Investigations of the role of D-amino acid oxidase and serine racemase in schizophrenia

Louise Verrall

Corpus Christi College
University of Oxford

A thesis submitted for the degree of
Doctor of Philosophy
Trinity 2008

1. INTRODUCTION

It has long been known that there is a heritable component to schizophrenia. Recently, significant progress has been made in identifying candidate susceptibility genes for the disorder and understanding how they contribute to pathophysiology. While the precise pathophysiological mechanisms remain unclear, the role of several brain regions and neurotransmitter systems is appreciated. In particular, the importance of glutamatergic deficits is emerging. Indeed, several recently identified susceptibility genes may impinge on glutamate pathways and contribute to *N*-methyl D-aspartate receptor (NMDAR) hypofunction in the disorder. D-amino acid oxidase (DAO) is genetically associated with schizophrenia and catabolises D-serine, the NMDAR co-agonist. It is therefore an interesting candidate gene. Moreover, reduced D-serine levels in schizophrenia have led to the suggestion that D-serine metabolic enzymes may be involved in the disorder. Thus, serine racemase (SRR), the D-serine synthetic enzyme, is also functionally implicated. However, at the time of conception of this thesis, an understanding of the potential role that DAO and SRR may play in schizophrenia, via regulating NMDAR activity, was limited. This thesis was designed to further investigate aspects of DAO and SRR neurobiology and their potential roles in schizophrenia. The following chapters detail investigations into the expression of DAO and SRR in the human brain and in schizophrenia, and attempts to investigate the role of D-serine metabolism in regulating NMDAR function. Firstly, however, the current understanding of schizophrenia and its aetiology and pathophysiology relevant to this thesis are overviewed. The current understanding of DAO, SRR and D-serine is then outlined.

1.1 SCHIZOPHRENIA; SYMPTOMS AND DIAGNOSIS

Schizophrenia is a severe and often chronic mental illness affecting around 1% of the population worldwide (reviewed in Andreasen, 1995), and thus exerting a major social and economic burden. The illness is heterogeneous and both outcome and presenting symptoms can vary greatly (reviewed in Messias *et al.*, 2007). Diagnosis is based on presenting symptoms and signs and their course (Andreasen, 1995) classified by the Diagnostic and Statistical Manual (DSM-IV; American Association of Psychiatry, 1994; Table 1.1) and the International Classification of Disease (ICD-10; World Health Organisation, 1992; Table 1.2).

The symptoms of schizophrenia are broadly categorized into three domains; positive, negative and cognitive. Positive symptoms include delusions, hallucinations and disordered thought and behaviour. Negative symptoms include flattening of emotional responses, withdrawal from social contact and apathy (Crow, 1985; Andreasen, 1995). Cognitive symptoms describe impairments in measures such as working memory, attention and executive function (Elvevag & Goldberg, 2000). The negative and cognitive symptoms are more resistant to pharmacological intervention and are most associated with long-term disability and poor outcome (Crow, 1985; Fenton & McGlashon, 1991; Andreasen, 1995; Green, 1996).

TABLE 1-1 DSM-IV Diagnostic criteria for schizophrenia.

A. Characteristic symptoms. Two (or more) of the following, each present for a significant portion of time during a 1 month period (or less if successfully treated).

a. Delusions
b. Hallucinations
c. Disorganised speech (e.g. frequent derailment or incoherence)
d. Grossly disorganised or catatonic behaviour
e. Negative symptoms, i.e. affective flattening, alogia or avolition

B. Social/occupational dysfunction. For a significant portion of the time since the onset of the disturbance, one or more major areas of functioning such as work, interpersonal relations, or self-care are markedly below the level achieved prior to the onset (or when the onset is in childhood or adolescence, failure to achieve the expected level of interpersonal, academic or occupational achievement).

C. Duration. Continuous signs of the disturbance persist for at least 6 months. This 6-month period must include at least 1 month of symptoms (or less if successfully treated) that meet criterion A (i.e. active-phase symptoms) and may include periods of prodromal or residual symptoms. During these prodromal or residual periods, the signs of the disturbance may be manifested by only negative symptoms or two or more symptoms listed in Criterion A present in an attenuated form (e.g. odd beliefs, unusual perceptual experiences).

D. Schizoaffective and Mood Disorder exclusion. Schizoaffective Disorder and Mood Disorder with Psychotic Features have been ruled out because either

a. No Major Depressive, Manic, or Mixed episodes have occurred concurrently with the active-phase symptoms; or
b. If mood episodes have occurred during active-phase symptoms, their total duration has been brief relative to the active and residual periods.

E. Substance/general medical condition exclusion. The disturbance is not due to the direct physiological effects of a substance (e.g. a drug of abuse, a medication) or a general medical condition.

F. Relationship to a Pervasive Developmental Disorder. If there is a history of Autistic Disorder or another Pervasive Developmental Disorder, the additional diagnosis of Schizophrenia is made only if prominent delusions or hallucinations are present for at least a month (or less if successfully treated).

Diagnostic criteria for Schizophrenia subtypes

1. Paranoid Subtype. A type of schizophrenia in which the following criteria are met:

a. Preoccupation with one or more delusions or auditory hallucinations
b. None of the following is prominent: disorganised speech, disorganised or catatonic behaviour, or flat or inappropriate affect.

2. Disorganised subtype. A type of Schizophrenia in which the following criteria are met:

a. All of the following are present ;i) Disorganised speech; ii) Disorganised behaviour; iii) Flat or inappropriate affect
b. The criteria are not met for catatonic type

3. Catatonic Subtype. A type of schizophrenia in which the clinical picture is dominated by at least two of the following:

a. Motoric inability as evidenced by catalepsy (including waxy flexibility or stupor
b. Excessive motor activity (that is apparently purposeless and not influenced by external stimuli)
c. Extreme negativisim (an apparently motiveless resistance to all instructions or maintenance of a rigid posture against attempts to be moved) or mutism
d. Peculiarities of voluntary movement as evidenced by posturing (voluntary assumption of inappropriate or bizarre postures), stereotyped movements prominent mannerisms, or prominent grimacing
e. Echolalia or echopraxia

4. Undifferentiated subtype. A type of Schizophrenia in which the symptoms that meet Criterion A are present but the criteria are not met for the Paranoid, Disorganised, or Catatonic Type.

Adapted from American Association of Psychiatry, 1994

TABLE 1-2 ICD-10 Diagnostic criteria for schizophrenia.

One very clear (and usually two or more if less clear-cut) symptom(s) belonging to one of the following groups:

a. thought echo, thought insertion, or withdrawal, and thought broadcasting; movements or specific thoughts, actions, or sensations; delusional perception;

b. delusions of control, influence or passivity, clearly referred to body or limb movements or specific thoughts, actions, or sensations; delusional perception;

c. hallucinatory voices giving a running commentary on the patient's behaviour, or discussing the patient among themselves, or other types of hallucinatory voices coming from some part of the body;

d. persistent delusions of other kinds that are culturally inappropriate and completely impossible, such as religious or political identity, or superhuman power and abilities (e.g. being able to control the weather, or being in communication with aliens from another world);

or symptoms from at least two of the following groups:

e. persistent hallucinations in any modality, when accompanied either by fleeting or half-formed delusions without clear affective content, or by persistent over-valued ideas, or when occurring every day or for weeks or months on end;

f. breaks of intentions in the train of thought, resulting in incoherence or irrelevant speech, or neologisms;

g. catatonic behaviour, such as excitement, posturing or waxy flexibility, negativism, mutism or stupor;

h. "negative" symptoms such as marked apathy, paucity of speech, and blunting or incongruity of emotional responses, usually resulting in social withdrawal and lowering of social performance; it must be clear that these are not due to depression or neuroleptic medication;

i. A significant and consistent change in the overall quality of some aspects of personal behaviour, manifest as loss of interest, aimlessness, idleness, a self-absorbed attitude, and social withdrawal;

Symptoms should have been clearly present for most of the time *during a period of 1 month or more*.

Adapted from World Health Organisation, 1992.

1.2 TREATMENT OF SCHIZOPHRENIA

Pharmacological treatment is integral to the clinical management of schizophrenia and it is established that antipsychotic drugs can improve psychotic symptoms of the illness and prevent their recurrence. The antipsychotic drugs are often described as falling into two classes; typical and atypical. As a rule, most antipsychotics have a high affinity for dopamine D_2 receptors. For typical antipsychotics this effect strongly correlates with their clinical potency (Seeman *et al.*, 1976; Kapur *et al.*, 2000), but may also lead to extra-pyramidal side effects (EPS). The atypical antipsychotics, on the other hand, have a more varied pharmacological profile and their D_2 receptor binding does not correlate as strongly with clinical outcome. They may be less likely to cause EPS (reviewed in Geddes *et al.*, 2000) but can be associated with other side effects of weight gain and hyperglycaemia (reviewed in Miyamoto *et al.*, 2005).

It had been thought that atypical antipsychotics were more clinically efficacious than typical antipsychotics. However, current thinking suggests that this is a misconception (Geddes *et al.*, 2000). The exception is the atypical antipsychotic clozapine, which has been shown to be effective for negative symptoms of the disorder and treatment-resistant patients (Kane *et al.*, 1988; Davis *et al.*, 2003). Coupled with the drug's potential effects on the glutamatergic system (reviewed in Heresco-Levy, 2003), clozapine is therefore an interesting therapeutic agent. However, its use can be associated with the potentially dangerous side effect of agranulocytosis, thus compromising its utility.

Since many patients fail to respond to antipsychotics, and given the adverse effects associated with them, current treatment of schizophrenia is limited. This

has prompted a change in rationale; firstly, to encompass new pathophysiological evidence in drug design; and secondly, to focus on narrower clinical targets, such as negative and cognitive symptoms, rather than the disorder as a whole (reviewed in Hyman & Fenton, 2003; Lewis & Gonzalez-Burgos, 2006). For example, several studies, pertinent to this thesis, have investigated the role of adjunctive therapies targeted at NMDAR in ameliorating negative and cognitive symptomology (discussed in section 1.9.1). In addition, the recent demonstration of the therapeutic effects of activation of metabotropic glutamate receptors (mGluRs) 2 and 3 (Patil *et al.*, 2007) attests to the potential utility in targeting the glutamatergic system in schizophrenia.

1.3 AETIOLOGY OF SCHIZOPHRENIA

The exact aetiology of schizophrenia is unclear. There is a strong heritable component, currently estimated to be ~80% (Sullivan *et al.*, 2003). Family studies indicate the mode of inheritance is non-Mendelian. Consequently schizophrenia is considered a polygenic disease, in which inheritance is complex and many genes predispose to the disorder. These genes likely act in concert, but individually will each account for only a small increment in risk (Harrison & Weinberger, 2005). Accordingly, identification of schizophrenia genes is difficult and genome-wide scans investigating linkage of chromosomal regions with schizophrenia have yielded inconsistent results. However, meta-analyses have identified loci at chromosomal regions 8p, 22q, 1q, 2p, 3p, 5q, 6p, 11q, 13q, 14p and 20p which may contain one or more susceptibility genes (Badner & Gershon, 2002; Lewis *et al.*, 2003). Using these data researchers may then identify candidate genes within these regions and look for their association with schizophrenia. Alternatively the same

approach may be taken with a gene that is a functional candidate rather than a candidate through its chromosomal location. Association is usually investigated through the identification of single-nucleotide polymorphisms (SNPs) within the gene and an analysis of their transmission in families or their frequencies in case-control samples. This approach has recently yielded the identification of several putative susceptibility genes for schizophrenia (Table 1.3). However, an important caveat is that the candidate SNP may not be causative, but is being transmitted along with the causative SNP i.e. is in linkage disequilibrium with that SNP.

Non-genetic factors have also been implicated in schizophrenia and include obstetric complications (Verdoux *et al.*, 1997; Geddes *et al.*, 1999), viral infections pre or peri-natally (Brown *et al.*, 2004), season of birth (Torrey *et al.*, 1997) and cannabis use in adolescence (Hall & Degenhardt, 2000; Veen *et al.*, 2004).

TABLE 1-3 Susceptibility genes for schizophrenia.

Gene	*Locus*	*Association with schizophrenia*	*Linkage to gene locus*
COMT	22q11	++++	++++
Dysbindin	6p22	+++++	++++
Neuregulin 1	8p12-21	+++++	++++
RGS4	1q21-22	+++	+++
mGluR3	7q21-22	+++	+
DISC1	1q42	+++	++
G72 (DAOA)	13q32-34	+++	++
DAO	12q24	++	+
PP3CC	8p21	+	++++
α7nAChR	15q13-14	+	++
PRODH2	22q11	+	++++
Akt1	14q22-32	+	+

Adapted from Harrison & Weinberger, 2005. COMT, Catechol-*O*-methyl transferase; RGS4, regulator of G-protein signalling 4; DISC1, disrupted in schizophrenia 1; G72, also known as DAOA, D-amino acid oxidase activator; mGluR3, metabotropic glutamate receptor subunit 3; PPP3CC, calcineurin gamma catalytic subunit; α7nAChR, α7 nicotinic acetylcholine receptor gene; PRODH2, proline dehydrogenase.

The neurodevelopmental hypothesis has become the main pathogenic model of schizophrenia and takes into account both genetic and non-genetic aetiological factors. It proposes that these act during a critical period of development and converge to affect the migration of neurons and the formation and remodelling of neuronal connections. Beginning *in utero*, these changes eventually lead to prominent psychopathology, presenting most commonly between 15 and 24 years (reviewed in Messias *et al.*, 2007), and triggered and/or exacerbated by environmental factors (Murray & Lewis, 1987; Weinberger 1987; Bloom 1993; Harrison 1999).

Several findings provide support to this theory (Table 1.4). For example, in animal models, neonatal hippocampal lesions (reviewed in Lipska & Weinberger, 2000) or developmental NMDAR blockade (Harris *et al.*, 2003) have been demonstrated to produce molecular and behavioural alterations in adulthood reminiscent of those in schizophrenia. In patients, the neurodevelopmental model is supported by observations that intellectual and behavioural differences occur in many children years before onset of schizophrenia (reviewed in Harrison, 2007). Moreover, neuropathologically, schizophrenic brains show no signs of neurodegeneration, and in the absence of a neurodegenerative mechanism brain pathology must presumably be neurodevelopmental (Harrison, 1999). For example, the absence of gliosis in the brain is taken to mean that pathological processes must have occurred prior to the third trimester (reviewed in Harrison, 1999). In addition, neuropathological observations of enlargement of the lateral and third ventricles, and loss of brain tissue, particularly prominent in the temporal lobe (reviewed in Harrison, 1999), can be present in first-episode unmedicated cases (Barr *et al.*, 1997; Whitworth *et al.*, 1998). This suggests that they are not consequent to medication or

TABLE 1-4 Key observations in support of a neurodevelopmental hypothesis of schizophrenia.

♦ Ventricular enlargement, decreased cortical volume and cognitive impairment present at onset of symptoms, if not earlier
♦ Presence and nature of cytoarchitectural abnormalities (e.g., altered cell positioning, packing density, and size)
♦ Absence of gliosis and other neurodegenerative features
♦ Increased prevalence of abnormal septum pellucidum
♦ Most known environmental risk factors operate pre-natally or in early childhood
♦ Children destined to develop schizophrenia in adulthood show neuromotor, behavioural and intellectual impairment
♦ Experimental neonatal lesions have delayed effects on relevant behavioural and neurochemical indices

Adapted from Harrison, 1999 and Harrison, 2007.

neurodegenerative processes. Further, young adults at risk of developing schizophrenia through their family history can manifest these alterations (Cannon *et al.*, 1993; Lawrie *et al.*, 1999), demonstrating that structural abnormalities in the brain can precede the onset of symptoms.

1.4 BRAIN REGIONS IMPLICATED IN SCHIZOPHRENIA

Several brain regions have been implicated in schizophrenia through behavioural tests and functional imaging, clinical observations and neuropathological findings. While the neuropathology of schizophrenia remains obscure it is now clear that the disorder is one of the brain, and that it has an anatomical basis. Some of the key macroscopic findings have been noted above (Table 1.4). Microscopic correlates of these (Table 1.5) include altered cell density, size, number and organisation. In addition, molecular studies demonstrate synaptic alterations in schizophrenia

(Table 1.5) (reviewed in Harrison, 1999). Many studies have focused on the hippocampus and dorso-lateral prefrontal cortex (DPFC) given the implication of these regions in the cognitive, negative and psychotic symptoms of schizophrenia (reviewed in Harrison, 1999). In addition, the cerebellum is increasingly recognized as an area important in schizophrenia and is central to some of the studies in this thesis. Therefore the hippocampus, DPFC and cerebellum in schizophrenia are discussed further below.

1.4.1 DPFC

At the functional level, the DPFC is involved in complex cognitive functions such as attention, executive function and working memory. Its processing capacity is deficient in schizophrenia, demonstrated, for example, by observations that schizophrenic patients have impaired working memory (reviewed in Knable & Weinberger, 1997; Weinberger *et al.*, 2001). Neuropathologically, post-mortem

TABLE 1-5 A summary of the major microscopic changes and synaptic alterations in schizophrenia.

Microscopic findings	
Incidence of gliosis	Unchanged
Hippocampal neuronal density	Unchanged
Hippocampal neuronal size	Reduced
Orientation of hippocampal neurons	Disarrayed?
Location of interstitial white matter neurons	Abnormal?
DPFC neuronal density	Increased
DPFC neuronal number	Unchanged
DPFC neuronal size	Decreased
Dorsal thalamic neuronal number	Decreased
Synaptic alterations	
DPFC presynaptic marker expression	Decreased
Hippocampal presynaptic marker expression	Decreased
DPFC dendritic spine density	Decreased
Hippocampal MAP2 dendritic marker expression	Decreased
Thalamic rab3a synaptic protein expression	Decreased

Adapted from Harrison, 1999. MAP2, microtubule-associated protein 2.

studies suggest reduced cortical thickness occurs in the DPFC (Daviss & Lewis, 1995; Selemon *et al.*, 1995) associated with reduced neuronal size (Rajkowska *et al.*, 1998; Pierri *et al.*, 2001) rather than number (Thune *et al.*, 2001). Neuron cell body size is proportional to the extent of the dendritic and axonal tree (Pierce & Lewin, 1994). Consistent with this, decreased expression of presynaptic markers (e.g. Davidsson *et al.*, 1999; Honer *et al.*, 1999; Karson *et al.*, 1999, but see e.g. Eastwood *et al.*, 2000a) evidences reduced neuropil - composed in part of axon terminals and dendritic spines - in the DPFC in schizophrenia. Therefore, altered synaptic connectivity may be the substrate for reduced DPFC neuropil, cortical thickness and perhaps function.

1.4.2 Hippocampus

At the functional level, imaging studies suggest that the hippocampus is involved in schizophrenic psychosis and cognitive impairments in the disorder such as memory and verbal learning (Tamminga *et al.*, 1992; Heckers *et al.*, 1998; Ongür *et al.*, 2006). Neuropathologically, evidence for altered neuronal density and number is weak (reviewed in Harrison, 1999) but hippocampal pyramidal neurons may be smaller in size in schizophrenia (Benes *et al.*, 1991; Arnold *et al.*, 1995; Zaidel *et al.*, 1997, but see Christison *et al.*, 1989). Again this could possibly reflect altered synaptic connectivity supported by demonstrations of reduced expression of presynaptic markers in the region (e.g. Browning *et al.*, 1993; Eastwood & Harrison, 1995, 1999; Young *et al.*, 1998; Vawter *et al.*, 1999; Fatemi *et al.*, 2001). Together the evidence suggests a synaptic pathology in the hippocampus in schizophrenia (Harrison & Eastwood, 2001) which may be a correlate of reduced neuronal size and perhaps aberrant hippocampal function.

1.4.3 Cerebellum

The cerebellum is traditionally considered to be primarily involved in motor control. However, patients with cerebellar degenerative diseases or those who have undergone cerebellar tumour removal, demonstrate cognitive and affective symptoms, suggesting its involvement in higher functions (Schmahmann & Sherman, 1998). Indeed, there is a move away from the central dogma of the cerebellum's exclusive involvement in proprioception, gait and motor control towards acceptance of its role in cognitive and affective behaviours (reviewed in Rapoport *et al.*, 2000; Schutter & van Honk, 2005; Konarski *et al.*, 2005). This role may be underpinned by circuitry which connects the cerebellum with the thalamus and prefrontal cortex (Schmahmann, 1991; Middleton & Strick, 1994). Accordingly, a theory proposed by Andreasen (Andreasen *et al.*, 1998; Andreasen, 1999) suggests that dysfunctions in cortico-cerebellar-thalamo-cortical circuits could impair the co-ordination of mental processes in schizophrenia and thence underpin some symptoms of the disorder.

Accompanying structural pathology at the macroscopic level is evidenced by cerebellar atrophy in schizophrenia (Weinberger *et al.*, 1979; Weinberger *et al.*, 1980; Lippmann *et al.*, 1982; Dewan *et al.*, 1983). However, associative microscopic changes have been inconsistent (Table 1.6). Consequently neuropathological abnormalities in the cerebellum in schizophrenia are inconclusive. Evidence exists for a synaptic pathology, however, based on altered cerebellar expression of synaptophysin (Eastwood *et al.*, 2001a, but see Davidsson *et al.*, 1999), snap-25 (Mukaetova-Ladinska *et al.*, 2002) and complexin II (Eastwood *et al.*, 2001a).

TABLE 1-6 Summary of microscopic pathology in the cerebellum in schizophrenia.

Finding		*Authors*
Purkinje cell density	↓	Reyes & Gordon, 1981
	↔	Lohr & Jeste, 1986; Tran *et al.*, 1998; Lingärde *et al.*, 2000; Bernstein *et al.*, 2001
Purkinje cell volume	↓	Reyes & Gordon, 1981; Tran *et al.* 1998
	↔	Lohr & Jeste, 1986; Andersen & Pakkenberg, 2003
Purkinje cell number	↔	Andersen & Pakkenberg, 2003; Andersen *et al.*, 2004

1.5 NEUROCHEMISTRY OF SCHIZOPHRENIA

At the neurochemical level, dopaminergic abnormalities in schizophrenia have been a central doctrine in research of the disorder, and are therefore briefly detailed below. More recently, however, and most pertinent to this thesis, the role of deficits in glutamatergic transmission have been appreciated. These are discussed further below. Other neurotransmitters such as GABA and serotonin are also likely related to schizophrenia pathophysiology and interactions between several neurotransmitter systems are suggested to occur.

1.5.1 Dopamine and schizophrenia

There are four main dopaminergic pathways in the brain; the tuberoinfundibular, nigrostriatal, mesolimbic and mesocortical tracts (Figure 1.1). In the prefrontal cortex, mesocortical dopaminergic terminals modulate the glutamatergic inputs to pyramidal neurons. In turn, a projection of cortical glutamatergic pyramidal neurons back to the limbic ventral tegmental area (VTA) is important for the physiological activity of this nucleus (reviewed in Sesack *et al.*, 2003).

The dopamine hypothesis of schizophrenia suggests that dopamine hyperactivity is responsible for the symptoms of schizophrenia (Matthysse, 1973). It was developed, in part, on the basis of pharmacological findings; firstly, that the clinical effects of typical antipsychotics are correlated with their D_2 receptor binding affinity (Seeman *et al.*, 1976; Kapur *et al.*, 2000); and secondly, that drugs which induce dopamine release produce psychosis in healthy volunteers and worsen the symptoms of schizophrenic patients (Lieberman *et al.*, 1987). A more recent revision to this theory suggests that both hyperfunction of mesolimbic projections and *hypo*function of mesocortical projections accounts for the symptoms of schizophrenia (Weinberger, 1987). Further still it is posited that the under-activity of mesocortical projections reduces cortical feedback inhibition of the mesolimbic pathway, and thereby might underpin subcortical dopamine hyperactivity (Weinberger, 1987). Consistent with this, modulation of subcortical

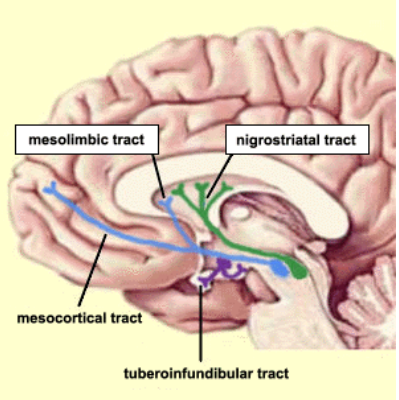

- ***Tuberoinfundibular tract:*** projects from the hypothalamus to the pituitary stalk.
- ***The nigrostriatal tract:*** projects from the substantia nigra to the caudate and putamen.
- ***The mesolimbic tract:*** projects from the VTA to limbic regions including the hippocampus, ventral striatum (nucleus accumbens) and amygdala.
- ***The mesocortical tract:*** projects from the VTA to cortical regions, especially the prefrontal cortex.

FIGURE 1-1 The four dopamine pathways in the brain. Taken from thebrain.mcgill.ca.

dopamine activity mediated via cortical dopamine activity has been demonstrated (Pycock *et al.*, 1980; Meyer-Lindenberg *et al.*, 2002).

Such revisions to the traditional dopamine theory in schizophrenia have implicated the neurotransmitter in the more cortical-based negative and cognitive symptoms of the disorder in addition to the psychotic symptoms. However, the disease as a whole is unlikely to be explained solely by dopaminergic deficits. Indeed, the role of glutamate in schizophrenia, and the interactions between the glutamate and dopamine systems, have taken on prominence in current views of schizophrenia neurochemistry.

1.5.2 Glutamate and schizophrenia

Glutamate is the major excitatory neurotransmitter in the brain, the effects of which are mediated by four receptors; the NMDAR, the alpha-amino-3-hydroxy-5-methyl-4-isoxazolepropionate (AMPA) receptor, the kainate receptor and the mGluRs. At glutamatergic synapses, the AMPA/kainate receptors and NMDARs mediate excitatory post-synaptic potentials (EPSPs) and are involved in synaptic plasticity of glutamatergic synapses, while the mGluRs are often modulatory. Astrocytes ensheathing glutamatergic synapses can modulate glutamate transmission through their expression of mGluRs and glutamate transporters and the release of glutamate and co-agonists of the NMDAR; so-called 'gliotransmitters' (Figure 1.2; reviewed in Halassa *et al.*, 2007).

A theory of glutamate dysfunction in schizophrenia stems, in part, from the effects of NMDAR blockade. In the 1950's and 60's, the drugs of abuse, ketamine and phencyclidine (PCP), were observed to precipitate psychotic syndromes in healthy human subjects (Luby *et al.*, 1959) and in schizophrenic patients (Itil *et al.*,

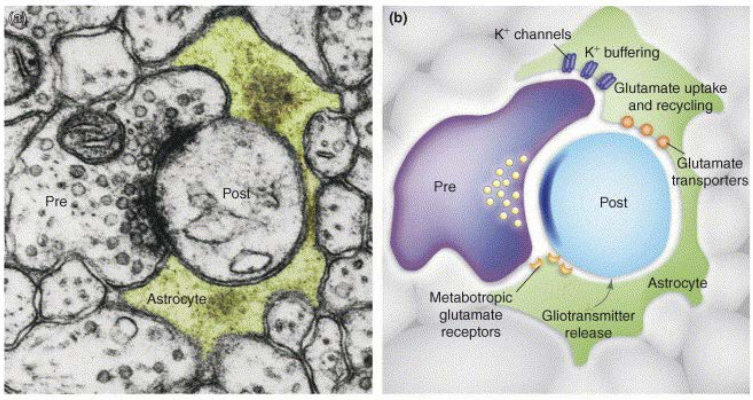

FIGURE 1-2 Electron micrograph (a) and schematic (b) showing the close association of astrocytic processes ensheathing pre- and post-synaptic cells at glutamate synapses. Astrocytes can have a key role in clearing glutamate from the synapse, clearing K^+ ions that accumulate following neuronal activity and releasing 'gliotransmitters', for example NMDAR co-agonists. Taken from Halassa *et al.*, 2007.

1967; Lahti *et al.*, 1995). These effects were proposed to be due to blockade of NMDARs (Javitt & Zukin, 1991). Consistent with this, in animal models, NMDAR blockade was shown to produce stereotyped behaviours and working memory deficits akin to those seen in schizophrenia (Verma & Moghaddam, 1996). In light of these observations, it has been suggested that NMDAR hypofunction models a disease mechanism underlying many of the symptoms of schizophrenia (Olney & Farber, 1995; Olney *et al.*, 1999; Moghaddam, 2003; Coyle, 2006).

The NMDAR hypofunction theory is attractive in its consistency with several other hypotheses of schizophrenia. Firstly, schizophrenia is thought to be a neurodevelopmental disorder (see above). The NMDAR is critical in developmental processes such as activity-dependent synaptic pruning and plasticity (Bear *et al.*, 1991; Hahm *et al.*, 1991; Poo & Isaacson, 2007) and cell differentiation and survival (Moran *et al.*, 1999; Alavez *et al.*, 2006). Thus, developmental NMDAR hypofunction could contribute to abnormal brain maturation in schizophrenia (reviewed in Bloom 1993; Harrison 1999; Weinberger 1987). A second appealing aspect to the

NMDAR hypofunction theory is its compatibility with dopaminergic hypotheses. Chronic NMDAR antagonist administration has been shown to produce reductions in mesocortical dopamine activity and excessive subcortical dopamine activity (reviewed in Jentsch & Roth, 1999). This may arise from disrupted glutamatergic control of VTA neurons since attenuation of glutamate transmission in the VTA has been shown to increase dopamine release in the mesolimbic pathway and reduce dopamine release in the mesocortical pathway (Takahata & Moghaddam, 2000). Thus, a model has been proposed whereby subcortical dopamine hyperactivity and cortical dopamine hypoactivity is consequent to NMDAR hypofunction (Carlsson *et al.*, 1999). Finally, the NMDAR hypofunction theory is appealing in its consonance with GABAergic deficits posited in schizophrenia. For example, chronic NMDAR blockade has been shown to down-regulate GABA transporter 1 (GAT) (Paulson *et al.*, 2003) and glutamic acid decarboxylase (GAD), the synthetic GABA enzyme, reminiscent of the schizophrenic brain (Woo *et al.*, 1998; Guidotti *et al.*, 2000; Volk *et al.*, 2000). Such observations are well received given that GABAergic deficits in schizophrenia are particularly robust findings, yet genetic evidence does not suggest that this is a primary deficit. Thus, they may be directly consequential to NMDAR hypofunction (Coyle, 2006).

Despite the attractiveness of the NMDAR hypofunction model, the theory nonetheless requires supporting evidence, for example from biochemical and genetic studies. Alterations may be expected in the NMDAR itself, in molecules impacting on NMDAR function, or in other glutamate receptors, which could result in a condition with the appearance of the effects of NMDAR hypofunction. Post-mortem data regarding NMDAR or AMPA receptor expression in

TABLE 1-7 A summary of post-mortem studies of glutamatergic receptor expression in schizophrenia.

Finding		*Authors*
NMDAR binding	↑ Temporal and frontal cortex	Ishimaru *et al.*, 1994; Nudmamud & Reynolds, 2001
	↔ DPFC and hippocampus	Kerwin *et al.*, 1988; Scarr *et al.*, 2005
NR1 mRNA	↑ DPFC	Dracheva *et al.*, 2001
	↓ Entorhinal cortex and hippocampus	Law & Deakin, 2001; Hemby *et al.*, 2002
NR2A mRNA	↑ DPFC	Dracheva *et al.*, 2001
	↔ Entorhinal cortex	Hemby *et al.*, 2002
GluR1 mRNA	↑ DPFC	Dracheva *et al.*, 2005
	↔ Entorhinal cortex	Hemby *et al.*, 2002
GluR1 protein	↑ Hippocampus	Eastwood *et al.*, 1997b
GluR6 mRNA	↓ Hippocampus	Porter *et al.*, 1997
	↔ DPFC and Entorhinal cortex	Hemby *et al.*, 2002; Scarr *et al.*, 2005
GluR5 mRNA	↓ DPFC	Scarr *et al.*, 2005
	↔ Entorhinal cortex	Hemby *et al.*, 2002
GluR2 mRNA	↓ Hippocampus and DPFC	Eastwood *et al.*, 1995; Eastwood *et al.*, 1997a; Vawter *et al.*, 2002
	↔ Entorhinal cortex	Hemby *et al.*, 2002
GluR2 protein	↓ Hippocampus	Breese *et al.*, 1995; Eastwood *et al.*, 1997b
AMPAR binding	↔ DPFC	Healy *et al.*, 1998

schizophrenia are sparse and inconsistent (Table 1.7). The discrepancies in these data likely arise from the different cohorts of patients and brain regions studied and the different techniques used. From these findings it is unclear whether NMDAR hypofunction is attributable to a primary deficit in NMDAR function or other glutamatergic deficits.

Genetic evidence, however, suggests NMDAR hypofunction may arise via molecules impinging on the receptor since many of the allelic variants which may contribute to schizophrenia pathophysiology (see Section 1.3, Table 1.3) are thought to do so by converging upon NMDAR function (Harrison & Weinberger, 2005; Harrison, 2007). For example, activation of mGluR3, which would reduce

glutamate transmission, may be overactive in schizophrenia and contribute to NMDAR hypofunction (Coyle, 2006). Further, dysbindin has been shown to regulate vesicular glutamate release (Numakawa *et al.*, 2004) and be down-regulated in schizophrenia (Talbot *et al.*, 2004; Weickert *et al.*, 2004), while neuregulin is involved in NMDAR-mediated signalling cascades (Gu *et al.*, 2005). Finally, G72 and DAO may impact on NMDAR function through the breakdown of D-serine (Chumakov *et al.*, 2002), the NMDAR co-agonist. The genetic implication of DAO in NMDAR function and thence schizophrenia forms a central premise of this thesis and will be detailed further below.

Taken together therefore, while the expression of the NMDAR itself may not be altered in schizophrenia, its function may be compromised through other molecules impacting on it. The final corroboration of NMDAR deficits in schizophrenia comes from pharmacological data which demonstrate that facilitation of NMDAR transmission is of therapeutic benefit in the disorder. Several strategies to this end have been employed and show improvements in patients, particularly in negative and cognitive symptoms (Coyle, 2006; Tuominen *et al.*, 2006). One of these strategies is D-serine, detailed further in Section 1.9.1. Evidence of the therapeutic potential of D-serine is clearly pertinent to the genetic association of its catabolic enzyme, DAO, with the disorder (Table 1.3) as well as to reports of reduced D-serine levels in schizophrenia (detailed further in Section 1.9). Thus, D-serine and DAO are implicated in schizophrenia through their functional roles in NMDAR transmission and genetic and pharmacological evidence. Consequently, theories of altered D-serine metabolism in schizophrenia contributing to NMDAR hypofunction have been proposed (Hashimoto *et al.*, 2003, 2005). Such theories led to the inception of the studies within this thesis. Before

these studies are detailed in the subsequent data chapters, a further description of the NMDAR, evidence for D-serine as the NMDAR co-agonist, and evidence for an involvement of D-serine and its metabolic enzymes in schizophrenia is given below.

1.6 THE *N*-METHYL D-ASPARTATE RECEPTOR

NMDARs are ionotropic glutamate receptors. They are characterised by voltage dependent Mg^{2+} block and a high permeability to calcium and consequently permit calcium entry only when a cell is depolarised. The NMDARs thus serve as coincidence detectors, responding to simultaneous pre- and post-synaptic activity (reviewed in Ozawa *et al.*, 1998).

Seven NMDAR subunits have been identified: one NR1, four NR2 (A-D) and two NR3 (A-B). Most NMDARs are heterotetrameric assemblies comprising two NR1 and two NR2 subunits. The NR1 subunit is encoded by a single gene and is mandatory for NMDAR function, while the NR2 subunits A-D, each encoded by a single gene and harbouring the glutamate binding site, modulate the biophysical and pharmacological properties of the receptor (reviewed in Llansola *et al.*, 2005; Köhr, 2006). The NMDARs have several modulatory sites including those for Mg^{2+}, Zn^{2+} and polyamine binding. A further 'glycine modulatory site' (GMS) located on the NR1 subunit binds glycine. Its occupancy has been shown as an absolute requirement in order for glutamate to open the NMDAR channel (Currás & Pallotta, 1996). Thus, endogenous glycine is considered a 'co-agonist' for the NMDAR. While some contention has surrounded whether the GMS is saturated *in vivo*, several studies have demonstrated that it is not (see below and reviewed in Wood, 1995; Javitt, 2006), suggesting that modulation at this site is integral to NMDAR function.

1.7 D-SERINE AS THE ENDOGENOUS NMDAR CO-AGONIST

In the early 1990's, several studies demonstrated substantial quantities of D-serine, a neutral D-amino acid, in the mammalian (Hashimoto *et al.*, 1992; Hashimoto *et al.*, 1993b,c; Nagata *et al.*, 1994a; Hashimoto *et al.*, 1995a,b; Hamase *et al.*, 1997) and human (Chouinard *et al.*, 1993; Hashimoto *et al.*, 1993a; Kumashiro *et al.*, 1995; Nagata *et al.*, 1995) brain. This was of interest given the traditional view that D-amino acids had limited function in nature with restricted roles in bacteria and lower invertebrates. It was of further interest, however, given that [^{3}H]glycine binding sites on NMDARs in the brain were found to be sensitive to displacement by D-serine (McDonald *et al.*, 1990). Moreover, at recombinantly expressed NMDARs, D-serine was shown to act as a full agonist of the GMS (McBain *et al.*, 1989; Watson *et al.*, 1990; Priestley *et al.*, 1995; Matsui *et al.*, 1995; Hess *et al.*, 1996) and in one report, more potently than glycine (McBain *et al.*, 1989). These studies suggested that D-serine in the mammalian brain had the potential to act as a potent NMDAR co-agonist.

Regionally, D-serine was found at high levels in the forebrain and low levels in the hindbrain and adult cerebellum, with a distribution correlating that of NMDARs (Hashimoto *et al.*, 1993c; Nagata *et al.*, 1994a; Kumashiro *et al.*, 1995; Hashimoto *et al.*, 1995a,b; Matsui *et al.*, 1995; Hamase *et al.*, 1997). Concurrently, seminal studies from Solomon Snyder's group reported D-serine distribution immunohistochemically. They described its enrichment in the grey matter of the forebrain, exclusively localized to astrocytes abundant in the neuropil around NMDAR 2A/B subunits (Schell *et al.*, 1995, 1997), consistent with correlated distributions of D-serine immunoreactivity and D-[^{3}H]serine binding sites (Schell *et al.*, 1995). Further, astrocytes were shown to release D-serine consequent to

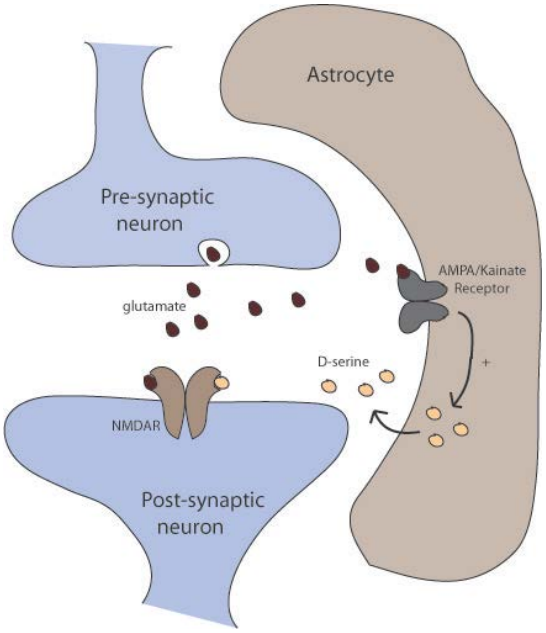

FIGURE 1-3 D-serine at the tripartate synapse. D-serine, localized to astrocytes ensheathing NMDAR bearing synapses, is released following AMPA/Kainate receptor stimulation. D-serine then potentiates the response of synaptic glutamate at post-synaptic NMDARs. Adapted from Martineau *et al.* (2006a,b).

AMPA/Kainate receptor stimulation (Schell *et al.*, 1995). These influential studies led to the proposal that D-serine is the endogenous NMDAR co-agonist in the forebrain where it acts as a 'gliotransmitter' at tripartate NMDAR-bearing synapses (Figure 1.3) (Schell *et al.*, 1995, 1997 and reviewed in Snyder & Kim, 2000; Snyder & Ferris, 2000; Wolosker *et al.*, 2002; Miller, 2004; Schell, 2004; Martineau *et al.*, 2006a,b; Oliet & Mothet, 2006; Wolosker, 2006). Consistent with this, several studies have demonstrated that exogenously applied D-serine potentiates the responses of NMDARs in cortical (e.g. Ito & Hicks, 2001; Chen *et al.*, 2003; Li & Han, 2007) and hippocampal slice preparations (e.g. Martina *et al.*, 2003; Krasteniakov *et al.*, 2005; Junjaud *et al.*, 2006) and the cerebellum *in vivo* (Wood *et al.*, 1989; Rao *et al.*, 1990). These studies provide evidence that the GMS is not saturated in these regions and that D-serine is capable of modulating NMDAR function. A role for *endogenous* D-serine was evidenced through demonstrations that its depletion attenuated NMDAR-dependent responses in the retina (Stevens *et al.*,

2003; Gustafson *et al.*, 2007), hippocampus (Mothet *et al.*, 2000; Yang *et al.*, 2003; Shleper *et al.*, 2005; Yang *et al.*, 2005), cortex (Katsuki *et al.*, 2004) and immature cerebellum (Mothet *et al.*, 2000). These studies therefore provided evidence that D-serine endogenously modulates NMDAR function in the forebrain and immature cerebellum. In the mature cerebellum some contention exists as to the presence of D-serine (e.g. Nagata *et al.*, 1992, 1994a; Schell *et al.*, 1997; Wang & Zhu, 2003; Williams *et al.*, 2006) and it is suggested glycine may serve as the NMDAR co-agonist in this region (Schell *et al.*, 1997; Mothet *et al.*, 2000). In agreement with its endogenous role in central NMDAR modulation, D-serine has since been implicated in a range of NMDAR-dependent behaviours including learning and memory, behavioural sensitization to cocaine, and pain processing (Wake *et al.*, 2001; Maekawa *et al.*, 2005; Guo *et al.*, 2006; Duffy *et al.*, 2007; Fernandez-Espejo *et al.*, 2007).

While the role of D-serine in modulating NMDAR function is central to this thesis, some additional, but more conjectural, neurochemical roles of the D-amino acid should briefly be pointed out. Firstly, D-serine has been shown to open NMDAR channels in the absence of glutamate binding in a subset of neocortical nerve endings (Paudice *et al.*, 1998). This raises the possibility of an exclusive role for D-serine in opening some NMDARs channels; although other studies show that D-serine only has potentiating effects on NMDAR responses and does not open the NMDAR channel alone (e.g. Guo *et al.*, 2005). In addition, D-serine has recently been shown to antagonize the AMPA glutamate receptor (Gong *et al.*, 2007). This suggests that it could exert both positive and negative modulatory effects at glutamatergic synapses, via NMDA and AMPA receptors respectively. D-serine also acts as an antagonist at NR1/NR3A or NR1/NR3B receptors, which are insensitive

to glutamate and activated by glycine (Chatterton *et al.*, 2002). Therefore, D-serine may modulate effects of glycine independently of its role in glutamatergic transmission. Speculatively, D-serine may also have a role in serotonergic signalling, given the demonstration that D-serine may bind 5-HT_3 receptors on human platelets (Fatima-Shad, 2006). Thus, while this thesis pertains to D-serine's co-agonist role at NMDARs, the actions of this D-amino acid are likely more complex than we are currently aware.

1.8 D-SERINE METABOLISM

D-serine is synthesized by SRR and broken down by its catabolic enzyme DAO. The presence of metabolic regulation of D-serine in the brain, and in particular the presence of a biosynthetic pathway, provides further evidence that D-serine plays a physiological role therein. In addition, transport systems for D-serine identified in the brain allow for regulation of its levels at localized sites. Thus, central D-serine availability likely depends upon the activities of its transporters and SRR and DAO. Presumably, therefore, metabolism and transport of D-serine may impact on its proposed function in NMDAR activation.

1.8.1 Serine racemase

The origin of D-serine in the mammalian brain was initially unknown, and thought possibly to arise from dietary and thence peripheral sources. Indeed transport at the blood brain barrier of D-serine has been demonstrated (Bauer *et al.*, 2005). However, D-serine was shown to be synthesized from L-serine in rat brain (Dunlop & Neidle, 1997) and thereafter a soluble enzyme, catalysing the direct synthesis of D- from L-serine, was purified (Wolosker *et al.*, 1999a). The enzyme demonstrated a

dependence on pyridoxal-5'-phosphate (PLP) for activity and was highly selective for L-serine over other L-amino acids. The purified SRR could also catalyse L- to D-serine but with six times less potency than D- to L-serine formation, such that D-serine formation is thought to principally occur under physiological conditions (Wolosker *et al.*, 1999a). SRR was subsequently cloned from mouse (Wolosker *et al.*, 1999b), rat (Konno, 2003) and human (De Miranda *et al.*, 2000; Xia *et al.*, 2004) and found to encode 339, 333 and 340 amino acid proteins respectively. High conservation among the sequences was demonstrated with 92% identity between rat and human and 96% between rat and mouse (Konno, 2003). Human SRR was found to comprise seven exons without a 5'untranslated region (UTR) exon (De Miranda *et al.*, 2000). However, Yamada *et al.* (2005) have subsequently described additional 5'UTR exons giving rise to four novel SRR transcripts, one of which was shown to be predominantly expressed in the brain. In addition, based on bioinformatics, three further putative transcripts have been described comprising novel combinations of SRR exons upstream of the 5'UTR (Xia *et al.*, 2004). However, western blot studies have reported only one predominant SRR protein in brain extracts (Wolosker *et al.*, 1999b; De Miranda *et al.*, 2000; Xia *et al.*, 2004; Steffek *et al.*, 2006; Bendikov *et al.*, 2007), suggesting that only one form of SRR may be translated in the brain.

Further studies on purified and recombinant SRR revealed that the enzyme is bifunctional and can also perform an α,β-elimination reaction which converts L-serine to pyruvate and ammonia (Figure 1.4; Panizutti *et al.*, 2001; De Miranda *et al.*, 2002; Foltyn *et al.*, 2005; Stříšovský *et al.*, 2003; Stříšovský *et al.*, 2005). D-serine was also shown to be a substrate for α,β-elimination, and it was suggested that this may be a physiologically relevant means of D-serine catabolism (Foltyn *et al.*, 2005).

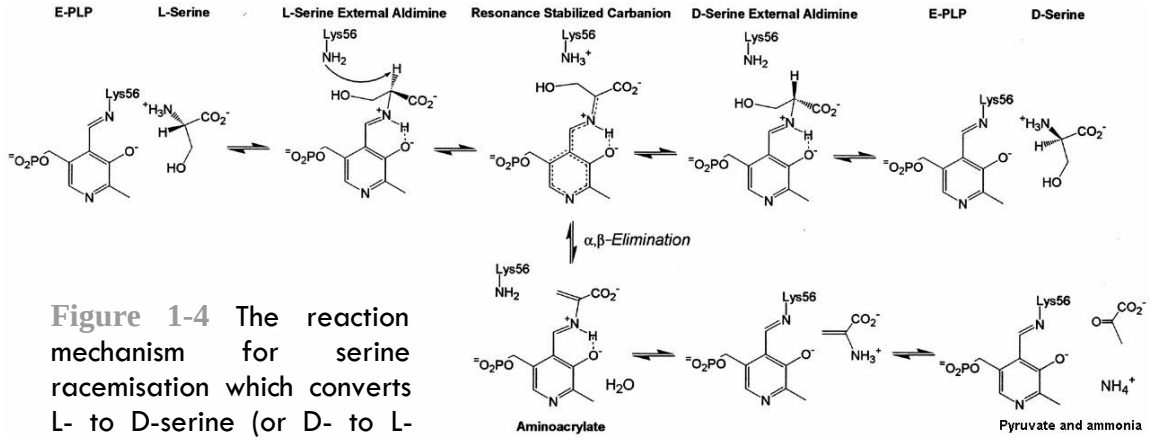

Figure 1-4 The reaction mechanism for serine racemisation which converts L- to D-serine (or D- to L-serine) and α,β elimination which generates pyruvate and ammonia from L- or D-serine. SRR catalysis is dependent on PLP. Adapted from Panizzutti et al., (2001).

However, others argue that this could only occur in cellular compartments where D-serine levels exceed those of L-serine given their relative affinities for SRR α,β-elimination (Stříšovský *et al.*, 2005).

Mg^{2+} and adenosine triphosphate (ATP) have been shown to stimulate SRR activity at physiologically relevant levels and in their presence, SRR was shown to make three molecules of pyruvate from L-serine for every one molecule of D-serine made (De Miranda *et al.*, 2002). Thus, ATP may partition SRR activity to favouring pyruvate formation (Foltyn *et al.*, 2005). Modulation of SRR activities becomes more intricate in light of demonstrations that the nucleotides adenosine diphosphate (ADP) and guanine triphosphate (GTP) can regulate SRR activity in place of ATP (Neidle & Dunlop, 2002), that Mn^{2+} and Ca^{2+} can replace Mg^{2+} in doing so (Cook *et al.*, 2002; Neidle & Dunlop, 2002; Stříšovský *et al.*, 2003), and that glycine is a competitive inhibitor of the enzyme at concentrations found intracellularly (Dunlop & Neidle, 2005; Stříšovský *et al.*, 2005). Further still, yeast-two hybrid systems have identified protein interacting with C-kinase 1 (PICK1; Fujii *et*

al., 2006) and glutamate receptor interacting protein (GRIP) as binding partners of SRR, the latter also shown to regulate the enzyme's activity (Kim *et al.*, 2005). Thus, elaborate control over D-serine synthesis, dependent on cellular compartmentalization, localized milieu and interacting proteins, likely occurs.

1.8.2 D-amino acid oxidase

DAO is a flavoenzyme, first described by Krebs in 1935 (Krebs, 1935), which oxidises neutral and basic D-amino acids including D-proline, D-alanine and D-serine. The enzyme non-covalently binds flavine-adenine-dinucleotide (FAD) as its prosthetic group and catalyses the conversion of D-amino acids to their corresponding imino acid with the concomitant reduction of FAD. The imino acid hydrolyzes in the presence of water to the corresponding α-keto acid and ammonia, and FAD reoxidises in the presence of oxygen which is reduced to hydrogen peroxide (Figure 1.5). This reaction was found to occur *in vivo* as well as *in vitro* (D'Aniello *et al.*, 1993) and DAO was localized to the mammalian brain (Neims *et al.*, 1966; Arnold *et al.*, 1979). However, its presence there was obscure until the discovery of D-amino acids in the mammalian nervous system (see above). D-serine immunoreactivity and DAO activity were then shown to have an inverse distribution in the rat brain (Schell *et al.*, 1995) suggesting a role for the enzyme in D-serine catabolism. Consistent with

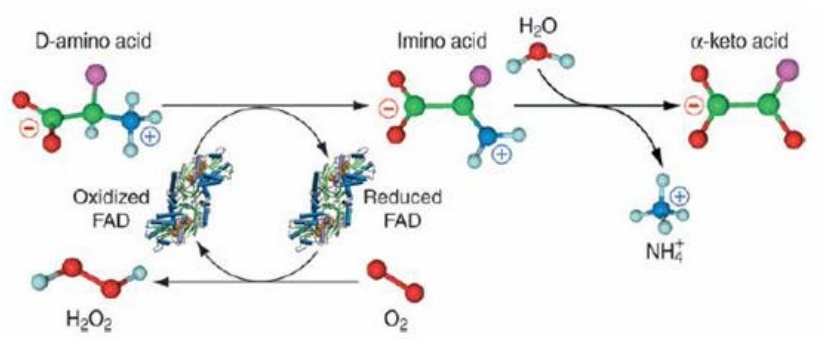

FIGURE 1-5
Schematic of the reaction catalyzed by DAO. Taken from Pollegioni *et al.*, (2007).

this, in mutant mice lacking DAO activity, D-serine levels were shown to be elevated in the cerebellum and hindbrain where DAO activity is normally present (Hashimoto *et al.*, 1993b; Nagata *et al.*, 1994b; Morikawa *et al.*, 2001; Hamase *et al.*, 2005). In the cortex, no change in D-serine levels was reported (Nagata *et al.*, 1994b; Morikawa *et al.*, 2001) in accord with low or undetectable DAO activity in this region (e.g. Horiike *et al.*, 1994; Schell *et al.*, 1995). However, others have reported a small but significant increase in cortical D-serine in mice lacking DAO activity (Hashimoto *et al.*, 1993b) and with pharmacological DAO inhibition (Adage *et al.*, 2007). Taken together therefore, a role for DAO *in vivo* in D-serine breakdown is firmly established in the cerebellum, while in the forebrain the presence of DAO and its catabolic regulation of D-serine is equivocal.

Within the cell, the oxidation reaction performed by DAO occurs in peroxisomes where the enzyme is localized (Arnold *et al.*, 1979; Perotti *et al.*, 1987; Usuda *et al.*, 1986; Moreno *et al.*, 1999). These organelles also contain other oxidising enzymes such as catalase (Usuda *et al.*, 1991). It is thought that DAO is trafficked through the peroxisomal membrane in an inactive form with a tertiary structure that is not fully formed (Caldinelli *et al.*, 2004).

At the molecular level, DAO has been cloned in the mouse (Tada *et al.*, 1990), rat (Konno, 1998) and human (Momoi *et al.*, 1988) and shown to encode 345, 346 and 347 amino acid proteins respectively. The rat and mouse sequences are 93% identical and the rat and human 77%, indicating evolutionary conservation (Konno, 1998). Human DAO resides on chromosome 12 and consists of 11 exons and 10 introns, the first exon comprising the 5'UTR and the last exon containing a peroxisomal targeting sequence (Fukui & Miyake, 1992). Alternative transcripts

involving 5'UTR deletions in the pig kidney (Fukui & Miyake, 1992) and human brain (Kapoor *et al.*, 2006) and 3'UTR deletions in the rat kidney, liver and brain (Konno, 1998) have been reported. However, western blot studies have reported only one predominant DAO protein in brain extracts (Gavazzi *et al.*, 1987; Moreno *et al.*, 1999; Almond *et al.*, 2006; Bendikov *et al.*, 2007).

1.8.3 D-serine transport

A further means of regulating D-serine levels is through transporters, which could potentially remove or release D-serine from and to NMDAR-bearing synapses or extra-synaptic regions. Recently, cDNAs encoding the alanine-serine-cysteine transporter 1 (Asc-1), a novel Na^+-independent neutral amino acid transporter, have been cloned from mouse (Fukasawa *et al.*, 2000) and human (Nakauchi *et al.*, 2000) brain. Their expression in heterologous expression systems resulted in the transport of D-serine with an affinity in the physiological range of D-serine levels (Fukasawa *et al.*, 2000; Nakauchi *et al.*, 2000), suggesting Asc-1 may be able to transport D-serine *in vivo*. Indeed, in knock-out mice Asc-1 has been shown to be the predominant mechanism for D-serine re-uptake in the forebrain and cerebellum (Rutter *et al.*, 2007). Asc-1 is expressed exclusively neuronally (Helboe *et al.*, 2003; Matsuo *et al.*, 2004), while remaining glial D-serine transport is thought to occur via the alanine-serine-cysteine transporter 2 (ASCT2) (Dun *et al.*, 2007; Rutter *et al.*, 2007; Ribeiro *et al.*, 2002). More recently, vesicular release of D-serine from glial cells has also been demonstrated (Mothet *et al.*, 2005).

1.9 D-SERINE IN SCHIZOPHRENIA

In view of D-serine's co-agonist actions at NMDARs, and hypofunction of these receptors in schizophrenia, interest prevailed as to whether reduced levels of the D-amino acid may be contributory. Indeed, reductions in D-serine levels and in D-serine as a percentage of total serine have been reported in the cerebrospinal fluid (CSF; Hashimoto *et al.*, 2005; Bendikov *et al.*, 2007) and blood serum (Hashimoto *et al.*, 2003; Yamada *et al.*, 2005) of schizophrenic patients. However, these findings have since not been replicated in the brain in schizophrenia (Bendikov *et al.*, 2007; Hashimoto *et al.*, 2007a), consistent with an earlier small study (Kumashiro *et al.*, 1995). Several reasons could account for the discrepancy between CSF/serum D-serine measurements and those in post-mortem brain tissue. It could be an effect of post-mortem interval (pmi) since D-serine levels are susceptible to pmi in rodents (Hashimoto *et al.*, 2007a). However, D-serine levels in schizophrenia were not found to be significantly altered even when controlling for the pmi effect calculated in rodents (Hashimoto *et al.*, 2007a). Alternatively, measuring D-serine in tissue homogenates may be less sensitive than in body fluids. Or, on the other hand, the results may be accurate such that CSF/serum D-serine measurements are not reflective of brain D-serine levels, a situation reported for other molecules (e.g. Thomas & Segal, 1998; Walker *et al.*, 2000). Notwithstanding this possibility, at the time of conception of this thesis, existing evidence from CSF and serum studies suggested an interesting reduction in D-serine levels in schizophrenia.

1.9.1 D-serine as an adjunctive treatment in schizophrenia

In light of D-serine's ability to potentiate NMDAR function, the D-amino acid, as well as other GMS agonists, have been utilised therapeutically in schizophrenia.

Administration of D-serine and its analogue D-cycloserine have been trialled as adjuncts to both typical and atypical antipsychotics (Table 1.8). The data show some inconsistencies, and of note, neither was effective in combination with clozapine. Indeed, in combination with clozapine D-cycloserine sometimes worsened symptoms (Table 1.8). Current meta-analyses have concluded that D-serine is beneficial for negative symptoms of schizophrenia and demonstrates a trend towards a positive effect on cognitive symptoms, while D-cycloserine is ineffective for the treatment of the disorder (Tuominen *et al.*, 2005; Tuominen *et al.*,

TABLE 1-8 Summary table of the studies trialling D-serine or D-cycloserine as an adjunctive therapy in schizophrenia and their main findings on symptom scales.

Authors	*Adjunct*	*Antipsychotics*	*Main finding*
Tsai *et al.*, 1998	D-serine	Typical and atypicals excluding clozapine	↓ P, N, C
Tsai *et al.*, 1999	D-serine	Clozapine	↔ P, N, C
Heresco-Levy *et al.*, 2005	D-serine	Atypicals excluding clozapine (olanzapine and risperidone)	↓ P, N, C
Lane *et al.*, 2005	D-serine	Atypical (risperidone)	↔ P, N, C
Cascella *et al.*, 1994	D-cycloserine	Typical	↑ P
Goff *et al.*, 1995	D-cycloserine	Typical	↓ N, C
Goff *et al.*, 1996	D-cycloserine	Clozapine	↑ N
Rosse *et al.*, 1996	D-cycloserine	Typical	↔ N
Heresco-Levy *et al.*, 1998	D-cycloserine	Typical and atypicals including clozapine	↓ N ↔ P
Goff *et al.*, 1999a	D-cycloserine	Typical	↓ N ↔ C
Goff *et al.*, 1999b	D-cycloserine	Clozapine	↑ N ↔ P
Van Berckel *et al.*, 1999	D-cycloserine	Typical	↑ P ↔ N
Evins *et al.*, 2002	D-cycloserine	Atypical (risperidone)	↓ N ↔ C
Heresco-Levy *et al.*, 2002	D-cycloserine	Typical and atypicals (olanzapine and risperidone)	↓ N ↔ P
Duncan *et al.*, 2004	D-cycloserine	Typical	↔ N, C
Goff *et al.*, 2005	D-cycloserine	Typical	↔ P, N, C

↑, increased symptoms; ↓, decreased symptoms; ↔, unchanged symptoms; P, positive symptoms; N, negative symptoms; C, cognitive symptoms.

2006). This may be explained by D-cycloserine's partial agonism at the NMDAR, and thus blockade of endogenous glycine or D-serine (Goff *et al.*, 1999b). D-serine has also been shown to exert effects in animal models of schizophrenia, consistent with its effect clinically. Systemic administration of D-serine in rodents has been shown to elevate D-serine levels in the brain, most prolonged in the cortex and hippocampus (Hashimoto & Chiba, 2004). Its administration was further shown to reverse NMDAR blockade-induced behavioural effects (Nilsson *et al.*, 1997; Andersen & Pouzet, 2004; Lipina *et al.*, 2005) and potentiate the effects of antipsychotics on conditioned avoidance response behaviour in rats, considered to be a test of predictive validity for antipsychotics (Olsen *et al.*, 2006).

Together these data indicate a beneficial role of administered D-serine in schizophrenia, likely through augmentation of NMDAR function. The data could support an involvement of D-serine metabolism in the disorder therefore, since D-serine administration may be ameliorative due to its reduced levels in the disease. On the other hand, D-serine may not be a pathophysiological determinant and administered D-serine may be beneficial by potentiating NMDAR responses hypofunctional through a different mechanism. However, further evidence that would support D-serine as a pathophysiological determinant comes from the genetic association of DAO with the disorder.

1.10 DAO IN SCHIZOPHRENIA

At the time of conception of this thesis, SNPs within the DAO gene had been associated with schizophrenia diagnosis in three independent studies (Table 1.9; Chumakov *et al.*, 2002; Liu *et al.*, 2004; Schumacher *et al.*, 2004). Given DAO's role in D-serine breakdown, these reports were clearly pertinent to demonstrations of

reduced CSF/serum D-serine in schizophrenia (Section 1.9). Subsequently, two further replications were demonstrated (Corvin *et al.*, 2007b; Wood *et al.*, 2007). However, six negative studies have also been reported (Fallin *et al.*, 2005; Yamada *et al.*, 2005; Liu *et al.*, 2006; Shinkai *et al.*, 2007; Vilella *et al.*, 2007). These non-replications may reflect the difficulty in demonstrating significant association of a single gene to a polygenic disorder such as schizophrenia. In addition, alleic heterogeneity, where different SNPs within the same gene may predispose to disease, can make the association of a given SNP with a disorder more difficult to detect. It can be easier to demonstrate the association of a gene with particular intermediate endophenotypes. These are underlying quantitative traits closer to the pathophysiological mechanisms exerted by a gene than the disorder as a whole (Meyer-Lindenberg & Weinberger, 2006). In this regard, Stefanis *et al.* (2007) have

TABLE 1-9 Summary of the schizophrenia-association studies for DAO.

Population	Polymorphisms studied	Subjects/ families studied	Association result	Publication
Case-control studies				
Canada	8	213	Positive	Chumakov *et al.*, 2002
Ireland	4	373	Positive	Corvin *et al.*, 2007b
Canada	4	168	Negative	Shinkai *et al.*, 2007
Germany	3	299	Positive	Schumacher *et al.*, 2004
Spain	5	589	Negative	Vilella *et al.*, 2007
USA	7	311	Positive	Wood *et al.*, 2007
China	6	547	Positive	Liu *et al.*, 2004
Japan (i)	6	50	Negative	Yamada *et al.*, 2005
Japan (ii)	6	570	Negative	Yamada *et al.*, 2005
Family-based studies				
USA	5	263	Negative	Fallin *et al.*, 2005
Canada	4	113	Negative	Shinkai *et al.*, 2007
Taiwan	3	218	Negative	Liu *et al.*, 2006
Japan	6	124	Negative	Yamada *et al.*, 2005

shown association of DAO with negative and disorganized schizotypy, while Corvin *et al.* (2007a) demonstrated association of DAO genotype with depression and anxiety, potentially relevant to the depressive symptoms of schizophrenia. However, Goldberg *et al.* (2006) failed to demonstrate association with the tested endophenotypes in their study. Taken together, these studies suggest a possible genetic involvement of DAO in schizophrenia. However, they are not definitive, possibly reflective of a contribution of DAO to disease in a particular subset of patients.

1.10.1 G72 in schizophrenia

In addition to the existing data implicating DAO in schizophrenia, prior to this thesis, the G72 gene, shown to be an activator of DAO (Chumakov *et al.*, 2002), was found to be robustly associated with schizophrenia (Chumakov *et al.*, 2002; Addington *et al.*, 2004; Hall *et al.*, 2004; Korostishevsky *et al.*, 2004; Schumacher *et al.*, 2004; Wang *et al.*, 2004). The association has since been replicated in ten studies (Fallin *et al.*, 2005; Zou *et al.*, 2005; Hong *et al.*, 2006; Korostishevsky *et al.*, 2006; Ma *et al.*, 2006; Nicodemus *et al.*, 2006; Corvin *et al.*, 2007b; Shin *et al.*, 2007; Shinkai *et al.*, 2007; Yue *et al.*, 2007) but not in a further six (Mulle *et al.*, 2005; Bakker *et al.*, 2007; Goldberg *et al.*, 2006; Liu *et al.*, 2006; Wood *et al.*, 2007; Vilella *et al.*, 2007). Association of G72 with the endophenotypes of persecutory delusions and working memory and attention have also been described (Schulze *et al.*, 2005; Goldberg *et al.*, 2006). Overall, two meta-analyses have concluded that G72 has either a weak (Li & He, 2007) or highly significant (Detera-Wadleigh & McMahon, 2007) association with schizophrenia. Based on the reported function of the G72 protein in activating DAO (Chumakov *et al.*, 2002), the potential mechanism by which G72 allelic

variation predisposes to schizophrenia was speculated to be through elevated levels or activity of G72 and thence DAO. This could result in reduced D-serine levels and thereby NMDAR hypofunction, and therefore supports the implication of D-serine metabolism in schizophrenia pathophysiology. However, others have since reported that G72 acts to reduce DAO stability (Pollegioni *et al.*, 2007), suggesting, conversely, that *decreased* G72 levels/activity could contribute to schizophrenia through an effect on DAO activity. A further study on the other hand, suggests that G72 is not a binding partner of DAO and has an independent cellular role in mitochondrial function (Kvajo *et al.*, 2007). Thus, previous support that the genetic association of G72 with schizophrenia provided for an involvement of D-serine metabolism in the disorder is now more tentative.

1.11 SRR IN SCHIZOPHRENIA

Given the accumulating evidence for an involvement of D-serine and DAO in schizophrenia, interest amounted in SRR as a functional candidate in the disorder since reduced SRR activity could contribute to reduced D-serine as well as elevated DAO catabolism could. Subsequently, some evidence was reported of a genetic involvement of SRR in schizophrenia. Goltsov *et al.*, (2006) demonstrated association between SRR and schizophrenia at borderline significance, while Morita *et al.* (2007) reported that the same SNP was associated with schizophrenia. This SNP was also found to be functional, reducing promotor activity and thus expression of the allele, in keeping with a hypothesized reduction of SRR in schizophrenia. However, two further studies have not replicated the association (Yamada *et al.*, 2005; Strohmaier *et al.*, 2007). The SRR binding partner PICK1, associated with schizophrenia in two studies (Hong *et al.*, 2004; Fujii *et al.*, 2006) has

also not been replicated in another (Ishiguro *et al.*, 2007). Thus, taken together the data suggest a possible minor contribution of SRR or molecules affecting SRR to schizophrenia.

1.11 AIMS AND OBJECTIVES OF THIS THESIS

As laid out above, at the time of conception of this thesis, evidence existed for a reduction in D-serine in the CSF and serum in schizophrenia and for a genetic involvement of D-serine's catabolic enzyme, DAO, and its putative activator, G72, in the disorder. Given the established role of D-serine as the co-agonist of the NMDAR, these findings were consistent with theories of NMDAR hypofunction in schizophrenia and led to the proposal of dysregulated D-serine metabolism in schizophrenia. Consequently, SRR, the D-serine synthetic enzyme, was also a further functional candidate in the pathophysiology of the disorder.

However, several questions existed as to the role of DAO and SRR in the brain and in schizophrenia. The distributions of DAO and SRR in the human brain, indicative of the central roles the enzymes may play, were unknown. Moreover, their described distributions in the rodent brain had yielded some inconsistent results such that the cellular expression of DAO and SRR needed clarification.

In addition the expression of DAO and SRR in schizophrenia had not been studied. If the enzymes were to be involved in dysregulated D-serine levels in schizophrenia, their altered expression in the disorder was an evident mechanism by which this could occur. Indeed, it would be hypothesized that elevated DAO and/or decreased SRR could account for reduced levels of D-serine in schizophrenia. Furthermore, the implications of DAO and SRR in schizophrenia depended on their effects on NMDAR function as the mechanism of their

involvement. However, the effects of D-serine metabolic activity on NMDAR function had largely not been studied. Therefore, this thesis aimed to further investigate the role of DAO and SRR in the brain, in schizophrenia and in NMDAR function. To achieve this, three objectives were set out: Firstly, to characterise the regional and cellular expression of DAO and SRR in the rodent and human brain. The study of the distribution of DAO and SRR in the human brain formed a prelude to the second objective; to examine the expression of DAO and SRR in the post-mortem brains of patients with schizophrenia and control subjects. Finally, the third aim was to examine the effects of D-serine metabolism on the NMDAR.

In the subsequent data chapters I outline the rationale for each of these objectives further and detail the methodology, findings and conclusion of each. In the final chapter I summarise the main findings of this thesis in the context of current literature and discuss future avenues of research stemming from these studies.

2. THE DISTRIBUTION OF SRR AND DAO IN RAT AND MOUSE BRAIN

2.1 INTRODUCTION

As described in Chapter 1, D-serine has been proposed as the endogenous NMDAR co-agonist in the forebrain where it acts as a gliotransmitter (Chapter 1, Section 1.7). This proposal is based on studies demonstrating that D-serine is a potent co-agonist of recombinant NMDARs (McBain *et al.*, 1989; Watson *et al.*, 1990; Priestley *et al.*, 1995; Matsui *et al.*, 1995; Hess *et al.*, 1996), and *in vivo* is concentrated to forebrain grey matter astrocytes abundant in the neuropil close to NMDARs (Schell *et al.*, 1995, 1997).

Consistent with the distribution of D-serine, SRR is expressed in the rat and mouse forebrain and therein to cortical and hippocampal grey matter astrocytes (Wolosker *et al.*, 1999b; Wang & Zhu, 2003; Xia *et al.*, 2004; Yoshikawa *et al.*, 2004; Kartvelishvily *et al.*, 2006), but is found at low levels in the mouse cerebellum (Almond *et al.*, 2006; Wang & Zhu, 2003). Conversely, DAO activity, shown to regulate D-serine levels *in vivo* (Hashimoto *et al.*, 1993b; Morikawa *et al.*, 2001; Almond *et al.*, 2006), is concentrated to the cerebellum and hindbrain, also astrocytically, but is absent in the cortex (Horiike *et al.*, 1987, 1994; Schell *et al.*, 1995, Wang & Zhu, 2003). The inverse distributions of SRR and DAO are therefore thought to account for the concentration of D-serine to the forebrain and low cerebellar and hindbrain levels.

However, several recent studies have questioned prevailing views on the localization of D-serine and its metabolic enzymes. For example, both D-serine and SRR have also recently been detected in neurons of rat and mouse brain (Yasuda *et al.*, 2001; Kartvelishvily *et al.*, 2006; Puyal *et al.*, 2006; Williams *et al.*, 2006), suggesting D-serine may not only function as a 'gliotransmitter'. In addition, D-serine immunoreactivity has been demonstrated robustly at localized sources in the mouse cerebellum (Williams *et al.*, 2006), consistent with SRR expression therein, albeit at lower levels than in the cortex (Yoshikawa *et al.*, 2004, 2005; Takeyama *et al.*, 2006; Hashimoto *et al.*, 2007b). This suggests D-serine may have a cerebellar as well as a cortical role. In addition, and in contrast to activity studies (Horiike *et al.*, 1987, 1994; Schell *et al.*, 1995, Wang and Zhu, 2003), DAO has been demonstrated immunohistochemically in the rat cortex (Moreno *et al.*, 1999) suggesting a role of DAO therein. In agreement, others have detected DAO protein (Almond *et al.*, 2006) and mRNA (Yoshikawa *et al.*, 2004, 2005; Takeyama *et al.*, 2006; Hashimoto *et al.*, 2007b) in the rat and mouse cortex. Moreover, inhibition or mutation of DAO *in vivo* has been shown in some studies to increase cortical D-serine levels in the rodent (Hashimoto *et al.*, 1993b; Adage *et al.*, 2007), raising the possibility of some cortical DAO activity as well as expression.

Thus, the roles of D-serine and its metabolizing enzymes, inferred by their distributions, are not definitive. Moreover, the published reports of the cellular distribution of SRR (Wolosker *et al.*, 1999b, Kartvelishvily *et al.*, 2006) and DAO (Moreno *et al.*, 1999) are limited. To extend these findings, and to clarify some of the issues surrounding SRR and DAO's cellular expression, the present study therefore aimed to characterise the cellular distribution of SRR and DAO immunoreactivities

in the rat and mouse brain. Since the studies of the cellular expression of DAO and SRR prior to this thesis were confined to rats and mice, this chapter also formed a prelude to examining SRR and DAO distribution in the human brain (described in Chapter 3).

2.1.1 Choice of tissue and regions for analysis

To extend previous findings of rodent SRR and DAO distribution which had been studied in rats and mice, the distribution of these enzymes was studied here in both species. The results were consistent and any exceptions of species differences are noted.

Sections were taken at the levels of the frontal cortex and cerebellum given SRR and DAO's respective concentration to these regions (Horiike *et al.*, 1987, 1994; Schell *et al.*, 1995; Wolosker *et al.*, 1999b; Wang & Zhu, 2003; Kartvelishvily *et al.*, 2006). In addition, sections were taken at the hippocampal level of rat and mouse brains as a comparison to previous immunohistochemical studies (Moreno *et al.*, 1999; Wolosker *et al.*, 1999b; Kartvelishvily *et al.*, 2006).

A subsequent study also utilised sections taken at the level of the substantia nigra (SN) and VTA in the adult rat. The aim was to study SRR and DAO distribution in regions of dopaminergic projection and innervation. This was based on studies showing; a) that DAO's catalytic site can bind D-DOPA, an exogenously administered precursor in dopamine synthesis (Kawazoe *et al.*, 2007); and b) that inhibition of DAO blocks D-DOPA induced behavioural effects in rats (Moses *et al.*, 1996). These studies therefore suggest DAO may be present and active in regions of dopamine synthesis.

2.1.2 Choice of methodology

The present study chose to analyse SRR and DAO distribution immunohistochemically since protein distribution has greater implications than messenger RNA (mRNA) localization (which may not necessarily be transcribed). A commercially available antibody to SRR and a novel antibody to DAO were used. These were initially characterised in western blotting studies conducted with rat, mouse and human brain extracts, prior to using the antibodies for immunohistochemical studies.

Co-localization studies using the antibodies to DAO and SRR were not optimised for this study. Therefore, as an attempt to delineate the cell types expressing DAO and SRR, glial and neuronal markers were utilised for immunohistochemistry in adjacent sections to those immunolabelled for SRR and DAO. This allowed a comparison of the morphologies of neuronal and glial cells and those stained for SRR and DAO. Antibodies used for these studies were to; NeuN, a neuronal marker which labels neuronal cell bodies (e.g. Gittins & Harrison, 2004); glial fibrillary acidic protein (GFAP), which labels astrocytes; and the 67kDa GAD isoform (GAD67), a marker of GABAergic interneurons.

2.2 MATERIALS AND METHODS

2.2.1 Animals and tissue processing

All animal procedures in this thesis were carried out in accordance with the Animals (Scientific Procedures) Act 1986 and associated Home Office guidelines. For immunohistochemistry experiments, Sprague-Dawley rats (Harlan-Olac, Bicester, UK) at post-natal day (P) 30 (n = 3), were sacrificed by lethal injection of pentobarbitone and their brains removed and fixed in 10% formalin for one week. Brains were then paraffin-wax embedded using standard techniques (carried out by Mary Walker, Dept Psychiatry, Oxford University). Control mice (CD1 strain; courtesy of Dr Sharon Eastwood, Dept Psychiatry, Oxford University) at P56 (n = 4), were deeply anaesthetised, perfused with PBS followed by 4% PFA in PBS, and the brains removed and paraffin-wax embedded as above. Rat brain sections were cut from frontal cortex (Bregma 2.7 - 4.2mm), hippocampus (Bregma -2.3 - -4.3mm) and cerebellum (Bregma -11.96 - -14.08mm) and mouse brain sections from frontal cortex (Bregma 2.80 - -2.10mm), hippocampus (Bregma -1.22 - -2.92mm) and cerebellum (Bregma -6.96 - -7.64mm) and collected onto Superfrost Plus coated slides (VWR International, Leicestershire).

2.2.2 Tissue used for protein extraction and western blotting

To validate the antibodies used for immunohistochemistry, preliminary experiments characterised them with western blotting. For these experiments, frozen sections of control rat (taken from the study conducted in Chapter 4; see Section 4.2.2) and mouse (courtesy of Dr S Eastwood, Dept Psychiatry, Oxford University) brains were used. For human cerebellar or DPFC extracts, tissue was taken from control subjects described in Chapter 3 (see Section 3.2.1).

2.2.3 Protein extraction and calculation of protein concentration

To extract protein from frozen mouse, rat or human brain, 2-3 slide-mounted tissue sections were homogenized in 200µl protein extraction lysis buffer (Appendix I), boiled for ten minutes, centrifuged at 13,000*g* for ten minutes, and the supernatant collected.

Total protein concentrations were assayed using Bradford reagent (Sigma, Poole, UK) according to manufacturer's instructions. Briefly, samples were diluted 1:4 in phosphate buffered saline (PBS; Appendix I). A standard curve of bovine serum albumin (BSA) (1.4mg/ml – 0.03mg/ml; Sigma) was made in a solution of protein extraction lysis buffer in PBS (1:4 v/v), since the sodium dodecyl sulphate (SDS) content of the standards affects the gradient of the standard curve and thus should be matched with that of the unknown samples. A 5µl volume of protein sample was mixed with 250µl Bradford reagent (Sigma) in triplicate and the absorbance read at 595nm. The sample concentration was calculated by comparing the mean absorbance of each triplicate sample to the standard curve.

2.2.4 Western blotting

Immediately before electrophoresis, equal concentrations of protein extracts were mixed in a 4:1 ratio with 5x loading buffer (Appendix I) and boiled for ten minutes. Protein samples and a molecular weight marker rainbow ladder (GE Healthcare, Buckinghamshire, UK or BioRad, Hertfordshire, UK) were fractionated by electrophoresis on a 12% SDS/polyacrylamide gel (Appendix I) performed in tris-glycine running buffer (Appendix I) and run at 100v. Protein was transferred onto polyvinyl difluoride (PVDF) membrane (Immobilon-P, Millipore, Watford, UK) in transfer buffer (Appendix I) in an electro-transfer chamber (Biorad) at 20v

overnight. PVDF membrane was pre-wetted in methanol and rinsed in transfer buffer before use. Following transfer, western blotting was carried out at room temperature on a shaking platform. The membrane was immediately immersed in blocking buffer (2% non-fat milk in PBS-0.1% Tween^{20}), to block non-specific binding sites, for one hour and then incubated in primary antibody at 4ºC overnight. Membranes were then washed three times for ten minutes in blocking buffer and incubated for one hour in horseradish peroxidise (HRP) -linked secondary antibody in blocking buffer. The membrane was washed four times for fifteen minutes in PBS-0.1% Tween^{20} (PBS-T) and rinsed in PBS. Immunoreactive bands were visualized by chemiluminescence using the ECL-Plus kit (GE Healthcare) in the dark, according to manufacturer's instructions. The membrane was then wrapped in Saran Wrap and exposed to photographic film (Kodak BioMax X-Omat AR film).

Primary antibodies used were anti-flag M2 (Sigma; 1:15,000), cyclophilin (AbCam, Cambridge, UK; 1:100,000) and anti-β-actin (Chemicon, Chandlers Ford, UK; 1:10,000). To detect SRR, a commercially available mouse SRR antibody (BD Biosciences, Oxford, UK) was used at 1:500 according to manufacturer's instructions. To detect DAO, a novel rabbit antibody (denoted GSK-DAO antibody) was used at 1:1000-1:3000. The GSK-DAO antibody, directed to a peptide sequence of human DAO (peptide H-CGRILEEKKLSRMPPSHL-OH; N-terminal Cys added for coupling), was produced as described (Verrall *et al.*, 2007) at Psychiatry DTG, GlaxoSmithKline (GSK), Harlow, UK and generously provided by Dr Isabel Benzel. The concentration of the GSK-DAO antibody was 0.77 mg/ml. Initial studies which validated the GSK-DAO antibody in HEK-293 cells over-

expressing DAO and Clontech protein medleys were carried out at GSK and are described in Verrall *et al.*, (2007).

Secondary antibodies used were HRP-conjugated anti-mouse immunoglobulin (DAKO, Cambridgeshire, UK) at 1:1000 for SRR, flag-M2 and β-actin and HRP-conjugated anti-rabbit immunoglobulin (Chemicon) at 1:5000 for GSK-DAO and cyclophilin. Specificity for all antibodies in western blotting was assessed in control experiments where the primary antibody was omitted. For DAO, a pre-adsorption control where the antibody was incubated in a 10 fold molar excess of the antigenic peptide (synthesized by Invitrogen, Paisley, UK) prior to application, was also carried out.

2.2.5 Immunohistochemistry

Paraffin-wax embedded sections were cut at 10µm using a Leica rotary microtome. Sections were de-waxed in xylene overnight, rehydrated in graded ethanol, and microwaved in antigen unmasking solution (Vector Laboratories, Peterborough, UK) at 100ºC for ten minutes. Tissue was pre-treated with 3% hydrogen peroxide (VWR International) and non-specific binding sites were blocked in 10% normal serum in PBS-0.3% $\text{Triton}_{\text{X-100}}$ (PBS-Tx) for one hour at room temperature. Sections were washed three times for five minutes in PBS-Tx and incubated overnight at 4ºC with primary antibody diluted in 2% normal serum in PBS-Tx.

The following morning, sections were washed three times for five minutes in PBS-Tx and incubated in biotinylated secondary antibody diluted in 2% normal serum in PBS-Tx for one hour at room temperature. Sections were washed three times for five minutes in PBS and the antibody localized by the avidin-biotin-peroxidase technique using the Vectastain Elite ABC kit (Vector Laboratories)

according to manufacturer's instructions. Sections were then washed three times for five minutes in PBS and incubated in 0.02% hydrogen peroxide, 0.025% (w/v) 3,3′-diaminobenzidine (DAB; Sigma) in PBS for ten minutes at room temperature to demonstrate the peroxidise reaction. Sections were rinsed in distilled water and dehydrated through graded ethanols. Cresyl violet (Appendix I) was used as a counter-stain for some sections. Sections were mounted with DPX (VWR International) and a coverslip. Some immunohistochemistry experiments for SRR were carried out by Nancy Rawlings, an MSc student.

To detect SRR, an antibody to SRR (BD Biosciences) was used at 1:500, according to manufacturer's instructions. To detect DAO, the GSK-DAO antibody was titrated in pilot studies with cerebellar tissue, known to express DAO (Arnold *et al*., 1979; Horiike *et al*., 1987, 1994; Schell *et al*., 1995; Moreno *et al*., 1999; Wang & Zhu, 2003). In rat and mouse tissue, 1:500 GSK-DAO antibody was selected for optimal detection of immunoreactivity in cerebellar tissue (Figure 2.1 A). This concentration was found to detect comparable immunoreactivity in frontal cortex also (Figure 2.1 B) and was therefore used in all further studies. Primary antibodies to NeuN (Chemicon), GAD67 (Chemicon) and GFAP (DAKO) were used at 1:500, 1:2000 and 1:1000 respectively, according to manufacturer's instructions.

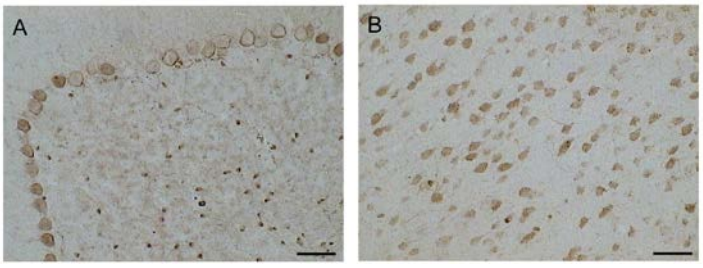

FIGURE 2-1 Optimisation of GSK-DAO antibody for immunohistochemistry. Representative image of 1:500 GSK-DAO antibody which showed robust detection of immunoreactivity in mouse cerebellar tissue (A) and frontal cortex tissue (B).

Secondary antibodies used were biotinylated horse anti-mouse (SRR, NeuN, GAD67) and goat anti-rabbit (DAO, GFAP) immunoglobulins (Sigma) at 1:100. Normal serums (Sigma) were horse (SRR, NeuN, GAD67) or goat (DAO, GFAP). Specificity for all antibodies in immunohistochemistry studies was assessed in control experiments where the primary antibody was omitted. For DAO pre-adsorption controls were carried out where the antibody, at the same concentration as that used under the experimental conditions, was pre-incubated at room temperature with a 10 fold molar excess of the antigenic peptide prior to use.

In immunohistochemistry results, based on morphology and immunostaining, cells were putatively identified according to the following criteria in Box 1.

Box 1. *Criterion used to identify putative cell types.*

a) Cells with a comparable morphology (shape and size) to those labelled by NeuN in adjacent sections were identified as neurons
   i) If these cells were large and with a triangular shape/visible apical dendrite they were identified as pyramidal neurons
   ii) If these cells were the same size and shape as GAD67 labelled cells in adjacent sections they were identified as interneurons

b) Large cells sometimes with apical dendrites located within the Purkinje cell layer of the cerebellum and comparable to those labelled for GAD67 in adjacent sections were identified as Purkinje cells

c) Immunoreactive cells which were small and not comparable in size and shape to NeuN immunolabelled cells in adjacent sections were identified as glia
   i) If these cells were also of comparable morphology to cells in adjacent sections which labelled for GFAP they were identified as GFAP-positive glial cells
   ii) If these were not of comparable morphology to cells in adjacent sections which labelled for GFAP they were identified as GFAP-negative glial cells
   iii) Presumed glia with a star-shaped/stellate morphology were identified as stellate glia
   iv) Particular glial populations, namely Bergmann glia, were identified based on their small size, rounded morphology and location within the Purkinje cell layer of the cerebellum
   v) Glial cells were speculatively identified as oligodendrocytes when they were visualized in rows (Hof *et al.*, 2003)

2.3 RESULTS

2.3.1 Validation of SRR and DAO antibodies by western blotting

To study the distribution of SRR, a commercially available SRR antibody was used and was first validated by western blotting in mouse, rat and human tissue. The antibody detected SRR as a single band at ~38kDa, the predicted molecular weight for SRR (Wolosker *et al*., 1999b; De Miranda *et al*., 2000), in human, rat and mouse brain (Figure 2.2). Omission of the primary antibody abolished the SRR immunoreactive band (data not shown).

To study the distribution of DAO, a novel GSK-DAO antibody was used. The GSK-DAO antibody had been previously validated by western blotting on lysates from human embryonic kidney (HEK)-293 cells over-expressing DAO and Clontech human protein medleys from different brain regions and peripheral tissues, all conducted at GSK. In these samples the antibody was shown to detect a single band at ~39kDa (Figure 2.3 A, B; Verrall *et al*., 2007), corresponding to the predicted molecular weight of DAO (Gavazzi *et al*., 1987; Moreno *et al*., 1999). The GSK-DAO antibody was then provided for the studies in this thesis and was further validated in our extracts of rat, mouse and human frozen tissue. The GSK-DAO antibody detected ~39kDa bands in rat, (Figure 2.3 C, Lane 2), mouse (data not shown) and human (Figure 2.3 C, Lane 1) cerebellum which were abolished by pre-adsorption of the GSK-DAO antibody with antigenic peptide (Figure 2.3 C, Lanes 3-4). In rat frontal cortical tissue, DAO immunoreactivity could not be detected by western blotting (data not shown) and in human DPFC tissue was variable and often negligible (Figure 2.3 D).

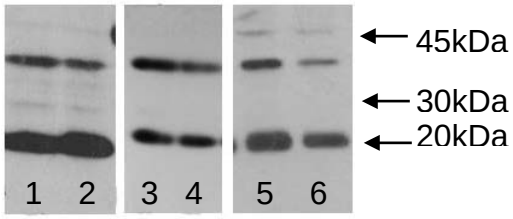

FIGURE 2-2 Representative western blot demonstrating the detection of SRR at ~38kDa and the loading control cyclophilin at ~20kDa in human (lanes1, 2), rat (lanes 3, 4) and mouse (lanes 5, 6) cortical (lanes 1, 3, 5) and cerebellar tissue (lanes 2, 4, 6).

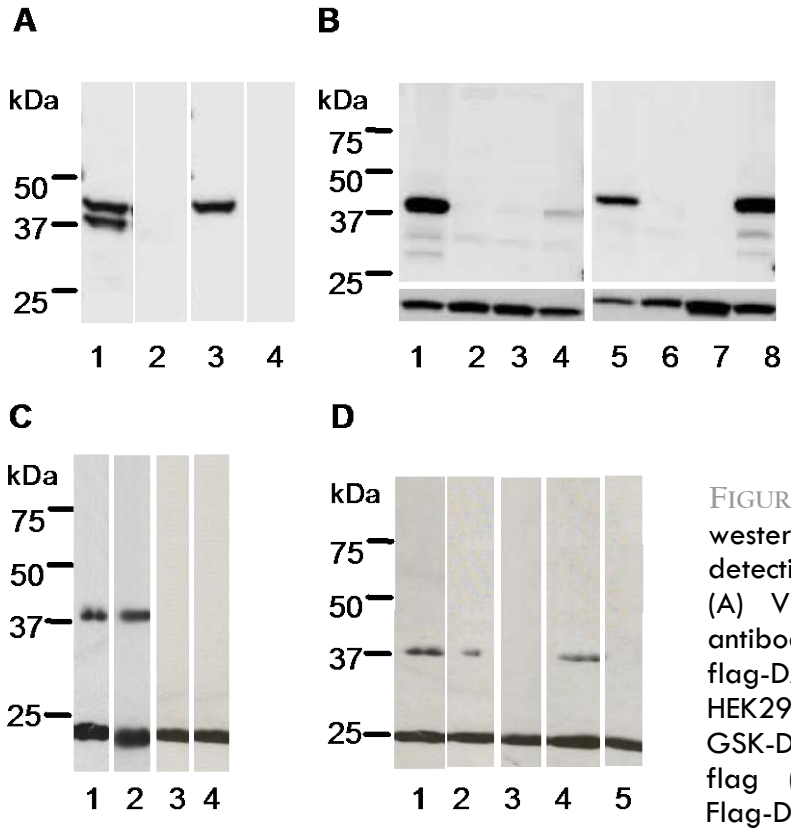

FIGURE 2-3 Representative western blots demonstrating the detection of DAO at ~39kDa. (A) Validation of GSK-DAO antibody using recombinant flag-DAO expressed in HEK293 cells. Detection with GSK-DAO (lanes 1-2) and anti-flag (lanes 3-4) antibodies. Flag-DAO is detected as a ~42kDa band with GSK-DAO antibody (lane 1) and anti-flag (lane 3) in flag-DAO transfected HEK293 cells but not respective mock transfected cells (lanes 2 and 4). Expressed untagged DAO is detected as a ~39kDa band, the predicted size for DAO, with GSK-DAO antibody (lane 1 lower band) but not anti-flag (lane 3). (B) Validation of DAO antibody using human tissue samples (Clontech protein medleys); lane 1: cerebellum, lane 2: amygdala, lane 3: hippocampus, lane 4: thalamus, lane 5: spinal cord, lane 6: lung, lane 7: heart, lane 8: kidney. A specific signal for DAO was detected at ~39 kDa in the cerebellum, spinal cord and kidney. Blots were re-probed with anti-β-actin as a loading control (lower panel). (C) Representative western blots of ~39kDa DAO (lanes 1-2) and DAO pre-adsorption control (lane 3-4) in protein extracts of post-mortem cerebellar tissue from human (lanes 1 and 3) and rat (lanes 2 and 4). Blots were simultaneously probed for cyclophilin as a loading control (lower band) which was detected at ~20 kDa. (D) Representative western blot of DAO detection in human DPFC extracts. Detection was variable and only evident in some subjects (upper bands at ~39kDa in Lanes 1, 2 and 4) compared to the loading control cyclophilin (lower bands at ~20kDa) present in all subjects. Adapted from Verrall *et al.*, (2007). Data in (A) and (B) were acquired by Dr Isabel Benzel at GSK, Harlow, UK.

2.3.2 Regional and cellular expression of SRR in the frontal cortex

In rat and mouse frontal cortex, SRR immunoreactivity localized to pyramidal cell bodies (Figure 2.4 B and C) and their apical dendrites. Staining was most prominently in layers II/III (Figure 2.4 A). Inferior cortical layers demonstrated milder neuronal labelling and intense immunolabelling of small round cells (Figure 2.4 C).

In adjacent sections, NeuN immunolabelling was uniform through all cortical layers and labelled pyramidal neurons and small round immunoreactive cells (Figure 2.4 E), too big for axonal processes in section, and smaller than GAD67 immunolabelled interneurons (Figure 2.4 F). Since they are neuronal, but not interneurons therefore, the small round NeuN immunolabelled cells putatively represent cell bodies in section. Given that SRR immunolabelled small round cells were distributed non-uniformly in layers where pyramidal neurons were less intensely stained, they probably do not reflect similar cell bodies in section. Based on their size, therefore, SRR immunolabelled small round cells are putative glia. However, GFAP immunolabelling localized predominantly to stellate cells with irregularly shaped cell bodies and extensive processes (Figure 2.4 G). Thus the rounded SRR-positive putative glia seen here might be GFAP-negative astrocytes or another glial subtype.

2.3.3 Regional and cellular expression of SRR in the hippocampus and surrounding structures

At the level of the hippocampus and surrounding structures, SRR immunoreactivity localized predominantly to cortical and white matter regions (Figure 2.5 A) including the retrosplenial cortex and corpus callosum. In the corpus callosum (Figure 2.5 B), scattered small round immunolabelled cells were

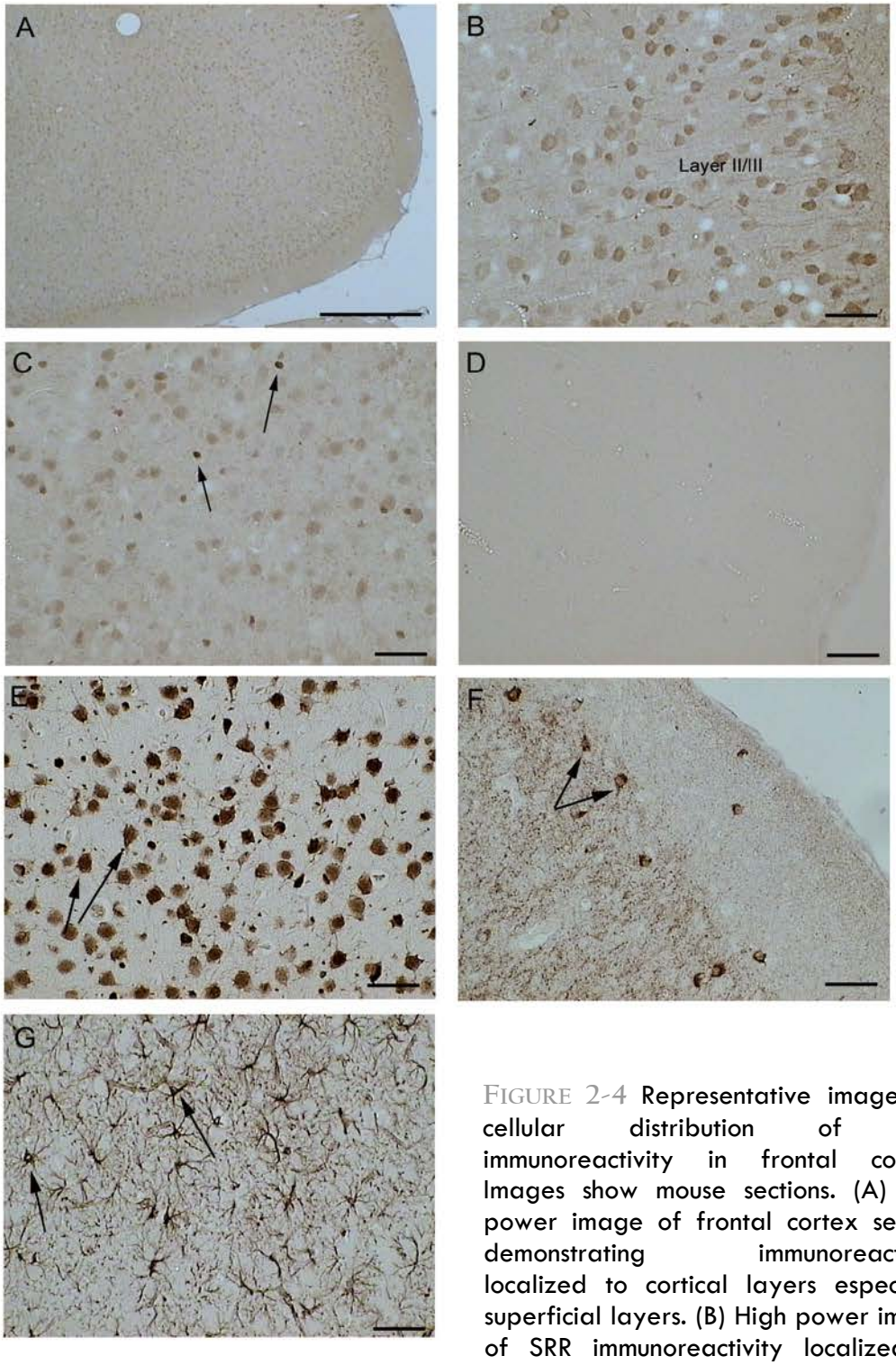

FIGURE 2-4 Representative images of cellular distribution of SRR immunoreactivity in frontal cortex. Images show mouse sections. (A) Low power image of frontal cortex section demonstrating immunoreactivity localized to cortical layers especially superficial layers. (B) High power image of SRR immunoreactivity localized to pyramidal neuron cell bodies and their apical dendrites in layers II/III. (C) High power image of moderate SRR immunolabelling of pyramidal neurons in inferior cortical layers and intense immunolabelling of small round cells (arrows). (D) No primary control for SRR in the frontal cortex. (E) NeuN immunolabelling in superficial layers of the frontal cortex demonstrating the intense labelling of pyramidal neurons (arrows). (F) GAD67 immunolabelling of interneurons (arrows) in the frontal cortex. (G) GFAP immunoreactivity in frontal cortex. Scale bars: A = 0.5mm; B-G = 50µm.

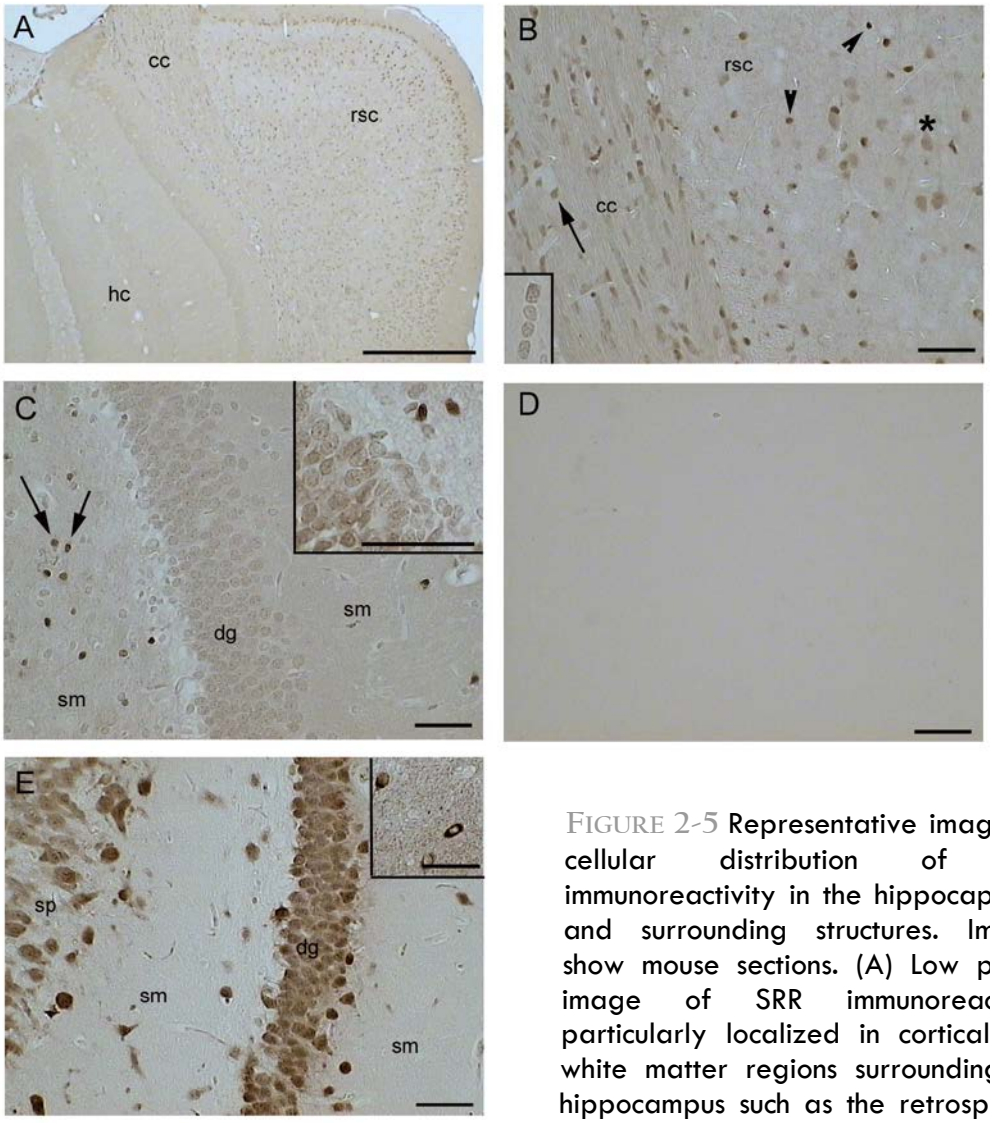

FIGURE 2-5 Representative images of cellular distribution of SRR immunoreactivity in the hippocapmpus and surrounding structures. Images show mouse sections. (A) Low power image of SRR immunoreactivity particularly localized in cortical and white matter regions surrounding the hippocampus such as the retrosplenial cortex and corpus callosum. (B) High power image of SRR immunoreactivity demonstrating the moderate labelling of cortical pyramidal neurons (asterix) and intense labelling of putative glia (arrowheads) in inferior layers of the retrosplenial cortex. Cells of a similar size to these are demonstrated in the corpus callosum (arrow), often seen in rows (inset). (C) Representative high power image of the hippocampal formation showing immunonegative granule cells of the dentate gyrus and scattered round immunopositive cells throughout the stratum moleculare (arrows). Sometimes granule cells of the dentate gyrus were moderately immunostained (inset). (D) No primary control for SRR in the hippocampus. (E) NeuN immunolabelling in the hippocampus demonstrating immunoreactive neurons in the dentate gyrus, stratum pyramidale and scattered cells in the stratum moleculare. Inset shows GAD67 immunolabelling of similarly sized cells in the stratum moleculare. hc = hippocampal formation; rsc = retrosplenial cortex; cc = corpus callosum; sm = strata moleculare; dg = dentate gyrus; sp = strata pyramidale. Scale bars: A = 0.5mm, B-E, 50µm.

visualized, sometimes in rows (Figure 2.5 B inset), a pattern reported for oligodendrocytes (Hof *et al*., 2003). In the hippocampal formation, immunostaining was limited to scattered round cells throughout the moleculare, oriens and lacunosum/radiatum (Figure 2.5 C) and occasional mild to moderate labelling of dentate gyrus granule cells (Figure 2.5 C inset).

NeuN immunolabelling in adjacent hippocampal sections revealed immunolabelling of dentate gyrus and stratum pyramidale neurons and scattered immunolabelled cells in the moleculare, oriens and lacunosum/radiatum strata (Figure 2.5 E) similar in shape and size to those immunolabelled by GAD67 (Figure 2.5 E inset). Since these were larger than the SRR immunoreactive cells in the same strata (Figure 2.5 C), it suggests the SRR immunoreactive cells are glia rather than interneurons characteristic of these strata.

2.3.4 Regional and cellular expression of SRR in the SN and VTA

SRR immunoreactive small round cells were visualized scattered throughout the substantia nigra pars reticulata (SNr) and pars compacta (SNc) and the VTA of the rat brain (Figure 2.6 A). In the neighbouring cerebral peduncle, intense immunolabelling of cells with irregular morphologies was visualized (Figure 2.6 A inset). Since this region did not stain for NeuN (Figure 2.6 B), these SRR positive cells are putative glia, and, given their irregular morphologies, may be putative stellate astrocytes. The NeuN stained cells in the SNc and SNr (Figure 2.6 B) did not morphologically resemble those stained for SRR in these regions, suggesting SRR positive cells in the SNc and SNr are putative glia (Figure 2.6 A).

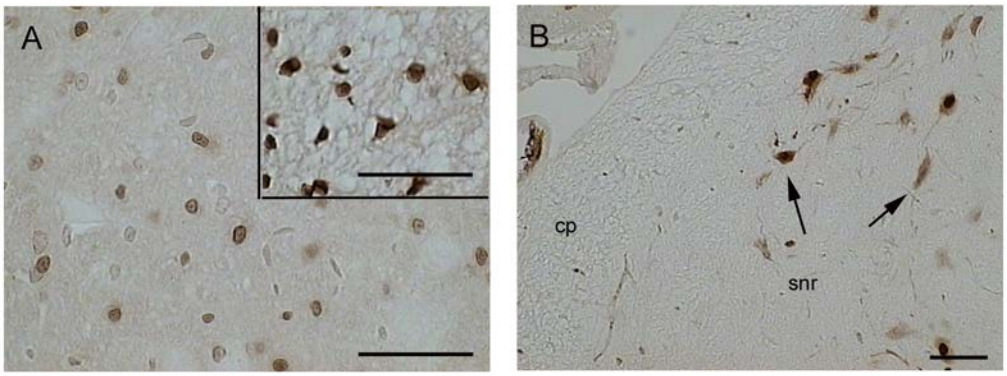

FIGURE 2-6 SRR immunoreactivity at the level of the SN and VTA in rat brain. (A) Representative high power image of SRR immunopositive round cells throughout the SNr. In the neighbouring cerebral peduncle (inset) cells with irregular morphologies were intensely immunolabelled. (B) NeuN immunolabelling in the SNr and neighbouring cerebral peduncle demonstrating scattered immunoreactive neurons in the substantia nigra pars reticulata (arrows) but no staining in the cerebral peduncle. cp = cerebral peduncle; snr = substantia nigra pars reticulata. Scale bars: A-B = 50μm.

2.3.5 Regional and cellular expression of SRR in the cerebellum

In both rat and mouse cerebellum, SRR immunoreactivity localized to granule and Purkinje cell layers and white matter (Figure 2.7 A). White matter demonstrated intense labelling of numerous cells often with irregular morphologies (Figure 2.7 B). In the granule cell layer, similar cells were strongly immunopositive (Figure 2.7 B). In Purkinje cell layers, occasional Purkinje cells were moderately immunoreactive (Figure 2.7 C) and concentrated to particular folia or particular regions within folia (Figure 2.7 C inset). Strong immunostaining of occasional scattered small round cells between Purkinje cells, putative Bergmann glia based on their location and morphology, was also observed (Figure 2.7 C).

NeuN labelling in adjacent sections demonstrated stained granule cells and immunonegative white matter (Figure 2.7 E). This suggests that white matter SRR-positive cells are glia. GFAP immunolabelling revealed stellate astrocytes in the granule cell layer (Figure 2.7 B top inset) and white matter (Figure 2.7 B lower

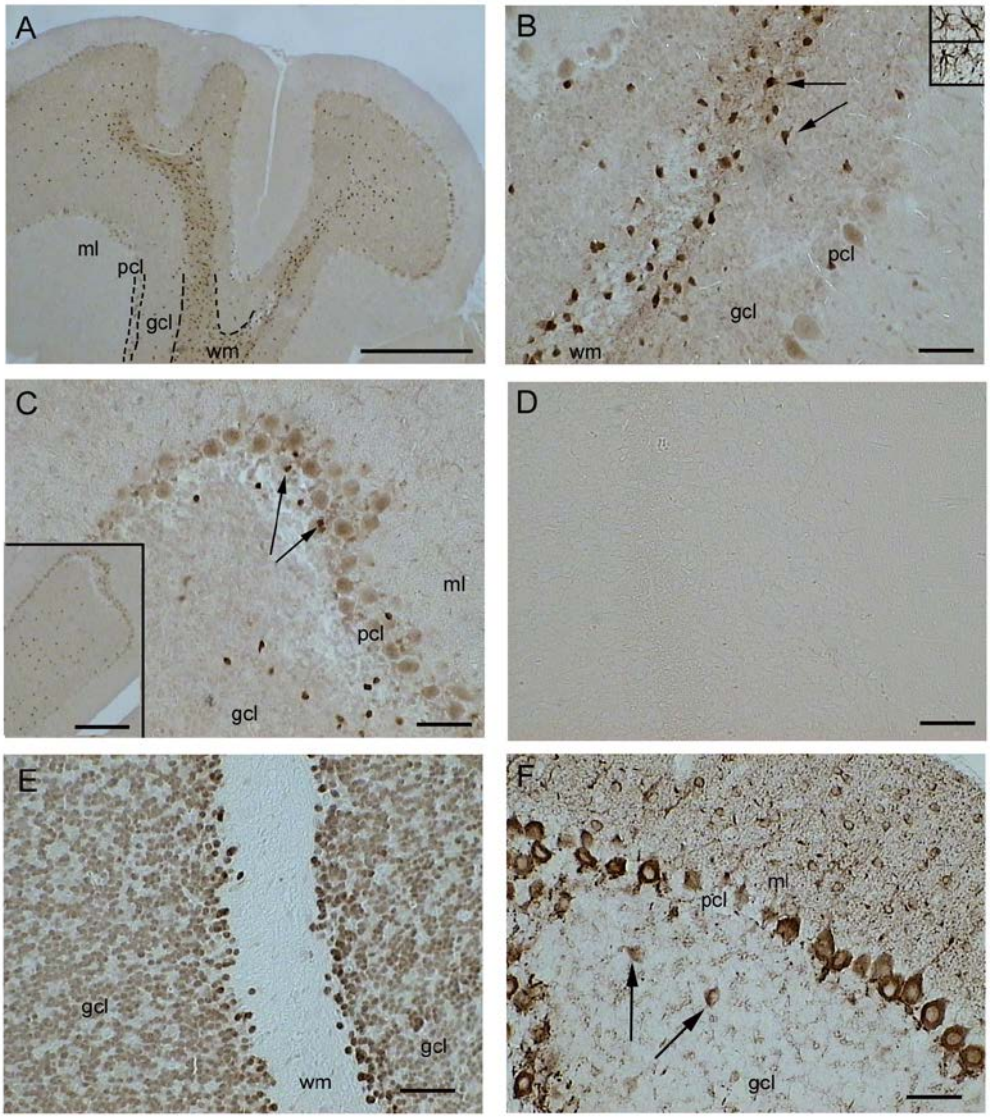

FIGURE 2-7 Representative images of the cellular distribution of SRR immunoreactivity in the cerebellum. Images show mouse sections. (A) Low power image demonstrating SRR immunoreactivity localized predominantly to white matter and granule cell and Purkinje cell layers. (B) High power image demonstrating intense immunolabelling of numerous cells in the white matter and of cells of a similar shape and size in the granule cell layer (arrows). Top inset shows GFAP immunolabelled cells in the granule cell layer. Lower inset shows GFAP immunolabelled cells in the white matter. (C) High power image demonstrating moderate immunolabelling of Purkinje cells. Immunostained Purkinje cells were often concentrated within a folia or particular regions of a folia (inset). Intense immunolabelling of occasional and scattered putative Bergmann glia within the Purkinje cell layer is also shown (arrows). (D) No primary control for SRR in the cerebellum. (E) NeuN immunolabelling in the granule cell layer and white matter of cerebellum. (F) GAD67 immunolabelling in the cerebellum localized to large cells in the granule cell layer (arrows). ml = molecular layer; pcl = Purkinje cell layer; gcl = granule cell layer; wm = white matter; igl = internal granule cell layer. Scale bars: A, C inset = 0.5mm; B-F = 50µm.

inset) with irregularly shaped cell bodies, similar in size and morphology to those immunoreactive for SRR in the same layers (Figure 2.7 B). This suggests SRR immunoreactive glia in the granule cell layer and white matter may be stellate astrocytes. Granule cell layer SRR-reactive cells are unlikely to be Golgi interneurons since GAD67 labelled larger cells in this layer (Figure 2.7 F).

2.3.6 Regional and cellular expression of DAO in the frontal cortex

In both rat and mouse frontal cortex, DAO immunoreactivity was widespread throughout cortical regions although more intense immunoreactivity localized to particular regions such as the prelimbic and cingulate cortices (Figure 2.8 A). Within the cortex pyramidal neurons were immunolabelled, often most prominently in layers II/III (Figure 2.8 B), and sometimes with a punctate appearance (Figure 2.8 C). Inferior cortical layers demonstrated mild pyramidal neuron labelling and intense immunolabelling of small round cells (Figure 2.8 D), which, based on NeuN and GAD67 immunolabelling (see above; Figure 2.4 E-F), are putatively glia.

2.3.7 Regional and cellular expression of DAO in the hippocampus and surrounding structures

At the level of the hippocampus and surrounding structures, DAO immunoreactivity predominantly localized to white matter (Figure 2.9 A). This immunostaining was attributable to punctate immunostaining and labelling of small round cells (Figure 2.9 B), putatively glia. In the retrosplenial cortex, labelled pyramidal neurons were clustered (Figure 2.9 C). In the hippocampal formation, immunoreactivity was limited to scattered moderately immunolabelled small round cells in the moleculare, radiatum/lacunosum and oriens strata (Figure 2.9 D). Their

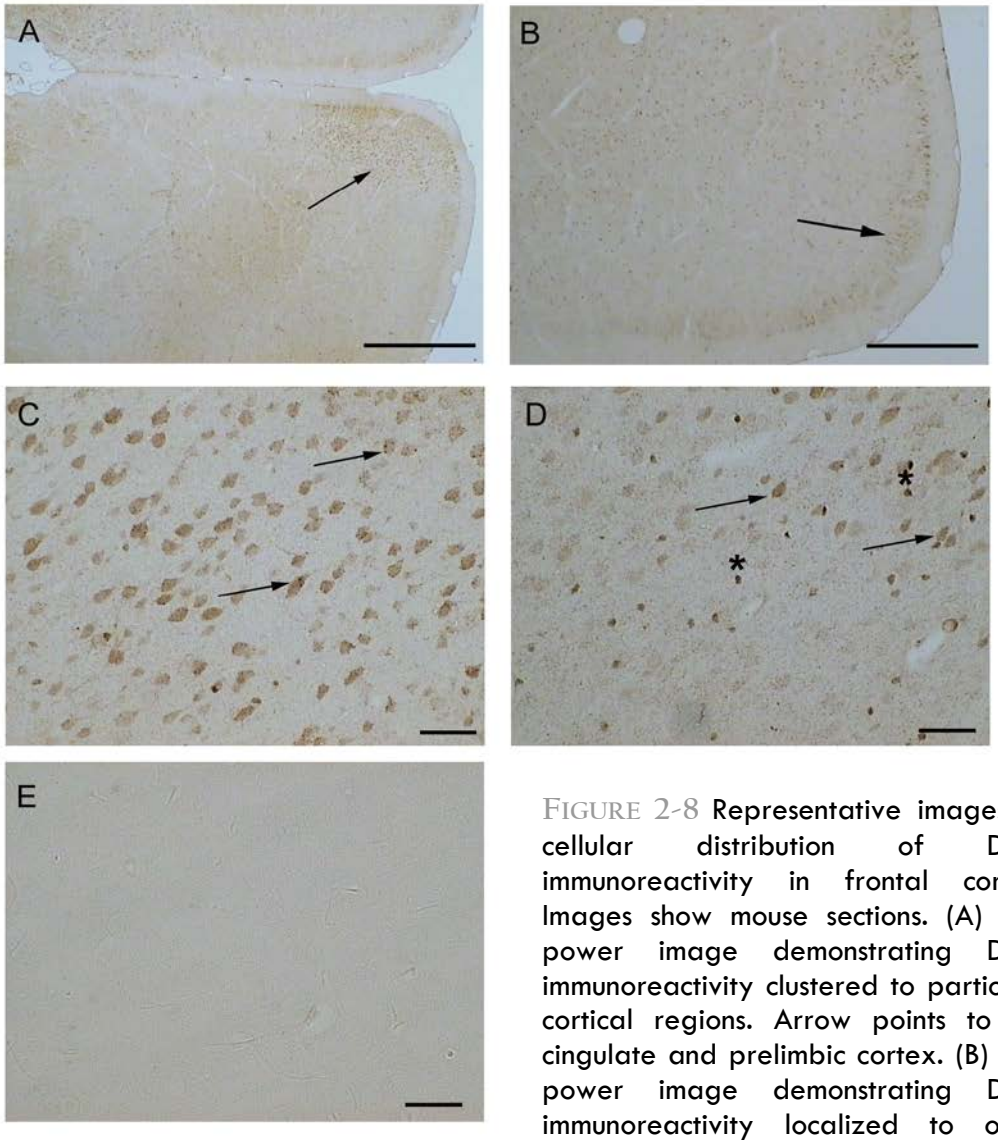

FIGURE 2-8 Representative images of cellular distribution of DAO immunoreactivity in frontal cortex. Images show mouse sections. (A) Low power image demonstrating DAO immunoreactivity clustered to particular cortical regions. Arrow points to the cingulate and prelimbic cortex. (B) Low power image demonstrating DAO immunoreactivity localized to outer cortical layers, particularly layers II/III (arrow). (C) High power image showing DAO immunoreactivity localized to pyramidal neurons. Staining within neurons was sometimes punctate (arrows). (D) High power image of inferior cortical layers demonstrating immunolabelled putative glia (asterix) and pyramidal neurons (arrows). (E) Pre-adsorption control for DAO in mouse frontal cortex. Scale bars: A = 0.5mm; B = 1mm; C-E = 50µm.

morphology is unlike that of cells immunoreactive for NeuN and GAD67 in these strata (see Figure 2.5 E), suggesting the SRR immunopositive cells in the moleculare, radiatum/lacunosum and oriens strata are putative glia.

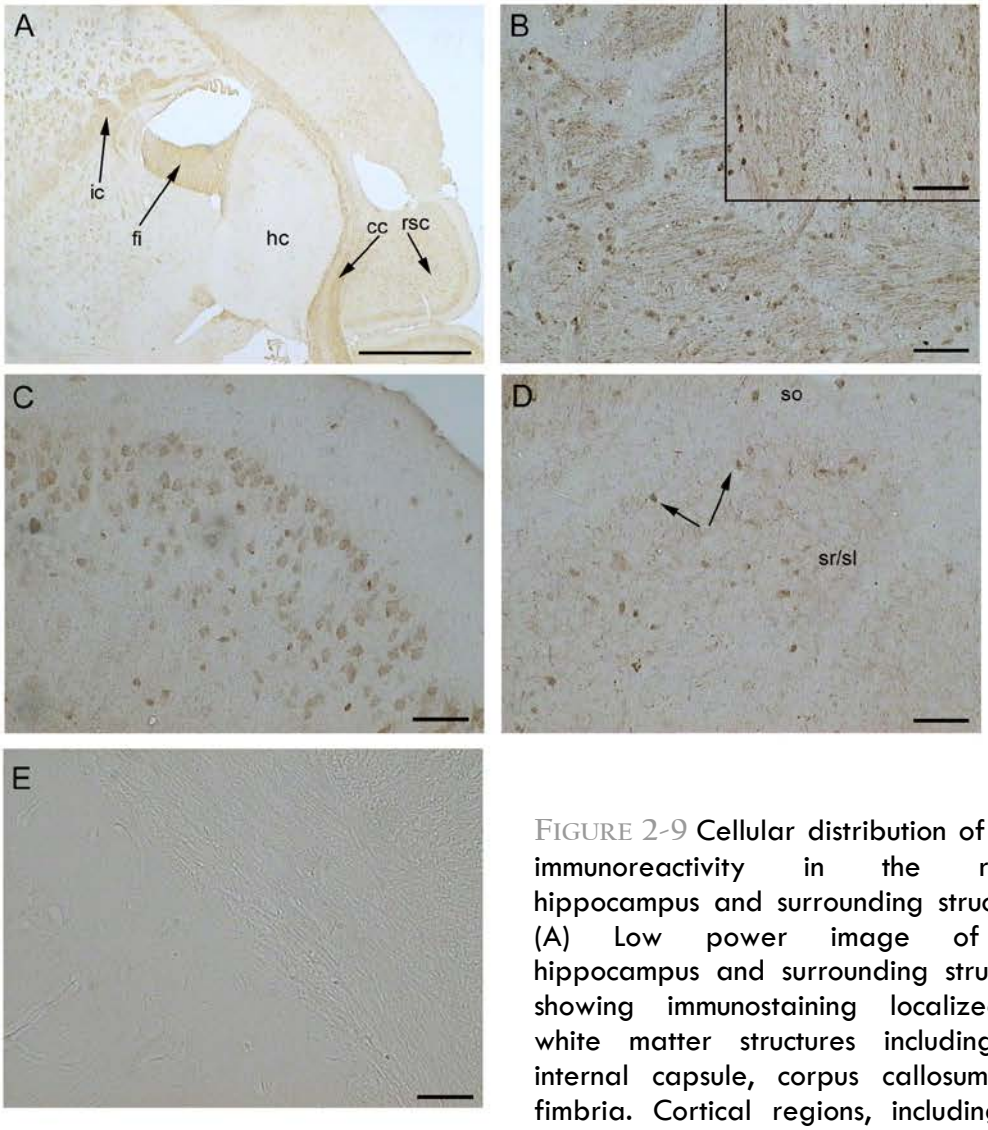

FIGURE 2-9 Cellular distribution of DAO immunoreactivity in the rodent hippocampus and surrounding structures. (A) Low power image of the hippocampus and surrounding structures showing immunostaining localized to white matter structures including the internal capsule, corpus callosum and fimbria. Cortical regions, including the retrosplenial cortex were also immunolabelled. The hippocampal formation was largely unstained. (B) High power image of DAO immunoreactivity in the internal capsule (main picture) and corpus callosum (inset) as punctate immunostaining and localized to small round cells. (C) High power image of DAO immunoreactivity localized to neurons in the retrosplenial cortex. (D) High power image showing DAO immunostaining in the stratum oriens, pyramidale and radiatum limited to moderate labelling of scattered small round cells (arrows). (E) Pre-adsorption control. ic = internal capsule; fi = fimbria; hc = hippocampal formation; cc = corpus callosum; rsc = retrosplenial cortex; so = stratum oriens; sr/sl = stratum radiatum/lacunosum. Scale bars: A = 0.5mm; B-E = 50µm.

2.3.8 Regional and cellular expression of DAO in the SN and VTA

DAO immunoreactivity localized to small round putative glia scattered throughout the SN, cerebral peduncle and VTA of the rat brain (Figure 2.10). DAO-positive

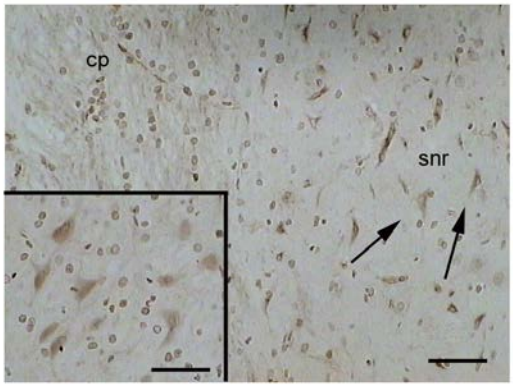

FIGURE 2-10 Representative image of DAO immunoreactivity at the level of the SN, VTA and cerebral peduncle of the rat brain. Immunoreactivity localized to numerous small round cells within these structures. Moderately immunolabelled neurons (arrows) were also visualized in the SN. In the VTA, moderately immunolabelled neurons were more abundant (shown in inset). cp; cerebral peduncle, snr; substantia nigra pars reticulata. Scale bars = 50μm.

cells visualized in the cerebral peduncle were sometimes visualized in rows, suggestive of oligodendrocytes (Hof *et al*, 2003). Scattered moderately DAO immunoreactive neurons were visualized in the SNr and SNc (Figure 2.10 arrows) and most abundantly in the VTA (Figure 2.10 inset).

2.3.9 Regional and cellular expression of DAO in the cerebellum

In adult mouse cerebellum, DAO immunoreactivity predominantly localized to granule and Purkinje cell layers and white matter with limited immunoreactivity in the molecular layer (Figure 2.11 A). Within the Purkinje cell layer, occasional scattered immunopositive putative Bergmann glia were visible (Figure 2.11 B). In this layer, Purkinje cell bodies were frequently immunostained, some more strongly than others (Figure 2.11 B), and often demonstrated peri-cellular rings of immunostaining (Figure 2.11 B inset).

The granule cell layer demonstrated scattered moderately DAO immunoreactive small round cells (Figure 2.11 C), similar to those labelled by SRR (see Figure 2.7 B, C) and GFAP (see Figure 2.7 B top inset) in this layer, and thus are putative glia. The cerebellar white matter demonstrated punctate DAO

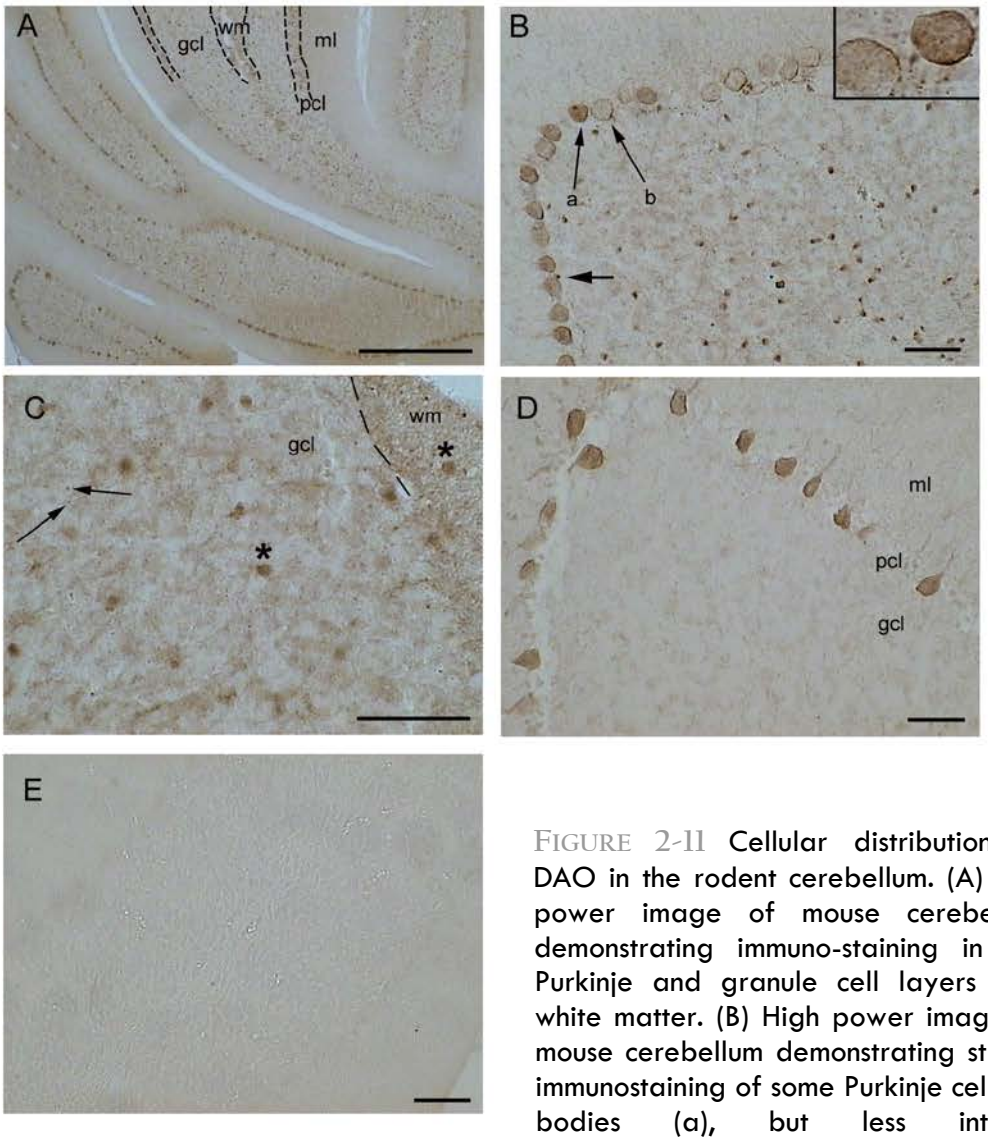

FIGURE 2-11 Cellular distribution of DAO in the rodent cerebellum. (A) Low power image of mouse cerebellum demonstrating immuno-staining in the Purkinje and granule cell layers and white matter. (B) High power image of mouse cerebellum demonstrating strong immunostaining of some Purkinje cell cell bodies (a), but less intense immunostaining in others (b); both sometimes demonstrated a peri-cellular ring of immunostaining (inset). Occasional and scattered immunoreactive putative Bergmann glia were sometimes visualized (arrow). (C) Mouse cerebellar granule cell layer and white matter demonstrating immunolabelling of small round cells (asterix) and white matter fibre staining. Punctate dots of immunoreactivity (arrows) could also be seen in all layers. (D) High power image of DAO immunoreactivity in the rat cerebellum localized to Purkinje cells and their processes but little immunoreactivity in the granule cell and molecular layers. (E) Pre-adsorption control. gcl = granule cell layer; wm = white matter; ml = molecular layer; pcl = Purkinje cell layer; igl = internal granule cell layer. Scale bars: A = 0.5mm; B-F = 50µm.

immunostaining and scattered moderately immunolabelled small rounded cells (Figure 2.11 C) unlabelled by NeuN in adjacent sections (see Figure 2.7 E) and thus putative glia. In the rat cerebellum, immunostaining of some Purkinje cells,

sometimes with punctate peri-cellular enhancement, consistent with observations in mice, was observed. However, the rat cerebellum demonstrated limited immunostaining in the granule cell layer (Figure 2.11 D) or white matter (data not shown).

2.4 DISCUSSION

2.4.1 Detection of SRR and DAO in the rat and mouse brain

In this study a commercial antibody to SRR and a novel GSK-DAO antibody against a human DAO peptide sequence were used. The SRR antibody detected a single band of predicted molecular weight in rat, mouse and human brain extracts (Figure 2.2) and detected SRR by immunohistochemistry in all regions of the rat and mouse brain studied (Figures 2.4 - 2.7).

The GSK-DAO antibody detected a band of predicted molecular weight in rat (Figure 2.3 C, Lane 2), mouse (data not shown) and human (Figure 2.3 C, Lane 1) cerebellum using western blotting. However, DAO could not be detected in the rat frontal cortex using this technique (data not shown), despite that the antibody worked reliably for immunohistochemistry in all areas examined in rat (and mouse) brain (Figures 2.8 - 2.11). The antibody's specificity for DAO is not questioned by this discrepancy, since pre-adsorption control in the cerebellum (Figure 2.3 C, Lane 4) demonstrated specificity of the immunoreactive band detected in this region. The phenomena was also seen for human tissue (discussed in Chapter 3, Section 3.4.1), where detection of DAO in the DPFC by western blotting was variable (Figure 2.3 D) but was robust with immunohistochemistry. A likely explanation for the disparity is that a regional difference in the antigenicity of DAO, possibly consequent to differences in post-translational modification or conformation, is differentially affected by western blotting and immunohistochemical protocols. That Almond *et al.*, (2006) could detect cortical DAO by western blotting in the mouse cortex, may therefore be due to their antibody, different to ours, being less susceptible to differences in DAO antigenicity.

TABLE 2-1 Qualitative summary of regional SRR and DAO immunohistochemistry in the rat and mouse brain and putative cellular expression.

	DAO	SRR
Cortical regions		
[Including frontal association, orbital, piriform, prelimbic, cingulate, motor, retrosplenial]		
Superficial layer pyramidal neurons	+++	+++
Superficial layer glia	+	+
Inferior layer pyramidal neurons	+	+
Inferior layer glia	+++	+++
White matter		
[Corpus callosum, internal capsule, fimbria]		
Non-stellate glia	++	++
Stellate glia	0	0
[Cerebral peduncle]		
Non-stellate glia	++	0
Stellate glia	0	+++
Hippocampal formation		
Dentate gyrus granule cells	0	0/+
Oriens, lacunosum/radiatum, moleculare strata		
Interneurons	0	0
Glia	++	+++
Midbrain		
SNc		
Neurons	+	0
Glia	++	++
SNr		
Neurons	+	0
Glia	++	++
VTA		
Neurons	++	0
Glia	++	++
Cerebellum		
Molecular layer	0	0
Purkinje cell layer		
Purkinje cells	0/++	0/++
Bergmann glia	++ (rat 0)	++ (rat 0)
Granule cell layer		
Granule cells	0	0
Golgi cells	0	0
Glia	++ (rat 0)	+++ (rat 0)
White matter		
Glia	++ (rat 0)	+++ (rat 0)

Immunoreactivity: 0, absent, +, mild-moderate, ++, moderate, +++, strong.

2.4.2 Regional and cellular distribution of SRR and DAO in the rat and mouse cerebral cortex

SRR immunoreactivity was detected in the rat and mouse cortex (summarised in Table 2.1) consistent with previous reports (Wolosker *et al.*, 1999b; Wang & Zhu, 2003; Yoshikawa *et al.*, 2004, 2005; Kartvelishvily *et al.*, 2006; Takeyama *et al.*, 2006; Hashimoto *et al.*, 2007b). At the cellular level, SRR immunoreactivity localized to pyramidal neuron cell bodies and their apical dendrites (Figure 2.4 B, C), most apparent in superficial cortical layers, particularly layers II/III (Figure 2.4 A). Inferior cortical layers on the other hand, demonstrated mild neuronal immunoreactivity with strong immunoreactivity localized to putative GFAP-negative glia.

These findings are discordant with Wolosker *et al.* (1999b) who described an enrichment of SRR to cortical grey matter GFAP-reactive astrocytes and no neuronal expression (Wolosker et al., 1999b). The SRR immunoreactive glia seen here were rounded, unlike the stellate GFAP-reactive glia of adjacent sections (Figure 2.4 G), and might therefore represent GFAP-negative glia, more typical of grey matter (Miller & Raff, 1984), oligodendrocytes or microglia (Wu *et al.*, 2004). The potential discrepancy in SRR reactive glial sub-types between the present findings and those of Wolosker *et al.* (1999b) may arise from methodological differences, for example the different SRR antibodies and tissue preparation used. However, this should be viewed tentatively, given that co-localization studies were not carried out.

The second inconsistency concerns neuronal SRR immunoreactivity. However, although Wolosker *et al.* (1999b) did not report neuronal SRR immunohistochemically in the rat brain, they did demonstrate low levels of SRR by

western blotting in rat primary neuron cultures. Moreover, others report equivalent levels of SRR mRNA and protein in rat neuronal versus glial cultures (Kartvelishvily *et al.*, 2006; Yoshikawa *et al.*, 2006) and SRR mRNA in rat brain neurons (Yoshikawa *et al.*, 2007). Consistent with this, and in agreement with our data, the Allen Brain Atlas demonstrates SRR mRNA localized to cortical neurons of the mouse brain, especially prominent in layer II (Allen Institute for Brain Science, 2008), while Kartvelishvily *et al.* (2006) reported SRR immunohistochemistry localized to pyramidal neuron cell bodies and apical dendrites of the rat brain. They also demonstrated SRR immunoreactivity localized to small round cells reminiscent of the SRR immunoreactive putative glia seen here in inferior layers.

Taken together, these findings provide evidence for a neuronal localization of SRR in the cortex, in addition to previous evidence of a glial localization. These findings therefore give credence to an emerging picture of both neuronal and glial SRR expression, and thence D-serine synthesis (Yasuda *et al.*, 2001; Kartvelishvily *et al.*, 2006; Puyal *et al.*, 2006; Williams *et al.*, 2006 and reviewed in Wolosker *et al.*, 2006). This contrasts with early and widely cited accounts of both SRR and D-serine's exclusive astrocytic localization (Wolosker *et al.*, 1999b; Schell *et al.*, 1995, 1997) and the emphasis on glial D-serine synthesis in several literature reviews (Snyder & Kim, 2000; Wolosker *et al.*, 2002; Schell, 2004; Miller, 2004). The demonstration of cortical neuronal SRR is consistent however with an early, but less widely cited report, of D-serine in purified synaptosomes (Wood *et al.*, 1996) and with recent D-serine immunohistochemical findings; for example, D-serine immunoreactivity has been localized to subsets of neurons in the mouse brainstem (Puyal *et al.*, 2006; Williams *et al.*, 2006). Moreover, others have localized D-serine

immunoreactivity to the cell bodies and apical dendrites of rat cortical pyramidal neurons (Yasuda *et al.*, 2001; Kartvelishvily *et al.*, 2006) consistent with localization of SRR in the present study. In addition, Kartvelishvily *et al.* (2006) replicated this latter finding using the antibody of Schell *et al.* (1995, 1997), suggesting that the early report of an exclusively glial localization of D-serine from these authors may be inaccurate.

The demonstration of SRR and D-serine in cortical neurons is pertinent to the distribution of the D-serine transporter, Asc-1. Asc-1 immunoreactivity was found to be exclusively neuronal in the rat brain and localize to cell bodies and apical dendrites (Helboe *et al.*, 2003; Matsuo *et al.*, 2004). Given the demonstration of neuronal D-serine release (Kartvelishvily *et al.*, 2006), together these results suggest that cortical pyramidal neurons can synthesize, release and re-uptake D-serine. Furthermore, based on the localization of DAO, discussed below, these cells may also possess the means to breakdown D-serine.

In both rat and mouse cortex, punctate DAO immunoreactivity was demonstrated in pyramidal neurons, predominantly in layers II/III (Figure 2.8 B, C). Inferior layers demonstrated immunolabelling of putative glial cells (Figure 2.8 D). These did not have the appearance of GFAP-reactive glia (Figure 2.4 G) and may therefore be of another glial sub-type such microglia, shown to express DAO mRNA (Urai *et al.*, 2002), oligodendrocytes or GFAP-negative astrocytes. DAO immunoreactivity was also sometimes observed to be particularly clustered in cortical regions, for example in the retrosplenial cortex (Figure 2.9 C). Of note, a similar regional predominance has also been reported for Asc-1 expression (Helboe *et al.*, 2003).

These findings are consistent with the detection of low levels of DAO mRNA in the rat and mouse cortex (Yoshikawa *et al*., 2004, 2005; Takeyama *et al*., 2006; Hashimoto *et al*., 2007b; Allen Institute for Brain Science, 2008) and DAO protein in the mouse (Almond *et al*., 2006) and rat (Moreno *et al*., 1999) frontal cortex. In agreement with our cellular findings, Moreno *et al*. (1999) described the enzyme immunohistochemically in cortical neurons. These authors also described interneuron DAO immunoreactivity in the cerebral cortex, which was not visualized here. This discrepancy may be due to methodological considerations, such as the antibodies used. It is important to note here that the antibody used by Moreno *et al*. (1999) was raised against a preparation of DAO shown subsequently to be contaminated by D-aspartate oxidase (DAspOx; Shleper *et al*., 2005). However, using an antibody to a peptide sequence of DAspOx, Zaar *et al*. (2002) do not report immunoreactivity in interneurons of the rat cortex, leaving DAO's localization therein equivocal.

However, despite the above reports of cortical DAO expression, *activity* has not been detected in the rodent cortex (Katagiri *et al*., 1991; Horiike *et al*., 1994; Schell *et al*., 1995; Wang & Zhu, 2003). Indeed, early reports which tried to describe DAO's cellular distribution on the basis of its activity with enzyme histochemistry led to a prevailing view that DAO is not in the cortex (Katagiri *et al*., 1991; Horiike *et al*., 1994; Schell *et al*., 1995). The expression of cortical DAO protein, but presumably therefore in a form of undetectable activity, is puzzling. One possibility is that inactive cortical DAO is a remnant from an earlier developmental function, although its continued robust expression would argue against this. Alternatively, cortical DAO may have a substrate other than D-serine, and/or catalyses a reaction not detected by commonly used activity assays. However, if this were the case, it

raises the question of how D-serine would be degraded in the cortex. Furthermore, while some reports show unchanged cortical D-serine levels in DAO mutant mice (Nagata *et al.*, 1994b; Morikawa *et al.*, 2001), others find a small but significant increase (Hashimoto *et al.*, 1993b). In addition, pharmacological inhibition of DAO has been shown to elevate cortical D-serine levels (Adage *et al.*, 2007) while others have detected DAO activity in cultured cortical astrocytes (Cristiano *et al.*, 2001). Together these findings suggest some endogenous DAO activity and regulation of D-serine levels may exist in the cortex, but perhaps commonly used activity assays may not be sensitive enough to detect it.

Overall, the distribution findings described suggest that DAO, SRR and D-serine may co-localize in the cortex to neurons and glia. Co-localization of DAO, SRR and D-serine has been reported in vestibular transitional cells (Dememes *et al.*, 2006) suggesting this is not unprecedented. However, the significance of such an arrangement is questionable, given that DAO, if active, could breakdown any D-serine synthesized by SRR. It is therefore noteworthy that DAO demonstrated a punctate pattern of immunostaining here, in keeping with its reported peroxisomal localization (Arnold *et al.*, 1979; Horiike *et al.*, 1987; Perotti *et al.*, 1987; Usuda *et al.*, 1986; Moreno *et al.*, 1999). Conversely, SRR was seen throughout the cytoplasm of cortical pyramidal neurons, in keeping with its concentration to the cytosolic fraction in subcellular fractionation studies (Wolosker *et al.*, 1999b; Kartvelishvily *et al.*, 2006). Therefore, these findings raise the possibility of spatially regulated D-serine metabolism within cortical neurons and glia.

2.4.2.1 Models of synaptic D-serine function in the rat and mouse cerebral cortex

Given early reports, widely cited, of SRR and D-serine's enrichment to grey matter cortical astrocytes (Schell *et al.* 1995, 1997; Wolosker *et al.* 1999b), a prevailing model of D-serine function at tripartate synapses has arisen: Activation of AMPA/Kainate receptors on astrocytes has been shown to cause SRR activation via GRIP (Kim *et al.*, 2005) and D-serine release (Schell *et al.*, 1995; Kim *et al.*, 2005), which may occur via ASCT2 transporters (Ribeiro *et al.*, 2002; Rutter *et al.*, 2007) or vesicular release (Mothet *et al.*, 2005), into the NMDAR bearing synapse ensheathed by the astrocyte (Figure 2.12). D-serine then acts in concert with neuronally released glutamate to activate post-synaptic NMDARs (for reviews see Snyder & Kim, 2000; Schell, 2004; Wolosker *et al.*, 2002; Miller, 2004; Martineau *et al.*, 2006a,b). The demonstration of SRR immunoreactivity localized predominantly to putative glia in inferior layers of the cerebral cortex in the present study is consistent with this model.

However, the results in the superficial layers of the cortex suggest a revision to the model is required. SRR and DAO immunoreactivity was demonstrated in cell bodies and apical dendrites of pyramidal neurons, particularly evident in layers II/III of the cortex. Kartvelishvily *et al.* (2006) have reported D-serine immunoreactivity localized to cortical neuron cell bodies and processes in all layers, while Asc-1 is reportedly expressed on neuronal cell bodies, apical dendrites and pre-synaptic terminals, predominantly in layers III and V (Helboe *et al.*, 2003; Matsuo *et al.*, 2004). Taken together therefore, this suggests SRR, DAO, D-serine and Asc-1 may co-localize in cortical neurons, particularly in layer III. Within this layer, post-synaptic NMDARs are predominantly localized to neuron cell bodies, as opposed to the apical dendrites of layer V/VI neurons (Currie *et al.*, 1994). Pre-

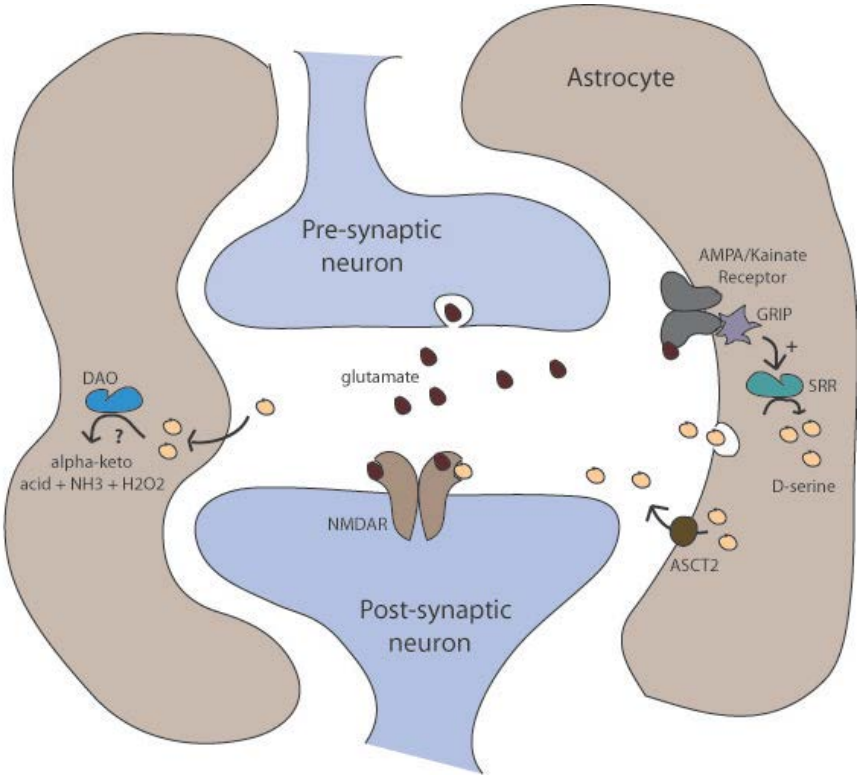

FIGURE 2-12 Astrocytic D-serine synthesis by SRR is stimulated in response to AMPA/Kainate receptor activation via GRIP. D-serine may be released via the ASCT2 transporter or through vesicular release into the NMDAR-bearing synapse to potentiate the effects of neuronally released glutamate. D-serine could then be re-uptaken into astrocytes for breakdown by DAO.

synaptic NMDARs in layer II/III of the cortex have also been demonstrated, activation of which increases glutamate release (DeBiasi *et al.*, 1996; Woodhall *et al.*, 2001). D-serine can potentiate both the responses in of pre- and post-synaptic layer II/III NMDARs (Ito & Hicks, 2001; Li & Han, 2007). In addition, D-serine can be released from neurons in a calcium-dependent manner in response to AMPA/Kainate and NMDAR stimulation (Kartvelishvily *et* al., 2006). Therefore a neuronal model of D-serine function can be described whereby D-serine is synthesized neuronally by SRR, released in response to glutamatergic inputs and then acts on post-synaptic NMDARs to potentiate NMDAR-mediated EPSPs and

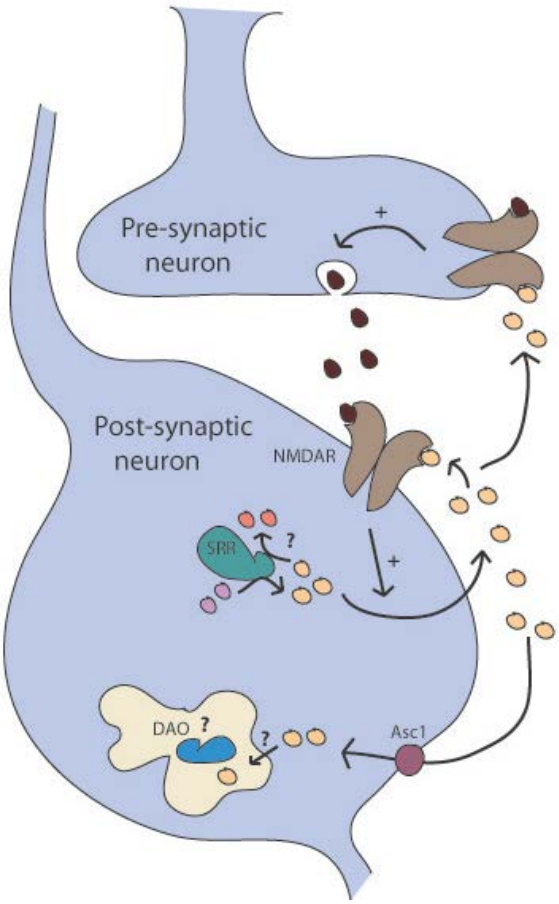

FIGURE 2-13 Neuronal D-serine synthesis, release, re-uptake and breakdown. D-serine (yellow circles) is synthesized by neuronal SRR from L-serine (pink circles) and may be released subsequent to NMDAR or AMPA/Kainate receptor stimulation. This may act on pre- or post-synaptic receptors to stimulate glutamate (brown circles) release or potentiate neuronal glutamate, respectively. The actions of D-serine may be terminated by Asc-1 re-uptake into neurons. Here peroxisomal DAO might break down D-serine, although a peroxisomal D-serine transporter is speculative. Alternatively SRR may catalyse an eliminase reaction of D-serine producing pyruvate and ammonia (orange circles).

release further D-serine, or acts on pre-synaptic NMDARs to stimulate glutamate release and consequently further D-serine release (Figure 2.13). In both scenarios, a positive feedback loop of NMDAR potentiation is initiated. Such a situation could conceivably function in NMDAR-dependent synaptic plasticity events. Indeed, Ito & Hicks (2001) have demonstrated that the co-agonist binding site of NMDARs is necessary for long term potentiation (LTP) expression in layers II/III of the visual cortex. Such a positive feedback loop of NMDAR stimulation could conceivably also have pathological consequences, and interestingly D-serine has been shown to contribute to NMDAR-mediated excitotoxicity in cortical neurons (Katsuki *et al.*, 2004; Kartvelishvily *et al.*, 2006).

The localization of Asc-1 (Helboe *et al.*, 2003; Matsuo *et al.*, 2004) and DAO (present study; Moreno *et al.*, 1999) to the same cortical layers and neuronal compartments as SRR and D-serine suggests that there is a mechanism whereby the actions of D-serine could then be terminated; D-serine could be re-uptaken by Asc-1 into the neuronal cell body and broken down by peroxisomal DAO (Figure 2.13). However, one should bear in mind the caveat of undetectable cortical DAO activity by some in the rat (Horiike *et al.*, 1994; Schell *et al.*, 1995) and the question of how else cortical D-serine may be degraded. In this regard it is worthy of note that SRR can perform an eliminase reaction, converting D-serine into pyruvate and ammonia (De Miranda *et al.*, 2000, Cook *et al.*, 2002; Neidle & Dunlop, 2002; Stříšovský *et al.*, 2003, 2005; Foltyn *et al.*, 2005). This reaction is proposed to occur physiologically (Foltyn *et al.*, 2005), suggesting a means whereby cellular milieu could control SRR activities depending on the requirements for D-serine. However others dispute the physiological relevance of SRR catalysed D-serine elimination (Stříšovský *et al.*, 2005) leaving the nature of termination of cortical D-serine activity ambiguous.

2.4.3 SRR and DAO distribution in the rat and mouse hippocampus, and surrounding structures and the rat SN and VTA

SRR immunoreactivity in the rat and mouse hippocampus, surrounding structures and SN and VTA (summarised in Table 2.1) localized predominantly to putative glia (Figures 2.5 and 2.6). Consistent with these findings, SRR has been previously been localized to glial cells in rat forebrain white matter (Wolosker *et al.*, 1999b) and stratum oriens (Kartvelishvily *et al.*, 2006). The predominance of glial staining in the hippocampus and surrounding structures contrasts with SRR

immunoreactivity in the cortex which was predominantly neuronal. In addition, staining appeared qualitatively less intense in the hippocampus and surrounding structures than in the cortex which could suggest a possible regional difference in the levels and cell types of SRR expression. However, SRR mRNA has been localized to the neuronal dentate gyrus and CA subfields of the mouse hippocampus, expressed at a level comparable to the cortex (Allen Institute for Brain Science, 2008) which could alternatively suggest our immunohistochemical detection of SRR was less sensitive in the hippocampus than in the cortex.

The putative SRR immunoreactive glia seen had a rounded morphology as opposed to the irregular morphologies characteristic of stellate astrocytes, except for in the cerebral peduncle. The arrangement of SRR immunoreactive putative glia in the corpus callosum in rows is reminiscent of the organization of oligodendrocytes (Hof *et al*., 2003), suggesting SRR positive glia may potentially be oligodendrocytic, as well as astrocytic or microglial (Wu *et al*., 2004).

DAO similarly localized to putative glia of the white matter (Figure 2.9 A, B), moleculare, radiatum/lacunosum and oriens in the hippocampal formation (Figure 2.9 D) and midbrain including the SN and VTA, consistent with low levels of DAO mRNA in these regions (Allen Institute for Brain Science' 2008). In the midbrain, especially the VTA, mildly immunolabelled neurons were also visualized (Figure 2.10). The DAO immunoreactive putative glia had rounded morphologies, not suggestive of stellate astrocytes. While their specific identity is speculative, the observation of DAO labelled glia in the cerebral peduncle in rows suggests that these may be oligodendrocytic (Hof *et al*., 2003).

These findings are discordant with those of Horiike *et al*., (1994) who reported absent DAO activity in the rat hippocampus, SN and cerebral peduncle

and localized enzyme activity to astrocytes only, not neurons or oligodendrocytes (Horiike *et al.*, 1994). The discrepancy is likely due to the different techniques utilised (immunohistochemistry and enzyme histochemistry) and perhaps the expression of DAO with undetectable activity (as discussed for the frontal cortex). Indeed, immunohistochemically DAO has been localized to glia of the corpus callosum, fimbria and cerebral peduncle and neurons of the VTA and SN (Moreno *et al.*, 1999) consistent with the present findings. However, these authors do not describe additional glial immunostaining in the VTA and SN, as is demonstrated here, and also report neuronal staining in the hippocampal formation, which was not seen here. Again, it is important to consider the potential cross-reactivity of the Moreno *et al.* (1999) antibody with DAspOx, itself expressed in hippocampal neurons (Zaar *et al.*, 2002).

Consistent with the findings of SRR and DAO distribution, D-serine immunoreactivity has been localized to astrocytes of the rat and mouse corpus callosum and in the rat hippocampal formation of the oriens, radiatum/lacunosum and moleculare strata (Schell *et al.*, 1995, 1997; Wolosker *et al.*, 1999b; Yasuda *et al.*, 2001; Dememes *et al.*, 2006; Williams *et al.*, 2006). This suggests that SRR, DAO and D-serine could be co-localized to glial cells in the hippocampal formation and surrounding white matter.

2.4.3.1 Functional implications in the hippocampal formation

In the hippocampal formation the localization of SRR (present study) and D-serine (Schell *et al.*, 1997; Dememes *et al.*, 2006; Williams *et al.*, 2006) predominantly to glial cells suggests that the D-amino acid may function at tripartate glutamatergic

synapses where glial DAO may be responsible for terminating the actions of released D-serine (Figure 2.12).

In agreement with this supposition, both exogenous and endogenous D-serine has been shown to facilitate NMDAR-dependent responses in hippocampal neurons (Thiels *et al.*, 1992; Watanabe *et al.*, 1992; Mothet *et al.*, 2000; Martina *et al.*, 2003; Krasteniakov *et al.*, 2005; Shleper *et al.*, 2005; Junjaud *et al.*, 2006; Sun *et al.*, 2007). Moreover, functional DAO in the hippocampus is suggested by enhanced hippocampal LTP and spatial learning in DAO mutant mice (Maekawa *et al.*, 2005). The glial origin of D-serine is potentially supported by the demonstration that D-serine rescues deficits in NMDAR-mediated synaptic plasticity induced by chronic lead exposure, a condition known to cause glial pathology (Sun *et al.*, 2007).

Within the hippocampus, SRR was localized to putative glia of the lacunosum/radiatum, moleculare and oriens strata. The moleculare, radiatum/lacunosum and oriens strata are characterised by the presence of interneurons (Duvernoy, 1998) such that glial released D-serine could act at glutamatergic inputs to this cell type. In agreement, Martina *et al.*, (2003) have demonstrated that D-serine enhances post-synaptic NMDAR-dependent responses in interneurons of the stratum radiatum.

2.4.3.2 Functional implications in the white matter

SRR and DAO both localized to putative glia in white matter regions. These had similar morphologies in some regions, such as the corpus callosum, where putative oligodendrocytes were labelled, and thus SRR and DAO could be co-localized. Presumably this is not the case in other regions, such as the cerebral peduncle

where SRR localized to putative stellate astrocytes and DAO to putative oligodendrocytes.

D-serine also shows pronounced localization to rat and mouse white matter (Schell *et al.*, 1997; Kartvelishvily *et al.*, 2006; Williams *et al.*, 2006). NMDAR expression by astrocytes and oligodendrocytes (Matute, 2006; Verkhratsky & Kirchhoff, 2007) presumably accounts for a requirement of D-serine metabolism in these regions. More specifically, the recent demonstration of vesicular glutamate release from axons in the white matter (Kukley *et al.*, 2007) might propound an involvement of D-serine in neuron-glial signalling (Figure 2.14). In addition, exocytic glutamate release from astrocytes (reviewed in Volterra & Meldolesi, 2005) suggests D-serine may potentiate NMDAR responses at glial-glial 'synapses'. For example, it is tempting to speculate this for astroglial-oligodendrocyte synapses (Verkhratsky & Kirchhoff, 2007) in the cerebral peduncle, where 'pre-synaptic' SRR containing astrocytes synthesize and release D-serine which is re-uptaken into the 'post-synaptic' oligodendrocyte for breakdown by DAO (Figure 2.14).

As well as possibly potentiating glutamate at NMDARs, the finding that glial NMDARs often comprise NR3 subunits (Verkhratsky & Kirchhoff, 2007), and that D-serine can antagonize a glycine-activated, glutamate-insensitive NR1/NR3 receptor (Chatterton *et al.*, 2002), may intimate a novel role of white matter D-serine (Figure 2.14).

However, despite established white matter NMDAR expression (Matute, 2006; Verkhratsky & Kirchhoff, 2007), presumably NMDAR-mediated responses are less widespread here than they are in the grey matter. Consequently others have suggested the predominance of white matter D-serine indicates a role for the D-

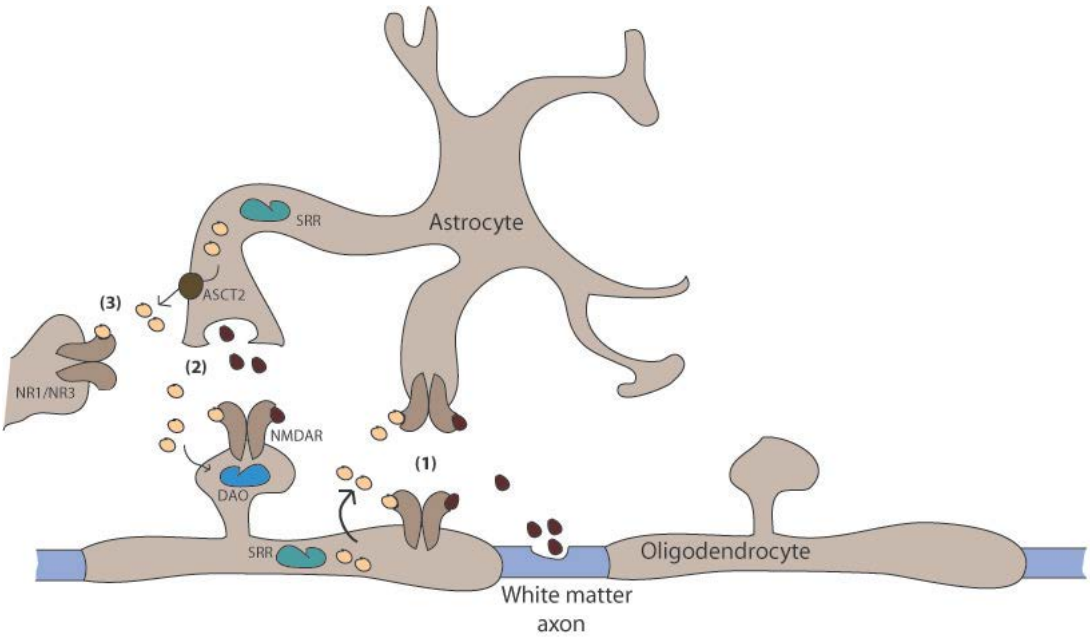

Figure 2-14 Potential D-serine metabolism and signalling in the white matter. (1) Neuronal-glial signalling; glial released D-serine (yellow circles) may act in concert with axonal glutamate release (brown circles) to activate astrocytic or oligodendrocytic NMDARs. (2) D-serine released from glia may act in concert with glutamate released exocytotically from astrocytes to activate glial NMDARs. ASCT2 D-serine transport has been demonstrated in astrocytes (Yamamoto *et al.,* 2004) while oligodendrocytic D-serine transport is speculative. DAO in oligodendrocytes could breakdown re-uptaken D-serine. (3) D-serine may also act without glutamate to antagonize glycine-activated NR1/NR3 receptors potentially expressed by glial cells.

amino acid, and thence its metabolism, in a process other than NMDAR activation (Williams *et al.*, 2006). One suggestion is a role in cellular energy requirements, given the ability of SRR to break down D-serine into pyruvate (Puyal *et al.*, 2006; Williams *et al.*, 2006).

2.4.3.3 Functional implications in the substantia nigra and ventral tegmental area

DAO and SRR localized to scattered putative glia in the midbrain, including the SNr, SNc and VTA. DAO also localized to scattered neurons in these regions, especially in the VTA. NMDARs are expressed on midbrain neurons (Ong *et al.*,1997;

Tse & Yung, 2000) which regulate their intra-cellular calcium levels and firing rates (Bennet & Gronier, 2007; Choi *et al*., 2003; Fernandez-Espejo *et al*., 2007). A role of D-serine at these receptors is suggested by the demonstration that intra-VTA D-serine administration augmented the expression of behavioural sensitization to cocaine in the rat, an effect dependent on NMDARs (Fernandez- Espejo *et al*., 2007). Furthermore, intra-VTA administration of sodium benzoate, a DAO inhibitor, had the same effect, suggesting that *endogenous* DAO and D-serine are active in the VTA (Fernandez-Espejo *et al*., 2007) consistent with our demonstration of SRR and DAO immunoreactivity in this region.

Since SRR was localized to glial cells in the rat SN and VTA, D-serine is presumably acting at tripartate synapses and could potentially affect the glutamatergic subthalamic nucleus inputs to GABAergic SNr neurons and dopaminergic SNc neurons (Chang *et al*., 1984; Bevan *et al*., 1994), and the prefrontal cortical and subcortical glutamatergic projections to dopaminergic and GABAergic VTA neurons (reviewed in Sesack *et al*., 2003). D-serine may be then re-uptaken into DAO expressing glia for breakdown, or in some cases perhaps, particularly in the VTA, into neurons, potentially GABAergic or dopaminergic. Mild Asc-1 immunoreactivity in the SN (Helboe *et al*., 2003) supports this possibility.

The speculated role of DAO above in D-serine breakdown and regulation of glutamatergic inputs to midbrain neurons could potentially affect either the dopaminergic or GABAergic neurons which exist in the mesencephalon. A demonstrable role, however, for DAO in *dopaminergic* neurons can be inferred. The enzyme has been shown to oxidise D-DOPA, an exogenously administered precursor to an alternative pathway of dopamine synthesis (Moses *et al*., 1996; Wu *et al*., 2006; Kawazoe *et al*., 2007) and DAO inhibition prevents D-DOPAs

ameliorative effects in Parkinsonian animals suggesting the enzyme's expression in cells expressing Dopa decarboxylase (i.e. dopaminergic cells) . While the presence of endogenous D-DOPA or other D-isomers of catecholamine precursors in mammals is, to our knowledge, unknown, DAO expression in these neurons allows conjecture that the enzyme could function in dopamine synthesis or breakdown.

2.4.4 SRR and DAO distribution in the rat and mouse cerebellum

SRR immunoreactivity was detected in the rat and mouse cerebellum (summarised in Table 2.1) qualitatively as robustly as in the cortex. Previous studies of cerebellar SRR have been conflicting. Wang & Zhu, (2003) could not detect SRR by western blotting in adult mouse cerebellum but could in the cortex. Consistent with this, high levels of HPLC measured D-serine are reported in the cortex with low or negligible levels in cerebellum (Nagata *et al*., 1992, 1994a; Hashimoto *et al*., 1993a,b,c, 1995a, b; Hamase *et al*., 1997; Morikawa *et al*., 2001; Wang & Zhu, 2003). However others have robustly detected cerebellar SRR mRNA (Yoshikawa *et al*., 2004, 2005; Takeyama *et al*., 2006; Hashimoto *et al*., 2007), at comparable levels as cortical SRR mRNA expression (Allen Institute for Brain Science, 2008) as well as localized sources of D-serine immunoreactivity (Schell *et al*., 1997; Wolosker *et al*., 1999b; Dememes *et al*., 2006; Williams *et al*., 2006). Moreover, intracerebroventricular administration of L-serine was shown to increase cerebellar D-serine levels in the rat cerebellum (Hashimoto, 2002), implying both SRR's presence and activity.

At the cellular level, immunolabelling was observed in putative glia in the rat and mouse cerebellum. Astrocytes of the cerebellar cortex are classified into three types; bushy stellate astrocytes, smooth astrocytes and Bergmann glial cells (Yamada & Watanabe, 2002). SRR localized to white matter and granule cell layer

glia (Figure 2.7 B) often with irregular morphologies, and therefore suggestive of stellate astrocytes. SRR also localized to occasional scattered Bergmann glia of the Purkinje cell layer (Figure 2.7 C). These results are consistent with previous demonstrations of both SRR and D-serine immunoreactivity in rat granule cell layer stellate astrocytes and Bergmann glia in the rat (Schell *et al.*, 1997; Wolosker *et al.*, 1999b; Dememes *et al.*, 2006; Williams *et al.*, 2006). Speculatively, the presence of D-serine at such localized sources could account for previous HPLC analyses of D-serine levels in homogenates of the whole cerebellum being low or negative (Nagata, 1992, 1994a; Hamase *et al.*, 1997; Hashimoto *et al.*, 1995a,b; Hashimoto *et al.*, 2003; Wang & Zhu, 2003). However, this is not an entirely unifying explanation for SRR's presence in the rat cerebellum, as Kartvelishvily *et al.*, (2006) detected negligible cerebellar D-serine with immunohistochemistry therein.

SRR immunoreactivity also localized to particular Purkinje cells in the rat and mouse, clustered in particular regions of cerebellar folia (Figure 2.7 C). Purkinje cells originate from a small pool of precursors (Baader *et al.*, 1996; Larouche & Hawkes, 2006) which are then dispersed through the adult Purkinje cell layer. However, given that mixing is not complete (Baader *et al.*, 1996), the occurrence of clustered cells of the same or a few clonal origins, some which potentially express SRR and others which do not, is possible. The presence of Purkinje cell SRR concords with SRR mRNA localization therein (Allen Institute for Brain Science, 2008) but is in disagreement, however, with previous reports of cellular SRR (Wolosker *et al.*, 1999b) and D-serine localization (Kartvelishvily *et al.*, 2006; Wolosker *et al.*, 1999b; Williams *et al.*, 2006; Dememes *et al.*, 2006; Schell *et al.*, 1995, 1997).

Taken together, these data suggest that SRR and D-serine are present in the cerebellum of rats and mice and are found at localized sites, namely Bergmann glia and stellate glia of the granule cell layer and white matter. SRR might additionally be localized to some Purkinje cells.

The presence of cerebellar DAO is undisputed (Arnold *et al.*, 1979; Horiike *et al.*, 1987, 1994; Schell *et al.*, 1995; Moreno *et al.*, 1999; Urai *et al.*, 2002; Wang & Zhu, 2003) and herein it is known to regulate endogenous D-serine levels, as demonstrated by increased cerebellar D-serine in DAO mutant mice (Hashimoto *et al.*, 1993b; Morikawa *et al.*, 2001). Consistent with this, robust cerebellar DAO immunoreactivity in rats and mice was detected here.

At the cellular level, differences in DAO immunoreactivity between mice and rats were observed. In the mouse, DAO localized to rounded putative glia in the white matter and granule cell layer (Figure 2.11 C), suggestive of the smooth cerebellar astrocytes (Yamada & Watanabe, 2002), and to occasional scattered Bergmann glia (Figure 2.11 B). In the rat cerebellum however, limited glial DAO was observed. Previously, DAO has been localized to white matter and granule cell layer astrocytes and Bergmann glia in adult rats including Sprague-Dawleys as were used here (Arnold *et al.*, 1979; Horiike *et al.*, 1987, 1994; Moreno *et al.*, 1999). This is consistent with the mouse findings of the present study but not rat. The reasons for the difference observed between the mice and rats here, and between the present rat findings and those of previous reports, are unknown. Since the rat and mouse data were concordant in other regions examined, and since the mouse findings here corroborate previous rat findings, there may have been a technical limitation in the immunostaining carried out for DAO in these rat sections.

DAO, in both mouse and rat, localized to many Purkinje cells, while others were less strongly immunostained (Figure 2.11 B, D). This accords with Purkinje cell layer DAO mRNA in the mouse brain (Allen Institute for Brain Science, 2008). This pattern of DAO immunoreactivity of variable expression among Purkinje cells has been previously observed (Moreno *et al.*, 1999) and again is a precedented observation for Purkinje cells (Baader *et al.*, 1996; Larouche & Hawkes, 2006). A prominent peri-cellular ring of DAO immunoreactivity was often observed around Purkinje cells, both those immunopositive and those immunonegative (Figure 2.11 B inset). This may arise from immunoreactive Bergmann glial appendages, which thoroughly surround Purkinje cell somata (Yamada & Watanabe, 2002).

In the present study, DAO immunoreactivity in cells suggestive of Golgi cells was not seen, discordant with the observations of Moreno *et al.* (1999). This discrepancy may again be attributable to the Moreno *et al.* (1999) antibody's potential cross-reactivity with DAspOx (see above), itself abundantly expressed in Golgi cells of the rat cerebellum (Zaar *et al.*, 2002).

2.4.4.1 Functional implications in the cerebellum

Taken together, these data indicate that; 1) Some scattered Bergmann glia express SRR and DAO and they may contain D-serine; 2) stellate astrocytes of the granule cell layer and white matter robustly express SRR and may contain D-serine; 3) smooth astrocytes of the granule cell layer and white matter express DAO; and 4) some Purkinje cells may express SRR and DAO.

Functionally, D-serine synthesis and breakdown in granule cell layer glia may regulate glial released D-serine levels potentially acting at glutamatergic tripartate synapses (Figure 2.12), namely mossy fibre inputs to granule cells. In the

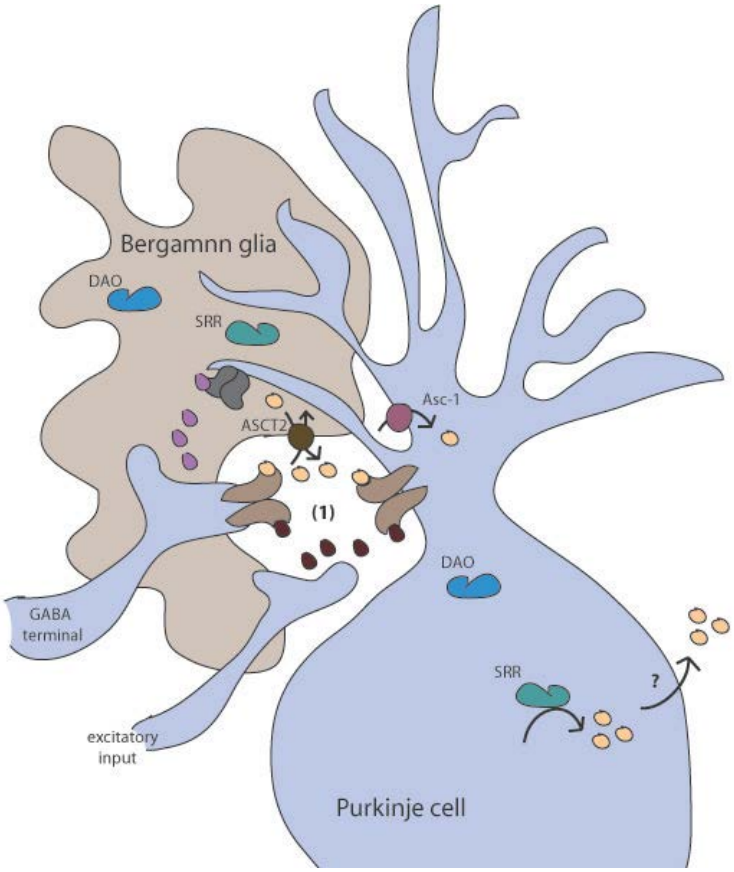

FIGURE 2-15 Potential D-serine metabolism and signalling in the cerebellum. (1) SRR in Bergmann glia may synthesize D-serine (yellow circles), released via ASCT2 which potentiates synaptic glutamate (brown circles) at post-synaptic or pre-synaptic NMDARs. Pre-synaptic NMDARs on GABA terminals regulate GABA release (pink circles). The actions of D-serine may be terminated by re-uptake into Purkinje cells by Asc-1 and breakdown by DAO. D-serine synthesis by Purkinje cell SRR and potential release is equivocal as D-serine has not been localized to these cells.

white matter, glial D-serine metabolism may have a role in regulating glial-glial or neuron-glial glutamatergic signalling, as described above (Section 2.4.3.2, Figure 2.14).

The localization of both SRR and DAO to some scattered Bergmann glia, which may also contain D-serine (Schell *et al.*, 1997, Williams *et al.*, 2006), is interesting as these cells enclose and regulate synapses onto Purkinje cells, the sole output of the cerebellar cortex (Cid & Ortega, 1993; Brockhaus & Deitmer, 2002; Huang & Bordey, 2004; Bellamy, 2006). Thus, Bergmann glial released D-serine may affect synaptic inputs to Purkinje cells, for example presynaptic NMDARs located on GABAergic interneurons that synapse onto Purkinje cells (Glitsch & Marty,

1999), or post-synaptic NMDARs receiving glutamatergic input from parallel and climbing fibres. Thus D-serine could modulate Purkinje cell miniature inhibitory post-synaptic potentials (IPSPs) and EPSPs and thence cerebellar long-term depression (LTD) and LTP which occurs at these synapses (Qiu & Knöpfel, 2007). To terminate the actions of D-serine, it may then be re-uptaken for breakdown into DAO expressing Bergmann glia or post-synaptic Purkinje cells. This latter suggestion is supported by the presence of Purkinje cell Asc-1 (Helboe *et al.*, 2003; Matsuo *et al.*, 2004) and the demonstration that neuronal Asc-1 regulates cerebellar D-serine levels *in vivo* (Rutter *et al.*, 2007).

However, these speculations on synaptic D-serine function should be viewed with caution given that *endogenous* D-serine was shown not to modulate cerebellar NMDAR-responses (Mothet *et al.*, 2000), although cerebellar NMDARs do respond to exogenous D-serine *in vitro* and *in vivo* (Wood *et al.*, 1989, 1990; Rao *et al.*, 1991; Vallebuona & Raiteri, 1995; Fedele *et al.*, 1997) and have elevated activity in DAO mutant mice (Almond *et al.*, 2006). In addition, it is somewhat paradoxical that SRR synthesized D-serine is thought to be rapidly degraded by DAO (Hashimoto *et al.*, 1993b; Morikawa *et al.*, 2001) questioning both why it is synthesized at all as well as SRR's robust cerebellar expression. Perhaps highly regulated levels of D-serine are necessary to cerebellar function. Alternatively, SRR could have a role outside of D-serine synthesis.

2.4.5 Limitations of the study and concluding remarks

The main findings if this study are; 1) the rat and mouse frontal cortex expresses both SRR and DAO in neurons, particularly in superior layers, and in glia, particularly in inferior layers; 2) the hippocampus expresses some SRR and DAO

which is predominantly glial; 3) glial cells in white matter regions express both SRR and DAO, sometimes in different subtypes of glia; 4) SRR is expressed by glial cells in the SN and VTA while these regions contain both DAO positive glia and neurons; 5) both SRR and DAO are expressed in the cerebellum, predominantly in glial cells with some Purkinje cell expression.

The data presented have both extended and questioned previous findings and views on the cellular and regional distribution of SRR and DAO in the rat and mouse brain. These findings may impact on the inferred roles of D-serine and its metabolizing enzymes at synapses within different regions of the brain. For example, neuronal SRR in the cortex suggests that D-serine should not only be considered as a gliotransmitter. Additionally, cortical and neuronal DAO expression in the cortex was highlighted, opposing previous views based on DAO activity of the enzyme's regional roles in the brain. In the cerebellum, the data adds to some accumulating evidence of the presence of cerebellar D-serine synthesis. In the white matter, the predominance of SRR suggests that the view of D-serine's enrichment to the NMDAR rich neuropil of the grey matter should be revised.

However, the study was limited by three factors. Firstly, pre-adsorption controls were only carried for the experiments with DAO. Whilst the antibody to SRR is a commercial antibody and its use has been previously validated for western blot detection of SRR (Steffek *et al.*, 2006) pre-adsorption controls to demonstrate its specificity in immunohistochemical detection of SRR in the present study would have been beneficial to further validate the SRR antibody. Secondly, co-localization studies were not carried out, in part due to an inability to optimise the SRR antibody for immunofluorescence. As a partial attempt to overcome this, labelling of adjacent sections with neuronal and glial markers was adopted. However, such comparisons between adjacently labelled sections can only provide

suggestive evidence for the particular cell types immunoreactive for SRR and DAO, and consequently truly definitive conclusions could not be drawn. The third limitation to this study is that D-serine was not studied. However, some controversy over reliable immunohistochemical detection of D-serine exists (e.g. Schell *et al*., 1997 and Kartvelishvily *et al*., 2006). Notwithstanding, this caveat means that the inferences drawn from SRR and DAO localisation's on D-serine's synaptic functions must be taken tentatively.

In addition, it should be borne in mind that these immunohistochemical studies are qualitative examinations of SRR and DAO expression. Thus, while immunoreactivity appeared qualitatively different across regions in some cases, for example SRR immunoreactivity appeared lower in the hippocampus than the frontal cortex, quantitative regional comparisons were not carried out.

Despite the limitations of the study, it has challenged some prevailing views of the localization of SRR and DAO and thus inferred roles of D-serine. Unsurprisingly, therefore, this study has also raised further questions. For example, what is the role of DAO in the cortex if it is inactive? It is possible its activity is compromised via protein-protein interactions, or perhaps an inactive splice variant is expressed. Alternatively cortical DAO may perform a novel function undetectable by common activity assays. Given the potential therapeutic candidacy of DAO to elevate D-serine levels in schizophrenia, investigating these questions is warranted. The paradox of SRR's expression and thence presumed D-serine synthesis in the cerebellum, where it is rapidly and efficiently degraded by DAO is also an interesting point highlighted in this study. One possibility is that cerebellar SRR also has functions outside of D-serine synthesis. This possibility is also suggested to account for SRR's robust white matter expression where it has been suggested SRR may be important in pyruvate formation. The study also raised the possibility of

novel synaptic functions of D-serine, for example as an antagonist at particular NMDARs. Investigating this prospect is important to advance an understanding of the role of this novel neuromodulator.

3. THE DISTRIBUTION OF SRR AND DAO IN THE HUMAN BRAIN

3.1 INTRODUCTION

The preceding chapter detailed the distributions of DAO and SRR in the rat and mouse brain. These findings extended previous studies contributing to an understanding of the cells within the brain in which D-serine metabolism potentially occurs. These studies also formed the prelude to investigating DAO and SRR distribution in the human brain. Detection of SRR (Steffek *et al.*, 2006; Bendikov *et al.*, 2007) and DAO protein (Bendikov *et al.*, 2007), although not DAO activity (Kapoor *et al.*, 2006), in the human cortex have previously been demonstrated. However, the cellular distribution of SRR and DAO in the human brain has not been studied. It is important to delineate the distribution of DAO and SRR in the human brain since it will impact on understanding the potential pathophysiological mechanisms by which D-serine metabolism may be involved in schizophrenia. Accordingly, the aim of this study was to characterise, and provide the first report of, the cellular distribution of SRR and DAO in the human brain. These studies were also carried out as a prelude to studying the expression of SRR and DAO in the brain in schizophrenia. The studies of SRR and DAO distribution in the human brain have been published (Verrall *et al.*, 2007).

3.1.1 Choice of tissue and regions for analysis

For this study brain tissue from control subjects was used. As described for the rats and mice, areas where DAO and/or SRR are reputedly abundant or biologically

implicated were chosen, namely the DPFC (Brodmann's Area 9/46), hippocampus, cerebellum and SNc. One of the tissue sections thought to contain the SNc was later realised, once immunostained, to be at the medullary level. Since interesting immunoreactivity was seen within the inferior olivary nucleus (IO) in this section, additional sections from further subjects were studied to characterise SRR and DAO distribution in the IO.

3.1.2 Choice of methodology

This study characterised the distribution of DAO and SRR using immunohistochemistry. In some cases, adjacent sections were labelled for Tyrosine Hydroxylase (TH) and GFAP in order to compare the morphologies of dopaminergic neurons and glial cells with SRR and/or DAO stained cells. Additionally, since we found DAO expression in the rodent brain (Chapter 2, Section 2.4.2) in regions of undetectable activity (Katagiri *et al.*, 1991; Horiike *et al.*, 1994; Schell *et al.*, 1995; Wang & Zhu, 2003), also reported for the human brain (Kapoor *et al.*, 2006), DAO activity was measured in the DPFC, hippocampus, cerebellum and SNc. The immunohistochemical findings for DAO in the human DPFC and hippocampus proved discordant to the results of activity assays in these regions. For this reason, DAO immunohistochemistry in the human brain was corroborated with *in situ* hybridisation histochemistry (ISHH), in order to demonstrate both mRNA and protein expression in the same cell types. This was carried out in human DPFC and hippocampus and, as a positive control, in the cerebellum where both DAO protein and activity were detectable.

3.2 MATERIALS AND METHODS

3.2.1 Human tissue

The brain tissue used in this thesis was collected at autopsy at two centres, Oxford and London, and approved by the Oxfordshire Psychiatric Research Ethics Committee. Demographic details of the subjects are shown in Table 3.1. Schizophrenia was diagnosed from case notes according to DSM-III-R (American Psychiatric Association, 1987) criteria. Most cases were initially of paranoid or disorganised subtype. All patients had received typical antipsychotics. Control individuals had no history of psychiatric or neurological illness. Neuropathological assessment of all brains did not identify any neurodegenerative abnormalities other than minor age-related changes.

Further brain tissue was taken from the Stanley Foundation collection, detailed in Torrey *et al.* (2000). Demographic details are shown in Table 3.2. The series comprises 15 subjects with schizophrenia, 15 with bipolar disorder, 15 with unipolar depression, all classified according to DSM-IV criteria, and 15 controls. Neuropathological assessment of all brains did not identify any neurodegenerative abnormalities other than minor age-related changes.

Brain tissue blocks from the Oxford series were dissected directly at autopsy and stored at -80ºC. Brain tissue blocks from the London series were dissected from previously snap-frozen coronal brain slices at -20ºC and returned to storage at -80ºC. Formalin-fixed paraffin-wax embedded blocks were also prepared from subjects from the Oxford series. Brains from the Stanley Foundations series were hemisected, with tissue blocks from one hemisphere frozen at -80ºC

TABLE 3-1 Demographic details of schizophrenia patients and control individuals from the Oxford and London brain series.

	Oxford series		London series		Combined series	
	Con	Scz	Con	Scz	Con	Scz
Number	12	12	10	9	22	21
Sex (M:F)	6:6	7:5	6:4	5:4	12:10	12:9
Age (years)	65(4.3)	53(5.1)	63(6.7)	62(6.4)	64(3.7)	57(4.0)
Range	25-79	19-71	26-85	32-87	25-85	19-87
pmi (hours)	39(4.9)	43(5.4)	38(5.2)	49(8.2)	39(3.5)	46(4.6)
Range	25-72	18-76	10-70	22-97	10-72	18-97
Brain pH	6.63(0.11)	6.42(0.07)	6.38(0.12)	6.36(0.08)	6.52(0.08)	6.40(0.05)
Range	6.2-7.71	6.05-6.72	5.9-6.97	6.04-6.8	5.9-7.71	6.04-6.8

Values are mean (standard error of the mean; sem). Con = control subjects, Scz = schizophrenic patients. Patients had been treated with the typical antipsychotic haloperidol. There are no significant demographic differences between diagnostic groups in the Oxford, London or combined series. Tissue was not available from all subjects for every experiment.

TABLE 3-2 Demographic details of subjects from the Stanley Foundation brain series.

	Schizophrenia	Bipolar Disorder	Unipolar Depression	Control subjects
Number	15	15	15	15
Age	44.2 (25-62)	42.3 (25-61)	46.4 (30-65)	48.1 (29-68)
Sex	9M, 6F	9M, 6F	9M, 6F	9M, 6F
pmi (hours)	33.7 (12-61)	32.5 (13-62)	27.5 (7-47)	23.7 (8-42)
Brain pH	6.1 (5.8-6.6)	6.2 (5.8-6.5)	6.2 (5.6-6.5)	6.3 (5.8-6.6)
Antipsychotic exposure (mg)	52,267 (62,062) 1 never	20,827 (24,016) 3 never, 1 >20 years	0	0

Values are mean (range); Antipsychotic exposure is mean (standard deviation; SD). Patients with schizophrenia had been treated with the typical and atypical antipsychotics thiothixene, risperidone, thioridazine, clozapine, haloperidol and chlorpromazine. There are no significant demographic differences between diagnostic groups in the series.

and, from the other, formalin-fixed and paraffin-wax embedded. All paraffin-wax embedding used polymer wax and a Leica automated processor.

For the studies described in this chapter, control cases only from all brain series were used. For immunohistochemistry, formalin-fixed paraffin-wax embedded blocks from the DPFC (n = 7), hippocampus (n = 5), midbrain containing the SNc (n = 7), medulla oblongata containing the IO (n = 5) and the cerebellum (n = 5) were taken and cut at 10 µm using a Leica rotary microtome. For ISHH, frozen tissue blocks from the DPFC (n = 5), hippocampus (n = 5) and cerebellum (n = 5) were cut at 18 µm and stored at -80°C. For DAO activity assays, frozen tissue blocks from the DPFC (n = 5), hippocampus (n = 2), midbrain containing the SNc (n = 5) and the cerebellum (n = 4) were cut at 18 µm and stored at -80°C. All sections were collected on Superfrost plus slides (VWR International).

3.2.2 Immunohistochemistry

Immunohistochemistry to detect SRR and DAO was carried out as described (Chapter 2, Section 2.2.5). Some immunohistochemistry experiments for SRR were carried out by Nancy Rawlings, an MSc student. To detect SRR, a commercial antibody (BD Biosciences), shown to detect a single band of the predicted molecular weight of SRR in human brain was used (see Chapter 2, Section 2.3.1 for characterisation). To detect DAO a novel GSK-DAO antibody was used. This had been shown to detect a single band of predicted molecular weight for DAO in the human cerebellum (see Chapter 2, Section 2.3.1 for characterisation).

For immunohistochemistry in human tissue, the antibody to SRR did not detect immunoreactivity in the DPFC at the recommended 1:500 dilution as had been used in rodent frontal cortex tissue (Chapter 2, Section 2.2.5). The antibody

was therefore titrated in pilot experiments and the lowest concentration demonstrating immunoreactivity in human DPFC tissue found to be 1:35 (Figure 3.1). This concentration also detected SRR in other regions studied and was used for all further experiments.

The GSK-DAO antibody was titrated in pilot studies in human tissue and selected for optimal detection of immunoreactivity at 1:500 in the cerebellum (Figure 3.2 A), SNc and IO. In DPFC and hippocampus tissue, 1:500 GSK-DAO antibody detected immunoreactivity (Figure 3.2 B), but it was less robust than that in the cerebellum, SNc and IO. Using 1:200 GSK-DAO antibody, immunohistochemistry signals in the DPFC and hippocampus were more robust (Figure 3.2 C) and were used in further experiments. In order to check that the increased signal in the DPFC with higher antibody concentration was antigen specific, microwaving (which enhances antigen retrieval; Cattoretti *et al.*, 1993) was reduced in the protocol. This was shown to give the same pattern of immunoreactivity but with less intense staining (Figure 3.2 D), demonstrating DAO immunoreactivity was antigen specific.

In immunohistochemistry results, based on morphology and immunostaining, cells were putatively identified according to the criteria in Box 2.

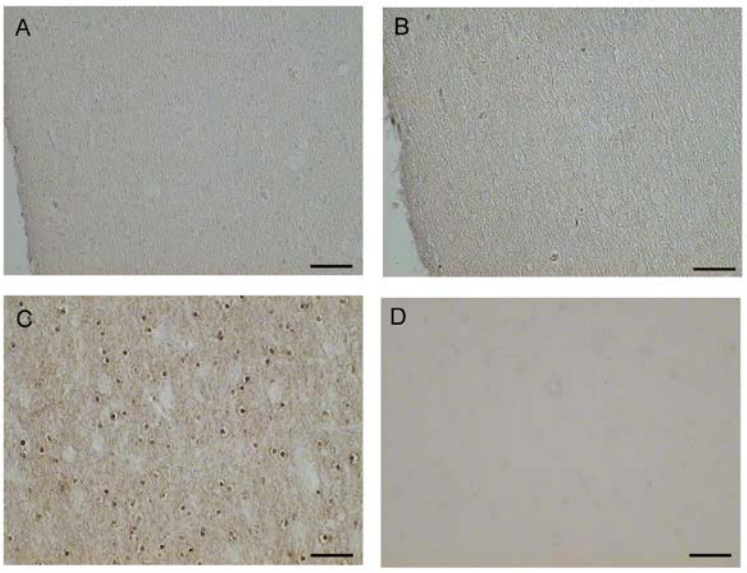

FIGURE 3-1 Titration of SRR antibody on DPFC tissue. (A) 1:500 anti-SRR. (B) 1:100 anti-SRR. (C) 1:35 anti-SRR. (D) No primary control. Scale bars = 50µm.

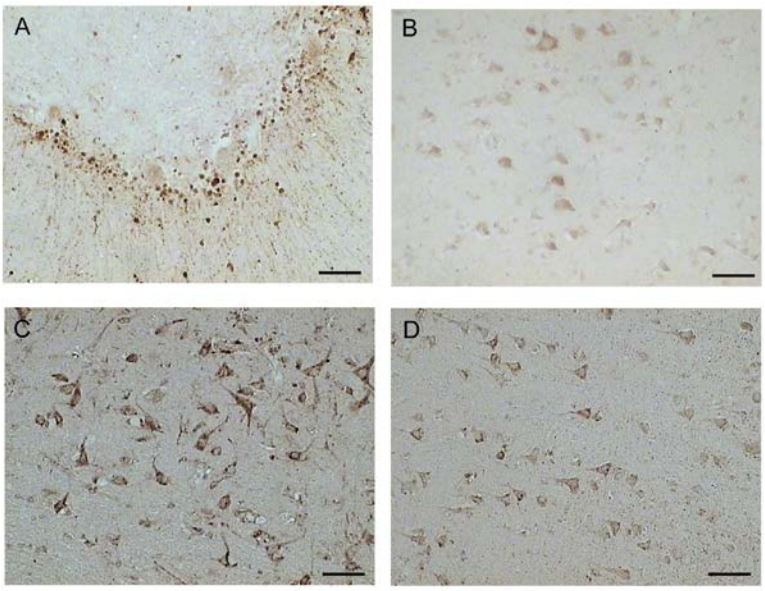

Figure 3-2
Optimisation of the GSK-DAO antibody for immuno-histochemistry.
(A) 1:500 GSK-DAO antibody in cerebellum. (B) 1:500 GSK-DAO antibody in DPFC tissue. (C) 1:200 GSK-DAO antibody in DPFC.
(D) 1:200 GSK-DAO antibody in DPFC tissue with reduced micro-waving. Scale bars = 50µm.

Box 2. *Criterion used to putatively identify immunolabelled cells.*

a) Pyramidal neurons were identified on the basis of their being large in size and triangular in shape often with a visible apical dendrite.
b) Large cells sometimes with apical dendrites located within the Purkinje cell layer of the cerebellum were identified as Purkinje cells
c) Large cells with apical dendrites and processes localized in known dopaminergic nuclei, containing lipofuscin pigment and comparable in size and morpholgy to those labelled for TH in adjacent sections were identified as dopaminergic neurons
d) Large cells with apical dendrites and processes within the IO were identified as putative neurons
e) Immunoreactive cells which were smaller than identified neurons and comparable in size and shape to GFAP labelled cells in adjacent sections were identified as glia
f) Immunoreactive cells which were smaller than identified neurons and localized in white matter were assumed to be glia
g) Small rounded immunostained cells in the midbrain, dissimilar to TH labelled neurons in adjacent sections were assumed to be glia
h) Bergmann glia immunostained cells were identified on the basis of their small size, rounded morphology and primarily their distribution within the Purkinje cell layer of the cerebellum
i) Oligodendrocytes were speculatively identified when visualized in rows (Hof *et al.*, 2003)

3.2.3 Ribroprobe synthesis

To synthesize a DAO ribroprobe, mRNA from human cerebellum was extracted, DNAse treated and reverse transcribed using standard techniques (described in Chapter 4, Sections 4.2.4, 4.2.5). DAO cDNA (400 base pair (bp) fragment, bp 441-840 of Accession # NM_001917) was amplified from human cerebellar cDNA with the following primers (F: CCTCTTCCATGAAGCCATTCC, R: TAGATGTT AAGGGGCATGTAG) and purified using standard techniques (described in Chapter 5, Sections 5.2.4, 5.2.8). DAO cDNA was ligated with 'blunt ends' into pGEM-T Easy Vector (Figure 3.3; Promega, Southampton, UK) following manufacturer's recommendations. Briefly, 105ng cDNA insert and 35ng plasmid were incubated with 1x ligation buffer (Promega) and 0.5U/µl final concentration T4 ligase enzyme (Promega) for one hour at room temperature. Plasmids were transformed into E. coli as described (Chapter 5, Section 5.2.6.2) and positive clones selected using blue-white reagent (Sigma) according to manufacturer's instructions. Clones were cultured and purified using standard techniques (described in Chapter 5, Sections 5.2.6.2, 5.2.7, 5.2.8). The DAO- pGEM-T construct was then linearized by restriction endonuclease digest. Briefly, 1µg plasmid was digested with 0.2U/µl *Sac*I or *Sac*II in a 20µl volume with 1x final concentration multi-core restriction endonuclease buffer (Promega) at 37ºC for two hours . To generate the ribroprobe, the linearized plasmid was then transcribed using SP6 (for Sac II linearized plasmid) or T7 (for Sac I linearized plasmid) RNA polymerases. Briefly, 1.5-2µg dried plasmid was incubated with nucleoside triphosphates (ATP, cytosine triphosphate; CTP, GTP each at 3mM final concentration), RNAsin (2-4U/µl final concentration), reaction buffer (1 x final concentration), T7 or SP6 enzymes (3–6 U / µl final concentration), dithiothreitol (DTT 10mM final concentration) (all from Promega) and [^{35}S]UTP

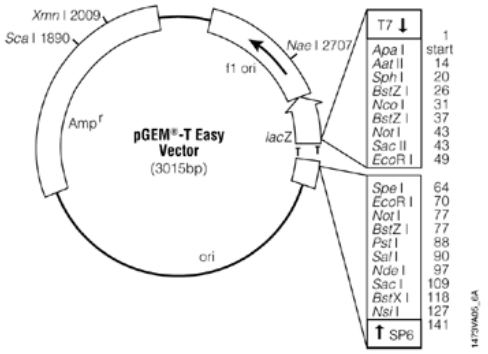

FIGURE 3-3 pGEM-T Easy Vector (Promega) containing a multiple cloning site within the ß-galactosidase gene, ampicillin resistance gene and T7 and SP6 RNA polymerase promotors.

(1000 C_i/mmol) (GE Healthcare) for 37ºC at sixty minutes. The plasmid was then degraded by incubation at 37ºC for five minutes in DNAse (0.3U/ul final concentration; Promega). The RNA was precipitated by adding sodium acetate (0.47mM final concentration), tRNA (0.58µg/µl final concentration; Promega) in a final volume of 43µl which was then mixed with 100µl isopropanol, stored at -20ºC for five minutes and centrifuged at 12000*g* for ten minutes to pellet the RNA. The pellet was washed in 75% ethanol and resuspended in 50µl nuclease-free water (Promega) and the radioactivity measured by scintillation counting. The ribroprobe was then hydrolysed in an equal volume of hydrolysis buffer (80mM $NaHCO_3$ in 120mM Na_2CO_3) incubated at 60ºC for twenty three minutes. Hydrolysed probe was precipitated by adding glacial acetic acid (4.35% final concentration) and sodium acetate (0.35mM final concentration) which was mixed with an equal volume of isopropanol, stored at -20ºC for five minutes and centrifuged at 12000*g* for ten minutes. The pellet was resuspended in 50µl nuclease-free water (Promega) and the radioactivity measured by scintillation counting.

3.2.4 *In situ* hybridisation histochemistry

Human tissue sections were thawed for fifteen minutes, fixed in 4% paraformaldehyde (PFA; VWR International) in diethyl pyrocarbonate (DEPC; Sigma) treated PBS and incubated in 100nM DEPC-treated triethanolamine (TEA; Appendix I) with 0.25% acetic anhydride to prevent non-specific probe binding. Sections were then dehydrated in graded ethanols, incubated in chloroform for ten minutes to remove tissue lipids, rehydrated to 95% ethanol and air dried.

The ribroprobe was diluted with hybridisation buffer with 20mM DTT added (Appendix I) to a final activity of 1.2 x 10^4 cpm/ml and 200 µl added to each slide of tissue sections. Slides were covered with a glass coverslip and incubated overnight at 50ºC in lidded Perspex trays lined with filter paper soaked with 3 x standard saline citrate (SSC; Appendix I)/75% formamide.

For post-hybridisation washing, slides were first rinsed in 2x SSC, incubated in RNase A (20µg/ml; Promega) for thirty minutes at room temperature, and immersed in 2x SSC at 55ºC for ten minutes, 0.5x SSC at 55ºC for sixty minutes and finally 0.5x SSC at room temperature for ten minutes. Slides were rinsed in ddH_2O, dried and apposed to X-ray film (Kodak) at room temperature. To localize cellular mRNAs, slides were emulsion-dipped in LM1 autoradiographic emulsion (GE Healthcare) diluted 2:1 with distilled water and, exposed at 4ºC for ~ six weeks and counterstained with cresyl violet (Appendix I).

3.2.5 DAO activity assay

Sections of frozen tissue (50-100mg) were homogenised in twenty volumes of DAO assay buffer (50mM Na_2HPO_4, pH= 7.4). Homogenates were centrifuged for one minute at 12,000g, and the supernatants stored at -70ºC prior to use. The DAO activity assay was performed using the Amplex Red kit (Molecular Probes,

Invitrogen) with D-proline as the substrate, (the D-amino acid DAO catabolises with the greatest activity; Gabler *et al*., 2000; Molla *et al*., 2006). The tissue extracts were incubated with 50µM Amplex Red, 0.125 units horse-radish peroxidise and D-proline (0.1-0.01µM) in a total volume of 10µl at 37ºC for sixty minutes, and the absorbance read at 571nm. Absorbance was normalised to the protein content of each sample, worked out using the Bradford assay (Chapter 2, Section 2.2.3). Addition of 10mM sodium benzoate (a competitive inhibitor of DAO; Singer '& Mason, 1967; Moses *et al*., 1996) blocked the colorimetric reaction (data not shown).

Initial pilot experiments were carried out to test if tissue had detectable DAO activity, prior to measuring DAO activity on the D-Proline standard curve (0.1-0.01µM). Tissue extracts from different regions were incubated with 0.1µM D-Proline; if the colorimetric reaction was not visualized as pink after incubation at 37ºC for sixty minutes, then DAO activity was deemed undetectable in that region, and further experiments were not carried out. All experiments were conducted in duplicate and cerebellar extracts used as positive controls for DAO activity detection.

3.3 RESULTS

3.3.1 Regional and cellular expression of SRR in the human DPFC

SRR immunoreactivity in the DPFC showed a white over grey matter enhancement (Figure 3.4 A) attributable to punctate labelling and immunostaining of small round cells more abundant in the white (Figure 3.4 B) than grey matter (Figure 3.4 C). In grey matter, immunolabelled cells were visible in the vicinity of unlabelled pyramidal neurons (Figure 3.4 D). Sub-cellularly some cells showed punctate or peri-cellular enhancement in immunostaining (Figure 3.4 C inset).

GFAP immunolabelling in adjacent sections demonstrated scattered immunoreactive cells in the grey matter (Figure 3.4 F). These were similar in size and shape to SRR immunoreactive cells, suggesting that the latter are GFAP-reactive astrocytes. In white matter, GFAP immunoreactivity localized to stellate cells (Figure 3.4 F inset). These were larger than SRR immunoreactive cells in the white matter (Figure 3.4 B), suggesting the latter are GFAP-negative cells. Given their size and location they are putative glia.

3.3.2 Regional and cellular expression of SRR in the human hippocampus

SRR immunoreactivity in the hippocampal formation predominantly localized to white matter regions such as the alveus (Figure 3.5 A) which demonstrated punctate immunostaining and immunolabelling of small round cells (Figure 3.5 B). Based on their size and location these are putative glia. Dentate gyrus granule cells (Figure 3.5 C) and pyramidal neurons (Figure 3.5 C inset) were immunonegative. In the radiatum/lacunosum strata, SRR immunoreactivity was punctate and localized to small round cells (Figure 3.5 D). GFAP labelling in adjacent sections stained small round cells in the strata radiatum/lacunosum (Figure 3.5 F) similar in size and

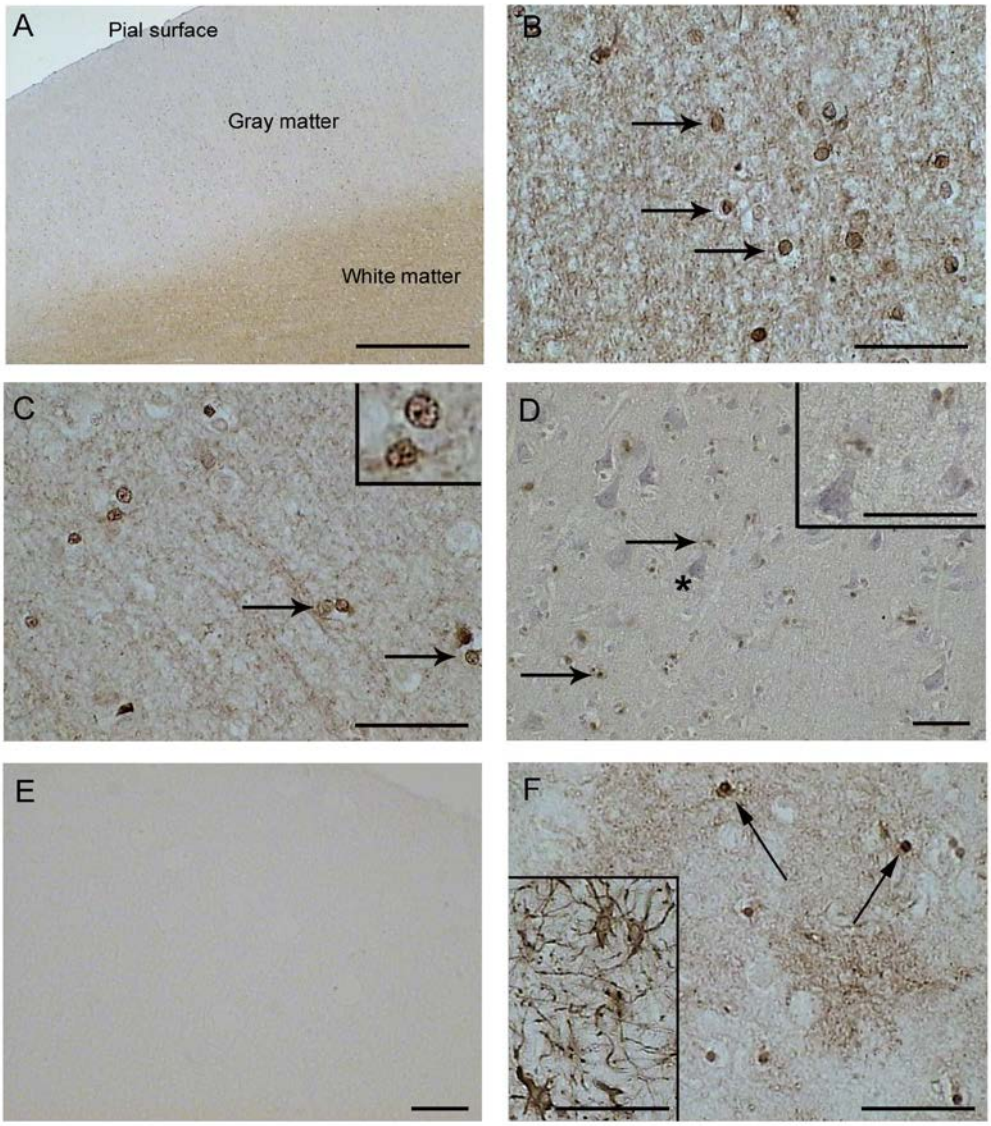

FIGURE 3-4 Cellular distribution of SRR in human DPFC. (A) Low power image of SRR immunoreactivity enhanced in the white compared to grey matter. (B) High power image of DPFC white matter demonstrating SRR immunoreactivity localized to putative glia (arrows). (C) High power image of DPFC grey matter showing immunolabelling of putative glia (arrows). Inset shows high power putative glia with peri-cellularly enhanced immunostaining. (D) High power image of DPFC grey matter counterstained with cresyl violet, demonstrating SRR immunolabelled putative glia (arrows) and immunonegative pyramidal neurons (asterix). (E) No primary control for SRR in the human DPFC. (F) GFAP immunolabelling of glia (arrows) in the grey matter (main image) and of stellate cells in the white matter (inset). Scale bars: A = 1mm; B-F = 50µm.

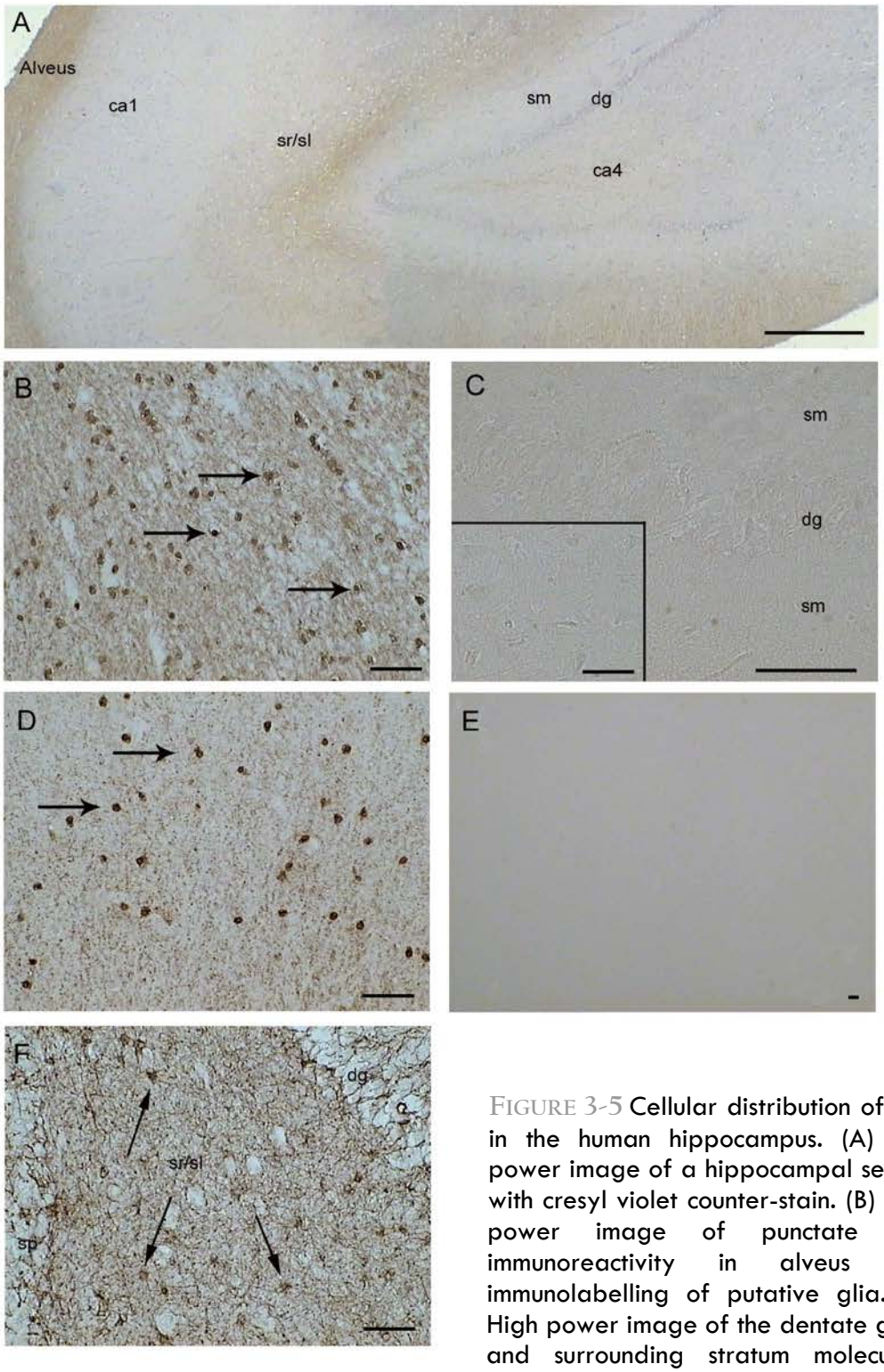

FIGURE 3-5 Cellular distribution of SRR in the human hippocampus. (A) Low power image of a hippocampal section with cresyl violet counter-stain. (B) High power image of punctate SRR immunoreactivity in alveus and immunolabelling of putative glia. (C) High power image of the dentate gyrus and surrounding stratum moleculare devoid of SRR immunoreactivity and of the cornu Ammonis subfields (inset) also devoid of SRR immunoreactivity. (D) High power image of the radiatum and lacunosum strata demonstrating SRR immunolabelling of scattered small round cells. (E) No primary control for SRR in the human hippocampus. (F) GFAP staining of small round cells (arrows) in the radiatum/lacunosum strata. ca1 = cornu Ammonis subfield 1; sr/sl = stratum radiatum/lacunosum; sm = stratum moleculare; dg = dentate gyrus; ca4 = cornu Ammonis subfield 4; sp = stratum pyramidale. Scale bars: A = 1mm; B-F = 50µm.

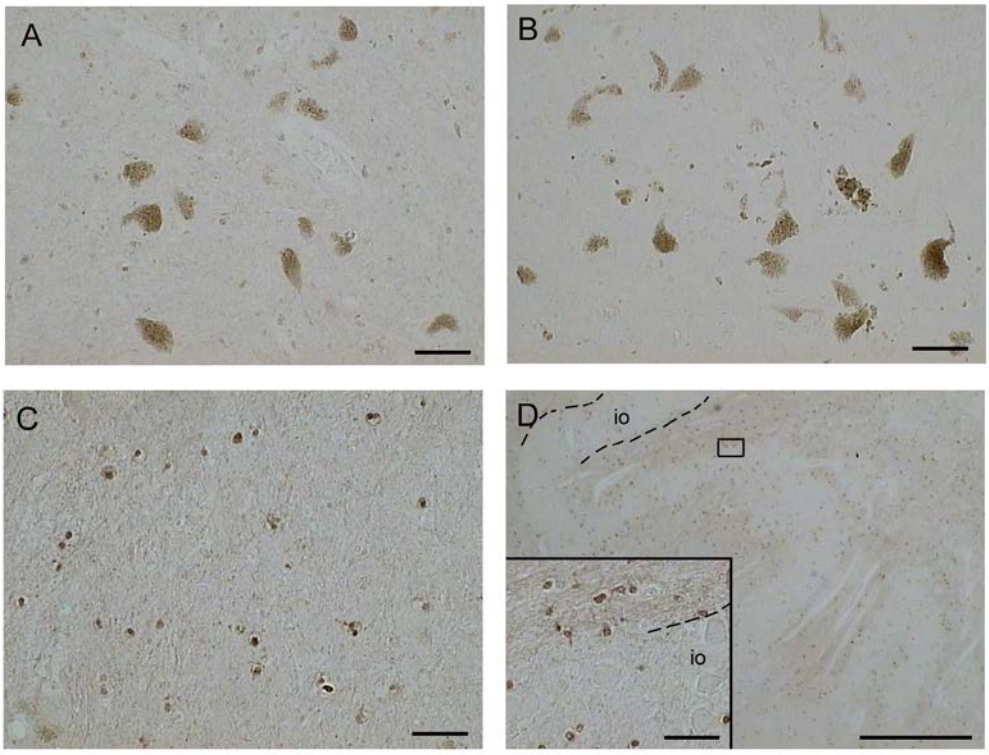

FIGURE 3-6 Cellular distribution of SRR immunoreactivity in the human SNc and IO. (A) High power image of SNc tissue immunonegative for SRR but demonstrating lipofuscin containing dopaminergic neurons. (B) High power image of no primary control for SRR in the SNc demonstrating lipofuscin containing neurons. (C) Representative high power image of scattered SRR immunopositive putative glia in the superior colliculus surrounding the SNc. (D) Low power image of SRR immunoreactivity in and around the IO. Inset shows a high power image of the boxed area, demonstrating neuropil SRR immunostaining surrounding the IO and scattered immunopositive putative glia within and surrounding the IO. io = inferior olivary nucleus. Scale bars: A-C, D inset = 50μm; D = 0.5mm.

shape to those labelled for SRR in these strata. This suggests the latter are putative astrocytes.

3.3.3 Regional and cellular expression of SRR in the human SNc and IO

In the SNc, large cells, putatively dopaminergic neurons due to the presence of lipofuscin, were not immunostained for SRR (Figure 3.6 A, B). Throughout the SNc (Figure 3.6 C) and particularly in surrounding structures such as the superior colliculus and cerebral peduncle, moderate SRR immunostaining of scattered small

round cells was visualized. Based on their size and morphology, these midbrain SRR immunoreactive cells are putative glia. Within the IO and surrounding the nucleus, SRR immunoreactivity localized to small round cells, again putative glia. These small round cells were most prevalent immediately surrounding the IO, where punctate immunostaining was also observed (Figure 3.6 D).

3.3.4 Regional and cellular expression of SRR in the human cerebellum

SRR immunoreactivity in the cerebellum was seen in all layers, but most prominently in the white matter (Figure 3.7 A). In the Purkinje cell layer, occasional moderately stained Purkinje cells were sometimes visualized (Figure 3.7 B inset) and putative Bergmann glia were frequently and intensely labelled (Figure 3.7 B). In the molecular layer, mild immunolabelling of putative Bergmann glia radial processes (Figure 3.7 B) and immunolabelled small round cells, sometimes with processes extending toward the pia matter (Figure 3.7 C), were visualized. Throughout the granule cell layer, scattered strongly immunopositive cells were observed which were round and slightly larger than granule cells (Figure 3.7 D). In the white matter, there was abundant and strong immunostaining of small round cells, similar in size and shape to those immunopositive in the granule cell layer, in addition to punctate labelling (Figure 3.7 E). Based on their size, the granule cell layer immunopositive cells are unlikely to be Golgi cells and, given their morphology and location, both granule cell layer and white matter stained cells are putative glia. Sub-cellularly SRR immunoreactivity was often observed to have a peri-cellular ring of labelling in each of these cell types (Figure 3.7 D inset).

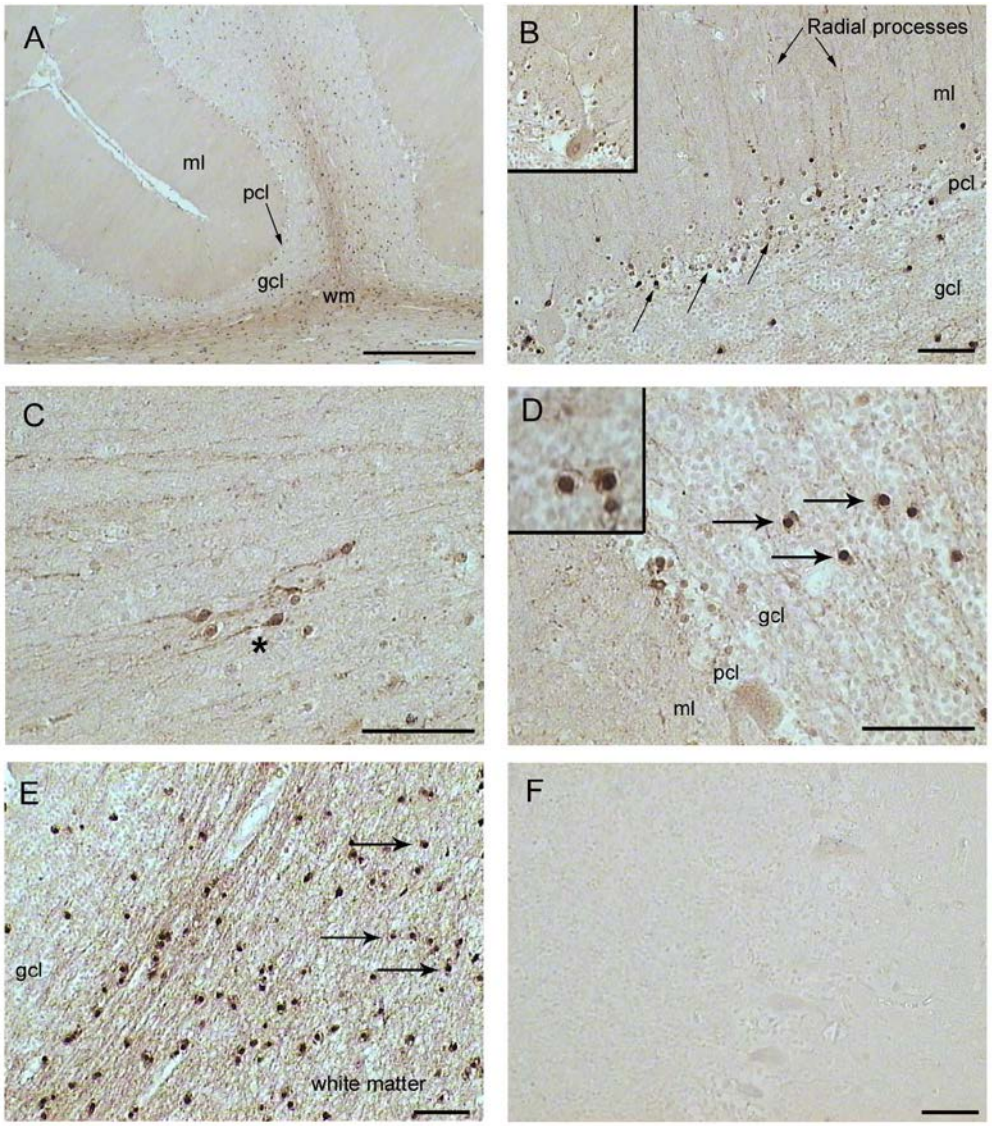

FIGURE 3-7 Cellular distribution of SRR immunoreactivity in the human cerebellum. (A) Low power image of the cerebellar cortex showing the molecular layer, Purkinje cell layer and granule cell layer and the underlying white matter. SRR immunoreactivity was seen in all layers and most prominently in the white matter. (B) High power image of the molecular, Purkinje and granule cell layers demonstrating immunostaining of Bergmann glia (arrows) in the Purkinje cell layer and moderate immunoreactivity of their radial processes. Purkinje cells sometimes demonstrated moderate immunostaining (inset). (C) High power image of the molecular layer demonstrating SRR immunoreactivity in small round cells within this layer, some of which had processes extending towards the pia matter (asterix). (D) High power image of the granule cell layer showing strongly immunopositive putative glia (arrows). Frequently immunopositive putative glia in the cerebellum demonstrated a peri-cellular ring in their staining (inset). (E) High power image of the granule cell layer and white matter demonstrating the immunolabelling of putative glia in the white matter similar to those immunolabelled in the granule cell layer and punctate labelling of the white matter. (F) No primary control for SRR in the human cerebellum. ml = molecular layer; pcl = Purkinje cell layer; gcl = granule cell layer; wm = white matter. Scale bars: A = 0.5mm; B-F = 50µm.

3.3.5 Regional and cellular expression of DAO in the human DPFC

In the DPFC, DAO immunolabelling was more prominent in the grey matter than white matter (Figure 3.8 A), which was attributable to labelling of layer II-VI pyramidal neurons (Figure 3.8 A, B). Immunoreactivity within pyramidal cells (Figure 3.8 C) and also of grey matter neuropil (Figure 3.8 D) was often punctate. Additionally, immunolabelled small round cells in grey matter were visible (Figure 3.8 D); these are putatively astrocytes based on their similarity in size and morphology to GFAP immunolabelled grey matter cells in adjacent sections (see Figure 3.4 F).

In white matter, moderate DAO immunoreactivity, sometimes with peri-cellular enhancement, was visible in numerous small round cells (Figure 3.8 E), which, based on their morphology and location, are putative glia. These were smaller than GFAP immunolabelled stellate white matter cells in adjacent section (see Figure 3.4 F inset).

Robust cortical and neuronal DAO immunostaining in the human brain were unexpected findings in view of the results of western blotting with human DPFC extracts (Chapter 2, Section 2.3.1, Figure 2.3 D) and activity studies (see below, Section 3.3.9). To validate these immunohistochemical results, DAO emulsion dipping of i*n situ* hybridised DPFC sections was carried out and revealed DAO mRNA signals clustered over pyramidal neurons (Figure 3.8 G and G`).

3.3.6 Regional and cellular expression of DAO in the human hippocampus

In the hippocampus, DAO immunoreactivity localized predominantly to pyramidal neurons (Figure 3.9 A) and was stronger in Cornu Ammonis (CA) 1 (Figure 3.9 B)

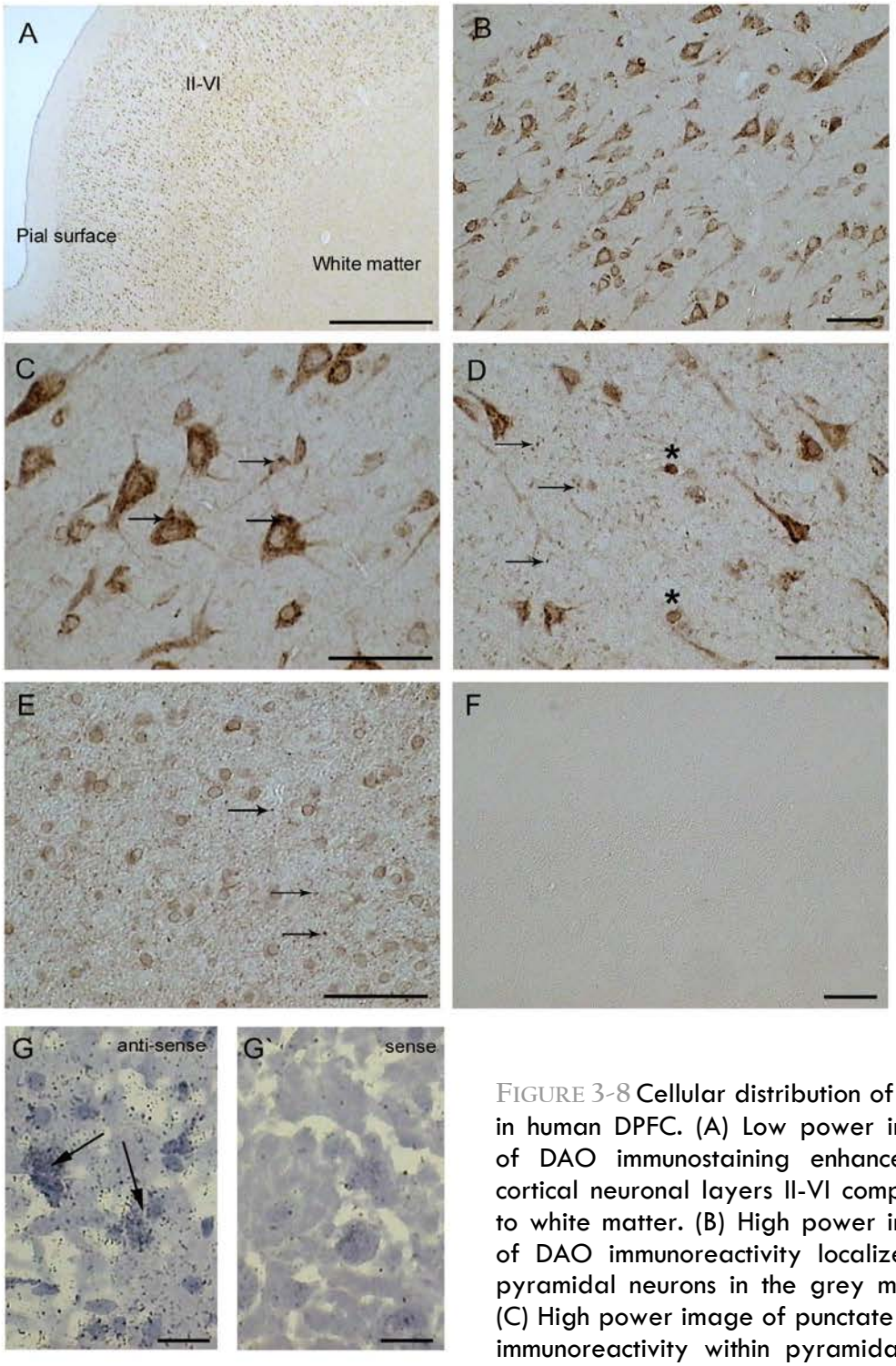

FIGURE 3-8 Cellular distribution of DAO in human DPFC. (A) Low power image of DAO immunostaining enhanced in cortical neuronal layers II-VI compared to white matter. (B) High power image of DAO immunoreactivity localized to pyramidal neurons in the grey matter. (C) High power image of punctate DAO immunoreactivity within pyramidal cell bodies (arrows). (D) High power image of punctate DAO immunoreactivity throughout grey matter neuropil (arrows). Immunolabelling of small round cells can also be observed (asterix). (E) High power image of DAO immunoreactivity in the white matter showing moderate immunostaining of small round cells. Throughout the white matter dark puncta can also be observed (arrows). (F) Pre-adsorption control for DAO in the DPFC. (G) Emulsion dipped antisense *in situ* hybridised DPFC sections showing localization of DAO mRNA to pyramidal cells (arrows). (G`) Corresponding image after sense probe hybridisation. Scale bars: A = 1mm; B-G` = 50µm.

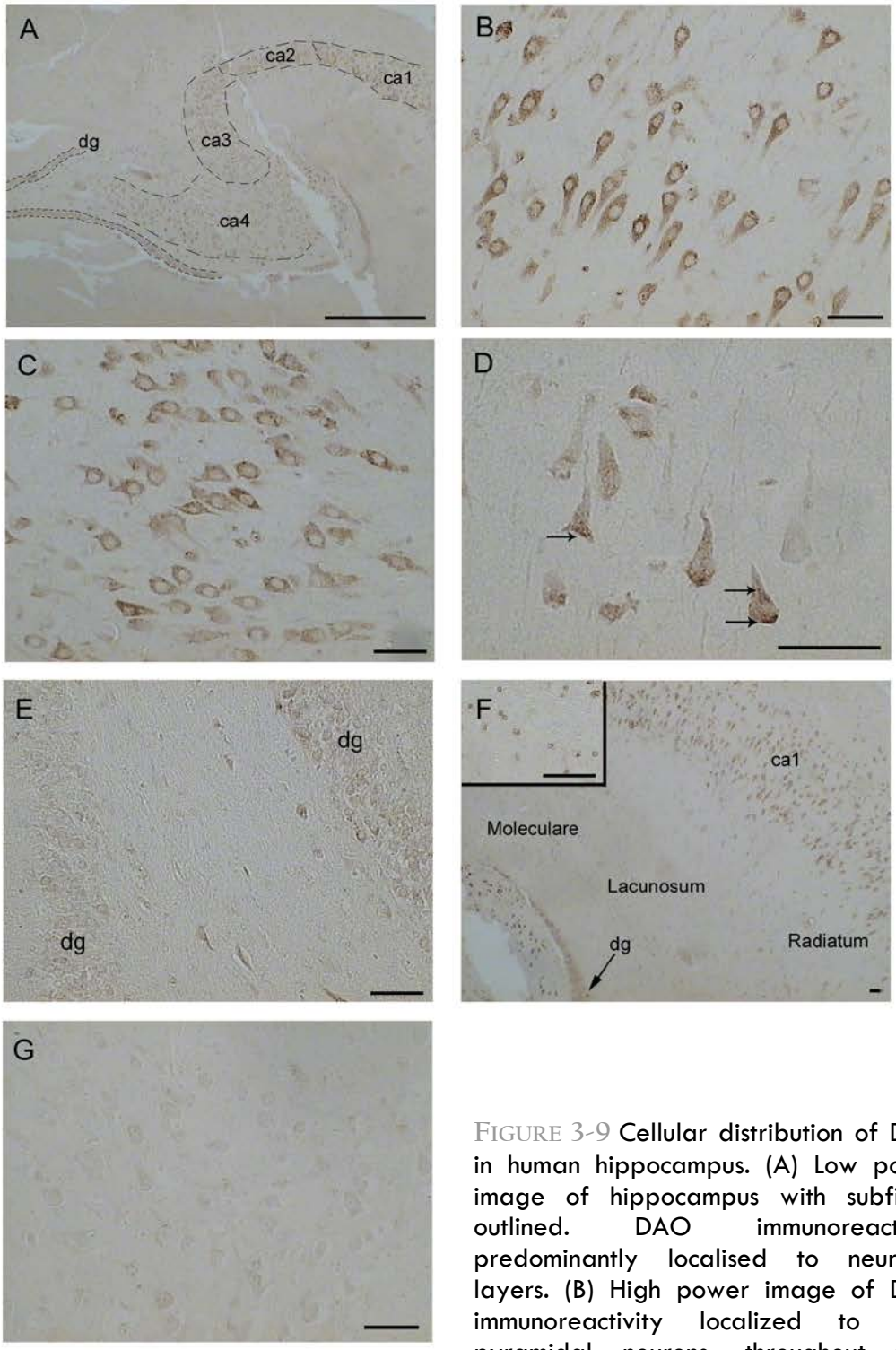

FIGURE 3-9 Cellular distribution of DAO in human hippocampus. (A) Low power image of hippocampus with subfields outlined. DAO immunoreactivity predominantly localised to neuronal layers. (B) High power image of DAO immunoreactivity localized to CA1 pyramidal neurons, throughout their cytoplasm. (C) High power image of DAO immunoreactivity localized to moderately stained CA2/CA3 pyramidal cells. (D) High power magnification of pyramidal neuron DAO immunostaining throughout cell bodies and sometimes punctate (arrows). (E) High power image of mild DAO immunoreactivity in the dentate gyrus. (F) Low power image showing DAO immunoreactivity localized to small round cells in the moleculare, lacunosum and radiatum strata, magnified in inset. (G) Pre-adsorption control for DAO in the hippocampus. dg = dentate gyrus; ca1-4 = cornu Ammonis subfields 1-4. Scale bars: A = 1mm; B-G, F inset = 50µm.

than CA2/CA3 and CA4 pyramidal cells (Figure 3.9 C). Immunostaining of pyramidal cell bodies was sometimes punctate (Figure 3.9 D). Consistent with our results in the cortex, ISHH and emulsion dipping of hippocampus sections revealed DAO mRNA signals clustered over pyramidal neurons in CA subfields (data not shown). In the dentate gyrus, mild immunoreactivity was seen in half of the subjects (Figure 3.9 E). In the radiatum/lacunosum and moleculare strata labelling of small round cells (Figure 3.9 F) was visible. Based on their similarity in size and morphology to GFAP immunoreactive cells in the radiatum/lacunosum strata of adjacent sections (Figure 3.5 F) these cells are putative GFAP-reactive astrocytes.

3.3.7 Regional and cellular expression of DAO in the human SNc and IO

In the SNc, DAO immunoreactivity localized to large cells, putatively dopaminergic neurons (Figure 3.10 A and B) based on the presence of lipofuscin pigment and their comparability to TH stained cells in adjacent sections. DAO also, in some cases, localized to small round cells (Figure 3.10 B). Cresyl violet stained sections (Figure 3.10 C) or those treated with pre-adsorbed GSK-DAO antibody (Figure 3.10 D) revealed putative dopaminergic neurons containing lipofuscin pigment but not immunoreactive. TH immunolabelling in adjacent sections revealed large dopaminergic neurons (Figure 3.10 E) morphologically similar to those labelled for DAO. The IO demonstrated strong DAO immunoreactivity (Figure 3.10 F), localized to putative neurons and small round cells (Figure 3.10 F inset). Based on their size and morphology, the small round cells immunopositive for DAO in the SNc and IO are putative glia.

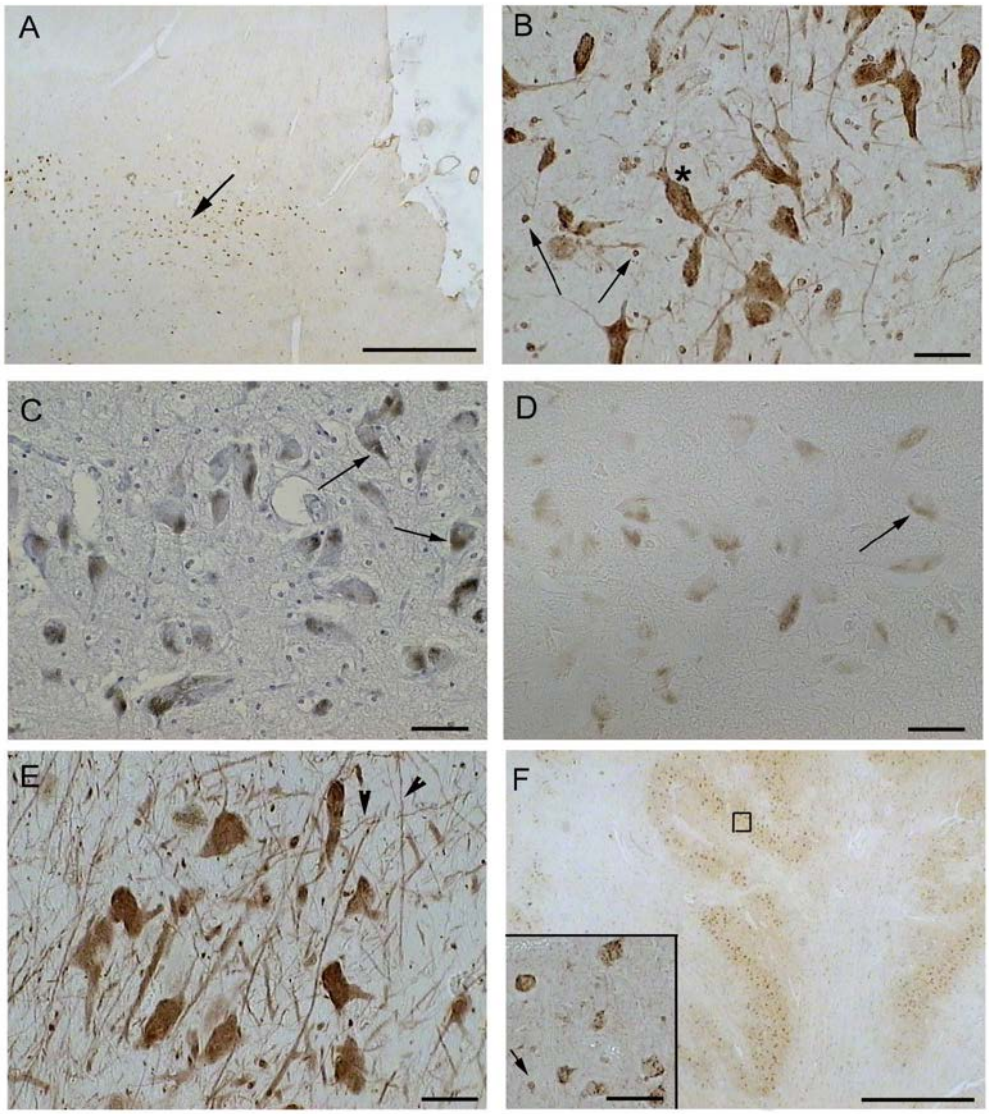

FIGURE 3-10 Cellular distribution of DAO immunoreactivity in the SNc and IO. (A) Low power image of DAO immunoreactivity localized to the SNc (arrow). (B) High power image of DAO immunoreactivity localized to dopaminergic neurons (asterix) and small round cells (arrows) within the SNc. (C) High power image of cresyl violet stained SNc demonstrating dopaminergic neurons containing lipofuscin pigment. (D) Pre-adsorption control for DAO in the SNc. (E) TH immunoreactivity in demonstrating immunolabelled large putative dopaminergic cells and processes (arrowheads). (F) Low power image of DAO immunoreactivity in the IO, shown in inset localized to large neuronal cells and putative glia (arrow). io = inferior olivary nucleus. Scale bars: A = 1mm; B-E, F inset = 50µm; F = 0.5mm.

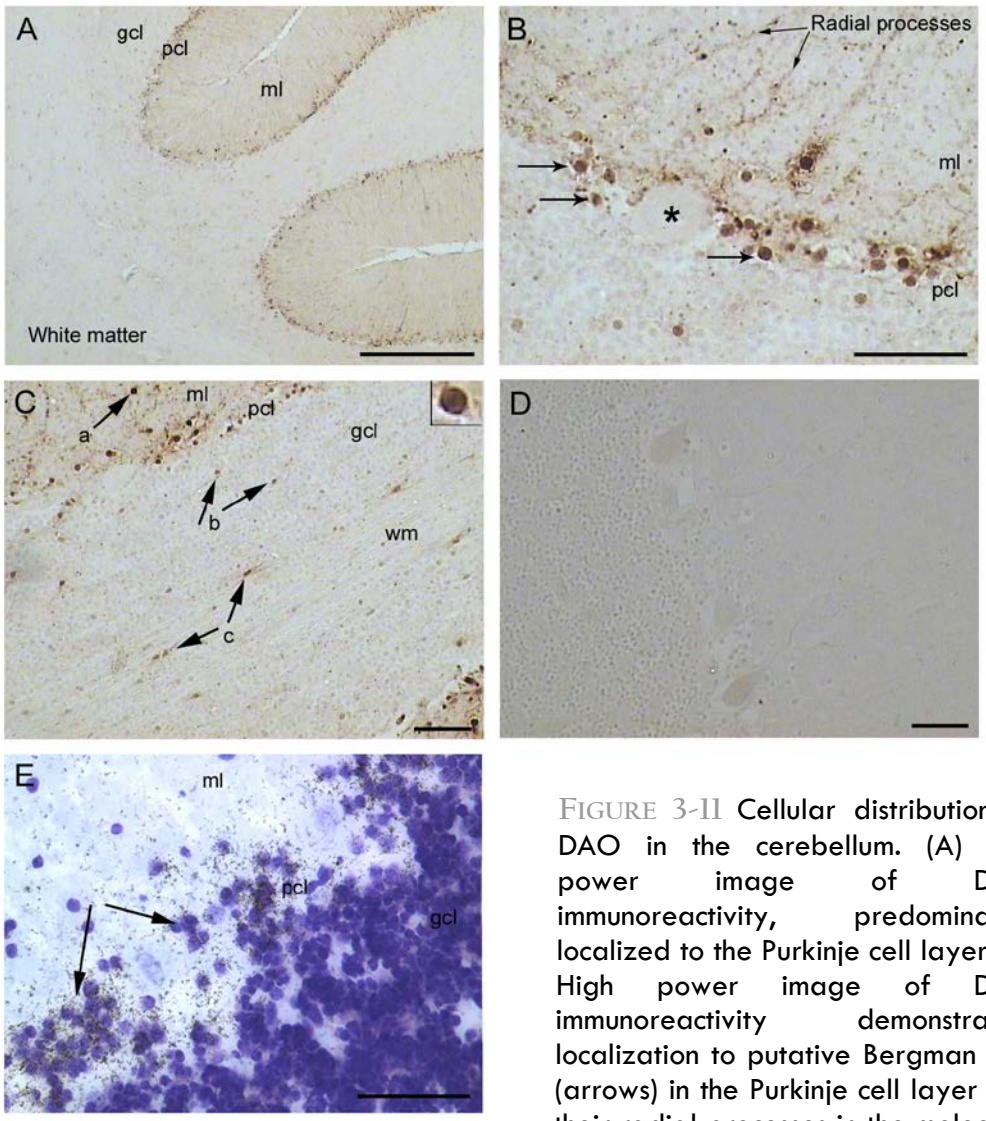

FIGURE 3-11 Cellular distribution of DAO in the cerebellum. (A) Low power image of DAO immunoreactivity, predominantly localized to the Purkinje cell layer. (B) High power image of DAO immunoreactivity demonstrating localization to putative Bergman glia (arrows) in the Purkinje cell layer and their radial processes in the molecular layer. Purkinje cells (asterix) were unstained. (C) High power image of DAO immunoreactivity localized to small round cells within the molecular layer (arrow a), granule cell layer (arrows b) and white matter (arrows c). Immunolabelling of these cells sometimes showed a peri-cellular enhancement (inset). (D) Pre-adsorption control for DAO in the cerebellum. (E) Emulsion dipped anti-sense *in situ* hybridised sections demonstrating silver grains clustered over putative Bergmann glia (arrows) but not over Purkinje cells (asterix) or the granule cell layer. gcl; granule cell layer, pcl; Purkinje cell layer, ml; molecular layer, wm; white matter. Scale bars (B-D) = 50µm.

3.3.8 Regional and cellular expression of DAO in the human cerebellum

DAO immunoreactivity in the cerebellum localized predominantly to the Purkinje cell layer (Figure 3.11 A) and therein to putative Bergmann glia, while Purkinje cells were unstained (Figure 3.11 B). In the molecular layer, putative Bergmann glia radial processes were immunoreactive (Figure 3.11 B) in addition to small round cells (Figure 3.11 C). In the granule cell layer, occasional small round cells, somewhat larger than granule cells and similar in size to those immunolabelled in the molecular layer, were stained (Figure 3.11 C). Based on their size, these are unlikely to be Golgi cells and are putative glia. Cells similar in shape and size to these were immunopositive in the white matter (Figure 3.11 C) and are again, putative glia. Sub-cellularly, many cells demonstrated a peri-cellular enhancement of immunolabelling (Figure 3.11 C inset). ISHH and emulsion dipping of cerebellar sections revealed DAO mRNA signals clustered predominantly over Bergmann glia of the Purkinje cell layer (Figure 3.11 E).

3.3.9 DAO activity in the human brain

Pilot studies were initially carried out with a single concentration of D-proline to see firstly whether DAO activity was detectable in the DPFC, hippocampus, SNc and cerebellum. Activity was detectable, as visualized by the colorimetric reaction, in the SNc and cerebellum from all subjects but not in DPFC or hippocampus tissue extracts run at the same time (data not shown). Tissue extracts were then incubated with a standard curve of D-proline concentrations. To compare the SNc and cerebellar DAO activities, tissue from both regions in the same subjects was used. Two such subjects were available and demonstrated higher DAO activity in the cerebellum than in the SNc (Figure 3.12).

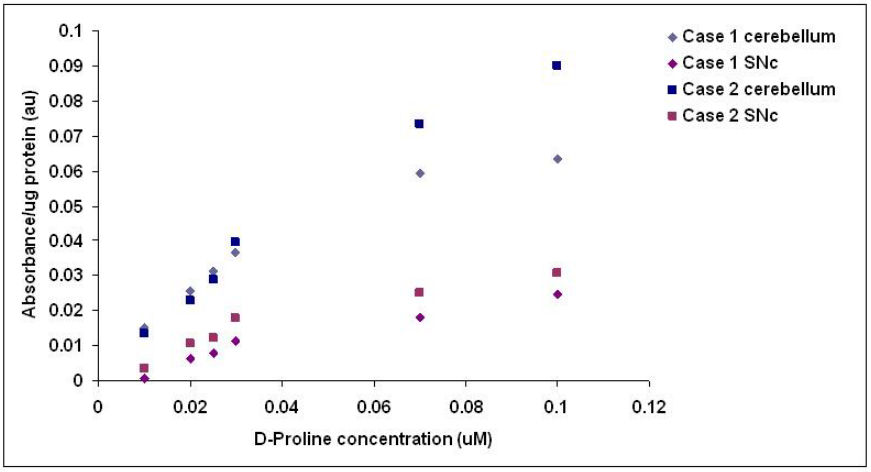

FIGURE 3-12 Within brain comparison of DAO activity in the SNc and cerebellum in two subjects, case 1 and case 2. Absorbance was measured at 571nm and normalised to the protein content within each sample and is directly proportional to the breakdown of D-proline.

3.4 DISCUSSION

3.4.1 Detection of SRR and DAO in the human brain

The antibodies used in this study had been validated by western blotting in the preceding chapter (Chapter 2, Section 2.3.1). The antibody to SRR detected a single band of predicted molecular weight for SRR in human brain extracts (Chapter 2, Section 2.3.1, Figure 2.2, Lanes 1-2). In immunohistochemistry in human tissue, the antibody detected immunoreactivity in all regions studied (Figures 3.4-3.7). This is in agreement with previous detection of SRR in primate (Xia *et al.*, 2004) and human (Steffek *et al.*, 2006; Bendikov *et al.*, 2007) hippocampus and frontal cortex. That a higher antibody concentration of the SRR antibody was required for human immunohistochemistry than in rodent tissue (Materials and Methods, Section 3.2.2), is likely due to the antibody having less affinity for human SRR; this is because the immunogen used to generate the antibody was a 121 amino acid peptide sequence of mouse SRR, which is not completely complementary to the human SRR.

In the preceding chapter, the GSK-DAO antibody to DAO was found to detect a single band of predicted molecular weight for DAO by western blotting in human cerebellum (Chapter 2, Section 2.3.1, Figure 2.3 B, Lane 1, Figure 2.3 C, Lane 1) but in human DPFC DAO detection was variable and sometimes negligible (Chapter 2, Section 2.3.1, Figure 2.3 D). However, the antibody reliably detected DAO by immunohistochemistry in all regions of the human brain studied (Figures 3.8 – 3.11). This disparity was also detailed for rodent frontal cortex western blotting and immunohistochemistry findings. As described (Chapter 2, Section 2.4.1) the disparity may be due to a regional difference in the antigenicity of DAO differentially affected by western blotting and immunohistochemical protocols.

Indeed, the human immunohistochemical findings were corroborated by ISHH (see below), providing evidence that the cortical cell types identified immunohistochemically do express DAO. Bendikov *et al.* (2007) were able to detect DPFC DAO by western blotting in human brain in contrast to the present findings. This may be due to their antibody, different to ours, being less susceptible to any differences in antigenicity of DAO.

3.4.2 Regional and cellular distribution of SRR and DAO in the human DPFC

SRR immunoreactivity in the DPFC (summarised in Table 3.3) was detected in both grey and white matter with an enhancement in the latter (Figure 3.4 A). Cortical grey and white matter SRR expression in the human brain is in agreement with rodent (see Chapter 2, Section 2.4.2, Table 2.1) and primate (Xia *et al.*, 2004) immunohistochemical findings. These findings are also consistent with the detection of SRR by western blotting in the human DPFC (Steffek *et al.*, 2006; Bendikov *et al.*, 2007) and the presence of D-serine in the human cortex (Kumashiro *et al.*, 1995; Bendikov *et al.*, 2007).

The greater cortical white than grey matter immunostaining for SRR is at odds, however, with the prevailing view of SRR and D-serine's enrichment in grey matter astrocytes reported from rodent studies (Schell *et al.*, 1995, 1997; Wolosker *et al.* 1999b). However, as discussed in the preceding chapter (Chapter 2, Section 2.4.2), both SRR and D-serine are likely prominent in rodent white matter also. Moreover, in the human brain, white matter D-serine concentrations are at least equal to those in grey matter (Kumashiro *et al.*, 1995). Taken together, these findings suggest cortical SRR in the human has a prominent role in the white as well as, or greater than that in grey matter.

TABLE 3-3 Regional SRR and DAO immunohistochemistry distribution in human brain and putative cellular expression.

	DAO	SRR
DPFC		
Pyramidal neurons	+++	0
Grey matter glia	++	++
Grey matter neuropil	+	+
White matter glia	++	+++
White matter neuropil	+	+++
Hippocampal formation		
Dentate gyrus granule cells	++/-	0
Stratum pyramidale neurons	+++	0
Radiatum/lacunosum strata glia	+	++
Moleculare stratum glia	+	0
SNc		
Dopamine neurons	+++	0
Glia	+/-	++
IO		
Neurons	++	0
Glia	+	++
Cerebellum		
Molecular layer		
Radial processes	+	+
Glia	+	+
Purkinje cell layer		
Purkinje cells	0	+/-
Bergmann glia	+++	++
Granule cell layer		
Granule cells	0	0
Golgi cells	0	0
Glia	++	+++
White matter		
Glia	++	+++

Immunoreactivity: 0, absent, +/- mild-moderate and variable, +, mild-moderate, ++, moderate, +++, strong.

Cellularly, grey matter SRR localized to putative glia, similar in morphology and size to GFAP-reactive astrocytes, thus positing their astrocytic identity (Figure 3.4). However, we cannot rule out additional microglial (Wu *et al.*, 2004) or

oligodendrocytic SRR expression. In counter-stained sections, putative SRR-positive astrocytes were seen in the vicinity of unlabelled pyramidal cell bodies (Figure 3.4 D), in contrast to neuronal SRR expression in the rodent cortex (Chapter 2, Section 2.3.2, Table 2.1). This difference could be a methodological limitation where the antibody was more sensitive to neuronal SRR in rodent than human tissue. Alternatively, there may be a species difference whereby neuronal SRR is not expressed in higher-order mammals. Consistent with this, Xia *et al.* (2004) do not find neuronal SRR in the rhesus monkey cortex and localize its immunoreactivity to grey matter GFAP-reactive astrocytes.

In white matter, SRR localized to putative glia, smaller than GFAP-reactive glia in adjacent sections, suggesting that they are GFAP-negative astrocytes, oligodendrocytes or microglia. These findings are consistent with our observations in the rodent of non-stellate glial SRR immunolabelling in telencephalic white matter such as the corpus callosum (Chapter 2, Section 2.3.3, Table 2.1).

DAO immunoreactivity in human DPFC was robustly detected with grey over white matter enhancement (Figure 3.8 A). At the cellular level, DAO localized predominantly to grey matter pyramidal neurons with a punctate appearance and to putative glia (Figure 3.8 B-D), possibly GFAP-reactive astrocytes. The punctate immunostaining in pyramidal neurons may reflect a peroxisomal location of DAO (Arnold *et al.*, 1979; Moreno *et al.*, 1999). In the white matter (Figure 3.8 E), moderate DAO immunoreactivity was observed in putative glia, smaller than GFAP-reactive astrocytes, and thus potentially GFAP-negative astrocytes, oligodendrocytes or microglia.

These findings were consistent with rat and mouse neuronal cortical DAO expression (Chapter 2, Section 2.3.6, Table 2.1). However, they were unexpected in

view of absent DAO activity in the human cortex (Kapoor *et al.*, 2006), replicated here, where DPFC DAO activity could not be detected with our assay when run alongside human cerebellar positive control extracts (Section 3.3.9). The immunohistochemical data were additionally unexpected since DAO could not be reliably detected by western blotting in the human DPFC (Chapter 2, Section 2.3.1 and discussed above). However, DAO mRNA also localized to DPFC pyramidal neurons (Figure 3.8) corroborating their DAO expression. Taken together therefore, the evidence suggests that DAO is expressed in the cortex, and therein to neurons, but presumably in a form with undetectable activity. This is consistent with the situation in the rodent, described in Chapter 2, Section 2.4.1 where some of the possible reasons for the paradox have been discussed.

3.4.2.1 Models of synaptic D-serine function in the human DPFC

In the human cortical grey matter, the exclusive glial expression of SRR suggests that the traditional model of glial D-serine functioning at tripartate synapses may occur (Chapter 2, Figure 2.12). Indeed, SRR positive astrocytes were sometimes seen in the vicinity of pyramidal neuron apical dendrites and thus potentially synaptic regions. However, an addition to this model is required given the demonstration of DAO expression in both neurons as well as glia, and thus potential breakdown of D-serine in post-synaptic neurons, possibly via Asc-1 re-uptake (Figure 3.13). Notwithstanding, the lack of detectable DAO activity in the DPFC means that D-serine breakdown by the enzyme, in either neurons or glia, is purely speculative. Again, as described for the rat and mouse, it is possible SRR contributes to DPFC D-serine breakdown (Panizzutti *et al.*, 2001; De Miranda *et al.*, 2002; Foltyn *et al.*, 2005; Stříšovský *et al.*, 2003; Stříšovský *et al.*, 2005).

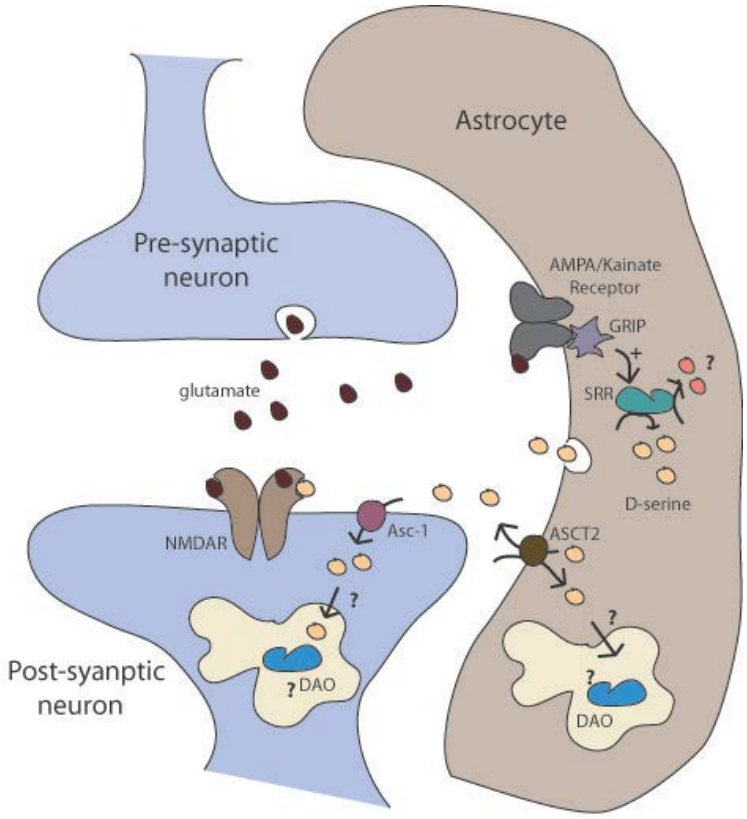

FIGURE 3-13 Model of D-serine synaptic function in the human DPFC. A revision of the tripartate synapse model: glial synthesized and released D-serine acts on post-synaptic NMDARs, and may be re-uptaken into both neurons and glia for breakdown by pero-xisomal DAO. However, DPFC DAO may not be active in D-serine breakdown and SRR may function in this capacity, eliminating D-serine to pyruvate and ammonia (orange circles).

In cortical white matter, the robust expression of SRR implies an important role for D-serine. As discussed for the rat and mouse (Chapter 2, Section 2.4.3.2, Figure 2.14), D-serine metabolism here may be important in glial-glial or neuronal-glial signalling (Figure 2.14) or in cellular energy requirements since SRR can generate pyruvate (Williams *et al.*, 2006, Puyal *et al.*, 2006).

3.4.3 SRR and DAO distribution in the human hippocampus

SRR immunoreactivity was detected in the human hippocampus (summarised in Table 3.3), consistent with previous reports in human (Steffek *et al.*, 2006); Bendikov *et al.*, 2007) and non-human primate (Xia *et al.*, 2004). Herein, SRR localized to putative GFAP-reactive astrocytes in the stratum radiatum/lacunosum (Figure 3.5) and alveus. Consistent with this, SRR and GFAP were demonstrated to co-localize in the primate hippocampus (Xia *et al.*, 2004) and rodent observations

(see Chapter 2, Table 2.1 for summary) demonstrated hippocampal SRR was glial. However, SRR-positive glia in the rat and mouse did not resemble GFAP-reactive astrocytes, suggesting a possible species difference in the glial sub-types expressing SRR.

DAO immunoreactivity was robustly detected in human hippocampus, consistent with previous detection of DAO protein expression in this region (Bendikov *et al.*, 2007) but discordant with undetectable DAO activity (Section 3.3.9). As described above for the DPFC, this could reflect the expression of DAO with undetectable activity.

Cellularly, DAO localized to putative glia of the radiatum/lacunosum and moleculare strata (Figure 3.9 F), consistent with our observations in rats and mice. Human DAO immunoreactivity was also prevalent in pyramidal neurons and in some cases in granule cells of the hippocampus (Figure 3.9 B-E), which was corroborated by DAO mRNA localization to the same cell types (data not shown). Neuronal DAO in the human hippocampus is discordant with rodent immunohistochemical observations (Chapter 2, Section 2.3.7, Table 2.1), but in agreement with the rat immunohistochemical observations of Moreno *et al.* (1999). However, the potential antibody cross-reactivity of the Moreno *et al.* (1999) antibody to DAspOx (Shleper *et al.*, 2005; discussed in Chapter 2, Section 2.4.2), which is expressed by pyramidal and granule cells in the rat (Zaar *et al.*, 2002), should be considered. If this cross-reactivity accounted for the findings of Moreno *et al.*, (1999) then the present data may indicate a species difference in neural hippocampal DAO expression.

Of the neuronal DAO expression, immunoreactivity was observed particularly prominently in CA1 pyramidal neurons. Differences in gene expression

between the pyramidal neurons of CA1 and other CA subfields are not unprecedented (e.g. Eastwood *et al.*, 2005) and presumably reflect the individual properties of this cell type (Duvernoy, 1998). More unusual, was the observation of DAO immunoreactivity in granule cells of the dentate gyrus in only half the subjects. Origin of tissue or demographics were not the cause of this variability, such that its source is unknown.

3.4.3.1 Models of synaptic D-serine function in the human hippocampus

As described for the rat and mouse, glial SRR expression and thence glial derived D-serine in the radiatum/lacunosum strata may act at tripartate synapses (Chapter 2, Section 2.4.3.1, Figure 2.12), presumably onto post-synaptic interneurons characteristic of these strata (Duvernoy, 1998). Therein, D-serine's actions at interneuron NMDARs may regulate the excitation-inhibition balance in the hippocampus (Martina *et al.*, 2003). As in the rodent, D-serine may be re-uptaken from these synapses into glia for breakdown by DAO. Alternatively, the prominent neuronal expression of DAO, particularly in CA1, implies that D-serine breakdown could also occur neuronally, concurring with expression of Asc-1 on hippocampal pyramidal neurons in the rat (Helboe *et al.*, 2003; Matsuo *et al.*, 2004). However, again, the caveat of undetectable DAO activity in the hippocampus applies.

3.4.4 SRR and DAO distribution in the human SN and IO

In the SNc, SRR localized to scattered putative glia, also observed throughout neighbouring structures including the superior colliculus and cerebral peduncle (Figure 3.6; summarised in Table 3.3). These observations agree with rodent

immunohistochemical findings (see Chapter 2, Table 2.1 for summary) and concord with the detection of SRR mRNA in the human SN (De Miranda *et al.* 2000).

DAO in this region localized to putative dopaminergic neurons (Figure 3.10, Table 3.3) consistent with rat and mouse immunohistochemical observations (Chapter 2, Table 2.1; Moreno *et al.*, 1999) and with DAO activity which was detected in the human SN (Section 3.3.9). This finding is of clinical significance given the demonstration that DAO can oxidise D-DOPA in an alternative pathway to dopamine synthesis, and the suggestion that D- and L-DOPA may be combined therapeutically for the treatment of Parkinson's disease (Brannan *et al.*, 1996; Moses *et al.*, 1996; Wu *et al.*, 2006; Kawazoe *et al.*, 2007).

Similarly in the IO, SRR localized to putative glia and DAO to putative neurons as well as glia (Figures 3.6 D and 3.10 F). The SRR immunoreactive glia were seen more predominantly surrounding the IO, while DAO immunoreactive neurons and glia were concentrated within the nucleus, producing an apparent inverse distribution of DAO and SRR.

3.4.4.1 Functional implications of D-serine metabolism in the SNc

The glial localization of SRR and predominantly neuronal localization of DAO in the SNc, where DAO was also found to be active, suggests that D-serine may be released from glia and re-uptaken into dopaminergic neurons for breakdown. As discussed for the rat and mouse (Chapter 2, Section 2.4.3.3), glial D-serine may potentiate the responses of NMDAR located on dopaminergic neurons and known to regulate their firing properties and intra-cellular calcium concentrations (Bennet & Gronier, 2007; Choi *et al.*, 2003; Fernandez-Espejo *et al.*, 2007). An alternative role

for DAO in dopamine synthesis is speculative (discussed in Chapter 2, Section 2.4.3.3).

Thus, in the SNc, D-serine metabolism may have an important role in regulating dopaminergic firing patterns. It would be interesting if this were also the case for dopaminergic cells of the VTA in the human which project in the mesolimbic and mesocortical pathways, implicated in the pathophysiology of schizophrenia (Chapter 1, Section 1.5.1). That VTA neurons were DAO positive in the rat and mouse (Chapter 2, Section 2.3.8), where the enzyme has been demonstrated to breakdown endogenous D-serine (Fernandez-Espejo *et al.*, 2007), adds some support to this possibility. Blockade of NMDARs on VTA neurons in the rat has been shown to increase their firing rate and stimulate DA release in the mesolimbic pathway (discussed in Bennett & Gronier, 2007). Given the implication of hyperactivity of the mesolimbic pathway in schizophrenia (Chapter 1, Section 1.5.1), DAO inhibition and thence D-serine elevation in the VTA region could be of therapeutic benefit.

3.4.4.2 Functional implications of D-serine metabolism in the I O

The IO is an incomplete capsule of grey matter, the aperture of which is the hilum. Olivocerebellar fibres project from IO, pass through the hilum, decussate and pass through and partly around the opposite IO. The fibres then ascend via the inferior cerebellar peduncle as the olivocerebellar tract to the cerebellum where they enter as climbing fibres synapsing onto Purkinje cells. Therefore the glia surrounding the IO, may be oligodendrocytes ensheathing these fibres or nearby astrocytes. As such, D-serine, potentially synthesized by SRR concentrated to glia surrounding the IO, may be involved in potentiating axonal glutamate actions in the white matter or

glial-glial signalling, as was discussed for white matter glial SRR expression in the rat and mouse (Chapter 2, Section 2.4.3.2, Figure 2.14). The functional implications of this are unknown, but glial SRR in this region and thence D-serine, could affect neural input to the cerebellum carried from the IO by olivocerebellar fibres.

Within the IO, D-serine synthesized in SRR immunoreactive putative glia may be released to act in tripartate synapses, potentiating responses of the NMDARs expressed on the soma and dendrites of IO neurons (Chen *et al.*, 2006). D-serine may potentially then be re-uptaken into neurons for breakdown post-synaptically by DAO. Blockade of the NMDAR co-agonist site on IO neurons has been shown to abolish the spontaneous oscillatory activity of these cells (Placeantonakis & Welsh, 2001) suggesting that D-serine metabolism in this region may impact on IO output. However, the greater DAO expression than SRR within the IO suggests that DAO would have a functional role outside of breaking down locally synthesized D-serine.

3.4.5 SRR and DAO distribution in the human cerebellum

SRR immunoreactivity was robustly detected in the human cerebellum (summarised in Table 3.3) and localized to putative granule cell layer, white matter and Bergmann glia, in addition to some moderately labelled Purkinje cells (Figure 3.7). These findings are broadly consistent with rat and mouse immunohistochemical observations for SRR (Chapter 2, Table 2.1; Wolosker *et al.*, 1999b) and D-serine (Schell *et al.*, 1995, 1997; Wolosker *et al.*, 1999b; Dememes *et al.*, 2006; Williams *et al.*, 2006). However, Bergmann glia labelling was more prevalent in the human cerebellum than rats and mice, while Purkinje cell labelling was observed more frequently and prominently in the rodent than human. This suggests

that there may be some switch of neuronal to glial SRR expression in the cerebellum between rodent and humans similar to the glial versus neuronal staining in the rodent compared to human frontal cortices.

Human cerebellar DAO activity and immunoreactivity were robustly detected. Immunoreactivity localized to Bergmann glia and their radial processes and putative granule cell layer and white matter glia. Occasional immunolabelling of small round cells in the molecular layer was observed, similar in size to those in the granule cell layer and white matter. These cell types were immunopositive for DAO in the mouse (see Chapter 2, Table 2.1 for summary) and accord to previous reports of DAO in white matter and granule cell layer astrocytes and Bergmann glia (Arnold *et al.*, 1979; Horiike *et al.*, 1987, 1994; Moreno *et al.*, 1999). However, the Bergmann glial staining was much more prominent in the human than rodent cerebellum, as noted for SRR staining also. In addition, unlike immunohistochemical observations in the rats and mice (Chapter 2, Table 2.1; Moreno *et al.*, 1999), human DAO was not expressed in Purkinje cells. This may reflect a species difference with more prominent D-serine metabolism in glial than neuronal cells in the human cerebellum.

Taken together therefore, in the human cerebellum, SRR and DAO immunoreactivities were observed within the same cell types, namely granule cell, white matter and Bergmann glia, suggesting that they could be co-localized with each other, and perhaps with D-serine (Schell *et al.*, 1995, 1997; Wolosker *et al.*, 1999; Dememes *et al.*, 2006; Williams *et al.*, 2006).

3.4.5.1 Models of synaptic D-serine function in the human cerebellum

The functional implications of DAO and SRR distribution in the human cerebellum are similar to those described for the rodent in Bergmann glia (Chapter 2, Section 2.4.4.1). Glial synthesized D-serine in human cerebellum may act at tripartate synapses (Chapter 2, Figure 2.12) potentiating glutamatergic inputs to granule cells in the granule cell layer, or in glial-glial or neuronal-glial synapses in the cerebellar white matter (Chapter 2, Figure 2.14). Bergmann glial D-serine may affect post-synaptic NMDARs on Purkinje cells or pre-synaptic NMDARs regulating input to Purkinje cells and thence Purkinje cell output (Chapter 2, Section 2.4.4.1, Figure 2.15). However, in the human cerebellum, D-serine is presumably cleared from these synapses into glia for breakdown by DAO rather than Purkinje cells. Indeed, since SRR and DAO show a greater glial than neuronal expression in human versus rodent cerebellum, these glial mechanisms of regulation of D-serine signalling are presumably more important.

3.4.6 DAO activity in the human brain

In the human brain, DAO activity was absent from DPFC and hippocampal homogenates but demonstrated in the cerebellum and SN (Figure 3.12). DAO activity was inhibited by sodium benzoate (data not shown), a competitive inhibitor of DAO (Singer & Mason, 1967; Moses *et al.*, 1996), demonstrating that the activity measured was DAO specific. The absence of DPFC and hippocampal DAO activity accords with previous findings in rats and mice (Horiike *et al.*, 1987, 1994; Schell *et al.*, 1995; Wang and Zhu, 2003) and human (Kapoor *et al.*, 2006) cortex and presumably means that DAO is expressed in the cortex and hippocampus in a form with activity undetectable by commonly used assays. If cortical DAO is indeed inactive in D-amino acid breakdown then it presumably has another function,

which is worthy of investigation. However, endogenous cortical DAO activity is suggested by two studies demonstrating that mutation (Hashimoto *et al.*, 1993b) and pharmacological inhibition (Adage *et al.*, 2007) of DAO in the rat led to small increases in cortical D-serine.

In the SN, robust DAO activity was detected, in contrast to Horiike *et al.*, (1994) who did detect activity in this region in the rat. This may reflect differential sensitivity of the DAO activity assays used. In the cerebellum, robust activity was detected in agreement with previous studies (Horiike *et al.*, 1987, 1994; Schell *et al.*, 1995; Wang and Zhu, 2003; Kapoor *et al.*, 2006).

3.4.7 Concluding remarks and limitations

The principal limitations of this study are those described for the rat and mouse study (Chapter 2, Section 2.4.5); namely that co-localization studies were not carried out and that D-serine itself was not measured. As discussed this was in part due to some controversy over reliable detection of D-serine immunohistochemically (e.g. Schell *et al.*, 1997 and Kartvelishvily *et al.*, 2006), required for cellular resolution.

The main findings of this study are; 1) the human DPFC expresses glial SRR, in contrast to the neuronal expression in the rodent; 2) the human DPFC robustly expresses DAO, predominantly neuronally, but DAO activity in this region is undetectable; 3) the hippocampus expresses predominantly glial SRR and neuronal DAO which was of undetectable activity; 4) SRR is expressed by putative glia in the SNc and surrounding structures and within and around the IO; DAO in the SN and IO was also neuronal and in the SN was active; 5) both SRR and active DAO are expressed in the cerebellum, predominantly in Bergmann glia and other glial

cells, while Purkinje cells are largely immunonegative; this contrasts to the lesser Bergmann glial and greater Purkinje cell immunoreactivities in the rodent.

These findings therefore extend knowledge on D-serine metabolism in the human brain. They provide novel data and highlight some species differences which underscore the caution required when extrapolating rat and mouse observations to the human brain. For example D-serine synthesis in the human appears to be exclusively glial but in the rats and mice there is a presumed neuronal component. The functional implications or reasons for this are unknown. Perhaps glial synaptic modulation at so called tripartate synapses is more sophisticated and/or prevalent in the human brain. DAO, on the other hand, showed neuronal expression in the cortex, hippocampus and SN but mainly glial in the cerebellum. The neuronal expression was more prevalent than in the rats and mice in the hippocampus and SN, but in the cerebellum was less so. The regional differences in the human also highlight that the differences in DAO activity are unlikely to be related to glial versus neuronal expression, since cerebellar DAO (predominantly glial) and SN DAO (predominantly neuronal) both exhibited detectable activity. The underlying reasons for the differences in DAO activity in the human between the cortex and SN/cerebellum are therefore unknown. It is interesting that antigenicity of DAO is presumably different in the cortex than cerebellum, and this may relate to differences in activity. Alternative DAO transcript expression in the cortex and cerebellum may be one possible reason for DAO's different properties in these regions. In addition, it is interesting that an inactive form of DAO is thought to be required for *in vivo* trafficking into peroxisomes (Caldinelli *et al*., 2004) suggesting that some intra-cellular regulation of DAO activity must exist.

Despite the questions unveiled by this study however, for example the role of cortical DAO and the reasons for apparent species differences, these data provide

an important prelude to studying the expression of SRR and DAO in the human brain and schizophrenia and understanding the possible cellular mechanism of their pathophysiological contributions.

4. THE EXPRESSION OF DAO AND SRR IN SCHIZOPHRENIA

4.1 INTRODUCTION

Impairment of D-serine function has been implicated in the pathophysiology of schizophrenia, based on reports of its reduced levels in the disorder (Hashimoto *et al*., 2003, 2005; Yamada *et al*., 2005), and its ability as an adjunctive therapy to ameliorate some symptoms of the disorder (Tsai *et al*., 1998; Heresco-Levy *et al*., 2005) (see Chapter 1, Section 1.9). It is possible that impaired D-serine function in schizophrenia may arise from its aberrant metabolism, a theory upheld by the association of DAO with the disorder (Chumakov *et al*., 2002; Liu *et al*., 2004; Schumacher *et al*., 2004; Corvin *et al*., 2007b; Wood *et al*., 2007, but see Fallin *et al*., 2005; Yamada *et al*., 2005; Goldberg *et al*., 2006; Liu *et al*., 2006; Shinkai *et al*., 2007; Vilella *et al*., 2007) and tentatively by evidence of a weak genetic contribution of SRR to schizophrenia (Goltsov *et al*., 2006; Morita *et al*., 2007, but see Yamada *et al*., 2005, Strohmaier *et al*., 2007).

Despite their implications in the disorder, at the time of this study no published reports had investigated the expression of DAO and SRR in schizophrenia. The aim of this study was therefore to quantify DAO and SRR expression, at both the mRNA and protein levels, in patients with schizophrenia compared to control subjects. It was hypothesized that increased DAO and/or decreased SRR expression could lead to reduced levels of D-serine in schizophrenia.

Any expression changes in DAO and SRR in the disorder could, in part, be conferred by SNPs in the DAO and SRR genes associated with illness. This is

because associated DAO and SRR SNPs are mostly intronic regions or in UTRs (Chumakov *et al*., 2002; Liu *et al*., 2004; Schumacher *et al*., 2004; Goltsov *et al*., 2006; Corvin *et al*., 2007b; Morita *et al*., 2007; Wood *et al*., 2007) and the mechanism by which such non-coding SNPs may contribute to disease pathophysiology is thought to be via altered gene expression (Harrison & Weinberger, 2005). While such a mechanism of gene expression alteration is less likely for SRR, where association to schizophrenia has not been demonstrated as robustly as it has for DAO, it is important to study SRR and DAO together. This is because the supposition that their altered expression could affect D-Serine levels would depend on there being no compensatory effects between them.

A second potential cause of altered gene expression in schizophrenia is antipsychotic medication. To explore this, the expression of SRR and DAO in antipsychotic treated rats was also investigated.

4.1.1 Choice of methodology

4.1.1.1 Real-time PCR for mRNA quantification

The method chosen to investigate SRR and DAO mRNA expression was real-time PCR using SYBR Green I to monitor fluorescence. PCR analysis involves the extraction of total RNA from individuals and the production of complementary DNA (cDNA) by reverse transcription. The levels of a specific target cDNA are then quantified by PCR using sequence specific primers. Under appropriate conditions, and during the exponential phase of the reaction, the amount of amplification product is directly proportional to the level of expression of the original target cDNA sequence and therefore reflects the amount of the complementary mRNA transcript within the starting sample. Thus PCR allows accurate and sensitive

quantification of the levels of a specific mRNA in different individuals. Real-time PCR is superior to conventional PCR methods because it utilizes fluorescence to monitor the reaction temporally and therefore allows gene expression to be quantified in the exponential phase of the reaction. An inexpensive method relies on double-stranded DNA binding dyes, such as SYBR Green I. These fluoresce upon binding to the double-stranded DNA product such that the amount of fluorescence is proportional to the amount of double-stranded amplification product (Yin *et al*., 2001; Wilson *et al*., 2004).

While real-time PCR is the most sensitive method of RNA quantification, it is also sensitive to error, given that any experimental variability will also be amplified exponentially. Such variability may arise inadvertently from different starting concentrations of mRNA, pipetting errors or different reaction efficiencies between individual samples and PCRs. The result is misinterpretation of the expression profiles of the target genes. To minimise these errors and sample-to-sample variation, an internal reference can be amplified simultaneously with the target sequence (Bustin, 2000). The internal standard should be a cellular RNA, to which other RNA values can be normalised and thus should be expressed at constant levels across experimental treatments, or diagnostic groups. Commonly used 'housekeeping genes' expressing such RNAs are ribosomal 18s (r18s), glyceraldehyde-3-phosphate dehydrogenase (GAPDH) and cyclophilin (Burnet *et al*., 1994; Eastwood *et al*., 1997a; Stefanis *et al*., 1998; Bustin, 2000). Because some contention exists over the use of particular housekeeping genes (Bustin, 2000), in the present study both r18s and GAPDH were chosen in order to verify that the normalised results from each were in agreement.

4.1.1.2 Western blotting for protein quantification

For this study, western blotting was chosen for quantification of DAO and SRR immunoreactivity. This technique allows measurement of a target protein whose authenticity can be verified on the basis of molecular weight. As with mRNA detection, variability in starting amounts of total protein and pipetting error can compound the analysed expression profiles of target proteins. For this reason a housekeeping gene is used as an internal reference or 'loading control'. Here cyclophilin was used as an internal reference, the expression of which has been shown to be unaltered in schizophrenia (Burnet *et al.*, 1994; Eastwood *et al.*, 1997a).

4.1.2 Choice of tissue and regions for analysis

For this study, two brain regions, the DPFC and the cerebellum, were chosen for analysis of DAO and SRR mRNA and protein abundance in schizophrenia. This was based on the reported preferential localizations of SRR and DAO to the DPFC and cerebellum respectively (Horiike *et al.*, 1987, 1994; Schell *et al.*, 1995; Wolosker *et al.*, 1999b; Wang & Zhu, 2003; Kapoor *et al.*, 2006).

Initially, brain tissue available from two sources was used: a series of brains from patients with schizophrenia and control subjects collected in Oxford and another collected in London. The investigation of DAO and SRR expression in schizophrenia with these brain series was carried out at the same time, and, given the limitations of tissue availability, the data sets were combined to allow for more robust statistical analysis. The results of this investigation have been published (Verrall *et al.*, 2007).

A subsequent study, based on the findings of the first, aimed to investigate SRR protein expression in the DPFC in the Stanley Foundation brain series. This

series is bigger than that utilised in the first study, comprising 60 well-matched cases, 15 each with diagnoses of schizophrenia, bipolar disorder and unipolar depression and 15 controls. Limited tissue and time precluded studying other variables in the Stanley Foundations brain series.

Finally, tissue from the frontal cortex and cerebellum of rats treated with antipsychotic medication was studied for SRR and DAO protein abundance to delineate any effects of medication on gene expression in these regions.

4.2 MATERIALS AND METHODS

4.2.1 Human tissue

The subjects used in this study came from the Oxford, London and Stanley Foundation brain series (described in Chapter 3, Section 3.2.1). Tissue blocks were processed as described (Chapter 3, Section 3.2.1). All material was coded and experiments carried out blind to diagnosis of the subject. Code-breaking and analysis for the Stanley Foundation series was performed by Prof P. J. Harrison.

4.2.2 Antipsychotic treatment in rats

Adult male Sprague-Dawley rats (Harlan-Olac) weighing 225-250g were treated with the typical antipsychotic haloperidol (1 mg/kg/day; $n = 8$), the atypical antipsychotic clozapine (25mg/kg/day; $n = 8$) or the same volume of saline ($n = 8$) by intraperitoneal injection once-daily for 14 days. Animals were sacrificed six hours after the final injection by a lethal injection of pentobarbitone and perfused transcardially with PBS. Brains were removed, frozen on dry ice/alcohol slurry and stored at -80ºC. Procedures were carried out by Dr Phil Burnet (Department of Psychiatry, Oxford). Sections were taken as described (Chapter 2, Section 2.2.1) and slides stored at -80ºC prior to use for protein extraction.

4.2.3 Protein extraction and western blotting

Protein was extracted from human DPFC and cerebellar sections and antipsychotic treated rat sections as described (Chapter 2, Section 2.2.3); for the Stanley Foundation series, ~200mg DPFC tissue was homogenised in 300µl protein extraction lysis buffer.

Western blotting was carried out as described (Chapter 2, Section 2.2.4) using primary antibodies to SRR at 1:500 and the GSK-DAO antibody at 1:1000-1:3000. Characterisation and validation of these antibodies is detailed in Chapter 2, Section 2.3.1 and Verrall *et al.* (2007). As a loading control, an antibody to the housekeeping gene cyclophilin (AbCam) was used at 1:100,000. Membranes were probed simultaneously for DAO and cyclophilin or SRR and cyclophilin overnight at 4ºC.

Secondary antibodies used were HRP-conjugated anti-mouse immunoglobulin (DAKO) at 1:1000 for SRR and anti-rabbit immunoglobulin (Chemicon) at 1:5000 for DAO and cyclophilin. Immunoreactive bands on photographic film were analyzed by densitometry using a light box with the AlphaImager analysis system and the optical density values for the target immunoreactive bands were normalised to those of loading control signals for the same sample. All experiments were run in duplicate and mean data used for analysis.

For studies using the Oxford and London brain series, individuals from each series were assigned at random and loaded onto two gels. For studies using the Stanley Foundation series, 15 individuals were assigned blind to diagnosis to each gel. In addition to these test samples, total protein from three individuals (Stanley numbers 10, 20 and 30) were loaded onto every gel, to allow data from different gels

FIGURE 4-1
Representative western blot (A) and standard curve (B) of linear protein detection. Image shows SRR and cyclophilin protein detection in the Stanley Foundation. A protein concentration in the linear range of detection for the target gene and loading control was chosen for all further studies.

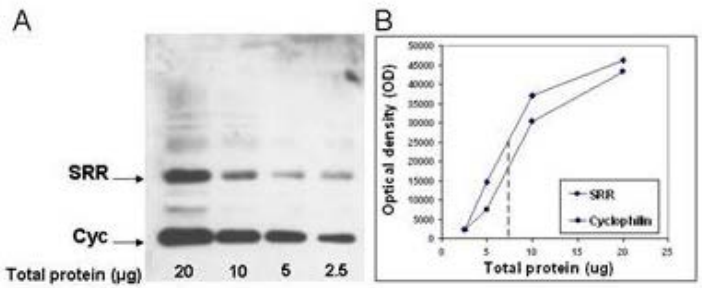

to be directly compared. The coefficient of variation of immunoreactivity measures for these samples was below 20% across gels (data not shown).

Before performing the main quantitative western blot study, pilot studies were carried out using a standard curve of protein (20µg – 2.5µg) made from pooled protein from all subjects to be studied within each brain series. A protein concentration was selected within the linear range of detection of SRR, DAO and cyclophilin of this standard curve and used for loading in all further experiments (Figure 4.1). For quantification of DAO and SRR in the Oxford and London brain series, 10µg total protein was used from each individual. For quantification of SRR in the Stanley Foundation brain series, 7.5µg total protein was used from each individual.

4.2.4 RNA extraction

To extract total RNA from human tissue, 2-3 frozen tissue sections were homogenized in 1ml Tri reagent (Sigma) using a 19-gauge needle and syringe and incubated at room temperature for five minutes. A 200µl volume of chloroform was

added and the sample mixed well and incubated at room temperature for ten minutes. The sample was centrifuged at 12000*g* for fifteen minutes at 4ºC and the aqueous phase, containing the RNA, removed. To precipitate the RNA, 500µl/ml isopropanol was added, incubated at 4ºC for twenty minutes and centrifuged at 12000*g* for fifteen minutes at 4ºC. The pellet was washed twice in 75% ethanol, dried, resuspended in nuclease-free water (Promega) and stored at -70ºC. Total RNA concentration was determined by spectrophotometric absorbance measurements at 260nm using a NanoDrop (NanoDrop Technologies, Wilmington, USA) according to manufacturer's instructions.

4.2.5 Reverse Transcription

RNA was DNAse treated to remove any contaminating DNA (which could be amplified in subsequent PCR reactions). 2µg RNA was treated for one hour at 37ºC with 1U RQ1 RNase-Free DNAse (Promega) and 24U RNasin ribonuclease inhibitor (Promega), then heated to 70ºC for five minutes to inactivate the DNAse. DNAse-treated RNA was then divided into two aliqouts: one was reverse transcribed using a High Capacity cDNA Archive Kit (Applied Biosystems, Warrington, UK) and the other subjected to the same reaction without the enzyme, thus serving as a negative control. Reverse transcription was carried out according to manufacturer's instructions. Briefly, 1 or 2µg of each RNA sample was incubated with 50U/ul MultiScribe RT, 1x reverse transcriptase buffer, 4x deoxynucleotide triphosphates (dNTPs) mix and 1x random hexamer mix to serve as primers at 25ºC for ten minutes followed by 37ºC for two hours. Solutions were diluted 1:10 or 1:20 in nuclease-free water (Promega) and stored at - 20ºC.

4.2.6 Primer design

Primers were designed for SRR, DAO, r18s and GAPDH (Table 4.1) using Primer 3 software (http://frodo.wi.mit.edu/cgi-bin/primer3/primer3_www.cgi). PCR products spanned exon-exon boundaries such that any contaminating genomic DNA would be unlikely to amplify given its size or, if it were, would be distinguishable by size from the PCR products. Specificity of primers for each transcript was confirmed using a nucleotide-nucleotide alignment search (http://www.ncbi. nlm.nih.gov/BLAST/). Primers were synthesized by Sigma.

TABLE 4-1 Sequences for real-time PCR forward (F) and reverse (R) primers.

Target gene	Sequence 5' - 3'	Product size (bp)
SRR	F; AACCTAGTGATGAGTCCAGAGAAA	79
	R; CTGGTTGGGATGTACCATGA	
DAO	F; CGCAGACGTGATTGTCAACT	169
	R; GGATGATGTACGGGGAATTG	
r18s	F; GTAACCCGTTGAACCCCATT	111
	R; CCATCCAATCGGTAGTAGCG	
GAPDH	F; AAGGTGAAGGTCGGAGTC	224
	R; GAAGATGGTGATGGGATTTC	

4.2.7 Real-time PCR

Real Time PCR was performed in an ABI Prism 7000 Sequence Detector system (Applied Biosystems), a combined thermal cycler and fluorescence detector. Reactions were performed in the presence of SYBR Green I to monitor fluorescence.

All reagents for the PCR reaction were supplied by Eurogentec (Southampton, UK), used according to the manufacturer's instructions, and were optimal for use with SYBR Green I and an ABI Prism Sequence Detector.

PCR reaction mix [1x reaction buffer, 3.5mM $MgCl_2$, 200µM dNTP mix, 100nM forward primer, 100nM reverse primer, 0.025 U/µl Hot GoldStar DNA polymerase, 1/2000 (in DMSO) SYBR Green (1/66000)] was added to 25ng of each sample of cDNA template in a final volume of 25µl. Thermal cycling was initiated with incubation at 50ºC for two minutes and 95ºC for ten minutes which was followed by 40 cycles of 95ºC for fifteen seconds for denaturing and 60ºC for one minute for annealing and extension.

All reactions were run in triplicate. A standard curve of known cDNA concentrations (100ng-1.56ng) was made from pooled cDNA from all samples in the brain series to be studied and assayed, in triplicate, simultaneously. PCR reactions were set up in a 96 well plate with optical density caps (Applied Biosystems). Target gene and housekeeping genes were studied on separate plates. To assess any chromosomal or aerosol DNA contamination within the sample, RNA samples that were not treated with the reverse transcription enzyme (negative controls) were subjected to PCR as above. These samples were run on the same plate as reverse transcribed cDNA samples in either duplicate or triplicate.

Following thermal cycling, a dissociation curve analysis was carried out where the PCR product is melted at 95ºC, equilibriated at 60ºC and then slowly re-heated back to 95ºC. The ABI Prism Sequence Detector software constructed derivative melting curves from the dissociation curve analysis, and constructed amplification plots of the fluorescent emission data collected during the PCR amplification plotted against Ct (cycle of threshold) values, corresponding to the number of PCR cycles. The Ct value was then measured for each sample at a given threshold of fluorescence emission intensity within the exponential phase of the PCR reaction. The mean Ct value for each triplicate sample was compared against the standard curve to calculate the relative concentration of target gene sequence.

This value was normalised to the relative concentration of r18s and GAPDH mRNA in the same sample.

4.2.8 Real-time PCR validation

To validate the specificity of the reaction, negative control samples and the data from the dissociation curve were inspected. The PCR product formed during cycling is considered pure when a single temperature of melting peak is demonstrated on the dissociation curve. It is necessary to check the specificity of each PCR reaction because SYBR Green I will bind any double-stranded DNA and thus fluorescence emission can result from contaminating double stranded DNA or primer dimers (Bustin, 2000) which would be evident as further peaks on the dissociation curve. Negative control samples demonstrated amplification at least 8 cycles later than positive samples, indicating limited contaminating DNA had been amplified, and all primer pairs amplified a single product as shown on the dissociation curve (Figure 4.2).

Before carrying out the main experiments, pilot studies were conducted to assess the linearity of the real-time PCR amplification of SRR, DAO, r18s and GAPDH with the above primer sets. PCR reactions were carried out on a standard curve of cDNA, made from pooled cDNA from all samples within each brain series to be studied. For an amplification reaction in the linear phase the R^2 value should be greater than 0.99. This was shown for amplification of each gene (Figure 4.3).

FIGURE 4-2 Representative dissociation curve for SRR showing a single strong peak of melting temperature in all reverse transcribed cDNA samples (§), indicative of the amplification of a single PCR product. Negative controls (*) show no peak, indicative of no DNA contamination.

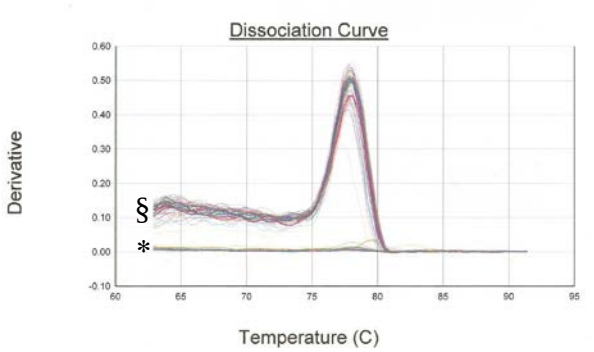

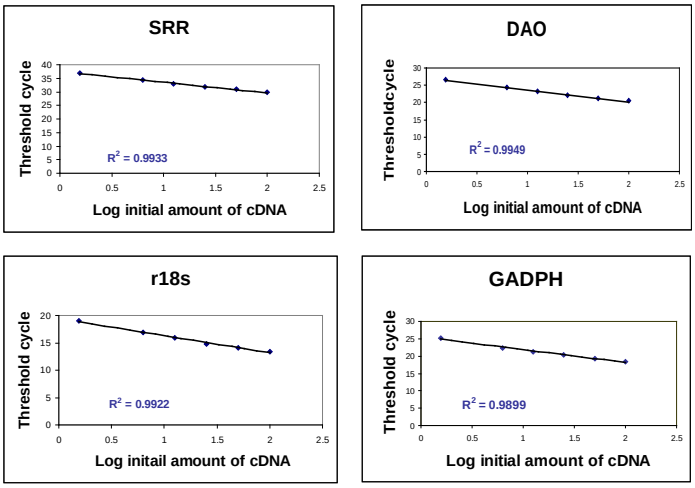

FIGURE 4-3 Representative standard curves for the amplification of SRR, DAO, cyclophilin and GAPDH transcripts showing cycle of threshold values against log cDNA concentration. In exponential amplification reactions there is an inverse linear relationship between the threshold cycle and log cDNA values. All amplifications occurred within the linear phase ($R^2 > 0.99$).

4.2.9 Statistical analysis

The initial study in this chapter analysed DAO and SRR expression in the Oxford and London brain series. The data from each series was inspected separately but for statistical analysis the data sets were combined to improve statistical power. However, previous studies have shown an effect of origin, whereby the mean abundance of some mRNAs and proteins differs between the two brain series (Eastwood *et al.*, 2000a, 2001a, b). In case a similar effect was seen here, Z-scores ([raw score – mean]/standard deviation) for the combined data set were computed (Eastwood *et al.*, 2001a). Z-scored data were inspected for normality using the Kolmogrov-Smirnoff test. The effects of the potential confounding factors age,

agonal state (brain pH) and pmi (Barton *et al*., 1993; Harrison *et al*., 1995) were investigated using Pearson's coefficient. Effects of diagnosis were investigated with one-way analysis of variance (ANOVA). Brain pH, pmi and age were included as co-variates in the ANOVA where the Pearson's correlation was significant ($p < 0.05$). For data not normally distributed, the Mann-Whitney *U* test was used.

A second study investigated SRR protein expression in the Stanley Foundation brain series. All data analysis was performed by Prof P.J. Harrison since the Stanley Foundation brain series is coded. The effects of the potential confounding factors of age of onset, duration of illness, brain pH, freezer storage time, pmi and lifetime antipsychotic dose were investigated using Pearson's coefficient on data partialled for diagnosis. Effects of diagnosis were investigated with one-way ANOVA and any potential confounding factors included as co-variates where the Pearson's correlation was significant. Least significant difference (LSD) post-hoc tests were carried out to look for differences between individual groups.

To test for an effect of antipsychotic drug treatment in rats, data were inspected for normality with the Kolmogrov-Smirnoff test and analysed by one-way ANOVA. Because an effect of antipsychotic compared to saline control was of interest (rather than a comparison of the antipsychotic drugs), one-way ANOVA was conducted with planned LSD post-hoc tests to compare the effect of each antipsychotic drug with saline.

4.3.1 DAO expression in schizophrenia in the Oxford and London brain series

In the cerebellum, DAO mRNA levels normalised to r18s correlated with brain pH (p = 0.048). No other effects of brain pH, age, or pmi were seen. DAO mRNA in the cerebellum was increased in patients with schizophrenia compared to control individuals whether normalised to r18s ($F_{1,26}$ = 10.01, p = 0.004; Figure 4.4 A) or GAPDH mRNA (Mann-Whitney U, p = 0.015; Figure 4.4 B). DAO immunoreactivity

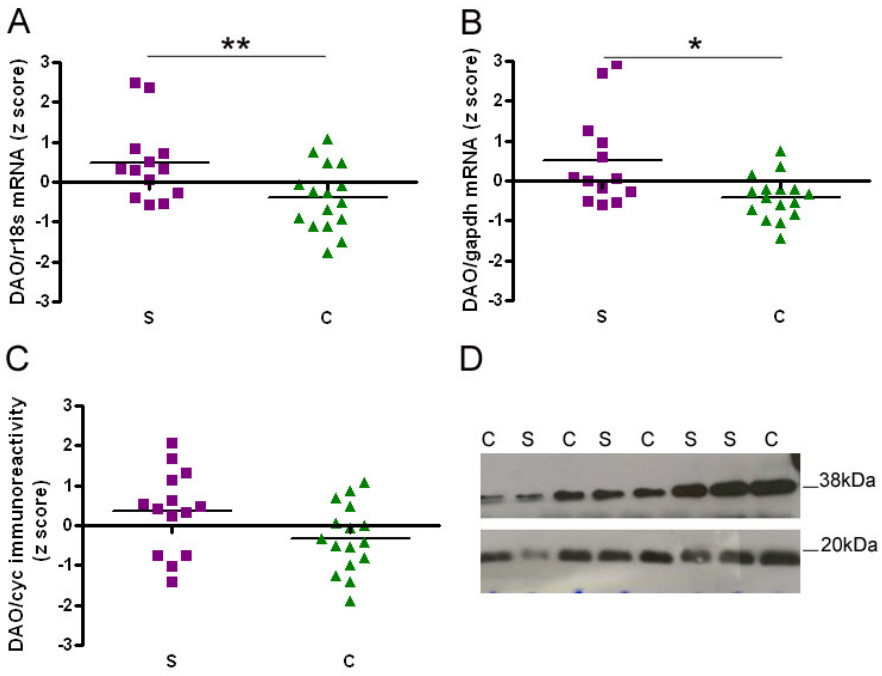

FIGURE 4-4 DAO expression in the cerebellum in patients with schizophrenia (S) and control subjects (C). (A) DAO mRNA abundance normalised to r18s. (B) DAO mRNA abundance normalised to GAPDH. (C) DAO immunoreactivity normalised to cyclophilin. (D) Representative western blot of DAO (top panel) at ~39kDa and cyclophilin (lower panel) at ~20kDa. ** p <0.01, ** p <0.05.

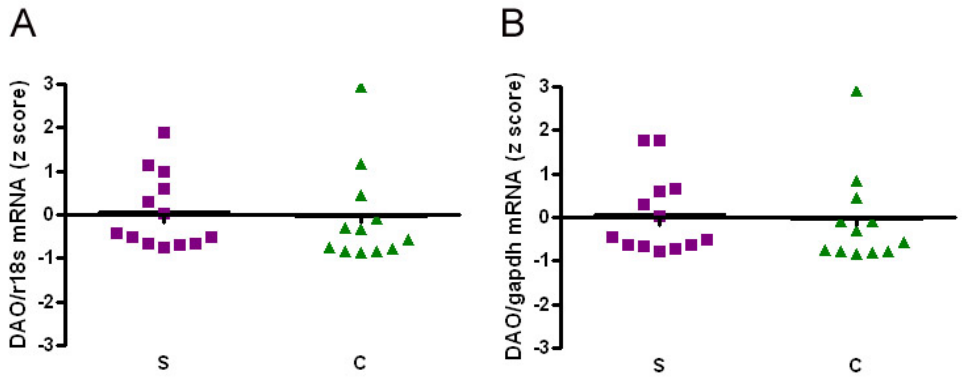

FIGURE 4-5 DAO mRNA abundance normalised to r18s (A) and GAPDH (B) in the DPFC in patients with schizophrenia (S) and control subjects (C).

in the cerebellum showed a trend to being increased in schizophrenia ($F_{1,28} = 3.79$, $p = 0.062$) (Figure 4.4 C, D). The direction of change in DAO mRNA and protein in the cerebellum in schizophrenia was consistent between the Oxford and London brain series, but the increase in schizophrenia appeared more marked in the London series (Table 4.2).

In the DPFC, DAO mRNA normalised to r18s (Mann-Whitney U, $p = 0.33$) or GAPDH (Mann-Whitney U, $p = 0.347$) was unchanged in schizophrenia (Figure 4.5 A, B). DAO immunoreactivity in the DPFC was extremely variable and most subjects expressed levels of DAO protein undetectable by western blotting (see Chapter 2, Section 2.3.1, Figure 2.3 D); consequently, no quantitation was attempted.

4.3.2 SRR expression in schizophrenia in the Oxford and London brain series

No effects of age, brain pH or pmi were seen on SRR mRNA or protein measurements. In the cerebellum, SRR mRNA was unchanged in schizophrenia, whether normalised to r18s ($F_{1,27} = 1.05$, $p = 0.32$) or GAPDH ($F_{1,27} = 2.533$, $p = 0.123$)

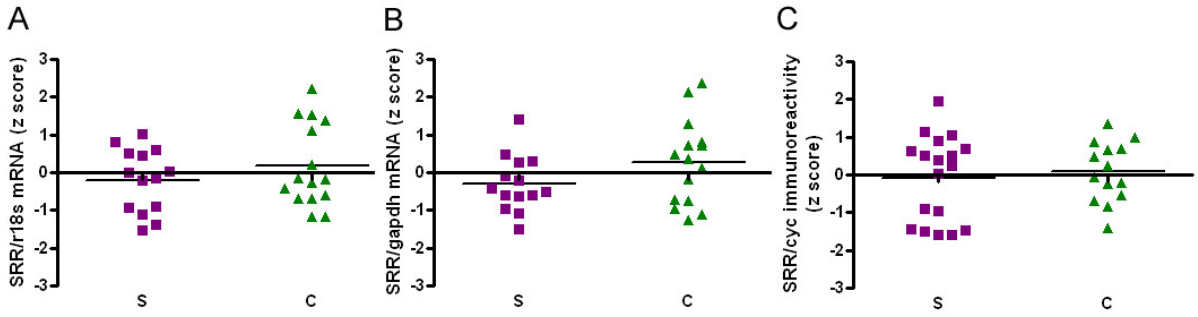

FIGURE 4-6 SRR expression in the cerebellum in patients with schizophrenia (S) and control subjects (C). (A) SRR mRNA normalised to r18s. (B) SRR mRNA normalised to GAPDH. (C) SRR immunoreactivity normalised to cyclophilin.

TABLE 4-2 DAO and SRR expression in the cerebellum and DPFC in patients with schizophrenia and control subjects divided by origin of tissue.

	Oxford series		*London series*	
	Control	Schizophrenia	Control	Schizophrenia
DAO	*n* = 6-9	*n* = 7-8	*n* = 6-7	*n* = 6
Cerebellum				
mRNA/r18s	7.65 ± 1.11	9.69 ± 1.43	11.74 ± 0.86	15.97 ± 1.29
mRNA/gapdh	11.41 ± 1.45	16.35 ± 3.15	25.90 ± 1.92	39.49 ± 5.94
IR	0.53 ± 0.06	0.60 ± 0.08	1.96 ± 0.44	3.40 ± 0.47
DPFC				
mRNA/r18s	8.70 ± 2.77	6.99 ± 0.90	4.34 ± 2.52	9.38 ± 3.69
mRNA/gapdh	15.99 ± 4.93	12.44 ± 1.66	4.26 ± 2.45	10.93 ± 4.56
IR	nd	nd	nd	nd
SRR	*n* = 6-8	*n* = 6-10	*n* = 7-9	*n* = 6-9
Cerebellum				
mRNA/r18s	1.18 ± 0.33	1.02 ± 0.21	1.10 ± 0.16	0.89 ± 0.15
mRNA/gapdh	1.08 ± 0.27	0.76 ± 0.13	1.23 ± 0.16	1.00 ± 0.14
IR	0.63 ± 0.08	0.70 ± 0.09	0.79 ± 0.05	0.66 ± 0.07
DPFC				
mRNA/r18s	1.02 ± 0.13	0.71 ± 0.17	0.95 ± 0.16	1.27 ± 0.10
mRNA/gapdh	0.33 ± 0.03	0.27 ± 0.07	0.85 ± 0.05	1.30 ± 0.18
IR	0.68 ± 0.08	0.88 ± 0.06	0.48 ± 0.06	0.59 ± 0.07

Values are mean ± sem. Immunoreactivity normalised to cyclophilin. nd; not determined. IR = immunoreactivity.

(Figure 4.6 A, B). SRR immunoreactivity in the cerebellum was also unchanged in schizophrenia ($F_{1,30} = 0.22, p = 0.64$) (Figure 4.6 C).

In the DPFC, SRR mRNA was unchanged in schizophrenia whether normalised to r18s ($F_{1,25} = 0.002, p = 0.96$) or GAPDH mRNA ($F_{1,24} = 0.881, p = 0.357$) (Figure 4.7 A, B). SRR immunoreactivity in the DPFC was increased in patients with schizophrenia compared to control individuals (Mann-Whitney $U, p = 0.027$) (Figure 4.7 C, D). This effect was seen in the same direction in both the Oxford and London series' (Table 4.2).

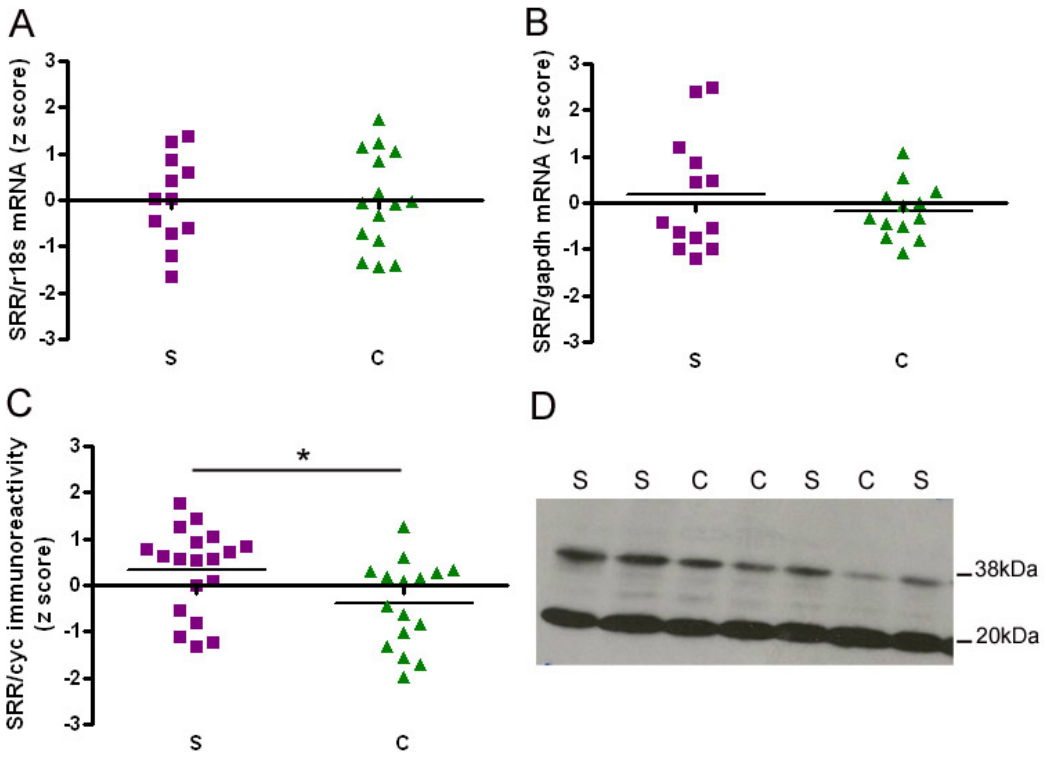

FIGURE 4-7 SRR expression in the DPFC in patients with schizophrenia (S) and control subjects (C). (A) SRR mRNA normalised to r18s. (B) SRR mRNA normalised to GAPDH. (C) SRR immunoreactivity normalised to cyclophilin. (D) Representative western blot of SRR at ~38kDa and cyclophilin at ~20kDa. *p<0.05.

4.3.3 SRR expression in the DPFC in schizophrenia, bipolar disorder and unipolar depression in the Stanley Foundation brain series

No effects of age, age of illness onset, duration of disorder, lifetime amount of medication, duration of tissue storage or brain pH on SRR immunoreactivity were identified. For pmi, a non-significant negative correlation was identified in each group. Because the direction of correlation was the same across groups, pmi was included as a co-variate in the one-way ANOVA. SRR immunoreactivity was unaffected by diagnosis ($F_{1,55}$ = 1.65, p = 0.188) (Figure 4.8). Since the focus was to confirm the elevation in SRR in the DPFC in schizophrenia in the Oxford and London brains (see above), and since a difference could be visualized between schizophrenic and bipolar groups (Figure 4.8), post-hoc tests were carried out to compare SRR immunoreactivity between individual groups. A trend increase in SRR immunoreactivity in the DPFC in patients with schizophrenia compared to control subjects (LSD test, p = 0.098) and patients with schizophrenia compared to

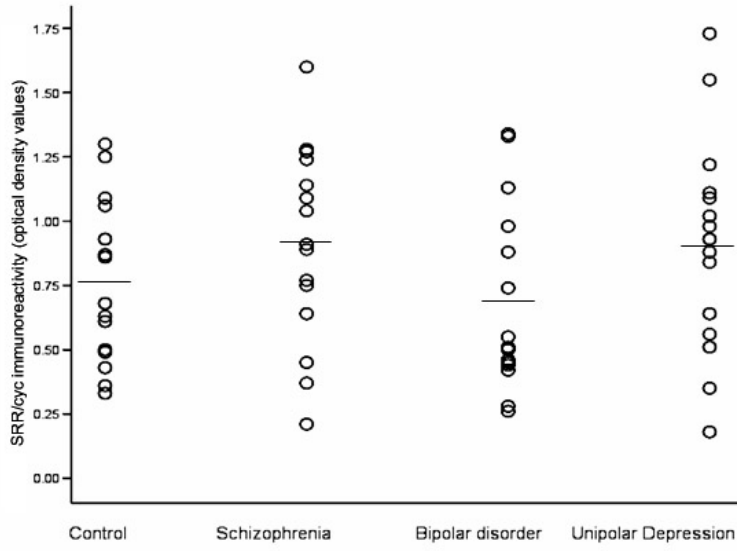

FIGURE 4-8 SRR immunoreactivity normalised to cyclophilin in the DPFC of patients with schizophrenia, bipolar disorder and unipolar depression and control subjects.

patients with bipolar disorder (LSD test, $p = 0.081$) was detected. No difference was detected between control subjects and patients with bipolar disorder (LSD test, $p = 0.976$).

4.3.4 DAO and SRR in antipsychotic treated rats

The administration of antipsychotics to rats did not change the levels of SRR immunoreactivity in the frontal cortex ($F_{1,2} = 2.441$, $p = 0.111$) or cerebellum ($F_{1,2} = 0.0.081$, $p = 0.922$) (Figure 4.9 A, B). However, post-hoc comparison revealed a trend effect of clozapine (LSD test, $p = 0.061$) on SRR protein levels in the frontal cortex compared to saline treated controls. DAO protein levels were unaffected by antipsychotic treatment in the cerebellum ($F_{1,2} = 0.627$, $p = 0.554$) (Figure 4.9 C).

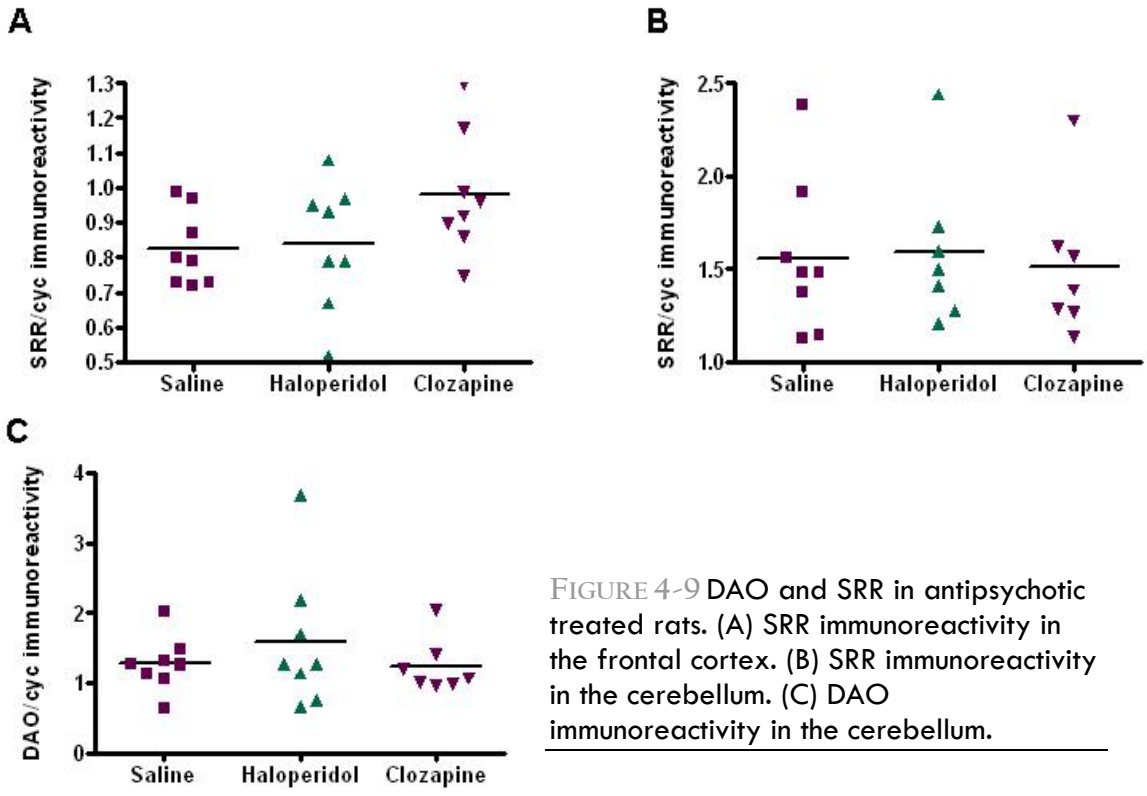

FIGURE 4-9 DAO and SRR in antipsychotic treated rats. (A) SRR immunoreactivity in the frontal cortex. (B) SRR immunoreactivity in the cerebellum. (C) DAO immunoreactivity in the cerebellum.

4.4.1 DAO expression in schizophrenia

DAO mRNA was found to be significantly elevated in the cerebellum in schizophrenia. That the effect was consistent after normalization with two housekeeping genes (Figure 4.4 A, B) supports its validity. This result is in agreement with a smaller study conducted by Kapoor *et al.* (2006) and with a subsequent study in a much larger sample set (35 patients with schizophrenia versus 35 control subjects) which demonstrated elevated cerebellar DAO mRNA levels normalised to the geometric mean of four housekeeping genes in schizophrenia (Burnet *et al.*, 2008a).

DAO immunoreactivity in the cerebellum, however, only demonstrated a trend increase (Figure 4.4 C). This could suggest that elevated mRNA levels were not translated into elevated protein. Precedents for this exist (Eastwood *et al.*, 1995; Eastwood & Harrison, 1995; Burnet *et al.*, 1996) and similarly Burnet *et al.*, (2008a) reported only a trend increase in DAO immunoreactivity to accompany a significant increase in cerebellar DAO mRNA in schizophrenia. However, both Burnet *et al.* (2008a) and Kapoor *et al.*, (2006) reported elevated DAO activity along with increased mRNA levels, and in the Burnet *et al.*, (2008a) study these correlated. One possibility to explain these findings is that mRNA levels for cerebellar DAO are up-regulated in schizophrenia but are not translated into elevated protein, whilst DAO activity is increased through an independent mechanism such as post-translational modifications. Alternatively, the above findings could suggest that elevated cerebellar DAO mRNA *is* translated into greater protein in schizophrenia such that elevated activity can be detected but the failure to demonstrate significant protein

increases reflects a reduced sensitivity of protein detection techniques compared to those for mRNA and activity detection. Notwithstanding either of these possibilities, taken together the findings here and those of Burnet *et al.* (2008a) and Kapoor *et al.* (2006) provide convincing evidence of increased DAO in the cerebellum in schizophrenia.

In the DPFC, DAO mRNA levels were unchanged. DAO immunoreactivity levels were not quantified since the GSK-DAO antibody used could not reliably detect cortical DAO (discussed in Chapter 3, Section 3.4.1). The mRNA findings are consistent with a previous report (Kapoor *et al.*, 2006) and accord with unchanged DAO protein levels in the DPFC in schizophrenia (Bendikov *et al.*, 2007). The possible reasons for the ability of Bendikov *et al.* (2006) to detect cortical DAO protein while we could not have been discussed (Chapter 3, Section 3.4.1).

Taken together therefore, these data provide convincing evidence for elevated DAO mRNA and activity in the cerebellum in schizophrenia, and unchanged DAO expression in the DPFC. Such region-specific changes in gene expression have been reported previously for the vesicular glutamate transporter 1 and complexins I and II (Eastwood & Harrison, 2005).

4.4.1.1 Mechanistic considerations

Increased cerebellar DAO in schizophrenia may arise for one of several reasons. The fact that DAO mRNA is increased indicates that the mechanism is likely to involve transcriptional regulation of DAO expression. This may relate to DAO's candidacy as a putative schizophrenia susceptibility gene, since the associated polymorphisms are all non-coding; thus, the mechanism of association is likely through an effect on gene expression (Harrison & Weinberger, 2005; Law *et al.*, 2006). The sample size

here was too small to investigate whether any of the schizophrenia-associated DAO polymorphisms contributed to the elevation in DAO expression. However, in a follow-up study, Burnet *et al.* (2008a) found that two associated DAO SNPs did not contribute to elevated cerebellar DAO mRNA or activity in schizophrenia. In addition, DAO SNPs are not thought to exert an effect on the reduced serum D-serine levels in the disorder (Yamada *et al.*, 2005), such that the function of schizophrenia associated SNPs in DAO is unknown. In any event, since DAO risk alleles are carried by only a minority of cases and by some control subjects as well, this seems unlikely to explain a diagnostic difference in DAO expression.

Instead therefore, increased cerebellar DAO in schizophrenia could arise as part of the broader pathophysiological processes downstream of other genetic, developmental or environmental influences. Relevant here is the demonstration that NMDAR blockade by MK801 or ketamine, models of the NMDAR hypofunction thought to occur in schizophrenia, caused elevated DAO mRNA levels four hours after administration (Takeyama *et al.*, 2006; Hashimoto *et al.*, 2007b). However, this would be a counter-intuitive mechanism for elevated DAO, since it could reduce D-serine levels and thence NMDAR function further. Moreover, chronic MK801 administration, which may more closely model NMDAR hypofunction in schizophrenia, was not found to alter DAO mRNA levels (Hashimoto *et al.*, 2007b) suggesting DAO alterations in schizophrenia would not be due to chronically reduced NMDAR function.

Another possibility, is the regulation of DAO activity by nitric oxide (NO; Shoji *et al.*, 2006) or G72 (Chumakov *et al.*, 2002). Shoji *et al.* (2006) have demonstrated that NO stimulated DAO activity in a glioblastoma cell line, which is particularly interesting in light of reported increases in NO in schizophrenia (Yao *et*

al., 2004; Yilmaz *et al.*, 2007) and the association of the NO synthetic enzyme, nitric oxide synthase (NOS) with the disorder (Shinkai *et al.*, 2002; Zheng *et al.*, 2005; Reif *et al.*, 2006). The G72 gene, associated with schizophrenia (reviewed in Detera-Wadleigh & McMahon, 2007; Li & He, 2007), is also thought to activate DAO (Chumakov *et al.*, 2002) and is reportedly over-expressed in the disorder (Korostishevsky *et al.* 2004). However, others have argued G72 acts to reduce DAO stability (Pollegioni *et al.*, 2007) suggesting that over-expression of G72 should reduce DAO activity rather than elevate it in schizophrenia. In addition, others still have disputed any interaction between G72 and DAO (Kvajo *et al.*, 2007) such that a link between elevated G72 and DAO in schizophrenia is tentative.

A further potential mechanism of elevated cerebellar DAO in schizophrenia, in this case downstream of environmental influence, is antipsychotic medication. Although there was no significant effect of antipsychotic administration in rats on cerebellar DAO protein, the mean in the haloperidol group was ~10% higher than that in the saline group (Figure 4.9). From these data therefore, it is possible that medication could have contributed to the DAO elevation seen in patients here. However, in the same animals, Burnet *et al.* (2008a) show unchanged cerebellar DAO activity consequent to antipsychotic treatment. In addition, in patients no correlation between lifetime antipsychotic exposure and DAO mRNA or activity levels was seen (Burnet *et al.*, 2008a). Taken together therefore, these data suggest that medication has limited, if any, effects on DAO expression.

4.4.1.2 Functional implications

The functional implications of elevated DAO in the cerebellum in schizophrenia are not straightforward. As described in Chapter 2 (Section 2.4.4), D-serine levels

measured in cerebellar homogenates are low or negligible (Nagata *et al.*, 1992, 1994a; Hashimoto *et al.*, 1993b,c, 1995a,b; Hamase *et al.*, 1997; Mothet *et al.*, 2000; Morikawa *et al.*, 2001; Wang & Zhu, 2003). However, a report demonstrating D-serine immunoreactivity highly concentrated at localized sites within the mouse cerebellum (Williams *et al.*, 2006) could suggest that D-serine is prevalent and that its discrete distribution accounts for low levels in homogenate preparations. However, Kartvelishvily *et al.* (2006) did not find D-serine immunohistochemically in the rat cerebellum such that D-serine levels in this region are equivocal.

The low D-serine in the cerebellum is thought to arise from DAO expression in the region, since mutant DAO mice show elevated cerebellar D-serine (Morikawa *et al.*, 2001). This therefore begets the question of the effect elevated cerebellar DAO (and constant SRR; see below) could have on D-serine if its levels are already minimal. However, it also suggests that tight regulation of cerebellar D-serine levels is required. In this regard, and in light of the findings of Williams *et al.* (2006) of D-serine immunoreactivity concentrated to cerebellar Bergmann glia, elevated DAO could perhaps exert an effect on this cell type at least. This is of particular note since DAO was observed localized most predominantly to Bergmann glia in the human cerebellum (Chapter 3, Section 3.3.8). Given that Bergmann glia regulate synaptic input to Purkinje neurons (Cid & Ortega, 1993; Brockhaus & Deitmer, 2002; Huang & Bordey, 2004), elevated DAO could therefore potentially affect cerebellar output via Purkinje neurons. As an example, Bergmann glia modulate presynaptic NMDARs on GABAergic interneurons that synapse onto Purkinje cells (Glitsch & Marty, 1999). They do so by regulating synaptic spill-over of glutamate, which activates these NMDARs, thus affecting the frequency of Purkinje cell miniature IPSPs (Huang & Bordey, 2004). Elevated cerebellar DAO (and constant

SRR levels) in schizophrenia could therefore lead to localized reduction of D-serine with consequent dysregulation of NMDAR activity and Purkinje cell inhibition.

However, such speculations must be taken with caution due to the caveats described. Furthermore, Mothet *et al.* (2000) reported that D-serine does not regulate NMDAR-dependent events in the cerebellum *in vivo*, suggesting D-serine is not the principle NMDAR co-agonist in this region. However, cerebellar NMDARs do respond to exogenous D-serine *in vitro* and *in vivo* (Wood *et al.*, 1989, 1990; Rao *et al.*, 1991; Vallebuona & Raiteri, 1995; Fedele *et al.*, 1997) and have elevated activity in DAO mutant mice (Almond *et al.*, 2006) making the supposition of Mothet *et al.* (2000) equivocal. Notwithstanding this, these authors and others have suggested that glycine rather than D-serine is the primary cerebellar NMDAR co-agonist (Schell *et al.*, 1997; Mothet *et al.*, 2000). DAO is not thought to oxidise glycine (D'Aniello *et al.*, 1993), however, or does so with very low affinity (Molla *et al.*, 2006) suggesting elevated DAO in schizophrenia would not affect NMDAR activity via glycine regulation. DAO does however oxidise D-alanine (D'Aniello *et al.*, 1993; Hamase *et al.*, 1997; Morikawa *et al.*, 2001; Molla *et al.*, 2006), also a possible NMDAR co-agonist (McBain *et al.*, 1989). Although D-alanine is less active at cerebellar NMDARs than glycine and D-serine (Wroblewski *et al.*, 1989), it is possible that elevated cerebellar DAO in schizophrenia has functional implications outside of D-serine metabolism. This is underscored by the finding that DAO genotype does not account for reduced serum D-serine in schizophrenia (Yamada *et al.*, 2005) and that brain D-serine levels are unchanged in the disorder (Kumashiro *et al.*, 1995; Bendikov *et al.*, 2007; Hashimoto *et al.*, 2007a), although this has not been studied in the

cerebellum. Taken together therefore it is possible that roles outside of D-serine metabolism may link DAO to schizophrenia.

While at the synaptic and cellular level the effects of elevated DAO in schizophrenia are difficult to interpret, at the regional level the increase would presumably exert some effect on cerebellar function. The involvement of this region in the disorder has traditionally been disregarded or overlooked. However, several reports do attest to its importance, as discussed in Chapter 1 (Section 1.4.3). For example, gene expression changes have been described in the region in schizophrenia (Eastwood *et al.*, 2001a,b, 2003; Mukaetova-Ladinska *et al.*, 2002) and while structural pathology is inconsistent, at the systems level the cerebellum is implicated in dysfunctions in cortico-cerebellar-thalamo-cortical circuits in the disorder (Andreasen *et al.*, 1998, 1999).

4.4.2 SRR expression in schizophrenia

SRR expression in the cerebellum was found to be unaltered in schizophrenia. In the DPFC, SRR immunoreactivity was elevated in patients with schizophrenia from the Oxford and London brain series (Figure 4.7). This was not replicated in a larger study, although a slight trend in the same direction was seen (Figure 4.8). From these data therefore, SRR expression in schizophrenia is inconclusive. Moreover, other reports are also ambiguous. Steffek *et al.* (2006) reported an elevation in SRR immunoreactivity in schizophrenia in the hippocampus but found unchanged levels in the DPFC. Therefore, their findings support an increase in SRR, although with a different regional effect. On the other hand, Bendikov *et al.* (2007) report a decrease in SRR in both the DPFC and hippocampus. Since all these studies used the same technique to quantify immunoreactivity, and the same

antibody was used here and by Steffek *et al.* (2006), the most likely explanation for the disparity is the different subjects used. All these studies used different cohorts of patients and controls and their different demographic characteristics could speculatively be related to different SRR expression. Bendikov *et al.*, (2007) additionally studied D-serine levels by HPLC in the parietal cortex in the Stanley Foundation brains and found no change in schizophrenia. Taken together therefore, these data show that the cortical SRR expression (DPFC and hippocampus) in schizophrenia is equivocal and in the Stanley cohort at least, not accompanied by D-serine changes. However, it is possible that SRR expression is altered in particular subsets of patients.

A slight trend increase in SRR immunoreactivity in the DPFC was seen in schizophrenic compared to bipolar patients, but not between bipolar and control subjects (Figure 4.8). Since this was a slight trend, any discussion of the implications of, or possible mechanisms for, the effect would be tentative. Parenthetically, differences in gene expression between patients with schizophrenia and bipolar disorder could occur due to different medications the patient's may have taken, different exposure to hospitalisation or the difference in the affective component of the phenotypes of these disorders.

4.4.2.1 Mechanistic and functional considerations

Detailed discussion of the elevated DPFC SRR immunoreactivity in schizophrenia in the Oxford/London brain series is not warranted given the lack of supporting data. However, if the change were real, albeit for a particular subset of patients, a few points are noteworthy. Cellularly, the glial localization of SRR described in the human DPFC (Chapter 3, Section 3.4.2) would infer increased SRR expression

would affect this cell type. In addition, the white over grey matter enhancement in SRR immunoreactivity described in the DPFC (Chapter 3, Section 3.4.2) could suggest a greater effect of elevated SRR in the white matter. This is potentially interesting in light of white matter alterations reported in schizophrenia (reviewed in Walterfang *et al.*, 2006).

Since the elevation was seen at the protein level and not the mRNA level, the mechanism of the alteration would be post-translational. An effect of the associated SNPs in SRR, which are in UTRs (Goltsov *et al.*, 2006; Morita *et al.*, 2007), on protein translation is unlikely. This is for the same reasons as those discussed above for DAO, and also given the weak association of SRR SNPs with the disorder (Yamada *et al.*, 2005; Goltsov *et al.*, 2006; Morita *et al.*, 2007; Strohmaier *et al.*, 2007). One plausible mechanism for elevated SRR protein in schizophrenia is via reduced protein degradation. SRR is degraded by the ubiquitin-proteasome system, modulated by the SRR binding partner Golga3 (Dumin *et al.*, 2006). Whether Golga3 is altered in schizophrenia is unknown.

Since an elevation in DPFC SRR levels would be expected to increase D-serine levels, its pathological involvement would be contrary to the NMDAR hypofunction model of schizophrenia. Rather, elevated SRR may be a compensatory response to NMDAR hypofunction in an attempt to restore homeostasis. In support of this, SRR induction by NMDAR blockade has been reported in both acute and chronic treatments (Takeyama *et al.*, 2006; Hashimoto *et al.*, 2007b), although the induction was at the mRNA level in which a change was not seen here. Further findings could be taken to support a homeostatic response to elevate SRR and thence D-serine in the disorder. For example, expression of GRIP, an SRR activator protein (Kim *et al.*, 2005), is increased in the DPFC in schizophrenia

(Dracheva *et al*., 2005) suggesting both the levels of SRR protein and the activation of the enzyme may be increased in the disorder. In addition, Asc-1, which transports D-serine away from the synapse (Helboe *et al*., 2003), is decreased in the DPFC in schizophrenia (Burnet *et al*., 2008b). Therefore, elevation in SRR may be part of a broader mechanism to increase synaptic D-serine levels. However, the potential eliminase ability of SRR (Panizzutti *et al*., 2001; De Miranda *et al*., 2002; Foltyn *et al*., 2005; Stříšovský *et al*., 2003; Stříšovský *et al*., 2005) means that elevated SRR could alternatively serve to reduce D-serine. In this context, a potential elevation in SRR in schizophrenia could contribute to reduced D-serine and thence NMDAR hypofunction in the disorder.

As described for DAO, another potential mechanism for gene expression changes is antipsychotic medication. This was unlikely for SRR here since haloperidol, the antipsychotic that patients in the Oxford/London series had been treated with, did not affect cortical SRR protein levels in drug treated rats (Figure 4.9 A). However, an interesting effect of clozapine, (not taken by the patients in this study) was seen, discussed further below.

The trend effect of clozapine on cortical SRR levels (Figure 4.9 A) is interesting. It is possible that a potential therapeutic affect of clozapine could, in part, stem from elevated SRR and, speculatively, thence D-serine levels. It is therefore relevant that D-serine has been shown to be an effective therapeutic adjunct when combined with typical antipsychotics (Tsai *et al*., 1998; Heresco-Levy *et al*., 2005) but its benefit in combination with clozapine is limited (Tsai *et al*., 1999). Taken together, these findings could suggest that D-serine and clozapine are exerting affects on the same pathway (culminating in NMDAR activation), and that their combination is not therapeutically beneficial, therefore, because it may

saturate the pathway. However, until a robust effect of clozapine on SRR immunoreactivity can be demonstrated this conjecture should be taken with caution.

4.4.3 Limitations of the study

The first part of this study investigated SRR and DAO expression in the Oxford and London brain series'. Given that they were studied at the same time, and due to the limitation of tissue availability, the cohorts were combined and *z*-scored for statistical analysis, as reported previously (Eastwood *et al.*, 2001b). However, the data values within each group were also inspected. Some measures of DAO expression, but not SRR, were found to differ between the two cohorts of brains studied (Table 4.2). The absolute values for DAO mRNA in the cerebellum were greater in the London brains than Oxford, while the cerebellar increase in DAO in schizophrenia appeared more marked in the London series at the mRNA and protein levels than the Oxford series. This observation is not unprecedented (Eastwood *et al.*, 2000a, 2001a, b), hence the use of *z*-scoring to overcome an effect of origin tissue when combining the data. However, since the basic demographics of the two series are similar (Chapter 3, Table 3.1 and 3.2) the reasons for this are unknown. For SRR on the other hand, measures were broadly consistent between the Oxford and London brain series. However, a second study with the Stanley Foundation brains failed to replicate the SRR change in schizophrenia seen in the DPFC in the Oxford and London brain series.

Taken together, therefore, these observations raise the issue of the general applicability of the findings of the present studies. They also underscore the

difficulties of post-mortem gene expression studies of this kind, particularly when looking for potentially subtle effects in a heterogeneous disorder.

The other main limitation here is that D-serine itself was not measured. This is despite the functional implications of altering DAO and SRR expression being largely implicitly or explicitly the result of their effect upon D-serine levels. While Bendikov *et al.* (2007) did measure D-serine levels in the human post-mortem brain, it was not carried out here, in part due to other reports of problematic detection of D-amino acids post-mortem (Kumashiro *et al.*, 1995; Hashimoto *et al.*, 2007a).

4.4.4 Conclusions

This study aimed to investigate the expression of DAO and SRR in schizophrenia in view of theories of altered D-serine metabolism in the disorder. Together with other reports, convincing evidence for elevated DAO in the cerebellum in schizophrenia has been outlined. However, the functional consequences of such an increase in this region are difficult to interpret and may not necessarily impinge on D-serine function. Future studies to investigate the molecular and cellular effects of elevated cerebellar DAO would help resolve this issue. For SRR, altered expression in schizophrenia is currently irresolute based on contradictory findings within this study, and compared to other studies. Larger cohorts of people, and perhaps studying defined subsets of patients, could potentially resolve whether altered SRR has a compensatory or pathophysiological role in the disorder.

5. DEVELOPMENT OF AN *IN VITRO* MODEL OF ABERRANT D-SERINE METABOLISM

5.1 INTRODUCTION

As outlined in Chapters 1 and 4, altered D-serine metabolism has been implicated in the pathophysiology of schizophrenia based on; reduced CSF and blood serum D-serine levels reported in the disorder (Hashimoto *et al.*, 2003, 2005; Yamada *et al.*, 2005; Bendikov *et al.*, 2007); the ameliorative effects of D-serine therapeutically (Tsai *et al.*, 1998; Heresco-Levy *et al.*, 2005); and potential genetic contributions of DAO and SRR to schizophrenia pathophysiology (see Chapter 1, Section 1.10 and 1.11). If altered D-serine metabolism were a pathophysiological determinant, it would presumably contribute to schizophrenia through a reduction in D-serine levels and thence NMDAR hypofunction. Indeed, numerous studies evidence the role of endogenous D-serine in potentiating NMDAR function (Mothet *et al.*, 2000; Stevens *et al.*, 2003; Yang *et al.*, 2003, 2005; Katsuki *et al.*, 2004; Shleper *et al.*, 2005; Gustafson *et al.*, 2007).

Given that some of the evidence for a role of D-serine in schizophrenia is the potential contributions of its metabolizing enzymes in pathophysiology, it is of interest whether DAO and SRR can themselves be demonstrated to impact on NMDAR function through regulating D-serine levels. Evidence that DAO does so is provided by studies showing that elevated DAO reduces NMDAR function in the retina and hippocampus (Mothet *et al.*, 2000; Stevens *et al.*, 2003; Yang *et al.*, 2003; Katsuki *et al.*, 2004; Gustafson *et al.*, 2007). Conversely, DAO mutant mice show

elevated extracellular D-serine levels and enhanced NMDAR function *in vivo* (Maekawa *et al.*, 2005; Almond *et al.*, 2006). Thus, increased DAO activity and expression in schizophrenia (Kapoor *et al.*, 2006; Verrall *et al.*, 2007; Burnet *et al.*, 2008a; Chapter 4, Section 4.3.1), might be expected to contribute to the disorder through reducing NMDAR function (but see Chapter 4, Section 4.4.1 discussion).

However, a hypothesis for SRR's involvement in schizophrenia is less parsimonious than that for DAO, given that SRR has both D-serine synthetic and eliminase activities which are intricately regulated (see Chapter 1, Section 1.8.1). While SRR over-expression in HEK-293 cells leads to elevated D-serine levels (De Miranda *et al.*, 2002; Xia *et al.*, 2004), the effects in neural cells are unknown. Indeed, the demonstration that SRR expression might be increased in schizophrenia (Steffek *et al.*, 2006; Verrall *et al.*, 2007, but see Chapter 4, Section 4.3.3 and Bendikov *et al.*, 2007) could point to a either a compensatory change (through increased D-serine) or a pathophysiological role (through decreased D-serine). This highlights the drawback of post-mortem gene expression studies, useful for identifying potential molecular pathophysiological determinants in schizophrenia but less for studying the functions of genes implicated in the disorder or consequences of their altered expression.

To probe gene function, researchers can adopt a genotype-to-phenotype experimental approach whereby gene expression can be manipulated and the phenotypic consequences examined. With the identification of schizophrenia risk genes, this approach has been readily adopted in research into the disorder. For example, transgenic or mutant mice for Neuregulin (Stefansson *et al.*, 2002), RGS4 (Grillet *et al.*, 2005), dysbindin (Li *et al.*, 2003), α7 nAChR (Orr-Urtreger *et al*, 1997) and DISC1 (Hikida *et al.*, 2007; Pletnikov *et al.*, 2007a) will likely provide insight into

the potential pathophysiological contributions of these genes. Another approach is the use of cell culture models, which cannot be used to probe the contributions of particular genes to behavioural phenotypes, but are amenable to studying the molecular and cellular consequences of gene manipulation. For example, *in vitro* over-expression of the schizophrenia risk gene DISC1 (Miyoshi *et al.*, 2003; Ozeki *et al.*, 2003; Kamiya *et al.*, 2005; Pletnikov *et al.*, 2007b), has identified its roles in neuronal differentiation and neurite outgrowth. A complementary approach is the knockdown of genes of interest in cell culture models. For example, knockdown of DNA methyltransferase 1 (Dnmt1) in primary cortical cultures evidenced its role in regulating reelin expression and provided support for the hypothesis of Dnmt1 hypermethylation in schizophrenia (Noh *et al.*, 2005). Similarly, dysbindin knockdown *in vitro* evidenced a role for this gene in dopamine D2 receptor signalling (Iizuka *et al.*, 2007). In addition, applying both over-expression and knockdown approaches can provide confirmatory evidence for a role of a gene in a particular process when their effects are opposite. For example, Numakawa *et al.* (2004) demonstrated that dysbindin over-expression in primary cortical cultures induced expression of pre-synaptic proteins SNAP25 and synapsin I and increased glutamate release, while knockdown of endogenous dysbindin reduced these parameters. Similarly, using both knockdown and over-expression of DISC1 in cell culture Hashimoto *et al.* (2006) and Shinoda *et al.* (2007) provided evidence of the gene's role in extracellular signal-regulated kinase (ERK) and Akt signalling and neurite growth. These studies therefore identified potential molecular and cellular mechanisms whereby DISC1 may contribute to schizophrenia pathophysiology,

At the time of conception of this thesis, no cellular or animal models of altered SRR levels were known. Moreover, delineating the precise role of SRR in

regulating D-serine levels and NMDAR function was required given the hypothesis of altered D-serine metabolism in schizophrenia and in light of the enzyme's dual functions. Due to the benefits in cost and time of cellular based models over animal models, the aim of this study was therefore to develop an *in vitro* model of altered SRR expression. If successful, the overall objective was to study the effects of altered SRR expression on D-serine levels and NMDAR expression and/or function. The study aimed to both over-express and knockdown SRR to provide complementary evidence of the role of the enzyme and focused on manipulating SRR due to; the enzyme's potentially more complicated regulation of D-serine levels, and thence NMDAR function, than DAO; the lack of cellular or animal models for SRR; and the constraints of time which prevented the development of *in vitro* models for both altered SRR and DAO expression.

Further detail on the methodology chosen for this chapter is firstly given below before describing the methods and results. The overall objective of this chapter was not met due to technical complications and this is dealt with in the discussion.

5.1.1 Choice of methodology

5.1.1.1 Cell culture system

This study chose to utilise the P19 cell line and primary cerebellar granule cell (CGC) cultures. P19 cells are embryonic carcinoma cells which are multipotential and may be easily maintained in tissue culture in an undifferentiated state (Jones-Villeneuve *et al.*, 1982; Bain *et al.*, 1994). Their particular advantage for this study is their ability to differentiate into co-cultures of neural- and glial-like cells in a simple and standardized procedure (Jones-Villeneuve *et al.*, 1982; Bain *et al.*, 1994).

This was important in selecting a biologically relevant model, given the ambiguity of whether SRR is predominantly neuronal or glial (discussed in Chapters 2, Section 2.4.2 and 3, Section 3.4.2). Morphologically, the P19 neural-like cells give off multiple processes which resemble neurites seen in primary cell culture (Finley *et al.*, 1996), express markers of neuronal differentiation (McBurney *et al.*, 1988) and segregate into axonal and dendritic compartments (Finley *et al.*, 1996). Moreover, these cultures use the neurotransmitter glutamate (MacPherson, 1997) and express glutamatergic receptors (Ray & Gottlieb, 1993; Turetsky *et al.*, 1993; Canzoniero *et al.*, 1996). Relatively few cell lines can be induced to differentiate into glial and neural-like cells forming glutamatergic networks (Svensson *et al.*, 2006), and as such P19 cells presented an ideal model system.

It was also aimed to utilise primary CGC cultures, advantageous over cell lines for their closer similarities to living systems. These cultures comprise granule cells and glial cells, with Purkinje cells few in number if present. SRR is expressed by cerebellar granule cells (Kartvelishvily *et al.*, 2006), and the enzyme is thought to regulate their migration *in vivo* (Kim *et al.*, 2005), suggesting CGC cultures as a relevant system to probe SRR function. In addition, these cells express NMDARs (Burgoyne *et al.*, 1988; Kilic *et al.*, 1991), which regulate neurite outgrowth in culture (Pearce *et al.*, 1987; Burgoyne *et al.*, 1993) and are potentiated by D-serine (Wroblewski *et al.*, 1989). The CGC cultures were additionally appealing in their relative ease to prepare, their preparation from neonatal animals rather than embryos, and their relatively high yield for a neuronal culture. To restrict the use of animals, however, this study sought to initiate and optimise gene manipulation studies in the P19 cell line with a view to later utilising primary CGC cultures.

The initial aim was to characterise these cell culture systems in order to ascertain their successful differentiation, culture and expression of SRR. The basal characteristics of SRR expression in P19 and CGC cultures were important to delineate prior to any attempts to manipulate SRR expression. In addition, these initial studies sought to ascertain whether DAO was expressed in these cultures given the potential for alterations in DAO expression to counteract those in SRR expression.

5.1.1.2 Manipulation of gene expression

This study aimed to both over-express and knockdown SRR in the chosen cell culture systems. For the former, a commercially available *myc*-tagged plasmid expression vector was chosen to express SRR under the cytomegalovirus (CMV) promotor which drives constitutive high level gene expression. *Myc*-tag containing expression vectors are frequently used (e.g. Kvajo *et al.*, 2007; Pletnikov *et al.*, 2007b) and provide a means to differentiate endogenous protein from the over-expressed protein on the basis of size.

To knockdown SRR, this study utilised RNA interference (RNAi), a powerful and increasingly popular technique in genotype-to-phenotype experiments. RNAi describes sequence-specific, post-transcriptional gene silencing. It is a highly conserved endogenous mechanism thought to be important in protection against viruses and in gene expression regulation (reviewed in Buckingham *et al.*, 2004; Trülzsch & Wood, 2004; Fountaine *et al.*, 2005). The phenomenon was first observed in *C. elegans* where the introduction of long double-stranded (ds) RNA was unexpectedly shown to reduce the levels of complementary mRNA (Fire *et al.*, 1998).

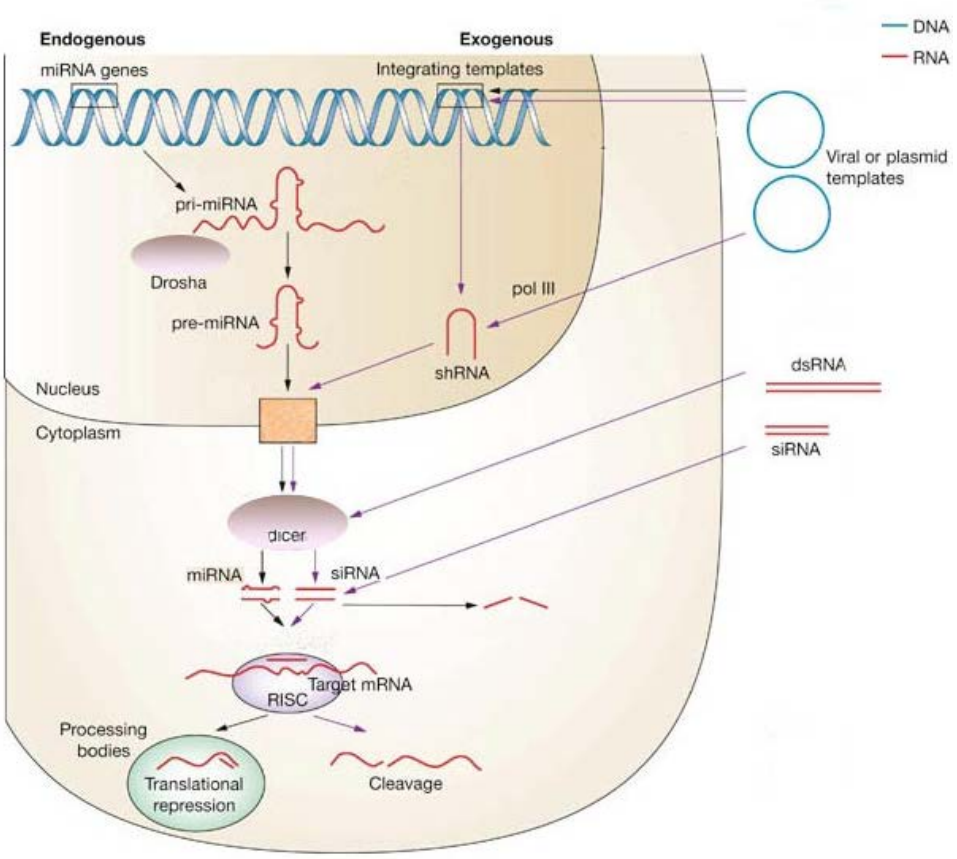

FIGURE 5-1 Endogenous and experimental RNAi. RNAi is triggered by long dsRNA from a variety of sources, including viruses, transposons and experimental application. Alternatively dsRNA in the form of shRNA can be transcribed by RNA polymerase III from viral or plasmid DNA templates and transported into the cytoplasm. The resultant dsRNA is processed by cytoplasmic Dicer to yield siRNA. Alternatively siRNA can be experimentally administered. The siRNA antisense strand (with respect to the eventual target) then binds to RISC, which mediates sequence specific degradation of complementary mRNA. Endogenously, miRNA genes are transcribed to produce pri-miRNA which is processed by Drosha to yield pre-miRNA. Exogenously, miRNAs can be engineered as pri-miRNAs and applied experimentally. Pre-miRNAs are transported into the cytoplasm and treated the same as other forms of dsRNA. They are cleaved by Dicer to produce miRNAs, which then associate with RISC and lead to post-transcriptional repression of complementary mRNAs. (Adapted from Fountaine *et al.*, 2005; Gonzalez-Alegre & Paulson, 2007).

Further studies demonstrated that long dsRNA is degraded by Dicer, a ribonuclease, yielding 21-23 bp small duplex RNAs termed small interfering RNAs (siRNAs). The antisense strand of the siRNA then associates with a multiprotein complex, the RNA-induced silencing complex (RISC), which guides the siRNAs to

their mRNA targets which are subsequently cleaved (Figure 5.1; Buckingham *et al.*, 2004; Trülzsch & Wood, 2004; Fountaine *et al.*, 2005; Gonzalez-Alegre & Paulson 2007). Attempts to replicate the effects of dsRNA seen in invertebrates in mammalian cells were initially unsuccessful as exposure to long dsRNA was found to generate a non-specific immune response (Kumar & Carmichael, 1998). Gene-specific silencing by RNAi was successfully achieved in mammalian tissue culture cells in 2001 (Elbashir *et al.*, 2001) through the introduction of siRNAs into cells, and later (Paddison & Hannon, 2002) through the introduction of plasmids expressing double-stranded short RNA hairpins (shRNA) which were processed by Dicer to yield siRNA duplexes (Figure 5.1). Both these approaches are now widely used experimentally. RNAi has now been successfully exploited to probe the functions of genes of interest in several neuronal cultures (e.g. Numakawa *et al.*, 2004; Noh *et al.*, 2005; Hashimoto *et al.*, 2006; Fountaine & Wade-Martins, 2007; Shinoda *et al.*, 2007) including CGC cultures (e.g. Leng & Chuang, 2006) and differentiated P19 cultures (e.g. Omi *et al.*, 2004; Trülzsch *et al.*, 2007). Moreover, RNAi is increasingly being used to probe the functions of neuropsychiatrically relevant genes (e.g. Numakawa *et al.*, 2004; Noh *et al.*, 2005; Hashimoto *et al.*, 2006; Shinoda *et al.*, 2007; see Hoyer, 2007 for review).

Endogenously, the RNAi system also processes microRNAs (miRNAs), generated from stem-loop RNA precursors. Both siRNA and miRNAs utilise the same processing machinery and both associate with RISC (Figure 5.1). However, depending on the level of sequence complementarity to an endogenous mRNA transcript, miRNAs can direct the degradation of that transcript or mediate more widespread translational repression (Valencia-Sanchez *et al.*, 2006; Sætrom *et al.*, 2006). Therefore, an important consideration in the exogenous application of

siRNAs is to ensure siRNA specific cleavage of an mRNA has occurred rather than miRNA mediated translational suppression.

5.1.1.3 Methodological considerations

The selection of functional siRNAs is one of the challenges in RNAi experiments and can rely on trial and error (Elbashir *et al.*, 2002). To overcome this, siRNAs to SRR were acquired commercially as a 'SMARTpool' from Dharmacon. The SMARTpool technology uses an algorithm developed from the systematic analysis of a large test set of siRNAs. The algorithm is used to identify siRNAs with a very high probability of potent and specific silencing, over 85% of which have been shown to reduce target mRNAs by > 95% (www. dharmacon.com). Four siRNAs to a gene are supplied within a pool for testing. The additional benefit of this is that, should more than one sequence be effective, multiplicity controls can be adopted. These add confidence to RNAi data by demonstrating similar effects with two or more siRNAs targeted to different sites within an mRNA (*Nature Cell Biology* (Editorial, 2003)). Additional important controls include; the titration of the siRNA to the lowest effective concentration to reduce the chance of side effects; and readout of knockdown at both the protein and mRNA levels to exclude miRNA effects (*Nature Cell Biology* (Editorial, 2003)). Both of these controls were planned in this study. However, protein levels were quantified as the initial knockdown readout (Elbashir *et al.*, 2002) which were assessed initially at the recommended 72hrs post-transfection (www. dharmacon.com; Elbashir *et al.*, 2002; Fountaine & Wade-Martins, 2007). A further planned control was the use of scrambled sequences. These comprise the nucleotides of the siRNA but in a non-targeting sequence (assessed by BLAST). They would therefore be designed and synthesized

once the effective siRNAs for the target gene have been selected from the SMARTpool. Thus for the initial experiments to screen the SMARTpool, no siRNA treatment controls were adopted.

For cellular delivery of siRNAs and over-expression vectors, several methods are available including electroporation, viral vectors and calcium-phosphate precipitation. Advantageous in time and cost over these methods is the use of cationic lipids. Cationic lipid formulations are amphiphilic and positively charged at physiological pH. They therefore complex spontaneously with nucleotide sequences through non-covalent bonding with negatively charged phosphates (McQuillin *et al.*, 1997). Internalization of the consequent lipoplex by cells is either by direct fusion of the lipoplexes with the plasma membrane or by endocytosis (Zabner *et al.*, 1995). *In vitro* the efficiency of lipid-based delivery is comparable to viral-based methods (Martin *et al.*, 2005; Rao & Gopal, 2006) and several studies have utilised lipid-based delivery of expression plasmids, oligonucleotides and siRNAs in neuronal culture models (Ohki *et al.*, 2001; Numakawa *et al.*, 2004; Noh *et al.*, 2005; Hashimoto *et al.*, 2006; Fountaine & Wade-Martins, 2007), including primary CGC cultures (e.g. Levkovitz & Baraban, 2001; Vesce *et al.*, 2005) and differentiated P19 cells (e.g. Omi *et al.*, 2004).

Given the advantages of lipid-based delivery methods, this approach was adopted here. Dharmacon recommend DharmaFECT lipid formulations with their siRNAs, while a widely used alternative is Lipofectamine^{2000} (Ohki *et al.*, 2001; Dalby *et al.*, 2004; Omi *et al.*, 2004; Noh *et al.*, 2005; Fountaine & Wade-Martins, 2007). For all lipid-based reagents, the ratio of lipid-DNA/siRNA is an important factor in transfection efficiency (McQuillin *et al.*, 1997; Rao & Gopal, 2006) and

manufacturers consequently provide guideline ratios which were taken into account in this study.

5.1.2 Aim of study

To achieve the goal of studying the effects of SRR on NMDAR function, the objectives of this chapter were to; firstly, successfully culture differentiated P19 and CGC cultures; secondly, characterise SRR and DAO expression in these cultures; and thirdly, establish SRR over-expression and knockdown in differentiated P19 cultures, with a view to extending this methodology to CGC cultures.

5.2 MATERIALS AND METHODS

5.2.1 P19 cell culture

P19 murine embryonal carcinoma cells (European Collection of Cell Cultures; ECACC, #95102107) were maintained in complete culture medium (Appendix II) at 37ºC humidified with 5% CO_2 and sub-cultured every 2 days at $3x10^6$ cells/ 25ml culture medium. Naïve (undifferentiated) P19 cells were induced to differentiate into neural- and glial-like cells by treatment with retinoic acid. $1x10^6$ cells were suspended in 10ml complete culture medium supplemented with 1µM *trans*-retinoic acid (Sigma), seeded on a 90mm bacteriological dish (Greiner Bio-One Ltd., UK) and incubated at 37ºC, 5% CO_2 for two days. In the presence of retinoic acid, cells aggregated into embryoid bodies. After two days embryoid bodies were seeded into fresh complete culture medium supplemented with 1µM *trans*-retinoic acid and incubated for a further two days.

Cell aggregates were rinsed with Dulbecco's PBS (Sigma). To dissociate the cells and dissolve DNA released from damaged cells, embryoid bodies were trypsinized in 3ml 1x trypsin - ethylenediaminetetraacetic acid (EDTA) solution (Sigma) and 50µg/ml DNAase I (Sigma) at 37ºC with the mixture agitated every two minutes for ten minutes. Cell viability was determined by Trypan Blue (Sigma) staining and $4x10^5$ live cells seeded per $2cm^2$ well in 24-well culture plates (Sarstedt Ltd, Leicester, UK). The following day (1 day in vitro; 1DIV) complete culture medium was changed and supplemented with Cytosine arabinoside (Ara-C; Sigma), at a final concentration of 10 µM, to inhibit division of non-neuronal cells (Finley *et al.*, 1996). Medium was exchanged two days later with complete culture medium and every 2-3 days thereafter. All cultures were morphologically examined daily.

5.2.2 Primary cerebellar granule cell cultures

Primary CGC cultures were prepared from 4-day old mouse pups (Harlan-Olac). Mice were put on ice to be anaesthetised and the heads removed: procedures were carried out by Dr Tracy Lane (Dept Psychiatry, University of Oxford). All buffers for primary culture preparation were made on the morning of the culture and are detailed in Appendix II. Cerebella were isolated, minced using a single edged razor blade and transferred to 10ml buffer A containing trypsin at room temperature to begin tissue disaggregation. Cerebella from one litter (five or six pups) were pooled for one culture. Following dissection (typically ~twenty minutes), buffer A containing minced tissue was incubated at 37ºC for fifteen minutes with occasional agitation. 10ml buffer B, which contained trypsin inhibitor and DNAse, was added to the buffer A/disaggregated tissue mixture and inverted three times to inhibit trypsinization and dissolve DNA released from damaged cells. The mixture was divided into two, centrifuged at 180*g* to pellet the tissue, and the supernatant removed. 1.5ml buffer C was added to the tissue which was then triturated using sterile glass Pasteur pipettes to produce a single cell suspension. Remaining aggregated tissue was left to settle and the single cell suspension removed. 1.25ml buffer C was added to the remaining tissue which was triturated again and the single cell suspensions from each trituration pooled. The cell suspension was centrifuged through 2ml buffer D (containing a 4% BSA gradient) for five minutes at 180*g* in order to remove cell debris. The supernatant was removed and the cells resuspended in CGC culture medium (Appendix II). Cell viability was assessed with Trypan Blue (Sigma) staining and cells seeded at 2.65×10^5 cells per $2cm^2$ well in poly-ornithine coated (Appendix II) 24-well culture plates. (Sarstedt). Ara-C was added (10µM final concentration) on 2DIV. Thereafter half of the medium was

replenished every 2-3 days with fresh cell culture medium. All cultures were morphologically examined daily.

5.2.3 Immunocytochemistry in cell cultures

For differentiated P19 cultures, cells were seeded on coated chamber slides (LabTekII chamber slide system, VWR International) and fixed at 3, 6 and 11 DIV. For CGC cultures, cells were seeded onto nitric acid cleaned (Appendix II) and poly-ornithine coated (Appendix II) glass coverslips and fixed at 4DIV.

Cells were washed once in PBS and fixed in 4% PFA (16% solution from Electron Microscopy Sciences, Science Services Ltd, London, UK) diluted in PBS for twenty minutes at room temperature. Cells were washed three times in PBS, blocked in 10% normal goat serum in PBS-0.5% $\text{Triton}_{\text{X-100}}$ (Sigma) for thirty minutes and incubated with primary antibodies for two hours at room temperature. Primary antibodies used were mouse MAP2 (Sigma) at 1:100 and GFAP. For differentiated P19 cultures, mouse GFAP (Chemicon) was used at 1:800. For CGC cultures, rabbit GFAP (DAKO) was used at 1:100 simultaneously with anti-MAP2.

Cells were washed three times for ten minutes in PBS and incubated with 1:50 fluorescein isothiocyanate (FITC) tagged anti-mouse and/or 1:50 rhodamine tagged anti-rabbit antibodies (both from Jackson Immunoresearch, Stratech, Suffolk, UK) in 2% normal goat serum in PBS-0.25% $\text{Triton}_{\text{X-100}}$ for one hour in the dark at room temperature. To visualize the nuclei in CGC cultures, 1:1000 Hoescht 33528 (Sigma) was added for the last fifteen minutes of secondary antibody incubation.

Cells were washed three times in PBS and once in ddH_2O, mounted with Vectamount (Vector Labs) and visualised by fluorescent microscopy with MCID Image analysis software (InterFocus Imaging Ltd, Cambridge, UK).

Additional studies attempted to localize SRR and DAO immunocytochemically in both primary CGC and differentiated P19 cell cultures with the above protocol using primary antibodies to SRR (BD Biosciences; see Chapter 2, Section 2.3.1 for characterisation) and DAO (GSK-DAO antibody; see 2, Section 2.3.1 for characterisation) at 1:35-1:500 and 1:35-1:500 µg/ul respectively. In addition, methanol and acetone fixation and permeabilizing cells with 0.1%Triton$_{X-100}$/0.01% SDS in PBS prior to blocking was also attempted.

5.2.4 RNA extraction and conventional PCR

To extract RNA from cell cultures, a column-based RNeasy mini kit (Qiagen, Crawley, UK) was used according to manufacturer's instructions. Briefly, cells were washed once in PBS and lysed and homogenized in lysis buffer RLT containing ß-mercaptoethanol using a 19-gauge needle and syringe. An equal volume of 70% ethanol was added and the mixture added to a mini-column which bound the total RNA. The column was then washed in one wash of buffer RW1 and two washes of buffer RPE and the RNA eluted in RNAse-free water.

Total RNA extracted from pooled differentiated P19 cultures was DNAse treated and reverse transcribed as described (Chapter 4, Section 4.2.5). To examine the expression of SRR, DAO and NMDAR subunits, 50ng cDNA was subjected to PCR using Taq Man beads (GE Healthcare) and each forward and reverse primer (Table 5.1) at 0.4µM final concentration in a final volume of 25µl according to manufacturer's instructions. The reaction was initiated with one minute at 94ºC twenty eight cycles of thirty seconds denaturing at 94ºC, thirty seconds annealing at 62ºC and thirty seconds extension at 72ºC.

TABLE 5-1 Sequences for Taqman PCR forward (F) and reverse (R) primers.

Target gene	Sequence 5' - 3'	Product size (bp)
SRR	F; CGTGCGCAGAGGTGTAAAGCT	138
	R; GGACTTTGATTGGCCCATCTT	
DAO	F; GATTATGGGCTACGGCTGGTT	438
	R; AGGGTGGGCTCCAGTTTACA	
NR1	F; GAGTCCAAGGCAGAGAAGGT	111
	R; GCTTGCAGAAAGGATGATGA	
NR2A	F; GCTTTCCTTGAACCCTTCAG	144
	R; AACTTAGCCAAAGGGAAAGCTCCCCAT	
NR2B	F; TTGGTGAGGTGGTCATGAAG	169
	R; ACCTTCTGCCTTCTTAGAGCC	
NR2C	F; GAGGCTTTCTACAGGCATCTG	106
	R; AATGGTTGTGATCGCTCTCA	

Primers were designed and synthesized as described in Chapter 4, Section 4.2.6.

5.2.5 Agarose gel electrophoresis to resolve DNA

PCR products or restriction digests were visualised by agarose gel-electrophoresis. Gels were prepared by boiling 2% w/v agarose (Promega) in 0.5x Tris-Borate-EDTA (TBE) buffer (Appendix I) containing 0.2µg/ml ethidium bromide (Sigma). Samples were mixed with loading buffer (0.25% Bromophenol blue, 40% sucrose), loaded onto the gel with DNA size ladder (123bp ladder, Sigma) and run at 80-120 V. Gels were visualized and photographed under ultraviolet light using the AlphaImager analysis system (Alpha Innotech, GRI Ltd, Braintree, UK).

5.2.6 Subcloning

5.2.6.1 Ligation of DNA

50-100ng plasmid DNA was incubated with a 1:3 ratio of DNA insert in 1x ligation buffer (Promega) and 0.1-0.3U/µl final concentration T4 DNA ligase (Promega) in a total volume of 10µl at room temperature for ninety minutes.

5.2.6.2 Transformation and culture of bacteria with plasmid DNA

E. coli competent cells (Promega) were thawed on ice and 50µl added to the ligation product and heat-shocked by incubation on ice for fifteen minutes, 42ºC for fifty seconds, and ice for a further two minutes. Cells were then grown in 1ml SOC medium (Sigma) to aid recovery for ninety minutes at 37ºC.

For selecting positive clones, 100µl bacteria/SOCS mixture was plated on Luria Bertani broth (LB; Sigma) agar plates (Appendix I) containing 40µg/ml ampicillin (Sigma) and incubated overnight at 37ºC. Colonies were selected using a pipette tip, grown in small scale cultures (5ml LB broth containing 40µg/ml final concentration ampicillin) at 37ºC overnight with rotation, purified (Section 5.2.7) and verified by restriction endonuclease digest (Section 5.2.10). For bacteria transformed with known positive clones, 100µl bacteria/SOCS mixture was grown directly in small scale cultures. For large scale cultures, 500µl of a small scale culture was used to inoculate 250ml LB broth containing 40µg/ml final concentration ampicillin and grown for 37ºC overnight with rotation.

5.2.7 Alkaline-lysis plasmid extraction

To purify small scale cultures, GenElute plasmid miniprep kit (Sigma) constituents were used as follows. A 4ml volume of bacterial culture was centrifuged at 12000*g*

for thirty seconds to pellet the cells which were resuspended in 200µl re-suspension buffer and vortexed. To lyse cells, 200µl lysis buffer was added and the mixture inverted several times. To precipitate genomic DNA and cell debris, 350µl neutralizing buffer was added, inverted several times and centrifuged at 12000*g* for ten minutes. To precipitate the plasmid DNA, the supernatant was added to an equal volume of isopropanol, mixed and centrifuged at 12000*g* for ten minutes. The pellet was washed in 75% ethanol and resuspended in nuclease-free water (Promega). Resuspended plasmid DNA was verified by restriction endonuclease digest where necessary and purified by phenol-chloroform purification. DNA concentrations were determined by spectrophotometric absorbance measurements at 260nm using a NanoDrop.

5.2.8 Phenol-chloroform purification of DNA

To purify DNA solutions with phenol-chloroform, 10µl sodium acetate was added (0.4mM final concentration) for every 90µl DNA solution and mixed. 90µl phenol: chloroform (9:1) was added, mixed until homogenous and centrifuged at 12000*g* for five minutes. The aqueous top phase containing the nucleic acid was removed and added to 90µl chloroform, mixed until homogenous and centrifuged at 12000*g* for five minutes. The aqueous top phase was removed and, added to an equal volume of isopropanol, stored at -20ºC for twenty minutes and centrifuged at 12000*g* to precipitate the nucleic acid. The resultant pellet was washed in 75% ethanol and resuspended in nuclease-free water (Promega).

5.2.9 Column-based purification of plasmid DNA

Large scale cultures were purified using a column-based Endo-Free Plasmid Maxi Kit (Qiagen) according to manufacturer's instructions. Briefly, plasmids were extracted by alkaline-lysis as follows. Bacteria were pelleted, resuspended in 10mls P1 resuspension buffer, added to 10mls P2 lysis buffer, inverted five times and incubated at room temperature for five minutes. To precipitate genomic DNA, 10mls chilled P3 neutralization buffer was added and the mixture inverted five times. Lysates were then cleared by filtration, 2.5mls endotoxin removal buffer added and the mixture inverted ten times and incubated on ice for thirty minutes. 10mls QBT DNA-binding buffer was added, column filtered and the lysate discarded. The column membrane was washed in two 30ml volumes of QC wash buffer and the DNA eluted in 15mls QN elution buffer. To precipitate the DNA, 10.5mls isopropanol was added, incubated for 4ºC overnight and centrifuged at 12000*g* for ten minutes. The pellet was washed in 75% ethanol and resuspended in endotoxin free TE buffer.

5.2.10 Restriction endonuclease digest

Plasmid DNA was digested by incubating 5µg plasmid in a 20µl volume containing 1x final concentration multi-core restriction endonuclease buffer (Promega) and 1U/µl final concentration of the relevant enzyme(s) at 37ºC for two hours. Digest products were then visualized on ethidium bromide-stained agarose gels (Section 5.2.5).

5.2.11 Short hairpin and small interfering RNAs

The siRNAs siGLO (a control siRNA targeting cyclophilin and tagged with the red fluorescent tag DY-547) and SRR1-4 (a 'SMARTpool' of four siRNAs targeting SRR; Table 5.2), were purchased from Dharmacon (Perbio Science, Northampton, UK).

The pGSU6-GFP plasmid (Genlantis; AMS Biotechnology, Oxford, UK) containing the kanamycin resistance gene (Figure 5.2) was used to express shRNA sequences corresponding to the siRNA sequences to SRR (Table 5.2) under the U6 promotor. The plasmid was provided linearized with Bam*HI* and Not*I*. For each target, forward and reverse oligonucleotides were synthesized (Sigma) (Figure 5.3). These comprised the sense and antisense 19mer siRNA sequences separated by a hairpin loop structure - 8 nucleotides including the *Hind*III restriction endonuclease site - and a polythymidine tract to terminate RNA polymerase III transcription. The 5' ends comprised the *BamH*I restriction endonuclease site (forward) and the *Not*I restriction endonuclease site (reverse) to enable 'sticky-end' ligation of the oligonucleotide into the linearized pGSU6-GFP plasmid in the correct orientation for transcription from the U6 promotor. The oligonucleotides were annealed and cloned into the pGSU6-GFP plasmid with the GeneSilencer shRNA Vector Kit (Genlantis) according to manufacturer's instructions. Briefly, 2µg of each oligonucleotide was incubated with annealing buffer in a 50µl volume at 90ºC for three minutes and then cooled to room temperature for ninety minutes. The annealed oligonucleotides were diluted to 10ng/µl and ligated as described (Section 5.2.6.1) but incubating 50ng vector and 10ng insert overnight. The shRNA vector was then transformed into bacteria, plated on LB agar plates and small scale

TABLE 5-2 Dharmacon SMARTpool siRNA sequences targeting SRR. Both sense and antisense strands have 3'UU overhangs. The antisense strand has a 5' phosphate (P).

SRR1	*Sense*:	GGAAUAGCCAUUACAAUUAUU
	Antisense:	5'-PUAAUUGUAAUGGCUAUUCCUU
SRR2	*Sense*:	GAGCAUCGAUAGUAUACUGUU
	Antisense:	5'-PCAGUAUACUAUCGAUGCUCUU
SRR3	*Sense*:	GAACAAUUGCCCUGGAAGUUU
	Antisense:	5'-PACUUCCAGGGCAAUUGUUCUU
SRR4	*Sense*:	GCUCAUAUCAACAUUCAAGUU
	Antisense:	5'-PCUUGAAUGUUGAUAUGAGCUU

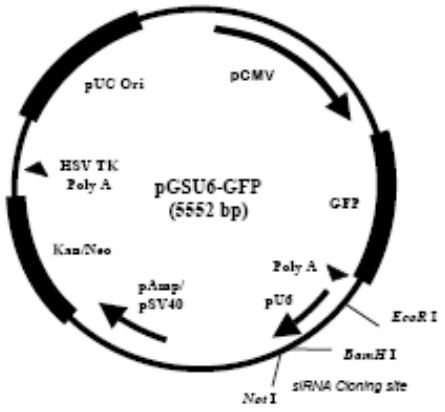

FIGURE 5-2 Map of the pGSU6-GFP plasmid (Genlantis) showing the kanamycin resistance gene, U6 promotor and siRNA sequence cloning site. The plasmid was provided linearized by Bam*HI* and Not*I*.

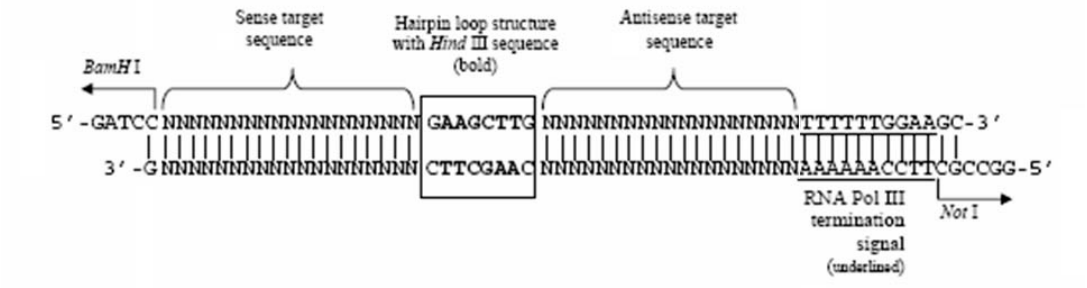

FIGURE 5-3 Forward and reverse oligonucleotide sequences. The sequences comprised 5' *Bam*HI and *Not*I sites respectively, the 19mer sense and antisense siRNA sequences (see Table 2.1) separated by a hairpin structure with the *Hind*III site, and a RNA polymerase III termination signal. Annealed forward and reverse oligonucleotides were cloned into the pGSU6-GFP plasmid containing the kanamycin resistance gene.

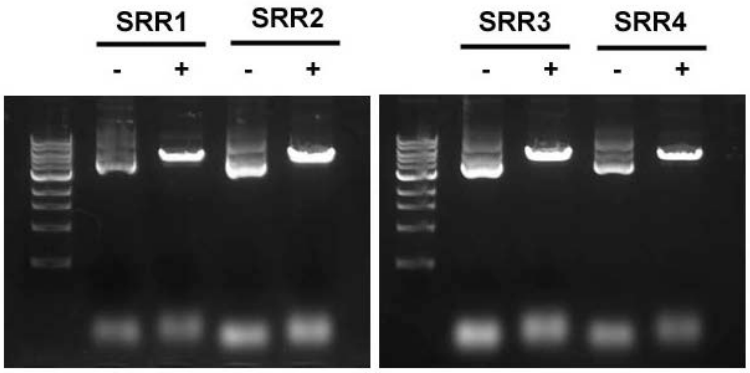

FIGURE 5-4 Restriction endonuclease digest resolved on ethidium-bromide stained agarose gel. Gel shows linear DNA for each shRNA (SRR1-4) cut with *HindIII* (+) which migrates higher than coiled shRNA counterparts not cut with *HindIII* (-).

cultures of selected colonies grown as described (Section 5.2.6.2) except; 10µl ligation reaction was transformed into 50µl SmartCell competent *E.coli* (Genlantis), added to 100µl SOCS and the 150µl transformation/SOCS mix added to LB agar plates containing 50µg/ml kanamycin (Sigma). Plasmids were then extracted, purified (Sections 5.2.7, 5.2.8), restriction endonuclease digested using the *Hind*III enzyme (Section 5.2.10) and visualized on agarose gels (Section 5.2.5). The insertion of the short-hairpin expressing sequence was verified by linearization of the plasmid by the *Hind*III enzyme for each shRNA (Figure 5.4).

5.2.12 Over-expression vectors

The SRR open-reading frame with 5' Bam*HI* and 3' Apa*I* restriction endonuclease sites was amplified as described (Section 5.2.4) using forward (CTAGATAGGGATCCA TGTGTGCTCAGTACTGCAT) and reverse (ATACGTACGGGCCCAACAGAAACCGTCTGGTAA G) primers. The forward primer contained the Bam*HI*, and the reverse primer the Apa*I*, restriction endonuclease sites (underlined). These were flanked by 5' nonsense sequences because the endonucleases cut more efficiently when the restriction site is not terminal (Dr P Burnet, personal communication). Amplified

SRR cDNA was purified as described (Section 5.2.8) and cut using *BamH*I and *Apa*I endonucleases as described (Section 5.2.10) but with 5µg DNA in a 50µl total volume. The pcDNA3.1/*myc*-His plasmid containing the ampicillin resistance gene and the CMV promotor (Figure 5.5; Invitrogen) was cut with *BamH*I and *Apa*I as described (Section 5.2.10) except 15-20µg plasmid was incubated in a 100µl total volume. Cut insert and plasmid were ligated (Section 5.2.6.1) and 3µl ligation mix transformed into bacteria which were plated, cultured (Section 5.2.6.2) and the plasmid purified by alkaline-lysis and phenol-chloroform purification (Sections

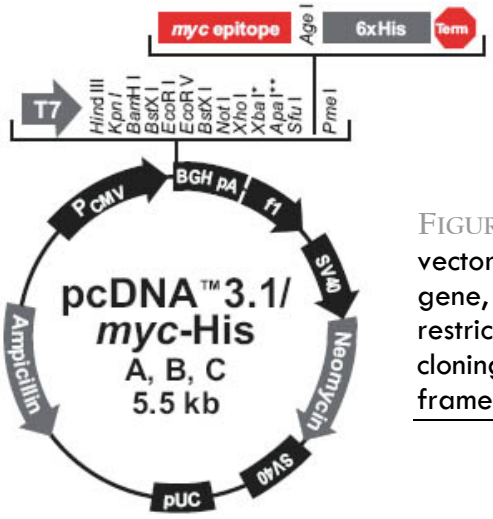

FIGURE 5-5 Features of the pcDNA 3.1*myc*-His vector (Invitrogen) showing the ampicillin resistance gene, the CMV promotor and the BamHI and ApaI restriction endonuclease sites within the multiple cloning site used to insert the SRR open-reading frame 5' to the *myc* tag and termination signal.

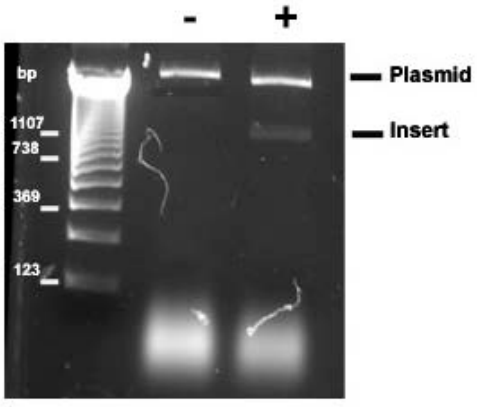

FIGURE 5-6 Verification of SRR over-expression plasmid synthesis. Representative restriction endonuclease digest showing resolved DNA on ethidium-bromide stained agarose gel. The insert of the SRR open-reading frame ~1000bp is cut from the synthesized SRR over-expression vector (+) but not from empty vector (-) following treatment with *BamH1* and *ApaI* restriction endonucleases.

5.2.7, 5.2.8) or column-based purification (Sections 5.2.9). Purified plasmids were verified by restriction endonucleases digest as described (Section 5.2.10) using *BamH*I and *Apa*I to cut the insert from the plasmid (Figure 5.6).

5.2.13 Transfections

Cells were plated at a density of $2x10^4$ (naïve P19), $4x10^5$ (differentiated P19) or $2.65x10^5$ (CGC) cells per $2cm^2$ well in 24-well plate format. Transfections were performed at 2-4DIV for differentiated P19 cultures and 1DIV for primary CGC cultures. Transfections were carried out using the cationic lipid reagents DharmaFECT3 (Dharmacon), Optifect (Invitrogen) or Lipofectamine^{2000} (Invitrogen) according to manufacturer's instructions. Briefly, for each well to be transfected, lipid reagent and siRNA or plasmid DNA were each resuspended in 50µl OptiMEM (Gibco, Invitrogen) and incubated at five minutes for room temperature. The mixtures were then combined and incubated for twenty minutes at room temperature to allow nucleic acid-lipid complexes to form. Culture media was removed from the cells, which were washed once in antibiotic free culture media, and the nucleic acid-lipid mixture then diluted in 400µl antibiotic-free culture media and the 500µl total volume added to the cells. Twenty four hours later, the medium was removed and exchanged entirely for antibiotic containing culture medium.

To knockdown cyclophilin in naïve P19 cultures, cells were transfected with 100nM final concentration siGLO using DharmaFECT3. To knockdown cyclophilin in differentiated P19 cultures, cells were transfected with 100nM final concentration siGLO using DharmaFECT3, Optifect or Lipofectamine^{2000}. Cells transfected with siGLO were visualized with fluorescence microscopy.

To knockdown SRR in differentiated P19 cultures, cells were transfected using Lipofectamine^{2000} with four siRNA sequences directed to SRR (Table 5.2) or four plasmids expressing shRNAs of these sequences (Section 5.2.11). To over-express SRR, the SRR expression vector was transfected with Lipofectamine^{2000} into differentiated P19 and primary CGC cultures.

For each 2cm^2 well to be transfected with siRNA, DharmaFECT3 was used at 0.5, 1 or 1.5µl/500µl total volume, Optifect at 3, 4.5 or 6µl/500µl total volume and Lipofectamine^{2000} at 1µl/500µl total volume. For each 2cm^2 well to be transfected with plasmid DNA, 1µg DNA and 2.5µl Lipofectamine^{2000} were used in 500µl total volume. Cells were visually examined daily.

5.2.14 Antibody affinity chromatography

An antibody to DAO, generated against purified porcine DAO (Sigma), was provided as a generous gift from Dr Cimini, University of L'Aquila, Italy (Moreno *et al.*, 1999). The antibody was purified in the laboratory of Dr Robert Sim, Department of Biochemistry, University of Oxford. To desalt the antigen, 5.45mg DAO (Sigma) (corresponding to 3mg actual enzyme) was dissolved in 1ml PBS-0.5mM EDTA (Sigma) and run through a Sephadex G-25M PD-10 Desalting column (GE Healthcare) according to manufacturer's instructions. The protein fraction was collected and verified by spectrophotometric absorbance measurements at 280nm. To prepare antigen coupled resin, 1g Cyanogen Bromide activated Sepharose 4B (Sigma) was dissolved in 200ml 1MHCl, filtered in a Buchner flask and the resin added to the desalted antigen. The mixture was incubated for two hours at room temperature on a rotary stirrer, to allow the antigen and resin to couple, and the supernatant filtered off using a Buchner flask. The resultant resin

was washed twice in 2M NaCl and incubated for two hours on a slow rotary stirrer at room temperature with 30ml 100nM ethanolamine HCl, 150mM NaCl, pH 8.5 to block non-specific antibody binding sites in the resin. 2mls resin was then added to a HiTrap-protein G affinity chromatography column (GE Healthcare) and run through with 10mls PBS-0.5mM EDTA. The DAO antibody serum was centrifuged at 15000*g* for five minutes to remove any precipitate and the supernatant added to the resin column with the tap off and incubated at 4ºC for an hour to allow the antibody to bind to the antigen. The DAO antibody serum was then run through the column followed by 20mls PBS-0.5nM EDTA until the fractions collected had spectrophotometric absorbance readings at 280nm of <0.04. To elute the antibody, 1ml ddH_2O followed by 6ml $MgCl_2$ and 1ml ddH_2O was run through the column and fractions containing the purified antibody verified by spectrophotometric absorbance measurements at 280nm. The solution was dialysed to remove $MgCl_2$ by adding the solution to 12-14kDa molecular weight cut-off dialysis tubing (Spectrum Laboratories, VWR International) placed in 1 litre PBS-0.5nM EDTA overnight. The resultant antibody solution measured spectrophotometrically at 280nm was 0.0171µg/µl.

5.2.15 Protein extraction and western blotting

To extract protein from cell cultures, 25-50µl radioimmuno-precipitation assay buffer (RIPA; Sigma) containing 1x protease inhibitor cocktail (Sigma) was added per cm^2 cell culture surface and homogenized by pipetting up and down several times. Cell debris was pelleted by centrifugation at 13,000*g* for ten minutes. The concentration of protein extracts was measured (Chapter 2, Section 2.2.3) and used for western blotting (Chapter 2, Section 2.2.4) as described.

For these studies, two primary antibodies to DAO were used. One was an antibody generated against purified porcine DAO (Sigma), provided by Dr Cimini, University of L'Aquila, Italy (Moreno *et al.*, 1999 antibody), and purified by affinity chromatography (Section 5.2.14). The Moreno *et al.* (1999) antibody was used at used at 1:50. A second antibody was the GSK-DAO antibody described in Chapter 2, Section 2.3.1 which was used at 1:500-1:1000. Primary antibodies to SRR (BD Biosciences; see Chapter 2, Section 2.3.1 for characterisation) and the loading controls cyclophilin (AbCam) and beta-tubulin (Sigma) were used at 1:500, 1:500,000 and 1:10,000 respectively.

5.2.16 DAO activity

DAO activity in primary CGC and differentiated P19 cell cultures was carried out as described (Chapter 3, Section 3.2.5) except cells were removed from the well in Ca^{2+} and Mg^{2+} free Dulbecco's PBS (Gibco, Invitrogen) using a cell scraper, pelleted by centrifugation at 180*g* for two minutes, and then homogenized.

5.2.17 High Performance Liquid Chromotography (HPLC)

For HPLC, cells were rinsed in PBS and lysed in ddH_20. Samples were frozen at -70ºC and sent to GSK, Harlow, UK. HPLC-mass spectrometry for D- and L-serine was generously carried out by Dr James Storey.

5.2.18 Data presentation and statistical analysis

All studies were carried out on triplicate wells of cells per experiment. Measurements from the three replicates of an experiment were averaged to provide the mean measurement for an *n* of 1. Experiments were then repeated for

subsequent *n*, on separate cultures. For differentiated P19 cells this is defined as a separate round of retinoic acid treatment and culture of these cells. For primary CGC cultures this is defined as a separate culture prepared from a different litter of animals. Therefore in this chapter, 'replicate' refers to a well of cells within one experiment/one culture. An 'experiment' or 'culture' represents three replicates and corresponds to an *n* of 1.

Statistical analyses were conducted with non-parametric tests owing to *n*'s of <5. To look for an effect of time *in vitro* on basal SRR immunoreactivity, a Spearman's correlation was performed in addition to a Kruskall-Wallis test to look for significant differences in SRR immunoreactivity amongst time-points. For knockdown and over-expression studies, Mann Whitney-*U* tests were performed to compare SRR immunoreactivity of siRNA or over-expression vector transfected cells with control SRR immunoreactivity levels.

5.3 RESULTS

5.3.1 Characterisation of differentiated P19 and CGC cultures

5.3.1.1 Characterisation of differentiated P19 cultures

MAP2, Tau and GFAP immunocytochemistry

To establish that P19 cells had been successfully differentiated with retinoic acid treatment into neuronal- and glial-like cells and cultured, cells were stained for the neuronal markers MAP2 and Tau and the glial marker GFAP. At 3 DIV, MAP2 and Tau staining was prominent and labelled cell bodies and neuronal processes while GFAP staining was not visible (data not shown). At 6 DIV, MAP2 and Tau staining was prominent and labelled cell bodies and extensive networks of neuronal processes (Figure 5.7 A). GFAP-reactive cells were visible but were few in number (Figure 5.7 C). At 11DIV, MAP2 and Tau staining had diminished due to fewer labelled cells and processes in total and due to clustering of neurons into clumps (Figure 5.7 B). GFAP-reactive cells were abundantly labelled at 11DIV (Figure 5.7 D).

Expression of SRR in P19 cultures

To examine whether differentiated P19 cultures express SRR, the gene was amplified from pooled 4DIV differentiated P19 cDNA (n = 2), which demonstrated amplification of a single product of predicted size (138bp; Figure 5.8 A). SRR protein expression in differentiated P19 cultures was examined by western blotting. A band at ~38kDa, the predicted molecular weight of SRR (Wolosker *et al.*, 1999b; De Miranda *et al.*, 2000), was detected (Figure 5.8 B). An additional fainter band at

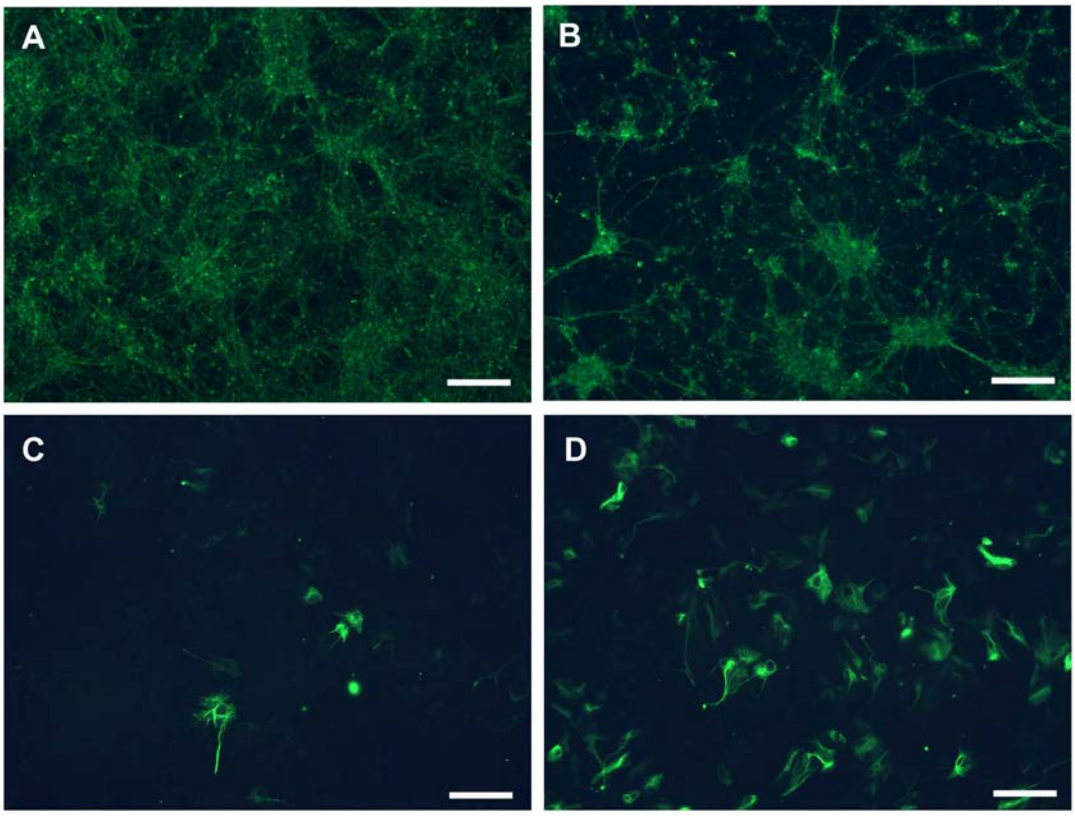

FIGURE 5-7 Expression of the neuronal markers MAP2 and Tau (A, B) and the glial marker GFAP (C, D) in differentiated P19 cultures at 6DIV (A, C) and 11DIV (B, D). Scale bars = 50µm (C, D), 100µm (A, B).

~50kDa was visualized in some replicates. No detectable immunoreactivity was visualized in naïve P19 cells (Figure 5.8 B). In differentiated P19 cultures, SRR immunoreactivity was detectable from 1DIV to 11DIV (Figure 5.8 C). No statistical effect of DIV on SRR immunoreactivity was observed (Kruskall-Wallis, $p = 0.468$), although a trend correlation of DIV with SRR immunoreactivity was (Spearman's correlation, $p = 0.068$). Attempts to delineate the cell type(s) expressing SRR protein with immunocytochemistry were unsuccessful, despite trying a range of fixation and permebalization methods and antibody concentrations (data not shown).

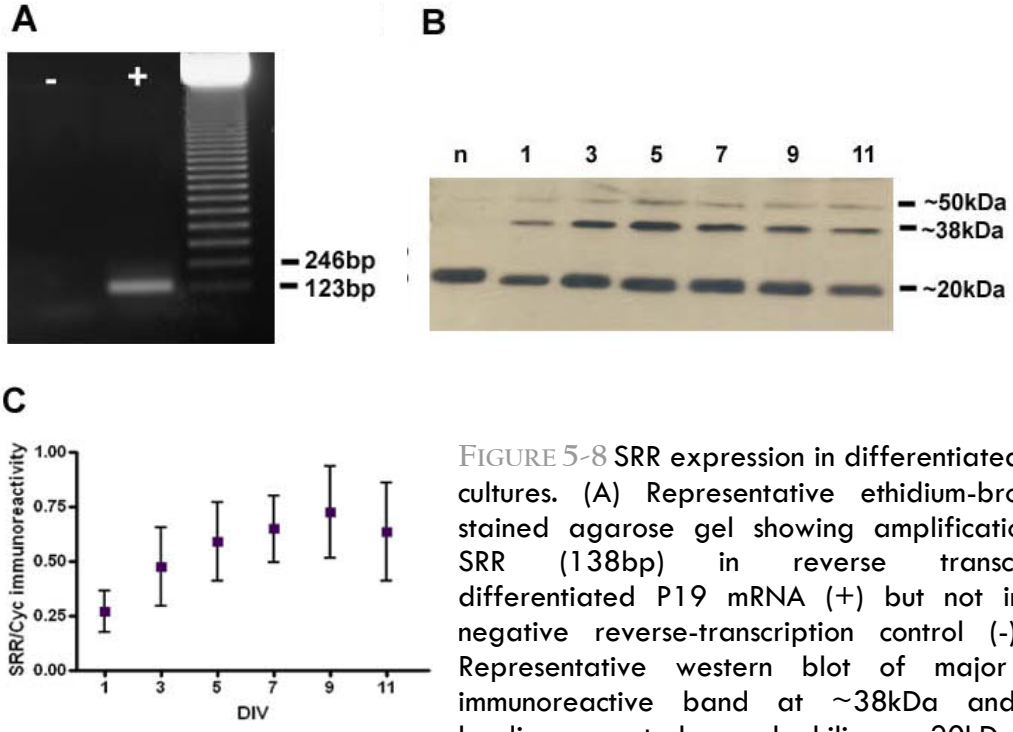

FIGURE 5-8 SRR expression in differentiated P19 cultures. (A) Representative ethidium-bromide stained agarose gel showing amplification of SRR (138bp) in reverse transcribed differentiated P19 mRNA (+) but not in the negative reverse-transcription control (-). (B) Representative western blot of major SRR immunoreactive band at ~38kDa and the loading control cyclophilin ~20kDa in differentiated P19 cell extracts (1 – 11 DIV). The ~38kDa band was not detected in naïve (n) P19 cell extracts. In some replicates a minor band ~50kDa was also visualized. (C) SRR immunoreactivity in differentiated P19 cultures 1DIV-11DIV (n = 3); data are mean ± sem.

Expression of DAO in P19 cultures

To examine whether differentiated P19 cultures expressed DAO, the gene was amplified from pooled differentiated P19 cDNA (n = 2), which demonstrated amplification of a single product of predicted size (438bp; Figure 5.9 A). Initial experiments attempting to detect DAO immunoreactivity in differentiated P19 cultures used an antibody generated against porcine DAO (Moreno *et al.* 1999 antibody). This antibody detected an immunoreactive band at ~39kDa, the predicted molecular weight of DAO (Gavazzi *et al.*, 1987; Moreno *et al.*, 1999), in purified porcine DAO (Figure 5.9 B, Lane 1) and rat cerebellum (Figure 5.9 B, Lane 2) and additional fainter bands at ~30kDa and ~50kDa. All bands were abolished by pre-incubation of the antibody with porcine DAO (Figure 5.9 B, Lane 3). In naive

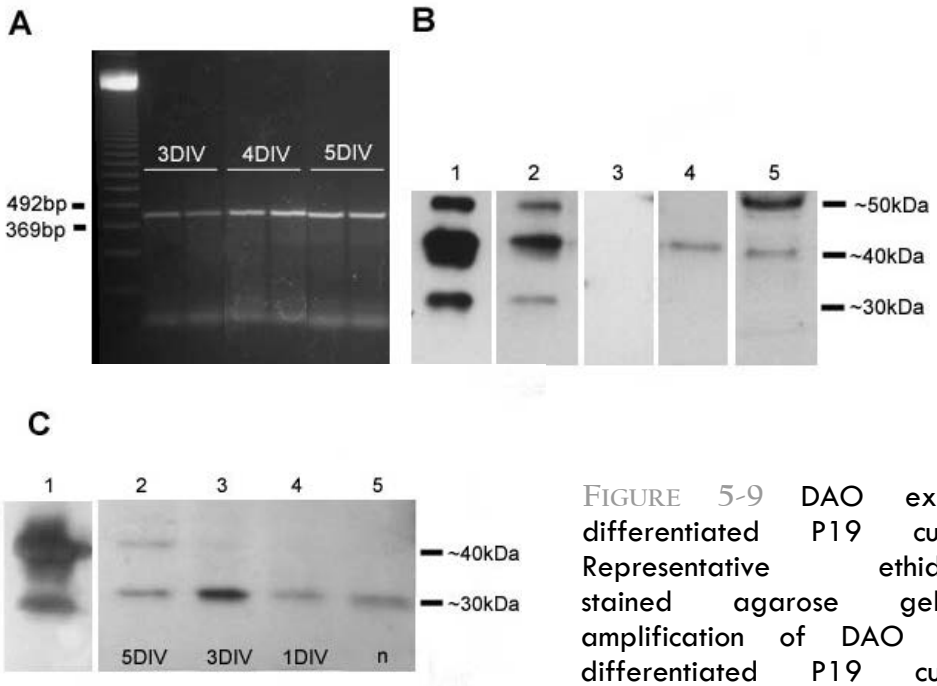

FIGURE 5-9 DAO expression in differentiated P19 cultures. (A) Representative ethidium-bromide stained agarose gel showing amplification of DAO (438bp) in differentiated P19 cultures. (B) Representative western blot showing detection of immunoreactive bands at ~39kDa, ~30kDa and ~50kDa with the Moreno *et al.* (1999) DAO antibody in purified porcine DAO (Lane 1), rat cerebellum (Lane 2), pre-incubation control (Lane 3), naïve P19 cells (Lane 4) and differentiated P19 cells (Lane 5). (C) Representative western blots showing detection of immunoreactive bands ~39kDa and ~30kDa with an anti-peptide DAO antibody (GSK antibody) in purified porcine DAO (Lane 1), differentiated P19 cells (Lanes 2-4) and naïve P19 cells (Lane 5).

P19 cells the ~39kDa band was detected (Figure 5.9 B, Lane 4) and additional bands at ~30kDa and ~50kDa detected in some replicates (data not shown). In differentiated P19 cells the ~39kDa and ~50kDa bands were detectable (Figure 5.9 B Lane 5). Subsequently, use of the Moreno *et al.* (1999) antibody was shown to be confounded by the demonstration that the porcine DAO preparation used as an antigen to generate the antibody, was contaminated by DAspOx (Shleper *et al.*, 2005). Consequently, experimentation with the Moreno *et al.* (1999) antibody was not pursued. Further studies were conducted with an antibody generated against a peptide sequence of DAO, the GSK-DAO antibody (see Chapter 2, Section 2.3.1 for characterisation). The GSK-DAO antibody was shown to detect a single

immunoreactive band, at ~39kDa, in human and rat cerebellum (Chapter 2, Section 2.3.1) and bands at ~39kDa and ~30kDa in porcine DAO (Figure 5.9 C, Lane 1). In P19 cells, the ~30kDa band was detected in naïve and differentiated cells, while an additional band at ~39kDa band was present in some replicates (Figure 5.9 C, Lanes 2-5). (However, two later attempts to detect DAO by western blotting in two naïve and two differentiated P19 cultures were negative (data not shown), despite the methodology being consistent). DAO could not be detected immunocytochemically in these cultures and nor could DAO activity be detected (data not shown).

Expression of NMDAR subunits in P19 cultures

To examine whether P19 cells expressed NMDARs, the NMDAR subunit NR1, NR2A, NR2B and NR2C transcripts were amplified from pooled naïve and differentiated P19 cDNA (n =3). Naïve P19 cells expressed negligible levels of NR1 and NR2C subunits and low levels of NR2A and NR2B subunits. Differentiated P19 cultures expressed robust levels of NR1, NR2A and NR2B subunits, detectable from 5 to 11DIV, and low levels of NR2C (Figure 5.10).

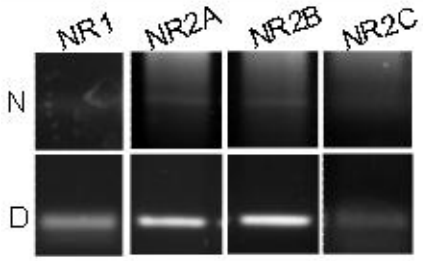

FIGURE 5-10 Representative ethidium-bromide stained agarose gels showing amplification of NR1, NR2A, NR2B and NR2C subunits in naïve (N) and differentiated (D) P19 (5DIV) cell extracts.

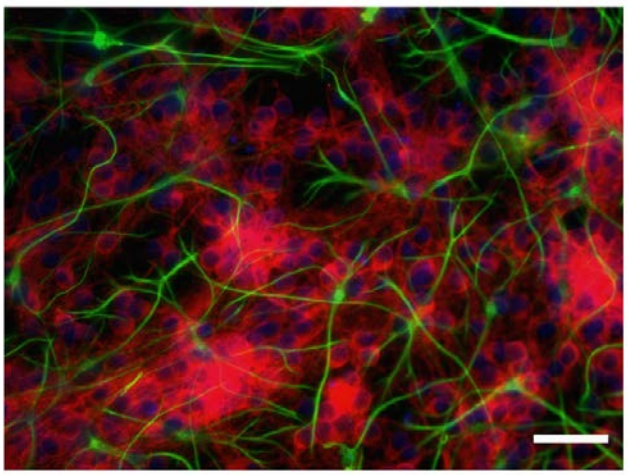

FIGURE 5-11 Representative image of CGC cultures (4DIV) stained for MAP2 and Tau (Red), Hoechst 33528 nuclear stain (Blue) and GFAP (green). Scale bar = 25µm.

5.3.1.2 Characterisation of primary CGC cultures

MAP2, Tau and GFAP immunocytochemistry

To establish that CGC cultures had been successfully generated, cultures were stained for the neuronal markers MAP2 and Tau and the glial marker GFAP. MAP2 and Tau labelled granule cell bodies and extensive neuronal processes and GFAP labelled numerous glial cells, many with stellate morphologies (Figure 5.11).

SRR expression in CGC cultures

Three SRR immunoreactive bands at ~38kDa, ~50kDa and ~150kDa were detected in primary CGC cultures, the predominance of which varied. In one culture the ~38kDa band was detected in all three replicates at 2, 4 and 6DIV and was the predominant band. Conversely, the ~50 and ~150kDa bands were detected in only one or two out of the three replicates for each time point in this culture (Figure 5.12 A). In a second culture all three bands were detectable at all time points and in all replicates except for one well which did not demonstrate the ~38kDa band. In this second culture the ~50kDa and ~150kDa bands were more intensely

immunoreactive than the ~38kDa (Figure 5.12 B). Quantification of the ~38kDa band - presumed to represent SRR based on the molecular weight - showed a visible increase in immunoreactivity with time *in vitro* (Figure 5.12 C) but an *n* of 2 precluded statistical analysis.

DAO expression in CGC cultures

Using the GSK-DAO antibody, two immunoreactive bands at ~30kDa and ~39kDa could be detected at very low levels in CGCs ($n = 2$) (Figure 5.13). DAO could not be detected immunocytochemically in these cultures and nor could DAO activity (data not shown).

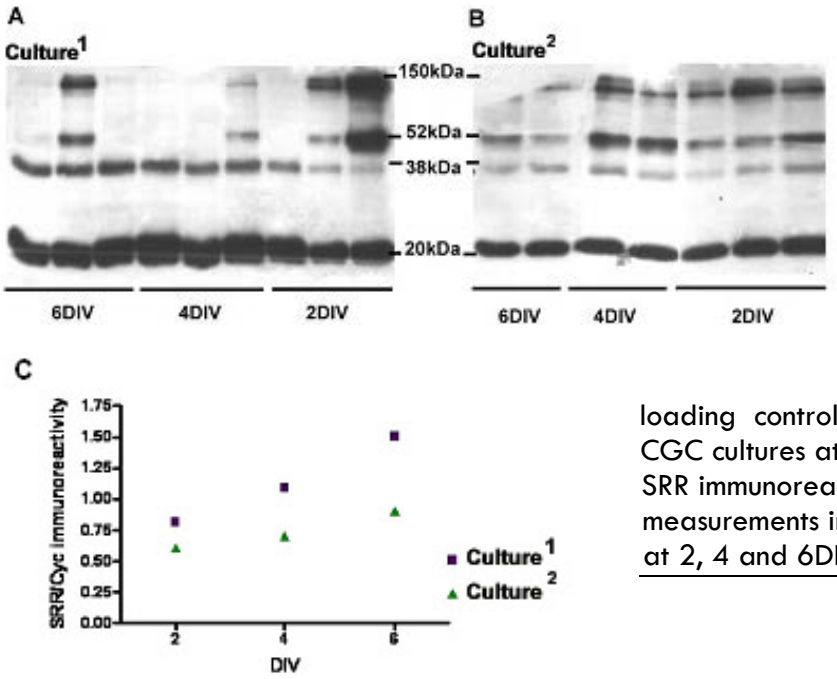

FIGURE 5-12 SRR expression in CGC cultures. (A) and (B) Western blot detection of immunoreactive bands at ~38kDa, 50kDa and 150kDa with SRR antibody and cyclophilin loading control at ~20kDa in two CGC cultures at 2,4 and 6DIV. (C) SRR immunoreactivity (~38kDa) measurements in two CGC cultures at 2, 4 and 6DIV.

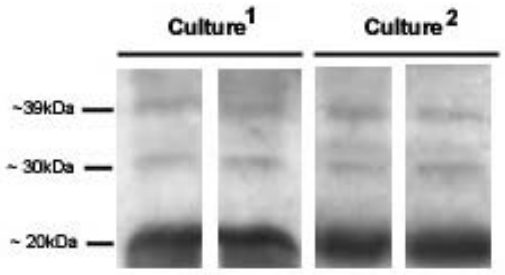

FIGURE 5-13 Representative western blots of DAO immunoreactivity at ~30kDa and ~39kDa in two CGC cultures. Cyclophilin loading control was detected at ~20kDa.

5.3.2 RNA interference in P19 cultures

5.3.2.1 Knockdown of cyclophilin in P19 cultures

Initial pilot experiments utilised an siRNA molecule, siGLO, targeted at cyclophilin and with a fluorescent tag. The activity of this siRNA is validated by Dharmacon and it therefore serves as a positive control: it allows transfection to be visualized via fluorescence microscopy and siRNA knockdown to be monitored via cyclophilin gene expression analysis, in order to verify RNAi in a given system. Initially the activity of siGLO was tested in naïve P19 cultures. 100nM siGLO was transfected with DharmaFECT3 at a range of recommended dilutions (0.5:500, 1:500, 1.5:500) in order to ascertain optimal transfection conditions. Under these conditions visible transfection was observed, greatest with 1:500 and 1.5:500 DharmaFECT3 (Figure 5.14 A-I). Transfection with 1:500 DharmaFECT3, the lowest amount of lipid producing the best transfection, induced knockdown of cyclophilin immunoreactivity 72hrs post-transfection (Figure 5.14 J) by 76% (Table 5.3).

Having tested the activity of siGLO in naïve P19 cultures, the siRNA was transfected into differentiated P19 cultures in order to validate RNAi in this system; the aim was to establish effective knockdown with siGLO in order to attempt SRR knockdown under the same conditions. 1:500 and 1.5:500 DharmaFECT3 dilutions demonstrated visible transfection of 100nM siGLO (Figure 5.15 A-F), whereas 0.5:500 showed no visible transfection (data not shown). Transfection was visualized in both neural and glial cells identified morphologically (Figure 5.15 G, H). Transfection with 1:500 and 1.5:500 DharmaFECT3 knocked-down cyclophilin by ~6 and 40% respectively 72 hours post-transfection (Figure 5.15 I; Table 5.3). This was lower than expected compared to siGLO cyclophilin knockdown in naïve P19 cultures. One hypothesized reason for this (see Discussion also) was that

TABLE 5-3 Cyclophilin knockdown with siGLO cyclophilin in naïve and differentiated P19 cultures under different transfection conditions. Knockdown was monitored 72 hours post-transfection, and for Optifect at both 72 and 96 hours post-transfection. $n = 1$

	Lipid reagent only (Cyc/ ß -tubulin immunoreactivity)	Lipid reagent + 100nM siGLO (Cyc/ß -tubulin immunoreactivity)	% Cyclophilin knockdown
Naïve P19 cultures			
DharmaFECT 3			
1:500	1.545	0.371	76
Differentiated P19 cultures			
DharmaFECT 3			
1:500	0.993	1.054	-6
1.5:500	1.301	0.782	40
OptiFECT_72			
3:500	0.656	0.479	27
4.5:500	0.763	0.670	12
6:500	0.850	0.756	11
OptiFECT_96			
3:500	1.126	1.179	-5
4.5:500	1.644	1.244	24
6:500	1.152	2.101	-82
Lipofectamine^{2000}	1.552	1.380	11

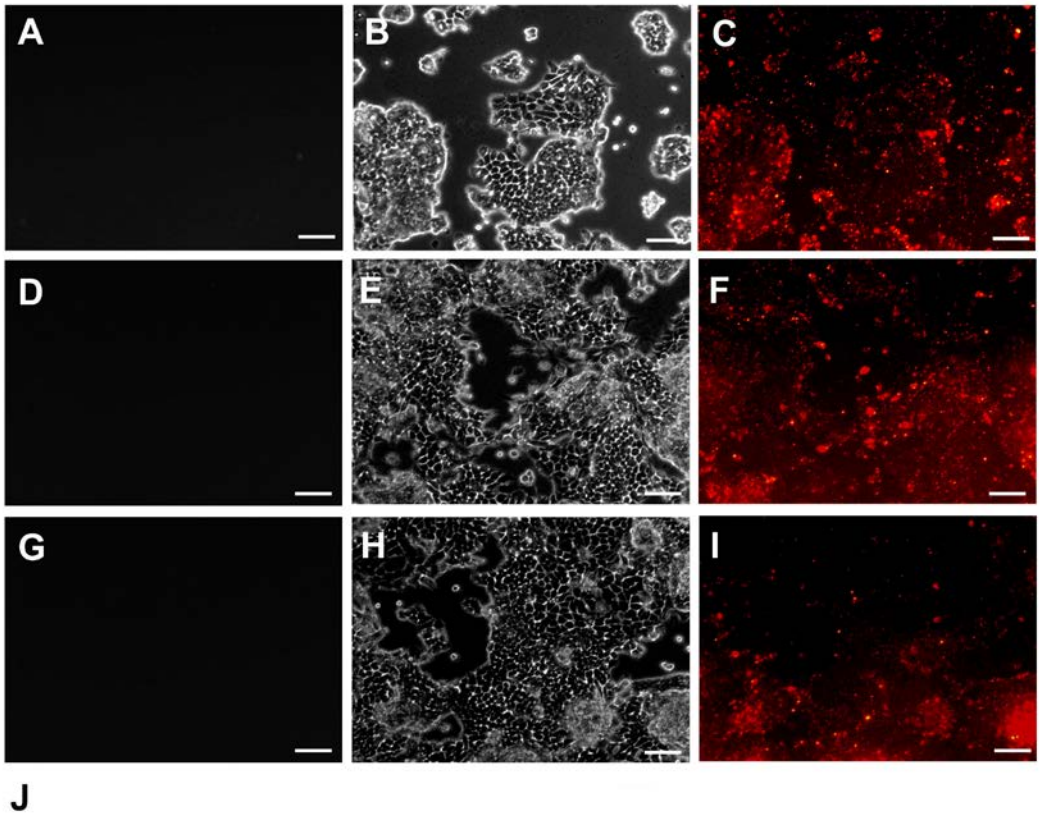

FIGURE 5-14 siGLO transfection and cyclophilin knockdown in naïve P19 cultures. Cells were treated with 1.5:500 (A-C), 1:500 (D-F) and 0.5:500 (G-I) DharmaFECT3 alone (A, D, G) or plus 100nM siGLO (C, F, I) and visualized with fluorescence microscopy 24 hours later. Corresponding live images are shown (B, E, H). Scale bar = 100μm. (J) With 1:500 DharmaFECT3, cyclophilin immunoreactivity (lower panel) was knocked down in siGLO transfected cells (+) but not lipid only treated cells (-) compared to the loading control beta-tubulin (top panel).

transfection was reduced in differentiated versus naïve cells. While transfection with DharmaFECT3 was visible it was hypothesized that levels may still have been too low for detectable cyclophilin knockdown. One factor that could have affected transfection efficiency was that differentiated cultures were often of a lower confluency than naïve P19 cultures. To probe these factors, 100nM siGLO cyclophilin was transfected into differentiated P19 cultures using Optifect, a lipid

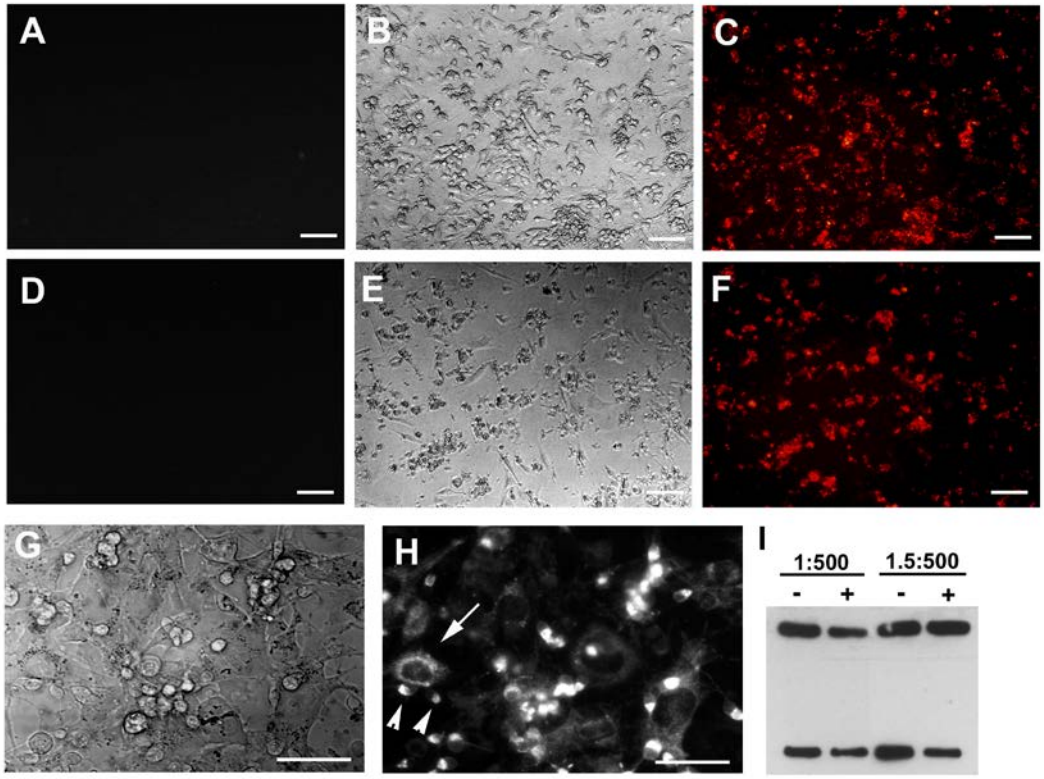

FIGURE 5-15 Transfection and knockdown with siGLO cyclophilin in differentiated P19 cultures. Cells were treated with 1.5:500 (A-C) and 1:500 (D-F) DharmaFECT3 alone (A and D) or plus 100nM siGLO (C and FI) and visualized with fluorescence microscopy 24 hours later. Corresponding live images are shown (B and E). (H) siGLO could be visualized with fluorescence microscopy in both glial (arrow) and neuronal (arrowheads) cells identified morphologically compared to corresponding live image (G). Scale bars = 100µm. (I) Representative western blot of cyclophilin immunoreactivity (lower panel) and the loading control beta-tubulin (top panel) following transfection of differentiated P19 cultures with siGLO cyclophilin (+) at 1:500 or 1.5:00 DharmaFECT3 compared to treatment with lipid only (-).

transfection reagent for low confluency or sensitive cells. Transfection was visible at 24 hours post-transfection with 3:500, 4.5:500 and 6:500 Optifect dilutions (data not shown) and cyclophilin knockdown of 11 – 27 % and 0 – 24 % was shown at 72 and 96 hours post-transfection respectively (Table 5.3). In two experiments, over-expression of cyclophilin was induced (Table 5.3). In a second attempt to modulate transfection, 100nM siGLO cyclophilin was transfected into differentiated P19 cultures using Lipofectamine^{2000}, effective for cells refractory to transfection

under standard conditions (Amarzguioui, 2004). Transfection of differentiated P19 cultures with 100nM siGLO cyclophilin and 1:500 Lipofectamine^{2000} was shown to knockdown cyclophilin by 11% (Table 5.3). Transfection with 1.5:500 Lipofectamine^{2000} caused cell death observed upon visual examination of cultures (data not shown) and these experiments were not continued.

5.3.2.2 Knockdown of SRR in P19 cultures

Since the overall aim of these experiments was to establish SRR knockdown, and given that low knockdown of cyclophilin in differentiated P19s may have been particular to knockdown of the cyclophilin gene, siRNAs to SRR were then tested. shRNAs targeted to the same sequences were tested in parallel, as some reports suggest that shRNAs have a greater potency than siRNAs targeted to the same sequence (Vlassov *et al.*, 2007). Lipofectamine^{2000} was initially chosen for these studies given its successful use in other siRNA experiments in neuronal cultures (Fountaine & Wade-martins, 2007) and its recognition as one of the most commonly used reagents in the literature for *in vitro* transfections.

A preliminary experiment ($n = 1$) revealed that transfection of shRNA plasmids led to knockdown of normalised SRR immunoreactivity by 26, 10, 10 and 16% respectively at 72hrs post- transfection (Figure 5.16 A and B). Transfection of siRNAs SRR1-4 and a cocktail of all four knocked-down SRR by 28±7 (mean ± sem), 34±2, 50±5, 45±8 and 34±4% respectively at 72 hours post-transfection (Figure 5.17). SRR immunoreactivity was significantly different between control cultures compared to SRR1 (Mann Whitney-*U*, $p = 0.037$), SRR2 (Mann Whitney-*U*, $p = 0.037$), SRR3 (Mann Whitney-*U*, $p = 0.037$), SRR4, (Mann Whitney-*U*, $p = 0.037$) and cocktail (Mann Whitney-*U*, 0.037) treated cultures. SRR3 and SRR4

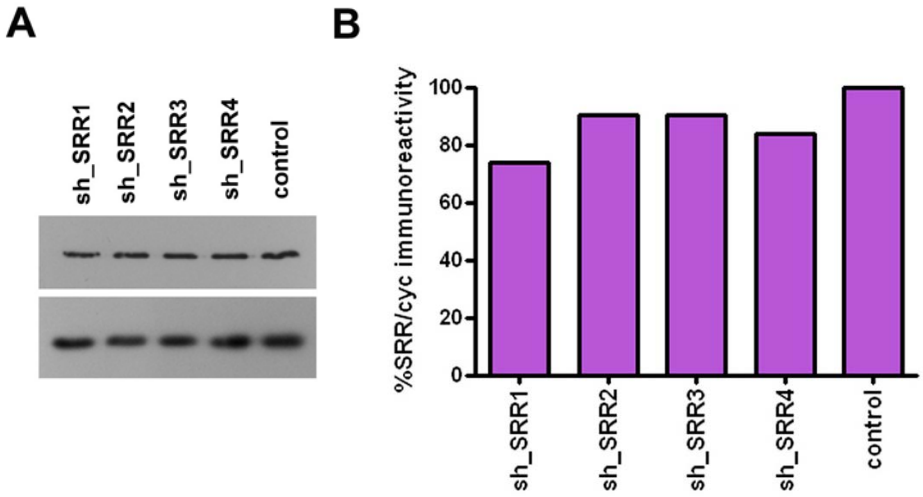

FIGURE 5-16 SRR knockdown in differentiated P19 cultures with shRNAs. (A) Representative western blot of SRR immunoreactivity at ~38kDa (top panel) and loading control cyclophilin immunoreactivity at ~20kDa (bottom panel) in cells treated with shRNAs (1-4) or Lipofectamine^{2000} only (control). (B) Percentage of normalised SRR immunoreactivity in differentiated P19 cultures (n = 1) treated with shRNAs 1-4 or Lipofectamine^{2000} only (control).

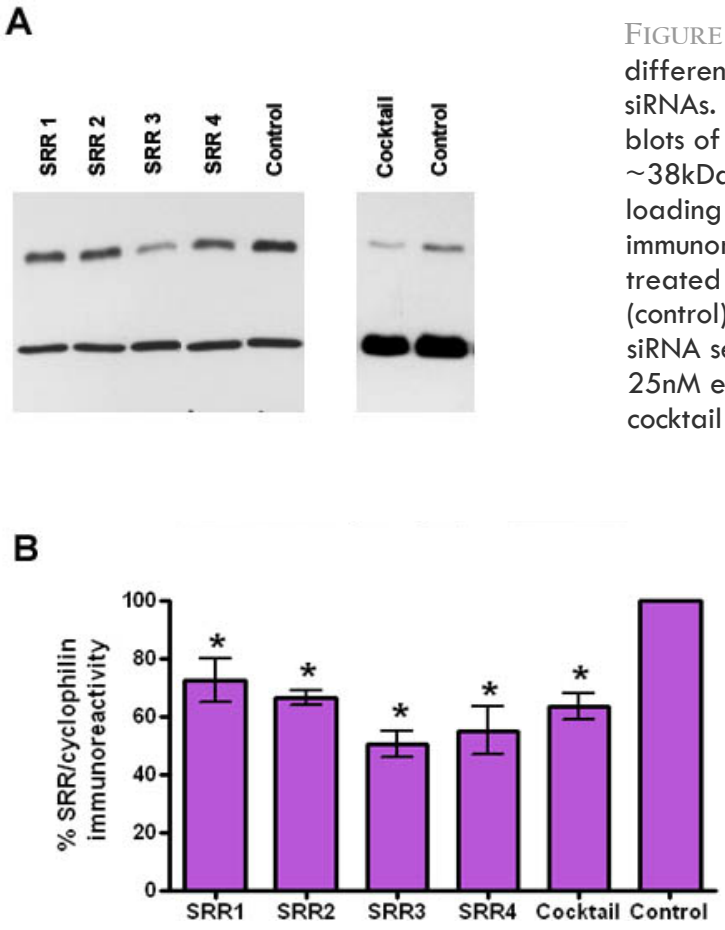

FIGURE 5-17 SRR knockdown in differentiated P19 cultures with siRNAs. (A) Representative western blots of SRR immunoreactivity at ~38kDa (top) and cyclophilin loading control at ~20kDa immunoreactivity (bottom) in cells treated with Lipofectamine^{2000} only (control) or 100nM of each of four siRNA sequences to SRR (SRR1-4) or 25nM each siRNA to SRR in a cocktail (cocktail). (B) Percentage normalised SRR immunoreactivity in differentiated P19 cultures (n = 3) treated with 100nM siRNA sequences SRR 1-4, a cocktail of 25nM of each or Lipofectamine^{2000} only (control). All siRNA treatments showed a significant (* $p < 0.05$) reduction in normalised SRR immunoreactivity compared to control samples. Bars show mean ± sem.

were then selected for further experimentation as they produced the greatest mean knockdown in this initial screen.

Titration of SRR3 and SRR4 from 100nM–12.5nM was found to produce less knockdown at any concentration than seen in the initial screen with 100nM. The maximum knockdown achieved was 15±22% (mean ± sem) with 12.5nM SRR3 and 16±15% (mean ± sem) with 25nM SRR4 (Figure 5.18). Intra-replicate (data not shown) and inter-replicate (Figure 5.18) variability was much greater than in the initial screen with 100nM siRNAs 1-4 to SRR (see Figure 5.17).

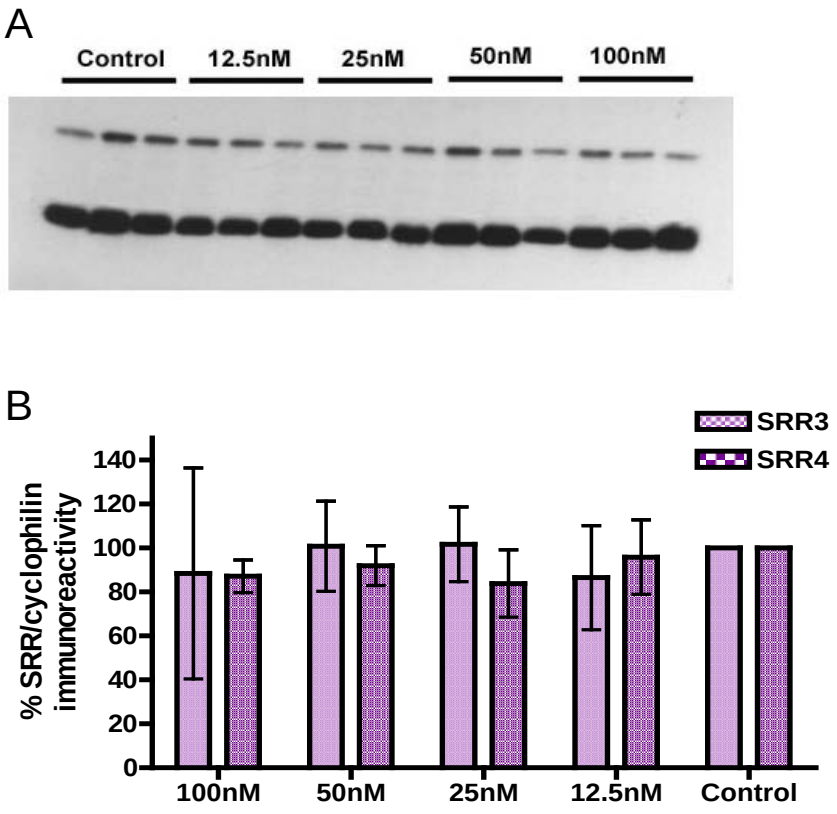

FIGURE 5-18 Titration of SRR siRNAs 3 and 4. (A) Representative western blot of SRR immunoreactivity (top row) and loading control cyclophilin immunoreactivity (bottom panel) in cells treated with Lipofectamine^{2000} only (control) or 12.5, 25, 50 or 100nM SRR3. (B) Percentage SRR immunoreactivity in cultures treated with 100, 50, 25 or 12.5nM SRR3 or SRR4 or Lipofectamine^{2000} only (control). Bars show mean ± sem, n =3.

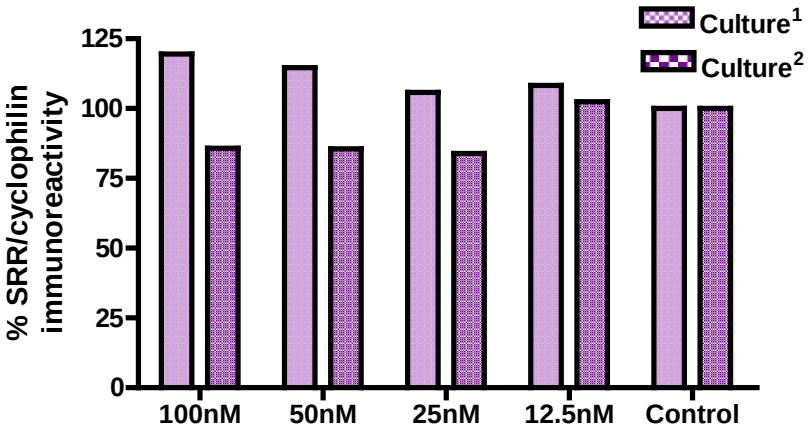

FIGURE 5-19
Repeated titration of SRR3 siRNA. Percentage SRR immunoreactivity in cultures treated with 100, 50, 25 and 12.5nM SRR3 or Lipofectamine2000 only (control) in two repeated experiments (culture 1 and culture 2).

The methodology between the initial screen and subsequent titration experiments was consistent. It was therefore hypothesized that a change in the health of the cells could possibly have contributed to the disparity in the results (see Discussion, Section 5.4.4 also). Therefore, at this point, a new batch of P19 cells were ordered, differentiated and cultured in two different laboratories with existing and newly ordered cell culture constituents. These cultures were visually compared and appeared healthy and morphologically similar. Repeated titration of SRR3 at this point, however, showed no demonstrable knockdown in one replicate and minimal knockdown in a second (Figure 5.19), as well as large intra-replicate variation (data not shown).

5.3.3 Over-expression of SRR

Significant difficulties had been faced in establishing reproducible knockdown of SRR in differentiated P19 cultures up to this point. Concomitant studies (detailed in Chapter 4) had investigated the expression of SRR in schizophrenia, and found an elevation in SRR levels in the DPFC of schizophrenia patients from the Oxford

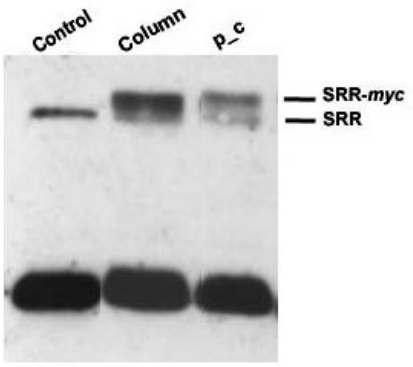

FIGURE 5-20 pSRR*myc* was purified using a commercial column-based method (column) and phenol-chloroform (p_c). The column purified vector showed a greater over-expression of SRR-*myc*, which migrates ~3kDa higher than SRR due to the *myc* tag, than phenol-chloroform purified plasmid did, compared to Lipofectamine^{2000} only treated cells (control).

and London series' (Chapter 4, Section 4.3.2). Since the aim of the present study was to establish a model of altered SRR expression that could allow exploration of the possible mechanism of SRR's involvement in NMDAR signalling and thence schizophrenia pathophysiological mechanisms, it was decided to subsequently concentrate on over-expression of SRR *in vitro*. At this point, the underlying basis for the variability in SRR knockdown observed in differentiated P19 cells was considered beyond the scope of this thesis. Over-expression of SRR in differentiated P19 cultures proved feasible but attempts to extend the manipulation to primary CGCs were not.

The SRR open-reading frame was inserted into *myc*-tagged plasmids under a CMV promotor (denoted pSRR*myc*). Initial studies first tested two methods of purification of this plasmid; phenol/chloroform purification, which is relatively quick and inexpensive and commercially available column purification kits which are more time-consuming and expensive but can be more efficient. Column purification was shown to produce greater over-expression of SRR-*myc* than phenol/chloroform purification (Figure 5.20) and was used in all further experiments.

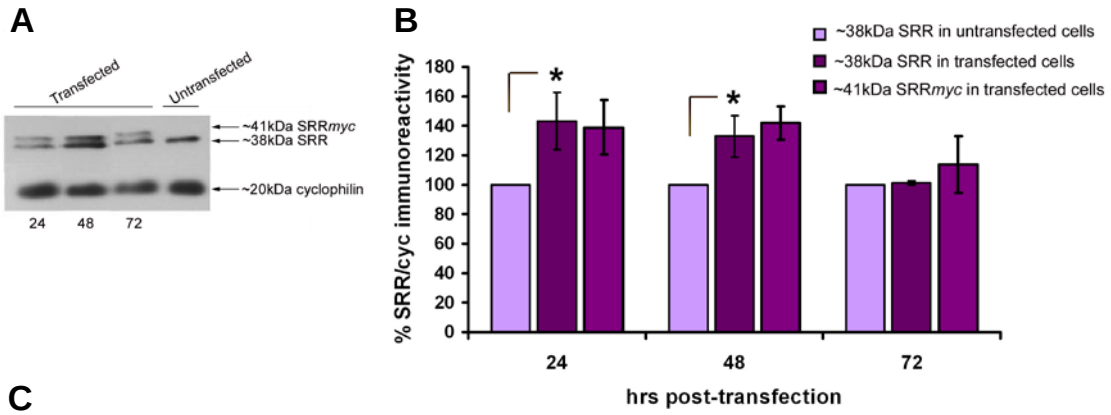

C

Hours post-transfection	~38kDa SRR/Cyc immunoreactivity Untransfected cells (%)	~38kDa SRR/Cyc immunoreactivity Transfected cells (%)	~41kDa SRR-myc /Cyc immunoreactivity Transfected cells (%)
24	100	143±19 * p =0.037	139±18
48	100	133±14 * p =0.037	142±11
72	100	101±1 p =0.317	114±20

FIGURE 5-21 SRR over-expression in differentiated P19 cultures. (A) Representative western blot showing loading control cyclophilin immunoreactivity at ~20kDa and SRR immunoreactivity in untransfected and transfected cells at 24, 48 and 72 hrs post-transfection. SRR immunoreactivity detects SRR at ~38kDa in both untransfected and transfected cells and SRR-*myc* at ~41kDa in transfected cells only, at 24, 48 and 72 hours post-transfection. (B) and (C) Percentage SRR immunoreactivity normalised to cyclophilin (cyc) in pSRR-*myc* transfected differentiated P19 cultures (n = 3) relative to untransfected cells. Transfection of pSRR-*myc* led to expression of ~41kDa SRR-*myc* in transfected cells at 24, 48 and 72 hours post-transfection. Transfection of pSRR-*myc* also led to statistically significant elevated expression of ~38kDa SRR in transfected compared to untransfected cells at 24 and 48 hours post-transfection.

Transfection of pSRR*myc* led to visible expression of SRR-*myc* at 24, 48 and 72hrs post-transfection. This could be visualized as a ~41kDa band, (compared to ~38kDa SRR), due to the molecular weight of the *myc*-tag (Figure 5.21 A). Levels of the newly synthesized SRR-*myc* were 139±18, 142±11 and 114±20% of the levels of ~38kDa SRR in untransfected cells at 24, 48, 72hrs post-transfection respectively.

In addition to over-expressed SRR-*myc*, levels of ~38kDa SRR in transfected cells were greater than those of SRR in untransfected cells by 43±19% (Mann Whitney-*U*, $p = 0.037$) and 33±14% (Mann Whitney-*U* , $p = 0.037$) at 24 and 48 hours post-transfection, but were equal to SRR levels in untransfected cells at 72 hours post-transfection (Figure 5.21 B and C).

Pilot experiments ($n = 2$), carried out at GSK, Harlow, UK, found intra-cellular D-serine was elevated in pSRR*myc* transfected cells compared to untransfected cells, while L-serine was unchanged (Table 5.4). These data could not, however, be replicated due to technical constraints.

Having established that transfection of pSRR*myc* led to SRR over-expression and possibly elevated D-serine levels in differentiated P19 cultures, the vector was transfected into CGC cultures under the same conditions. Cells were harvested at 48 hours post-transfection for analysis of SRR immunoreactivity and for planned studies on NMDAR expression following SRR over-expression.

TABLE 5-4 Intra-cellular D- and L-serine HPLC measurements in SRR over-expressing differentiated P19 cultures. ($n = 2$)

		D-serine (µM)	L-serine (µM)	D-/L-serine
Transfected cells				
Culture 1		0.11	5.56	0.02
Culture 2		0.51	5.74	0.09
	Mean	*0.31*	*5.65*	*0.05*
Untransfected cells				
Culture 1		0.09	6.10	0.01
Culture 2		0.06	5.37	0.01
	Mean	*0.07*	*5.66*	*0.01*

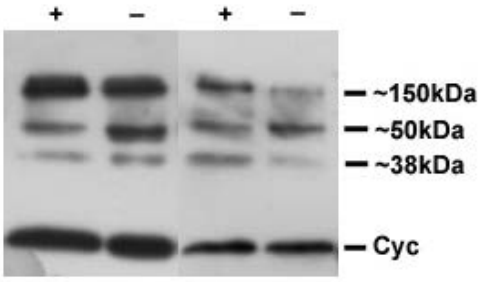

FIGURE 5-22 Representative western blot showing loading control cyclophilin (cyc) immunoreactivity and SRR immunoreactivity ~38, 50 and 150kDa in pSRRMYC transfected (+) and untransfected (-) CGC cultures.

Visible SRR-*myc* could not be seen by western blotting in transfected CGC cultures (n = 4) which demonstrated the three endogenous SRR immunoreactive bands (Figure 5.22) that had been seen previously in primary CGCs (see above) but no bands of the size of SRR-*myc*. Quantification of ~38kDa band, presumed to be SRR based on its molecular weight, showed SRR immunoreactivity in transfected cultures was 101±6% (mean ± sem; n = 4) of SRR immunoreactivity in untransfected cells. This indicated that SRR over-expression in primary CGC cultures had failed (the reasons for which are discussed below), and precluded further experiments on NMDAR expression and signalling in this model system.

5.4 DISCUSSION

The aim of this chapter was to develop an *in vitro* model of altered SRR expression to study the effect of SRR on NMDAR function. To reach this aim the objectives were to; successfully culture differentiated P19 cells and primary CGCs; characterise their basal expression of SRR and DAO; and to establish SRR over-expression and knockdown in these cultures. The main findings of this study are: 1) these cultures were both successfully generated and maintained, 2) their basal expression of SRR and DAO was assessed and a potential novel variant of DAO detected, 3) knockdown of SRR was achieved in differentiated P19 cells but was not reproducible, and 4) over-expression and of SRR was achieved in differentiated P19 cells but not primary CGC cultures. These findings are discussed in turn below.

5.4.1 Culture of differentiated P19 and primary CGC cultures

Retinoic acid treatment was shown to successfully differentiate P19 cells into neural- and glial-like cells based on immunocytochemistry for neuronal and glial markers (Figure 5.7). Consistent with previous reports (Tanaka *et al.*, 1992; Tang *et al.*, 2002; Trülzsch, 2004), neural-like cells extended neurites and stained for MAP2 and Tau from 3 DIV. The MAP2/Tau staining had begun to diminish by 11DIV (Figure 5.7 B), which likely reflects a loss of neurons over time in culture as has previously been reported for differentiated P19 cells (Omi *et al.*, 2004). Only limited GFAP staining was visible in differentiated P19 cultures at 6DIV but was prominent by 11DIV (Figure 5.7 C, D). Consistent with this, reports suggest that the terminal differentiation of glia into astrocytes is later than the adoption of neuronal phenotypes in differentiated P19 cultures (Shen *et al.*, 2004) and that

GFAP labelling is detectable only by ~8 DIV (Belliveau *et al.*, 1997; Tang *et al.*, 2002; Shen *et al.*, 2004), although others report detection of GFAP at 1DIV (Santiago *et al.*, 2005).

Differentiated P19 cultures were shown to express NMDAR mRNAs including the obligatory NR1 subunit (Figure 5.10), in keeping with previous reports evidencing functional NMDAR transmission in these cultures at 8DIV (Turetsky *et al.*, 1993; Morley *et al.*, 1995; Canzoniero *et al.*, 1996). Differentiated P19 cells were found to express NR1 mRNA from 5DIV while naïve P19 cells did not, in agreement with a previous report (Okamoto *et al.*, 1999) and suggesting the NMDAR phenotype may be switched on post-differentiation. Differentiated P19 cells were also found to express NR2A and NR2B subunit mRNAs but negligible NR2C, consistent with Ray & Gottlieb (1993) who reported NR1 and NR2B mRNA expression at 8DIV in differentiated P19s in the absence of detectable NR2C expression. However, they could not detect NR2A in these cultures (Ray & Gottlieb, 1993), which we could here, perhaps reflecting differences in the sensitivity of the PCR reactions used.

Primary CGC cultures were successfully generated as demonstrated by immunocytochemistry for MAP2/Tau and GFAP (Figure 5.11), showing neuronal and glial phenotypes at 4DIV, consistent with previous reports (Cambray-Deakin *et al.*, 1987; Hockberger *et al.*, 1987).

Taken together, the expression of MAP2, Tau, GFAP and NMDAR subunits in P19 cells, demonstrates that this cell line can be successfully differentiated into a neural- and glial-like cell culture expressing NMDARs, establishing its benefit to the present study. In addition, proof-of-principle was demonstrated for the preparation and culture of CGCs in our hands.

5.4.2 Basal expression of SRR in differentiated P19 and CGC cultures

Differentiated P19 cultures were found to express SRR mRNA (Figure 5.8 A) and protein by western blotting at ~38kDa (Figure 5.8 B), the predicted molecular weight of SRR (Wolosker *et al.*, 1999b; De Miranda *et al.*, 2000). SRR immunoreactivity was not detected in naïve P19 cells, possibly suggesting that SRR expression is switched on post-differentiation, perhaps concomitantly with that of NR1 subunit expression (see above). SRR protein at ~38kDa was also detected in CGC cultures (Figure 5.12 A, B) consistent with a previous report (Kartvelishvily *et al.*, 2006).

In differentiated P19 cultures, no statistical effect of DIV on SRR immunoreactivity was detected, although a trend correlation was observed (Figure 5.8 C). These results might suggest SRR expression increases developmentally with time *in vitro*, but further replications are required to establish statistical significance. In primary CGC cultures, an effect of time on SRR immunoreactivity was visible (Figure 5.12 C), although an *n* of 2 precluded correlation or statistical analysis. Notwithstanding, this is consistent with a previous observation of increasing SRR expression with CGC culture age (Kartvelishvily *et al.*, 2006) and, given the cerebellar origins of primary CGC cultures, may also be consistent with an increase in SRR expression from P1 to P7 in the developing mouse cerebellum *in vivo* (Wang & Zhu, 2003).

Kartvelishvily *et al.* (2006) reported that in primary CGCs, SRR was localized to the neuronal as well as glial cell populations in this culture. We were interested in the neuronal versus glial expression of SRR in these cultures given some contradictory findings of SRR expression in these respective cell types in the rat and mouse brain (discussed in Chapter 2, Section 2.4.2). However, attempts to

address this with immunocytochemistry failed, despite trying several methodological modifications.

In differentiated P19 cultures, an additional SRR immunoreactive band at ~50kDa could sometimes be detected (Figure 5.8 B). Again for CGC cultures a ~50kDa band was sometimes detectable as well as a further ~150kDa band. The relative predominance of the ~50 and ~150kDa bands in CGC cultures was variable across cultures and across replicate wells within the same cultures (Figure 5.12 A and B). While evidence from EST clustering, northern blotting and RACE experiments has identified possible alternative mRNA variants for SRR (Konno, 2003; Xia *et al.*, 2004; Yamada *et al.*, 2005), such variants could not account for these additional bands given that they are bigger than the predicted molecular weight of the protein encoded from the entire SRR open-reading frame. Thus one possibility is that these bands represent artefact. This conjecture could be supported by several previous reports with different SRR antibodies which only demonstrate a single ~38kDa immunoreactive band in various tissues (Wolosker *et al.*, 1999b; De Miranda *et al.*, 2000; Xia *et al.*, 2004; Steffek *et al.*, 2006; Bendikov *et al.*, 2007). However, the SRR antibody used here also only detected a single immunoreactive band for SRR ~38kDa in human, rat and mouse brain (Chapter 2, Section 2.3.1). This suggests that the additional immunoreactive bands seen in differentiated P19 and CGC cultures may be reflective of a genuine antibody-SRR interaction rather than non-specific properties of the antibody per se. In this case, a parsimonious explanation for the multiple SRR immunoreactive bands visualized is the demonstration of SRR homodimers and homotetramers reported for *Arabidopsis thalina* (Fujitani *et al.*, 2006), *Pyrobaculum islandicum* (Ohnishi *et al.*, 2007) and mammalian (Cook *et al.*, 2002; Wu *et al.*, 2004) SRR. However, bands at ~50kDa and

~150kDa are not two and three fold sizes of ~38kDa SRR. This could reflect a non-linear relationship between the electrophoretic mobility of a protein and its dimer/trimerization. The variability in the relative detection of the different bands for SRR across cultures could be due to variation in the dimer/trimeriztion of SRR in these cultures, or differences in the denaturation of SRR in individual protein extracts during the western blotting protocol.

5.4.3 Basal expression of DAO in differentiated P19 and CGC cultures

Differentiated P19 cultures were found to express DAO mRNA (Figure 5.9 A). Consistent with this, western blotting with the Moreno *et al.* (1999) antibody detected a band of ~39kDa, the predicted molecular weight of DAO (Gavazzi *et al.*, 1987; Moreno *et al.*, 1999), in differentiated P19 cells and rat cerebellum (Figure 5.9 B). However, the porcine DAO preparation used as an antigen to generate this antibody was subsequently shown to be contaminated with DAspOx (Shleper *et al.*, 2005), suggesting this antibody may detect both DAspOx and DAO. Since DAspOx is also ~40kDa (Setoyama & Miura, 1997; Yamada *et al.*, 1996), it is possible the band detected at ~39kDa represented DAspOx rather than DAO. However, using the GSK-DAO antibody, directed against a DAO specific C-terminal peptide sequence of the protein, a ~39kDa band was detected in differentiated P19 cells (Figure 5.9 C, Lanes 2-4) and purified porcine DAO (Figure 5.9 C, Lane 1). This suggests that the porcine DAO used as an antigen for the Moreno *et al.* (1999) antibody does contain ~39kDa DAO and that this antibody detects, at least in part, DAO in differentiated P19 cells. However, detection of DAO in differentiated P19 cells with the GSK-DAO antibody was variable (Section 5.3.1.1). This is unlikely to be because the GSK-DAO antibody does not detect DAO in mouse differentiated P19 cells, since this antibody

detected DAO in mouse brain (see Chapter 2, Section 2.3.1). This therefore suggests that if differentiated P19 cells do express DAO it is either at low and variable levels or in a conformation more readily detectable by the Moreno *et al.* (1999) antibody than the GSK-DAO antibody.

Both antibodies also detected an immunoreactive band at ~30kDa in differentiated P19 cells (Figure 5.9 B and C). This was also detected in porcine DAO by both antibodies (Figure 5.9 B, Lane 1 and C, Lane 1), suggesting that purified porcine DAO and differentiated P19 cells may both contain a ~30kDa form of DAO. Moreover, ~30kDa forms of DAspOx have not been reported to our knowledge, suggesting that the Moreno *et al.* (1999) antibody was detecting ~30kDa DAO rather than DAspOx. Since the detection of DAO mRNA in differentiated P19 cells was with primers which did not span the entire open-reading frame, an mRNA variant that could express a truncated form of DAO could not be verified. Possible alternative transcripts previously described (Fukui & Miyake, 1992; Konno, 1998; Kapoor *et al.*, 2006) involve UTR deletions and would therefore not encode a smaller protein. Interestingly though, a variant which would predict a truncated protein of ~30kDa has been reported in mouse (Strausberg *et al.*, 2002). However, its nucleotide sequence has a frame-shift such that the C-terminal peptide sequence of the predicted encoded protein would not be detectable by the GSK-DAO antibody (which is generated against a C-terminal DAO sequence). It is possible the sequencing reported by Strausberg *et al.* (2002) for this variant is inaccurate and thus the variant could account for the ~30kDa band detected here. However, it is also possible that both the Moreno *et al.* (1999) and GSK-DAO antibodies detected an artefactual ~30kDa band. Notwithstanding this possibility, the potential of a DAO variant is worthy of investigation. Indeed the ~30kDa band detected by the

GSK-DAO antibody appeared more prevalent than the ~39kDa band in differentiated P19 cells, suggesting it might be the dominant form in this cell type. That DAO activity was undetectable in differentiated P19s (Section 5.3.1) may therefore be due to the levels of ~39kDa DAO being below the threshold for activity detection. Or, speculatively, this finding could also be accounted for by the more predominantly expressed ~30kDa DAO form in differentiated P19 cells being inactive.

A further ~50kDa band, detected in differentiated P19 cells by the Moreno *et al.* (1999) antibody was not detected by the GSK-DAO antibody, and may represent DAspOx detection. In primary CGC cultures, the GSK-DAO antibody similarly detected only ~39kDa and ~30kDa bands, but at low levels (Figure 5.13).

Taken together therefore, two different antibodies to DAO were found to detect two immunoreactive bands at ~39kDa and ~30kDa in purified porcine DAO and in two different cell types. These findings are by no means definitive, given the potentially confounding DAspOx detection with the Moreno *et al.* (1999) antibody and the variable detection of both bands in differentiated P19 with the GSK-DAO antibody discussed. However, further investigation of a possible DAO variant is warranted. Future studies could amplify the reported DAO variant (Strausberg *et al.*, 2002) using primers spanning the boundary of the exons either side of the missing exon. Replicated sequencing of the amplified product could then assert whether a frame-shift occurs or whether the mRNA variant could theoretically encode a ~30kDa product with the original C-terminal peptide sequence, and thus detectable by the GSK antibody. *In vitro* translation could be used to then investigate whether the variant is translated and its enzymatic function measured with the DAO activity assay. Alternatively, although more costly, the ~30kDa band

could be analysed by mass spectrometry to reveal its identity. Further, future studies of a DAO variant in the human brain developmentally and in schizophrenia would be of topical interest in furthering an understanding of the gene's role and given DAO's therapeutic candidacy (Brandish *et al.*, 2006; Adage *et al.*, 2007).

5.4.4 RNA interference in P19 cells

Initial RNAi experiments with siGLO in naïve cells found that transfection of 100nM siGLO with 1:500 and 1.5:500 DharmaFECT3 produced visible transfection, and with 1:500 DharmaFECT3 produced 76% knockdown of cyclophilin immunoreactivity 72 hours later (Table 5.3). This is in keeping with reported levels of siRNA induced protein knockdown at this time-point (e.g. Fountaine & Wade-Martins, 2007) and in naïve P19 cells (Trülzsch *et al.*, 2004). However, in differentiated P19 cultures, while the same lipid dilutions produced visible transfection of 100nM siGLO in both neurons and glia (Figure 5.15 G and H), 1:500 and 1.5:500 DharmFECT3 dilution produced ~6 and 40% cyclophilin knockdown, respectively (Table 5.3). This could reflect a low turnover of the target protein (Choi *et al.*, 2005) in differentiated versus naïve P19 cells. While 72 hours is the recommended time point to study protein knockdown (*Nature Cell Biology* (Editorial, 2003)) some proteins show greater knockdown at 96 than 72 hours post-transfection (Trülzsch *et al.*, 2004). Another possible cause may have been lower levels of transfection in terminally differentiated cells (Brunner *et al.*, 2000) versus naïve P19s. For example, it was also noted that plated differentiated P19 cells were often of a lower confluency than naïve P19 cells when transfected, which could have had an effect on the transfection. However, transfection of 100nM siGLO with Optifect, a lipid reagent for sensitive or low confluency cell types, was not

found to improve the % knockdown above that seen with DharmaFECT3 either at 72 hours post-transfection or at 96 hours post-transfection (Table 5.3). This suggested that Optifect was not superior to DharmaFECT3 in transfecting the cells, and that knockdown was not improved at 96 compared to 72 hours post-transfection. In fact, conversely, over-expression of cyclophilin, by 82%, was seen at 96 hours post-transfection with the highest amount of Optifect (Table 5.3). The reason for experimental variability in the direction of over-expression to this degree is unknown. While siRNA-induced gene over-expression phenomena have been reported, this applies to a particular sequence of siRNA that has inducing *rather than* knockdown capabilities (Li *et al.*, 2006). This does not explain the over-expression seen here, therefore, by an siRNA which also shows knockdown capability. Such variance in knockdown as that seen here is gravely concerning for reproducible experiments.

While modulating transfection - a possible reason for low cyclophilin knockdown in differentiated P19s - with Optifect did not improve knockdown, an additional means to improve transfection with Lipofectamine^{2000} was nevertheless tried. This was because Lipofectamine^{2000} has been reported as being superior to other lipid formulations for the transfection of post-mitotic neurons (Ohki *et al.*, 2001) and cells refractory to transfection under other conditions (Amarzguioui, 2004) as well as being one of the most commonly used lipid reagents in the literature. However, cyclophilin knockdown (11% at 72 hours post-transfection) was not improved using Lipofectamine^{2000}.

In summary therefore, attempts to modify transfection of the cells did not improve knockdown, and measurement of knockdown at 96 rather than 72 hours did not improve knockdown. This could suggest that cyclophilin is more stable in

differentiated than naïve P19 cells, but that knockdown would require analysis at time points later than the 72 and 96 hours tried. Indeed, the stabilization (reduced turnover) of proteins during neuronal differentiation is not unprecedented (Coulombe *et al.*, 2003). Alternatively the results could suggest that the RNAi machinery is less efficient in differentiated P19 cells compared to naïve P19 cells. However, Omi *et al.* (2004) report that RNAi in naïve and differentiated P19 cells does not differ, lending credence to the low knockdown of cyclophilin in differentiated compared to naïve P19 cells being due to its increased stabilization.

Since our overall aim was to manipulate SRR expression, the siRNAs to SRR were then tested in differentiated P19 cells. At this time, it was decided to pursue Lipofectamine^{2000}, given its successful use in transfecting neuronal cells (Ohki *et al.*, 2001; Noh *et al.*, 2005; Fountaine & Wade-Martins, 2007) and its common use within the literature. Concomitantly, plasmids expressing shRNAs of the four siRNA sequences to SRR were tested, in case their action was more potent than siRNAs, as reported in some cases (Vlassov *et al.*, 2007).

In fact, it was found that the siRNAs were more potent than the shRNAs to the same sequences at the time-points tested (Figure 5.16 and 5.17). Of the siRNAs, SRR3 and SRR4 produced the greatest knockdown of 50±5% and 45±8% respectively (Figure 5.17). This was slightly greater than that seen for cyclophilin knockdown in differentiated P19 cells (Table 5.3), and the intra-replicate variability was lower than that seen for cyclophilin knockdown (data not shown). This suggested therefore, that the lower and variable cyclophilin knockdown in differentiated P19 cells was not due to compromised RNAi machinery, although its efficiency may still be less than that in naive P19s. Indeed, the levels of knockdown of SRR in the differentiated cells were lower than expected compared to similar

reports of siRNA-induced knockdown in neuronal cultures (Fountaine & Wade-Martins, 2007).

Notwithstanding the lower than expected levels of SRR knockdown, SRR3 and SRR4, which had shown the best knockdown at ~50%, were pursued. The aim was to titrate the siRNAs and then study a time-course of their knockdown. The time-course experiment allows the appropriate point for phenotypic analysis to be selected based on the time of maximal gene knockdown, which varies from gene to gene based on the half-life of the target protein (Choi *et al.*, 2005). The titration experiment is an important one to carry out because reducing the amount of siRNA used for effective knockdown reduces the likelihood of non specific side-effects (*Nature Cell Biology* (Editorial, 2003)).

The results from the initial titration experiment showed large intra-replicate variability (data not shown), large inter-replicate variability and minimal knockdown (~15-16%) with any concentration of siRNA (Figure 5.18). This was therefore discrepant with the previous knockdown achieved with 100nM of these siRNA sequences (Figure 5.17).

The main limiting factor in the degree of knockdown achievable is known to be transfection efficiency (*Nature Cell Biology* (Editorial, 2003)). Consistent with this, in reporter gene assays, Hollon & Yoshimura (1989) demonstrated that the high variability they observed among measurements of reporter enzyme activity was due to variation in the overall level of transfection efficiency from one experiment to another. It was found that this could vary by a factor of at least ten (Hollon & Yoshimura, 1989). Thus, differences in transfection efficiency between replicates and between repeated experiments might plausibly account for the variability in knockdown seen within the titration experiment.

However, this would not explain why the knockdown was lower or even negligible in the titration experiment compared to the initial screening experiment or why the variability was larger in the titration experiments compared to the initial screen experiments. Moreover, no conditions in the methodology had changed between the initial screen of the SRR siRNAs and the SRR3 and SRR4 titration experiment. Consequently, it was hypothesized that the disparity in results may represent a change in the health of the cells from the initial screen experiments to the titration experiments, although cells had been morphologically examined daily. Nonetheless, a change in cell health could have potentially affected the ability to transfect the cells or the efficiency of the RNAi machinery. Indeed, the general health of cells prior to transfection is known to be a source of variability from one transfection to another (Dalby *et al.*, 2004), (although this would not account for the intra-replicate variability seen). However, when a new batch of P19 cells were ordered, differentiated and cultured in two different laboratories with existing and newly ordered cell culture constituents, all cultures visually appeared morphologically comparable and healthy. Furthermore, when titration of SRR3 was again attempted in two cultures at this time, limited SRR knockdown was observed (Figure 5.19) and intra-replicate variability was apparent (data not shown). Therefore, factors outside of cell health may have contributed to these findings. Differences in cell density at the time of transfection are a common source of variability in over- or knockdown of gene expression (Dalby *et al.*, 2004), however a standard seeding protocol following cell counting of live cells was used in these studies which should over-come such a source of irregularity. It is therefore difficult to find a reasonable explanation for the variability seen here, given that standardized protocols were used and attempts to overcome common sources of

variation were undertaken. One possibility is that, for unknown reasons, complexing of nucleic acid and cationic lipids can be a variable process. It has been shown that this therefore creates a heterogenous population of complexes (Zabner *et al.*, 1995) and thus it is possible that some complexes will transfect better than others.

Discussion of further possible causes of, or moreover precedents for, the variability seen here, are difficult to find within the literature given a probable publication bias towards reporting of positive data. Some reports do exist however. For example, Choi *et al.* (2005) generated stable cell lines of enhanced green fluorescent protein (EGFP) knockdown using shRNAs in HEK-293 cells and found that the reduction in EGFP fluorescence among the clones varied remarkably. This variation could be due to variability in the transcription of the plasmid or due to variability in the RNAi machinery from clone to clone. Similar variability has been reported in ***Histoplasma capsulatum*** transformants carrying stem-loop RNA episomes (which generate shRNAs and thence siRNAs) (Rappleye *et al.*, 2004; see Woods, 2005 for comment). Such reports, and the experience in this study, create concern over the popular use of RNAi in genotype-to-phenotype experiments, when the source of the variability is difficult to identify.

5.4.5 SRR over-expression in differentiated P19 and CGC cultures

Up to this point, difficulty had been encountered in establishing reproducible SRR knockdown. Having adopted standardized procedures and demonstrated comparable cultures morphologically after controlling for cell batch, cell culture constituents and cell culture facilities, the source of the variance observed was difficult to identify. Further analysis of the cause of the irregularity was considered

beyond the scope of the thesis. Concomitant experiments, however, had revealed that SRR expression was elevated in the DPFC in subjects with schizophrenia from the Oxford and London brain series' (Chapter 4, Section 4.3.2). At this time therefore, a second strategy to develop a model of aberrant D-serine metabolism, SRR over-expression, was focused on, the relevance of which was underscored by these schizophrenia expression data.

A pSRR-*myc* plasmid was generated and purified using a commercial column-based kit. This was found to lead to greater SRR-*myc* over-expression assessed visually by western blot than phenol-chloroform purification. It is likely therefore, since the same amount of plasmid was transfected, that the commercial column-based purification method yielded purer plasmid preparations than phenol-chloroform purification.

Transfection of pSRR-*myc* led to expression of ~41kDa SRR-*myc* at 24, 48 and 72 hours post-transfection, which was not present in untransfected cells (Figure 5.21). This is consistent with the observation that peak transient expression is seen 24-72hrs post-transfection (Dalby *et al.*, 2004). At these respective time-points, the levels of SRR-*myc* were 139±18, 142±11 and 114±20% of the level of endogenous ~38kDa SRR expression in untransfected cells. Therefore, transfection of the plasmid led to the expression of SRR-*myc* around 1-1.5x the levels of SRR in untransfected cells. This would therefore effectively just over double the total SRR/SRR-*myc*. In addition, the level of ~38kDa SRR in transfected cells was significantly greater than the level of ~38kDa SRR in untransfected cells at 24 and 48 hours post-transfection. This suggests that transfection of pSRR-*myc* could have induced endogenous SRR expression. Alternatively, processing of the novel SRR-*myc* within the cells may have led to cleavage of the *myc* tag, yielding additional but

untagged SRR. However, precedents for this are unknown despite common use of *myc*-tag plasmids. At 72 hours post-transfection the SRR immunoreactivity in transfected and untransfected cells was equal, suggesting that any potential induction of endogenous SRR was not occurring at this time-point. Possible explanations for this are unknown, but it could represent intra-cellular feedback signalling to restore homeostatic levels of endogenous SRR.

Pilot data of intra-cellular D- and L-serine measurements in differentiated P19 cells over-expressing SRR demonstrated an elevation of D-serine levels but unchanged L-serine levels compared to untransfected cells (Table 5.4). This experiment could not be repeated, due to difficulties in our collaboration with GSK as discussed (Section 5.3.3). Thus, based on a single experiment, speculation over the result must be cautious. However, the data could tentatively suggest that the elevated SRR and/or SRR-*myc* drove the synthesis of more D-serine. This would be consistent with SRR over-expression in HEK-293 cells (De Miranda *et al.*, 2002; Xia *et al.*, 2004) and suggests that the *myc* tag did not effect SRR enzyme activity. However, if the pSRR-*myc* plasmid induced endogenous SRR expression, as discussed, this could have led to elevated D-serine, irrespective of SRR-*myc* expression.

Having established SRR over-expression, we next attempted to extend this manipulation to primary CGC cultures. Primary cultures are beneficial for their closer relationship to living systems than cell lines. Moreover, primary CGC cultures were particularly pertinent to this study given their established expression of SRR (here and Kartvelishvily *et al.*, 2006) and the role of SRR in the migration and development of these cells (Kim *et al.*, 2005). However, attempts to replicate SRR over-expression in primary CGC cultures failed. Transfection of the SRR

vector under the same conditions as those used to transfect differentiated P19 cultures, was found to lead to undetectable levels of SRR-*myc*, and equal levels of SRR in transfected and untransfected cells. Lipofectamine^{2000} based transfection of primary neuronal cultures has been reported, and while some suggest transfection may be as low as 3% (Uo *et al*., 2005), others report transfection of 20-30% (Ohki *et al*., 2001). Since the SRR-vector used in transfecting CGC cultures was the same as that used in transfecting differentiated P19 cultures, reduced transfection efficiency in the CGCs compared to the differentiated P19s would be the most likely explanation for the observed result. Thus, future experiments would require optimisation of transfection in this cell type, in our hands, with reporter vectors and perhaps alternative transfection methods (see below).

5.4.6 Limitations and conclusions

This study aimed to develop an *in vitro* model of altered SRR expression as a basis for studying the effects of D-serine metabolism on NMDAR function, relevant to pathophysiological theories of D-serine metabolism in schizophrenia. Initial proof-of-principle experiments with cyclophilin knockdown demonstrated low knockdown in differentiated P19 cells. The main limitation of these studies was a sample size of 1 used in trying different transfection conditions. At the time these experiments were carried out it was thought that the three replicates (wells) of a single experiment would represent sufficient replication. However, with later experience it was realised that three replicates in an experiment should be combined as a single *n*; this should then be repeated with independent cultures or generations of cells for subsequent *n* numbers. This knowledge was utilised for later experiments of SRR knockdown and over-expression.

Attempts to knockdown SRR encountered considerable variation which, given the scope and time constraints of this thesis, precluded continuation of these studies. However, future studies should examine the source of the variation beyond that which was attempted here. It is important to understand such irregularities in RNAi methodology, given the popular utilisation of this technique in genotype-to-phenotype studies.

The second strategy of over-expressing SRR was successful in differentiated P19 cultures and pilot data was indicative of a phenotypic consequence on intra-cellular D-serine levels. However, the study was limited by the fact that these data were only preliminary and further HPLC analysis of D-serine levels consequent to SRR over-expression could be not be continued. Thus, if time and resources permitted, future studies would have extended these D-serine measurements. In addition, further phenotypic analysis of the effects of SRR over-expression on NMDAR function in differentiated P19 cells would have been warranted. Had these studies not been beyond the constraints of time here, they would have been carried out utilising NMDAR expression analyses and measurements of NMDAR activity with calcium imaging.

Subsequent attempts to over-express SRR in primary CGC cultures were unsuccessful, speculatively due to factors affecting transfection of these cells. Therefore the overall aim of studying NMDAR expression/function following perturbation of SRR expression and thence D-serine metabolism in a biologically relevant system was not achieved here. To conduct this analysis in the CGC culture system would presumably require the optimisation of alternative delivery methods in future studies. While beyond the scope of this thesis, future studies could attempt to optimise methods such as viral-based delivery, electroporation or calcium-phosphate precipitation. Once optimised the phenotypic consequences of

SRR over-expression in CGC cultures could be analysed, again through NMDAR expression analyses and calcium imaging measurements of NMDAR activity. A further future and attractive study would be to analyse NMDAR internalisation through NMDAR expression in membrane versus cytosolic cell fractions, as was planned but not carried out here, or live receptor internalisation imaging.

6. GENERAL DISCUSSION

6.1 OVERVIEW OF THESIS

While the precise aetiology and pathophysiology of schizophrenia remains unclear, the last decade has seen considerable progress in understanding the contribution of susceptibility genes to the disorder. In addition, traditional dopaminergic theories in schizophrenia have now been incorporated into a greater understanding of other neurochemical abnormalities in the disorder, particularly glutamatergic ones. However, theories of NMDAR hypofunction in schizophrenia have not been supported by robust evidence of altered expression of these or other glutamate receptors. Consequently, attention has been given to those molecules impinging on NMDAR function; not least the several recently described schizophrenia susceptibility genes thought to do so (Harrison & Weinberger, 2005). DAO is one of these identified susceptibility genes, and is functionally implicated in schizophrenia through its catabolism of D-serine. Since D-serine is thought to be the endogenous co-agonist of the NMDAR, at least in the forebrain (Schell *et al.*, 1995; Schell *et al.*, 1997), and its CSF and serum levels are reportedly reduced in schizophrenia (Hashimoto *et al.*, 2003, 2005; Yamada *et al.*, 2005; Bendikov *et al.*, 2007), brain D-serine and its metabolism have been highlighted in the disorder.

The research detailed in this thesis was designed to investigate D-serine metabolic enzymes further, with three objectives; firstly, to investigate a potential contribution of DAO and SRR to the function of the brain through studying their regional and cellular distribution; secondly, to investigate a potential contribution of DAO and SRR to schizophrenia through studying their expression in the

disorder; and thirdly, to investigate the role of SRR in NMDAR activity, this being a potential mechanism of SRR's putative involvement in schizophrenia.

In chapters 2 and 3, the distribution of DAO and SRR were investigated immunohistochemically in the rodent and human brain respectively. At the time of conception of this thesis, the distribution of DAO and SRR in the human brain was unknown, and knowledge of their regional and cellular expression was required to gain an understanding of the potential pathophysiological roles they may play. Moreover, the proposed role of D-serine as the NMDAR co-agonist, relevant to NMDAR hypofunction theories in schizophrenia, was based largely on studies of its distribution and that of its metabolic enzymes in the rodent brain. However, controversies over these data had begun to emerge and thus it was important to study the distribution of DAO and SRR in the rodent brain as well as human.

In chapter 4, the expression of DAO and SRR in the schizophrenic brain, previously unknown, were examined. These studies were designed to investigate a potential dysregulation of D-serine metabolism, and thence D-serine levels, in schizophrenia through the altered expression of DAO and SRR. Specifically, it was hypothesized that DAO expression may be elevated in schizophrenia and/or SRR expression reduced. This underscores the rationale in this thesis for studying both DAO and SRR, since any changes in one enzyme in schizophrenia may be counter-balanced by an opposite change in the other.

In chapter 5, an attempt was made to develop an *in vitro* model of aberrant SRR expression with the goal of studying an effect of SRR on NMDAR function. This was important since the hypothesis of an involvement of D-serine metabolic enzymes in schizophrenia centred on their regulation of D-serine and thence NMDAR activity. The overall aim of this chapter was, however, largely unmet. The study characterised two potential model systems, (differentiated P19 and primary

CGC cultures), and highlighted some of the potential technical issues surrounding SRR knockdown and over-expression in these systems. However, technical constraints precluded an analysis of the role of SRR in NMDAR activity.

Since the conception of this work, several studies have been published of direct relevance to the hypotheses and aims of this thesis. The main findings of the investigations carried out are therefore discussed here in the context of current literature. Future extensions of the research stemming from this thesis and a summary of the overall view on the potential involvement of DAO and SRR, and thence D-serine, in schizophrenia are given.

6.2 The Distribution of SRR and DAO in the Brain

In chapters 2 and 3, immunohistochemical studies were carried out to characterise DAO and SRR distribution in the rodent and human brains respectively. In the rodent, both DAO and SRR were localized to the frontal cortex and therein to neuronal and glial cells. For SRR, these findings have added to more recent accounts of neuronal SRR expression and thence D-serine synthesis in the rodent (Yasuda *et al.*, 2001; Kartvelishvily *et al.*, 2006; Puyal *et al.*, 2006; Williams *et al.*, 2006). This contrasts to the traditional view of an exclusively glial expression of SRR (Wolosker *et al.*, 1999b; Xia *et al.*, 2004) and D-serine (Schell *et al.*, 1995, 1997) and challenges the view of D-serine solely being a gliotransmitter. Consequently a reconciliation of these traditional and novel views has been required, underscoring the importance of both replicating and extending studies and the continued questioning of accepted views. Wolosker (2006) has therefore recently discussed the potential of neuronal as well as glial D-serine signalling at NMDARs and the possibility that neuronal and glial D-serine serve different roles. This latter point is

particularly interesting in light of the exclusive glial localization of SRR in the human cortex described in Chapter 3. The findings here therefore raise the possibility of an interesting species difference in D-serine signalling and highlight the caution that must be taken when extrapolating from rodent to human. The use of human tissue for studies such as these is therefore an important and valuable commodity.

The white over grey matter enhancement of SRR expression observed in the human cortex may also challenge the original proposal that D-serine primarily serves as a gliotransmitter at NMDAR bearing synapses in the cortical grey matter (Schell *et al.*, 1995, 1997). While these seminal studies were widely cited, the data presented here add to an increasing appreciation of white matter SRR and D-serine (Williams *et al.*, 2006). Moreover, while white matter D-serine synthesis by SRR could be involved in NMDAR potentiation, the data may suggest that other roles of SRR, such as in pyruvate formation and cellular energy requirements (Williams *et al.*, 2006; Puyal *et al.*, 2006), should be considered.

For DAO, the neuronal expression of the enzyme in the rodent frontal cortex is noteworthy given previous reports of its undetectable activity in this region. Both the immunohistochemical expression of DAO in cortical neurons and the lack of detectable cortical DAO activity was replicated in the human brain (Chapter 3, Sections 3.3.5 and 3.3.9). Conversely, in both rodent and human cerebellum, DAO was robustly expressed, consistent with previous reports including those localizing its activity there. These data therefore highlight a paradox where DAO is both present and active in the cerebellum but its robust continued expression in the frontal cortex is unaccompanied by detectable activity. This is of particular note given the apparent difference in cortical and cerebellar

DAO antigenicity demonstrated from western blotting versus immunohistochemical findings (Chapter 2, Sections 2.3.1 and 2.3.2-2.3.9). The reasons for the difference in cortical and cerebellar DAO properties are unknown. It is attractive to contemplate these data with reference to the findings discussed in Chapter 5 however. In these studies, a smaller ~30kDa DAO band was the dominant DAO form expressed in differentiated P19 cells and could speculatively account for the lack of detectable DAO activity in these cells. Thus, it is tempting to conjecture a possible contribution of alternative splicing to the expression of cortical versus cerebellar forms of DAO with differences in both antigenicity and activity. In addition, that an inactive form of DAO is thought to be required for *in vivo* trafficking into peroxisomes (Caldinelli *et al*., 2004; see Chapter 1, Section 1.8.2) suggests that some intra-cellular regulation of DAO activity must exist. These possibilities may impact upon therapeutic interest in DAO inhibition in schizophrenia (Brandish *et al*., 2006; Adage *et al*., 2007), particularly given the importance of the cortex in the disorder (see Chapter 1, Section 1.4).

SRR expression in both rodent and human cerebellum was, unlike that for DAO, less expected. This is due to conflicting reports of cerebellar SRR expression (Wang & Zhu, 2003; Yoshikawa *et al*., 2004, 2005; Takeyama *et al*., 2006; Hashimoto *et al*., 2007b) as well as the low reported levels of cerebellar D-serine (Nagata *et al*., 1992, 1994a; Hashimoto *et al*., 1993b,c, 1995a, b; Hamase *et al*., 1997; Morikawa *et al*., 2001; Wang & Zhu, 2003; Kartvelishvily *et al*., 2006). While more recent immunohistochemical studies of D-serine distribution may refute this (Williams *et al*., 2006), the presence of SRR expression and inferred activity (Hashimoto, 2002)in a region where D-serine is possibly low, or more certainly in a region where DAO acts to breakdown the majority of any synthesized D-serine (Morikawa *et al*.,

2001), is puzzling. Our findings of cerebellar SRR expression may therefore highlight an importance in tight regulation of D-serine levels or the importance of its localized sources in this region. Alternatively, SRR could be carrying out a different role in the cerebellum. This pertains to the robust expression of white matter SRR also, and highlights the caution that must be taken when speculating over distribution data, since the functional correlates of gene expression are unknown.

The expression of SRR and DAO were studied in the SN and VTA of the rodent and SN of the human brain and both were evident in these dopaminergic regions. The demonstration that DAO can oxidise D-DOPA (Moses *et al*., 1996; Wu *et al*., 2006; Kawazoe *et al*., 2007) could allow speculation that DAO in dopaminergic cells could take part in alternative dopamine synthetic pathways. However, in the absence of a known endogenous substrate to enable this (discussed in Chapter 2, Section 2.4.3) it may seem unlikely. However, the expression of SRR, and presumably therefore D-serine synthesis, in these regions, coupled with DAO expression, suggests the enzymes may impact at a site of glutamatergic and dopaminergic interaction. Further study of a role of DAO in glutamate-dopamine interaction, such as an analysis of the effects of DAO over-expression or inhibition on dopamine levels *in vivo* or *in vitro*, may be interesting as well as of potentially therapeutic relevance. Indeed, the discussion here highlights the lack of functional insight that can be drawn from distribution studies and thus the requirement for further experiments.

6.3 THE EXPRESSION OF SRR AND DAO IN SCHIZOPHRENIA

In Chapter 4, the expression of DAO and SRR in the DPFC and cerebellum in schizophrenia were examined. These areas were focused on given the reported preferential localizations of SRR and DAO to these regions respectively (Horiike *et al.*, 1987, 1994; Schell *et al.*, 1995; Wolosker *et al.*, 1999b; Wang & Zhu, 2003; Kapoor *et al.*, 2006). At the time of conception of this thesis, the expression of these enzymes in schizophrenia was unknown and it was important to analyse this in light of hypotheses of reduced D-serine in the disorder (Hashimoto *et al.*, 2003, 2005; Yamada *et al.*, 2005). In addition, the SNPs in DAO (Chumakov *et al.*, 2002; Liu *et al.*, 2004; Schumacher *et al.*, 2004; Corvin *et al.*, 2007b; Wood *et al.*, 2007 but see Fallin *et al.*, 2005; Yamada *et al.*, 2005; Liu *et al.*, 2006; Shinkai *et al.*, 2007; Vilella *et al.*, 2007) and SRR (Goltsov *et al.*, 2006; Morita *et al.*, 2007 but see Yamada *et al.*, 2005; Strohmaier *et al.*, 2007), genetically associated with schizophrenia, may exert their effect through altered expression of these genes (Harrison & Weinberger, 2005).

In Chapter 4, evidence was provided for an elevation in cerebellar DAO expression in schizophrenia, a conclusion made more robust by later findings (Kapoor *et al.*, 2006; Burnet *et al.*, 2008a). This work has therefore made an important contribution to an understanding of the role of DAO in schizophrenia. However, the relationship of this increase to the genetic association of DAO with schizophrenia is unclear (discussed in Chapter 4, Section 4.4.1.1). Moreover, the relationship of the elevation of DAO in the cerebellum with decreases in D-serine in the disorder is questioned given reportedly low cerebellar D-serine levels (see above; Nagata *et al.*, 1992, 1994a; Hashimoto *et al.*, 1993b,c, 1995a, b; Hamase *et al.*, 1997; Morikawa *et al.*, 2001; Wang & Zhu, 2003) and recent evidence that D-serine

in the brain (as opposed to CSF/serum) is not decreased in schizophrenia (Bendikov *et al.*, 2007; Hashimoto *et al.*, 2007a). Thus, the functional and pathophysiological implications of elevated DAO in schizophrenia in light of these findings are unclear. Possibilities, such as D-alanine breakdown or effects on localized sources of D-serine have been discussed (Chapter 4, Section 4.4.1.2). However, these suggestions are only speculative since post-mortem expression data cannot probe functional consequences, underscoring the main limitation of such studies. Thus, future work would benefit from investigations aimed at analysing the functional consequences of DAO over-expression in the cerebellum *in vivo* or in cerebellar cultures *in vitro*. Such experiments could evaluate whether elevated DAO would exert any effect on localized sources of D-serine, perhaps with immunoautoradiography of D-serine and D-alanine in sections or cultures of cerebella over-expressing DAO. The consequences on NMDAR function could perhaps then be evaluated with calcium imaging or *in vivo* electrophysiology. Moreover, these over-expression studies are attractive given the ability to rescue the effect through pharmacological DAO inhibition or knockdown of DAO using RNAi. Again such experiments would be of interest pharmacologically. Indeed, the therapeutic potential of DAO exists irrespective of its status as a pathophysiological determinant and may be supported by its elevated expression in schizophrenia. Additionally interesting in this regard would therefore be to study whether DAO expression is elevated in dopaminergic brain regions (striatum and VTA) in schizophrenia, to complement functional studies on the effect of DAO on glutamate-dopamine interactions (discussed above).

The studies conducted in Chapter 4 analysed SRR expression in schizophrenia in the Oxford and London brain series and attempted to replicate

these findings in the Stanley Foundation brain series. The elevation in SRR immunoreactivity in the DPFC observed in the Oxford and London brains was not replicated in the Stanley Foundation brains. Others have reported elevated hippocampal SRR expression, but unchanged DPFC expression in schizophrenia (Steffek *et al.*, 2006), and others still decreased SRR expression in the DPFC in schizophrenia (Bendikov *et al.*, 2007). As discussed (Chapter 4, Section 4.4.2), robust evidence for SRR alterations in schizophrenia therefore does not exist. While the relationship of diagnostic expression changes and genotype is unclear (discussed in Chapter 4, Section 4.4.2.1), it is noteworthy that analyses of association of SRR with schizophrenia are not robust in light of recent non-replications (Yamada *et al.*, 2005; Strohmaier *et al.*, 2007). In addition, the demonstrations that D-serine is unaltered in the brain in schizophrenia (Bendikov *et al.*, 2007; Hashimoto *et al.*, 2007) in contrast to CSF and serum (Hashimoto *et al.*, 2003, 2005; Yamada *et al.*, 2005; Bendikov *et al.*, 2007) question the original hypothesis of altered D-serine metabolism in schizophrenia. While this argument also applies to DAO, where association studies have also yielded negative results (Fallin *et al.*, 2005; Yamada *et al.*, 2005; Liu *et al.*, 2006; Shinkai *et al.*, 2007; Vilella *et al.*, 2007), the robust expression change and pharmacological interest in DAO support its importance. For SRR on the other hand, the current data would suggest it may not be integral to schizophrenia pathophysiological mechanisms, whether causative or compensatory. Notwithstanding this, the enzyme itself is interesting in light of a suggested involvement of D-serine signalling in pain (e.g. Wake *et al.*, 2001), the potential therapeutic strategy to target SRR in conditions of excessive NMDAR activity and the intriguing possibility of a dual function of the enzyme (Panizutti *et*

al., 2001; De Miranda *et al*., 2002; Foltyn *et al*., 2005; Stříšovský *et al*., 2003; Stříšovský *et al*., 2005).

6.4 Development of an In Vitro Model of Altered SRR Expression

In chapter 5 an attempt was made to generate an *in vitro* model of aberrant SRR expression as a means of studying the consequences of dysregulated D-serine metabolism. Studying the consequences on NMDAR activity would be integral to the hypothesis that D-serine metabolic enzymes are involved in schizophrenia through reducing D-serine levels and consequently NMDAR activity.

In this study, proof-of-principle was established for generating and maintaining neuronal and glial differentiated P19 and primary CGC cultures. During the initial characterisation studies, the expression of DAO and SRR in differentiated P19 and primary CGC cultures was studied. For DAO the possibility of the existence of a truncated ~30kDa form of the enzyme was highlighted.

For SRR, additional immunoreactive bands were also observed in primary CGC protein extracts. Their possible identity has been discussed (Chapter 5, Section 5.4.2). The observation of these additional immunoreactive bands raises an important point about the applicability of cell culture systems. The choice of primary CGC cultures was made as an attempt to have a biologically relevant model in which to study the effects of SRR manipulation. However, the demonstration of SRR immunoreactive bands at ~50 and 150kDa in these cultures, unseen in human and rodent protein extracts, questions their biological relevance. Notwithstanding this caveat, the use of model systems is an absolute requirement in light of the limitations of post-mortem studies in probing gene function (see above). However, the use of *in vivo* models may overcome the shortfalls of using

primary cultured cells where their *in vitro* development in relation to their normal *in vivo* development is unknown. This is a more important consideration for cell lines, which are transformed to allow continued replication.

The attempts to knockdown SRR in differentiated P19 cultures were hindered by substantial experimental variability. Some of the possible sources (e.g. batch of cells, culture facilities/materials) were investigated but did not yield an answer, and in light of the use of standardized procedures, an explanation for the irregularities in knockdown observed was not achieved. Further studies into this were beyond the scope of this thesis. However, the grave concern that such variability generates for reproducible genotype-to-phenotype studies means that future investigation into the underlying reasons are warranted; although the nature of such experiments is hard to envisage given that no obvious source of the disparities was identified here. Perhaps comparing knockdown of different genes across different cell types could identify whether differentiated P19 cells or SRR expression is particularly prone to biological variability. Since transfection can be a frequent source of variation in knockdown experiments the optimisation of other transfection techniques and their comparison in ability to achieve reproducible knockdown could be insightful (discussed in Chapter 5, Section 5.4.4).

Over-expression of SRR in differentiated P19 cells was achieved in preliminary studies and a pilot study suggested this may lead to elevated D-serine synthesis. However, in the absence of verification this finding requires replication. In primary CGC cultures, over-expression was not achieved, and as discussed (Chapter 5, Section 5.4.5), may represent a limitation in transfection of these cells. Thus future studies would aim to extend these findings by replicating SRR over-expression and consequent D-serine elevation in differentiated P19 cultures and

optimising alternative transfection techniques in order to achieve SRR over-expression in primary CGC cultures. Once established the consequent effects on NMDAR activity could be studied.

The main limitation to the studies carried out in Chapter 5 is their small sample numbers, the reasons for which have been discussed (Chapter 5, Section 5.4.6). If time and resources permitted, and if these studies were to be carried out again, the use of larger *n* numbers from the beginning would have allowed a better analysis of SRR expression alterations and any variability. In light of current literature, however, the rationale for manipulating SRR expression in a model system with regard to schizophrenia is now questioned. The gene was chosen in this study as time and resources prevented the manipulation of both DAO and SRR, and the neurobiology of SRR was unclear. The data outlined in this thesis, and in this discussion however, now suggest that evidence for reduced D-serine in schizophrenia and altered SRR expression in schizophrenia is not strong. While SRR may still be an interesting molecule and potential therapeutic target, for example in pain, modelling its role in NMDAR function in the context of understanding pathophysiological mechanisms in schizophrenia now has less impetus.

6.5 Final Summary

The work presented in this thesis has advanced an understanding of the neurobiology of DAO and SRR, and their potential roles in schizophrenia. The novel data accrued on DAO was of particular importance and overall, the enzyme appears particularly interesting in light of novel distribution findings and its expression in schizophrenia. Specifically, DAO shows:

- robust cortical expression
- expression in dopaminergic regions and neurons, and sites of glutamate-dopamine interaction
- robust elevation in the cerebellum in schizophrenia.

These findings may impact on current pharmacological and interest in the enzyme and generate further interesting questions. Indeed, future studies are required to resolve the role of DAO in the brain and in schizophrenia. The current data represents the initial step to this end.